TEMPERATURE DISTRIBUTION MODELS FOR DOUBLE GLAZED WINDOWS AND THEIR USE IN ASSESSING CONDENSATION OCCURRENCE

Nasser Abodahab

Ph.D. **July 1998**

Temperature Distribution Models for Double Glazed Windows and Their Use in Assessing Condensation Occurrence

Nasser G. A. Abodahab

A thesis submitted in partial fulfilment of the requirements of Napier University for the degree of DOCTOR of PHILOSOPHY

Department of Mechanical,
Manufacturing and Systems Engineering
Napier University

July 1998

Table of Contents

June 1996, Computational Mechanics Publications, Southampton, UK, 1996

E. N. Abodahab and T. Muneer, Free convection analysis of a window cavity and its longitudinal temperature profile, Energy Conversion and Management, Vol. 39, No. 3/4, 1998

F. T. Muneer, N. Abodahab, and A. Gilchrist, Combined conduction, convection, and radiation heat transfer model for double glazed windows, Building Services Engineering Research & Technology (BSER&T), Vol. 18 (4), pp 183-191, London, England, 1997

G. T. Muneer and N. Abodahab, Frequency of condensation occurrence on double glazings in the United Kingdom, Energy Conversion and Management, Vol. 39, No. 8, pp 717-726, 1998

Microsoft Excel Workbooks on Floppy Disk

H. *UVal.xls*: U-value calculation of a given window design

I. *LongTemp.xls*: Longitudinal (centreline) temperature profile for double glazed window

J. *Conduct.xls*: Edge-seal conduction, convection and radiation analysis and their effect on window edge temperature

K. *Condense.xls*: Analysis of the frequency of occurrence of condensation

Acknowledgements

I wish to express my sincere appreciation to my supervisor Dr. Tariq Muneer for his criticism, encouragement and the help he extended throughout the work. I am also grateful to Dr. Alistair Gilchrist, my external supervisor, for his instructive suggestions and valuable contributions towards this work.

I am also indebted to Professor Jorge Kubie, Head of MMSE Department; Mr Tom Truslove, Deputy Head of MMSE Department and my internal supervisor; Professor Alex Young, the former Head of MMSE Department, for their support throughout the work.

I acknowledge the friendship and moral support of David Kinghorn, Dr. Baolei Han, Torkild Aas, Andy Gibson, Dr. Bill Bailey, Gillian Weir, Steve Bremner, Abdulla Elammari, Dr. Abdelmadjid Bensalem, Harbi Ahmed and Dr. Kamal.

I would like to thank Bill Young, Ken Russell, Kevin McCann, Ian Campbell, Chris Anthony, Donald Ross, John Fairley, Caroline Middleton, Cheryl Thomson, and Eileen Lyons for their ever-willingness to offer help and technical advice.

Many thanks are due to Mr George Pringle, the Chief Technician of the MMSE Department, for his generous help.

Finally, I dedicate this thesis to all the members of my family who have supported and encouraged me throughout the research period.

Abstract

Condensation might be described as the modern disease of buildings. In dwellings, condensation on window glazing may obstruct the view and, if it becomes so excessive and no means for drainage is provided within the window frame, condensed water will run off causing damage to woodwork, furniture and decorations. The present research contributes to the furtherance of understanding of the temperature distribution in double glazed windows, the mechanism behind such variations and their effect on condensation occurrence on the inward pane.

Herein, it has been proven via measurements that there is a longitudinal temperature variation along the height of the inward glass of any double glazed window. It has also been shown that condensation always initiates at the bottom edge of windows and it progresses upwards with the drop in external temperature and/or the increase in the indoor relative humidity. It is postulated that this temperature stratification is primarily due to the buoyancy driven flow of gas within the sealed enclosure. An analytical model which computes the temperature at any given location along the vertical centre-line of the window has been developed. In this respect a new heat transfer dimensionless group has been introduced. This group is a function of Rayleigh and Prandtl numbers, glazing U-value and the height along the window centreline.

A two-dimensional numerical model for obtaining the longitudinal temperature distribution for the bottom part of double-glazed windows has also been developed. In contrast to previous studies which solely addressed the spacer conduction effects, this model additionally includes inter-pane radiative exchange and natural convection effects. It has been shown that the cavity gas convection is an important factor in the reduction of the bottom edge temperature. Cold bridging is also a significant factor for the conductive loss of heat at the edge surface. However, the present analysis has shown that the relative weighting for the cold bridging conductive loss is only 17% for air filled windows. The temperatures computed by this model were found to be in good agreement with the corresponding measured temperatures. Statistically, the average values of the mean bias error (MBE) and the root mean square error (RMSE) were found to be 0.5 and 0.7 degree Celsius respectively. The model is thus of significant use for the precise quantification of the condensation problem so commonly encountered in dwellings.

As an aid in quantifying the condensation problem a simplified model for assessing the nocturnal temperature drop within buildings has been developed. Using this model it has been shown that frequency of condensation occurrence can be substantially reduced by using modern, super-insulated windows. For example, condensation occurrence will be reduced by about 40-50% if an air-filled, float-glass double glazed window is replaced by a xenon-filled double glazed window using low-emissivity coating on both panes.

Microsoft Excel workbooks are included to enable the user to perform a number of relevant computations such as U-value for a given window design, window longitudinal temperature profile, and an assessment of condensation occurrence.

Nomenclature

$\dot{m}$	air mass flow rate, kg/s
q_F	fabric heat loss, W
$\Delta T_{H_w/2}$	temperature difference between the centre-glazing and the core of infill gas (= $t_3 - T_f$), ^{0}C
$\bar{R}$	universal gas constant (8.3144 kJ/kmole K)
$\dot{V}_i$	volume flow rate of air entering the building space, m^3/s
$\dot{V}_o$	volume flow rate of air exiting the building space, m^3/s
A	material cross sectional area perpendicular to the heat flow direction, m^2
A_b	building surface area, m^2
A_{cg}	projected area of glazing, m^2
A_{eg}	projected area of window edge-seal, m^2
A_f	projected area of window frame, m^2
A_F	surface area of fabric, m^2
A_n	node surface area with unit depth, m^2
A_o	surface area of window outer pane with unit depth, m^2
A_{pf}	projected area of the entire fenestration, m^2
A_r	aspect ratio of the window cavity
C	heat exchange by convection, W
c	specific heat, J/kg K
c_1	constant
c_o	constant
c_p	specific heat at constant pressure, J/kgK
d	total thickness of glass panes, m
ΔT	differential temperature, ^{o}C
ΔT_{edge}	temperature difference across edge-seal, K
ΔT_X	temperature difference at any height (x) between a given node and the infill gas (= $T_n - T_f$), ^{0}C

Δx	material thickness, m
E	heat loss by evaporation, W
F	angle of the glass surface from the vertical, degrees
F_{no}	view factor of nodal element with respect to the outer glass pane
g	gravitational acceleration, m/s^2
Gr	Grashoff number
h	heat transfer coefficient from the building surface to external air, W/m^2K
H	height along glass pane from the bottom edge, m
h_c	convection heat transfer coefficient, W/m^2K
h_{ca}	convection heat transfer coefficient for window air cavity, W/m^2K
h_{ci}	internal convection heat transfer coefficient, W/m^2K
h_i	combined heat transfer coefficient for internal surface, W/m^2K
h_o	combined heat transfer coefficient for external surface, W/m^2K
h_r	radiation heat transfer coefficient, W/m^2K
h_{ra}	radiation heat transfer coefficient for window air cavity, W/m^2K
h_{ri}	internal radiation heat transfer coefficient, W/m^2K
h_s	infill gas heat transfer coefficient, W/m^2K
h_t	conductance of multiple glazed unit, W/m^2K
H_w	window height, m
K	heat exchange by conduction, W
k	thermal conductivity, W/mK
K_{cl}	heat conduction through clothing, W
k_{edge}	thermal conductivity of window edge-seal, W/mK
k_g	thermal conductivity of glass, W/mK
k_i	constant, i = 1 to 11
L	cavity width, m
L_g	thickness of glass, m
l_g	length of inner perimeter of window frame, m
ln	natural logarithm
M	gas molecular weight, kg/kmole
m	constant

MBE	mean bias error
MET	heat generated within the human body by metabolism, W
N	number of window cavities
n	air change rate per hour, $hour^{-1}$
Na	Napier number
n_d	number of days
Nu	Nusselt number
p	gas pressure, Pa
Pr	Prandtl number
P_w	partial pressure of water vapour, Pa
P_{ws}	saturation pressure of water vapour, Pa
Q	angle of the enclosure cavity from the horizontal, degree
q	heat flux, W/m^2
q_e	linear heat flow through window edge-seal, W/m
q_r	net radiative heat transfer, W/m^2
q_v	rate of transfer for ventilation energy, W
R	correlation coefficient
R_a	window cavity resistance, m^2K/W
Ra	Rayleigh number
Ra^*_H	constant heat flux Rayleigh number
RAD	heat exchange by radiation, W
R_{cond}	thermal conduction resistance, m^2K/W
R_{conv}	convection resistance, m^2K/W
RES	heat exchange by respiration, W
r_g	thermal resistivity of glass, m K/W
R_{g1}	outside pane thermal resistance, m^2K/W
R_{g2}	inside pane thermal resistance, m^2K/W
RMSE	root mean square errors
R_{rad}	thermal radiation resistance, m^2K/W
R_s	surface resistance, m^2K/W
R_{si}	inside surface resistance, m^2K/W

R_{so}	outside surface resistance, m^2K/W
R_T	overall thermal resistance, m^2K/W
R-value	centre-glazing thermal resistance, m^2K/W
S	rate of heat storage in the human body, W
T	absolute internal dry bulb temperature, K
t	t-test statistic
T(x)	temperature of glass pane at distance x from edge-seal, K
T*	dimensionless temperature
T_1	temperature of the hot side wall, K
t_1	outer pane external temperature at centre-glazing level, ^0C
T_2	temperature of the cold side wall, K
t_2	outer pane cavity-side temperature at centre-glazing level, ^0C
t_3	inner pane cavity-side temperature at centre-glazing level, ^0C
t_4	inner pane room-side temperature at centre-glazing level, ^0C
T_a	the mean of the air space surface temperatures, ^0C
T_b	outer pane bottom temperature, ^oC
t_d	indoor dew-point temperature, ^oC
$T_{e,w}$	temperature of inner pane edge-seal, K
T_f	infill gas film temperature, ^oC
t_g	inner pane bottom edge temperature (at H = 5 mm), ^oC
T_i	internal ambient temperature, ^oC
t_i	temperature of the inner glass pane at an arbitrary point, ^0C
T_n	node temperature, n represents node number (3, 4, 5, or 6)
T_o	external ambient temperature, ^0C
T_{si}	inside mean surface temperature, ^0C
T_{so}	outside mean surface temperature, ^0C
T_t	outer pane top temperature, ^oC
U	centre-glazing U-value, W/m^2K
U_{eg}	edge-of-glass U-value, W/m^2K
U_F	fabric U-value, W/m^2K
U_f	frame U-value, W/m^2K

U_o	window overall U-value, W/m^2K
U_{ref}	reference glazing U-value (at T_i =20° and T_o =0 °C), W/m^2K
V	volume, m^3
V_w	wind speed, m/s
W	external work, W
x	distance from edge-seal, m
Y*	dimensionless height
Y_1	constant
Y_2	constants

Greek Letters

α	infill gas thermal diffusivity, m^2/s
β	infill gas volumetric thermal expansion coefficient, K^{-1}
δt	thermal boundary layer thickness, m
ε	surface emissivity
ε_1	emissivity of window outer pane
ε_2	emissivity of inner window pane
ε_{eff}	effective emissivity of the parallel glass surfaces
ε_h	hemispherical emissivity of the coated surface
ε_n	nodal surface emissivity
ϕ	relative humidity
μ	infill gas dynamic viscosity, kg/ms
ν	infill gas kinematic viscosity, m^2/s
ρ	density, kg/m^3
ρ_i	density of air entering the building space, kg/m^3
ρ_o	density of air exiting the building space, kg/m^3
σ	Stefan-Boltzmann constant ($\sigma = 5.678 \times 10^{-08}$ W/m^2K^4)
τ	time, seconds

ψ_g	linear thermal transmittance due to the combined thermal effects of the spacer, glazing and frame, W/mK

1 Introduction

1.1 Human thermal comfort

Thermal comfort is often defined as that condition of mind which expresses satisfaction with the prevailing thermal environment [1.1]. This definition emphasises that comfort is a psychological phenomenon and not related to physical environment or physiological state [1.2]. An understanding of feelings of thermal comfort or discomfort reported by humans is complex and not completely understood. The human response to thermal environments is affected by four basic environmental parameters (air temperature, radiant temperature, humidity, and air movement) and two personal parameters (the metabolic heat generated by human activity and clothing worn by a person). Humans respond to the interaction of these six parameters. The thermal comfort is often assessed in terms of air temperature alone but, in fact, it is not exclusively a function of air temperature as the other five parameters are also relevant. For example, thermal comfort in offices or vehicles may be greatly affected by solar radiation and specifying comfort limits in terms of air temperature alone will be inadequate [1.2].

Heat transfer into the body and generated within it must be balanced by heat outputs from the body in order to maintain the body's internal temperature at around 37 ^{0}C. The heat balance equation for the human body can be represented in the following form [1.3],

$$S = MET \pm W \pm RAD \pm C \pm K - E - RES \qquad 1.1$$

where,

C heat exchange by convection, W

E heat loss by evaporation, W

K heat exchange by conduction, W

MET metabolism, W

RAD heat exchange by radiation, W

RES heat exchange by respiration, W

S rate of heat storage, W

W external work, W

A heat balance is reached if the storage S = 0. When dealing with a clothed person with no contact for conduction (K = 0) and by assuming that the heat transfer from/to the non-clothed parts of the person's body is negligible, the heat transfer through the person's clothes (K_{cl}) should be taken into account. For S = 0, Equation 1.1 can be written as follows,

$$MET \pm W - E - RES = \pm K_{cl} = \pm RAD \pm C \qquad 1.2$$

Equation 1.2 implies, that the metabolism (MET) plus the external work (W) minus the heat loss by evaporation (E) and respiration (RES) is equal to the heat conduction through the clothing (K_{cl}) and equal to the heat loss or gain by radiation (RAD) and convection (C) from the outer surface of the clothing.

The provision of thermal comfort is fundamental to human existence. A human has to adjust his/her clothing and activity and regulate his/her position with regard to heat sources (artificial or natural) in order to meet their requirements. In hot climates, consideration is generally given to how to cool indoor environments to provide thermal comfort. In cooler climates, consideration is given to how to heat environments to provide comfort. When humans become thermally uncomfortable, health and productivity can be affected, morale can fall and workers may refuse to work in such an environment. For this reason, there has been interest in research into the conditions which produce thermal comfort.

A modern building is expected to provide a satisfactory thermal environment. Windows, as key elements of building construction, influence occupant thermal comfort by [1.4]:

- heat gain or heat loss through the glass, which either raises or lowers the room air temperature
- radiation exchange between glass and occupant

For an occupant close to a window, the internal glass surface temperature influences thermal comfort as a result of heat loss produced by long wavelength radiation exchange between the occupant and the window [1.4]. In winter, the long wavelength radiation exchange between the cold surface of window glass and the occupant contributes to a sensation of cold discomfort. In summer, the situation is reversed, the internal surface of glass can be much hotter owing to the absorption of solar radiation. The long wavelength radiation exchanged between the window glass and the occupant and also direct short wavelength solar radiation received by the body through the glass contribute to a sensation of hot discomfort.

Within the United Kingdom the Health and Safety regulations demand that the temperature within occupied buildings should not be over 28 0C for 1% of the working year.

1.2 Windows

1.2.1 Introduction

Recently, higher levels of insulation, lower infiltration rates and larger areas of glazed aperture have been demanded of building. In view to this increasing demand, the conventional window has become the weakest thermal fabric in a building. Studies [1.5 and 1.6] have shown that 6% of the United Kingdom's energy consumption is due to domestic glazings alone. In addition to their poor thermal performance, conventional windows can create comfort problems and damaging accumulations of condensation. These malfunctions have strengthened the desire for windows with higher thermal performance. The use of double glazed windows is still the most common method of providing a reasonable level of thermal resistance. Various technologies have been

introduced to double glazed windows to further enhance their performance. Examples of these new advances include spectrally selective low emissivity coatings on glass and on thin plastic films, solar control coatings, infrared transparent glazings, anti-reflective surface treatments, low conductivity infill gases, honeycombs, silica aerogels, multi-layer film suspension systems, holographic coatings, optically switchable glazings, polarised glazings, and evacuated enclosures.

Most double glazed windows currently manufactured consist of two panes of glass separated from each other by an edge-seal. The edge-seal isolates the cavity between the glazings, thereby creating an enclosure suitable for non-durable coatings and/or substitute infill gases. The edge-seal creates a thermal bridge between internal and external environments. This phenomenon is called cold bridging. It causes energy loss at the perimeter of the window hence reducing the window's overall thermal performance. Cold bridging may also cause condensation occurrence on the bottom part of the window inner pane. Better window glazing calls for a parallel development in edge-seal and frame technology [1.7].

Windows provide humans with a variety of functions which include the supply of the interior spaces of buildings with light, solar energy, air and view according to the desires of the occupants and to shield them from dust, noise, rain and excessive heat or cold. Windows also provide the passers-by with attractive views into buildings, e.g. commercial buildings and houses. Some of these functions which are of importance to this research project will be explained briefly in the following sections.

1.2.2 Windows and energy conservation

Most of the energy used today originates from fossil fuels (gas, oil and coal). Burning fossil fuels emits pollutants, including carbon dioxide and gases that cause acid rain. As carbon dioxide and other gases build up in the atmosphere, more of the sun's heat is trapped (the greenhouse effect). This could result in the earth becoming hotter (global warming), which may also increase the risk of storms, coastal flooding and drought.

Using energy more efficiently is one of the most cost effective means of reducing emissions of carbon dioxide and also helps to conserve fossil fuels.

Buildings account for 60% of the total energy budget of the United Kingdom. Over 80% of energy consumption in the 20 million homes in the United Kingdom is due to space and water heating. This accounts for 25% of the national energy budget. At least one-quarter of the domestic heating bill is due to the thermal energy loss through glazings because they are the weakest thermal components in a building.

Therefore, improving the thermal insulation of the window will contribute to energy conservation and environmental betterment by reducing the heat loss from a building shell. This, in turn, reduces the amount of fossil fuels to be burnt and hence the greenhouse gases, such as CO_2 released into the atmosphere.

Heat is lost through windows by conduction, convection and radiation. Detailed analysis of the mechanism of heat loss through single and double glazed windows will be discussed in Chapter 3. It is convenient to combine all types of heat loss in a single parameter which describes the air-to-air behaviour of a double glazed window. This parameter is called the thermal transmittance or U-value (W/m^2K). It represents the rate of heat loss per square metre, under steady state conditions, for a temperature difference of one Kelvin between the inner and outer environments separated by the glazing. The lower the window U-value, the better is its thermal insulation and the more energy it can conserve. Present research is targeted to achieve U-values below 0.35 W/m^2K [1.4]. Better U-values can be achieved by using modern technology. Examples of this technology will be given later in this chapter.

In order to investigate the effect of window insulation betterment and CO_2 curbing, life cycle analysis for different gas-filled double glazed windows is required. The results of one such study [1.8] shows that the use of inert gases in double glazed windows is economically favourable.

1.2.3 Windows and daylight

Daylight is one of the vital necessities that occupants require from buildings. Occupants need adequate amounts of daylight to be able to perform indoor tasks such as reading and machine operation. Task lighting cannot be provided by daylight alone for the entire working day throughout the year, some form of artificial lighting is required to supplement the available daylight [1.4]. Daylight is also required to enhance the appearance of an interior and its contents by admitting areas of light and shade that give shape and detail for objects. Electrical lighting in the UK accounts for an estimated 5% of the total primary energy consumption and buildings may consume up to 60% of their total energy in the form of electric lighting [1.9]. Therefore, by reducing reliance on artificial lighting, daylight can be an effective means of saving energy and reducing environmental impact. However daylight and artificial light may need to be integrated to avoid lack of proper lighting within a building. The inclusion of daylight in the work place provides workers with social and physiological benefits. Daylight, for instance, may increase the ability of office workers to do desk work.

Using a low emissivity coating to improve a double glazed window performance has very little effect on daylight transmissivity. The daylight transmissivity for a double glazed window with 4 mm thick float glass is 80% and if one low-e coating is added, while other conditions remain the same, the transmissivity becomes 75% (5% decrease). However, as a consequence of using the low-e coating, the U-value is reduced by 53% [1.9].

Daylight can, however, be troublesome in some situations. For example, occupants may feel discomfort due to the excess of illumination in their field of view. This phenomenon is called glare. If the level of glare becomes very high, it may cause disability to carry out a task such as reading or writing. Interior objects such as furniture and paintwork may suffer visual degradation and fading if subjected to daylight for longer periods of time. The use of excessive glazed area in an attempt to admit more daylight may give rise to solar overheating. Some windows using special low-e coatings,

especially in commercial buildings, can reflect solar energy while admitting the worthwhile daylight, thus reducing cooling loads without increasing the lighting load.

1.2.4 Windows and sound insulation

Sound insulation within a building is as important as other building services, such as heating, ventilation and lighting. Noise usually is communicated to rooms within a building via many different paths, from noise sources elsewhere in the building and/or from noise sources outside the building [1.10]. Examples of these sources are road traffic, railways, aircraft, industry, and building mechanical services. Modern architecture using light-weight structures, often with large windows allow more sound to be transmitted into the building rather than the heavy, load-bearing walls of older buildings.

Noise is defined as unwanted sound. It has many effects on human beings. Noise causes annoyance or dissatisfaction, affects communication, causes damage to hearing, affects performance of tasks, and causes permanent changes in the normal functioning of the human organism which results in mental and/or physical deterioration [1.11].

Sound insulation does not mean eliminating all sources of sound. Humans need contact with the outside world through hearing desired sound. Windows are usually the weakest link in the sound insulation of a building. A single double glazed window provides about 25 dB of sound insulation and a well-designed double glazed window can provide over 40 dB of sound insulation [1.12].

The fundamental principle of the sound insulation of windows is the mass law, which demonstrates that, with each doubling of glass thickness, the corresponding sound insulation is increased by about 4 dB [1.4]. Other factors contributing to the sound insulation of a multiple glazed window are air-tightness, the gap width of the window cavity and the acoustical isolation of the absorbent material around the edges of the air space. The best air gap for sound insulation has a width of at least 150 mm [1.12]. Ideally, for best thermal insulation and lower cost, the optimum air gap width should

only be 20 mm. Windows based on this design cavity width are commonly used. However, for larger widths there is not a serious degradation in the thermal performance. Thus there may be a compromise struck between thermal and acoustic considerations.

1.2.5 Window technology

During the last decade window technology has seen more dramatic changes than any other building technology. Spurred by the spiralling oil prices of the late 1970s, new technology has touched upon every aspect of the window performance [1.13]. In the past, the addition of extra glazing was the only option for improving window thermal performance. Recently, modern technology has introduced low emissivity coatings, inert infill gases, insulating edge spacers and low conductive frames in the window design. Windows having the combination of these technologies are referred to as superinsulated windows. For instance, a German window company, Interpane, has brought onto the market a window with a U-value of 0.4 W/m^2K [1.9] which is as good as an insulated wall.

In addition to reducing energy loss from buildings, superwindows also offer the following advantages [1.9]:

- The improvement of comfort through the elimination of cold downdraughts and radiation exchange.
- Excellent noise attenuation performance.
- An increase in the total light admission in residential and other buildings by allowing greater window areas to be employed without increasing the overall energy losses.
- With appropriate selective coatings, a reduction in overheating problems in temperate and tropical zones in summer, leading to a reduction in the need for indoor cooling.

- Greater flexibility and freedom for architects, designers and users.
- A reduction in condensation problems at the window edge area.

Research in all aspects of windows is still very active. New technology in material, design, manufacturing and installation is being developed. The following are some of window technologies presently in the market.

1.2.5.1 Wavelength selective coatings

These coatings can be used to reflect or absorb certain bands of radiation whilst allowing the transmission of others. Some of the technologies utilising coating techniques are mentioned below.

A. Low-emissivity coatings

A low-e coating is a low absorptive coating to suppress infrared radiation exchange. Absorption equals emissivity at any given wavelength and hence it is called low-e coating. Transmission in the longwave infrared (far infrared) equals zero for nearly all materials. Hence low-e coatings have a high far infrared reflection. However their reflectivity for the shortwave infrared is low. Most of the solar energy is shortwave infrared whilst the energy radiated from warm objects is far infrared. A low-e glazing, therefore, acts as a selective reflector where solar transmission is quite high, solar reflectance is low and the reflectance of the far infrared emitted from internal objects is very high. These characteristics are appreciated by building occupants as in winter more daylight and solar energy are welcome and less heat loss from the interiors is required. Sixty per cent of the heat lost through ordinary windows is through longwave infrared. A low-e window essentially doubles a window's thermal resistance because the low-e coating nearly shuts down the infrared conduit [1.14].

Commercial buildings produce so much heat from people, lights and equipment. That in many instances the solar energy is hardly desirable, particularly in the summer. External

window shading and tinted glazing were always considered effective means for reducing undesirable solar energy and glare. Some low-e coatings are formulated to reflect solar energy away while admitting the worthwhile daylight. Such coatings can reduce cooling loads in commercial buildings without increasing the lighting load.

Low emissivity films are generally of the type dielectric/metal/dielectric or dielectric/metal. The preferred metals are silver, gold and copper, although silver is the most widely used.

B. Spectral splitting and cold mirrors

Spectral splitting coatings can be used to divide the solar spectrum into different broadband regions. In this way various glazings can be tailored to particular photovoltaic or photothermal needs. By tailoring the solar energy to that of the photovoltaic response, the overall system efficiency can be increased. The cold mirror coating has the opposite spectral response to that of the transparent low-e film. The cold mirror exhibits a high reflectance in the visible region and transmits highly in the infrared. Cold mirrors are generally multilayer dielectric interference films. A simple design utilising a conventional dielectric/metal/dielectric low-e coating might be used to separate the visible and the near infrared portions of the solar spectrum. The visible portion could be used for photovoltaic conversion and the infrared portion could be used for photothermal conversion. Also, the photovoltaic will operate more efficiently if infrared heating is eliminated. If transparent low-e coatings with different spectral characteristics were used, the solar spectrum could be partitioned from low to high energy as the low-e transition wavelengths become shorter. Also, liquid crystals can be used as optical filters in that they are aligned and solidified by polymerisation. This process can give pre-set optical properties.

C. Holographically coated glazings for wavelength selection

Holographic coatings can be tuned to reflect any waveband in the solar spectrum whilst allowing 75 - 80% transmittance in the visible wave band [1.15]. The holographically

coated film would be laminated between two glazing substrates for protection. These coatings are already used in head-up displays (HUD) for cockpit and automobile windscreens where instrument information is projected optically on to the screen and reflected to the pilot or the driver.

1.2.5.2 Superwindows

Superwindows are glazing systems comprising of multiple panes of glass or plastic films, one or more low emissivity coatings, gas cavity fillings and insulating frame and spacers.

For triple glazing with two low-e coatings of emissivity (ε=0.1) and using air in the window cavity, the U-value is approximately 1.0 W/m^{2}K. For triple glazing, with two low-e coatings of emissivity (ε=0, which is the ideal case), the U-value is about 0.9 W/m^{2}K. Thus it can be seen that this technology is reaching its ideal limit [1.9]. By filling glazing cavities with gases of lower conductivity than air, e.g. xenon, the U-value is about 0.4 W/m^{2}K.

Superwindows are now commercially available and the range will increase in the future. Potential problems of cost, weight and sealing durability are constraining multiple glazing technology and preventing the theoretical level of U-value being achieved.

1.2.5.3 Transparent insulation materials

Transparent insulation material (TIM) are materials which allow solar energy to be readily transmitted, but minimise the amount of heat which can be transferred through the surface.

The air space between window panes can be filled with aerogel, a microporous silicate foam material which reduces thermal transmission. Two forms of aerogel exist for use in windows, monolithic (in the form of continuous slabs) and granular (in the form of

granules). The granular form is easier to produce and therefore cheaper but has poorer properties.

Monolithic aerogel has excellent properties, being both highly transparent and having thermal properties approaching that of an opaque wall. It is predicted that only slight evacuation would be required to achieve a heat loss coefficient of 0.37 W/m^2K for a double glazed window with a 2 cm layer of aerogel [1.9].

Granular aerogel, of various diameters (typically 1 - 10 mm), can be poured into the cavity of a double glazed window. The resulting heat loss coefficient for a 2 cm thick space of granules between glass panes is 0.98 - 1.15 W/m^2K depending on the size of the granules. However, the translucent nature of this design makes it less suitable for normal windows than monolithic aerogel [1.9].

1.2.5.4 Vacuum windows

Evacuated windows circumvent the high cost of gas filling. These windows utilise a vacuum in combination with a low-emissivity coating on one of the internal surfaces, an approach which eliminates cavity gas convection and most of the radiant heat transfer. Conduction through the spacers becomes the major vehicle of heat transfer. The U-value for such windows can be as low as 0.13 W/m^2K. This technology is currently being developed to overcome the following problems:

- The seal must be able to maintain the vacuum required. The pressure within the cavity has to be maintained to extremely low values, e.g. of the order of 0.001 Torcelli.
- The exceptionally low heat transfer across the glazing requires special attention be given to the frame of the glazing unit.
- The temperature difference between the outer and inner panes will be large, producing thermal expansion that could overstress rigid edge seals.
- Spacers are needed in the evacuated cavity to keep the glass layers from collapsing.

Heat transfer through a vacuum window is by thermal radiation, conduction through low pressure gases, conduction through pillars and edge conduction. Radiation losses can be reduced by the use of low-e coatings. Hard coats (ε=0.1) are technically possible, vacuum compatible and will withstand the high temperatures involved in processing vacuum windows.

1.3 Condensation in buildings

1.3.1 Introduction

Condensation might be described as the modern disease of buildings [1.16]. Surveys have indicated that millions of households in the UK are affected to a greater or lesser extent by condensation, and in some instances these problems have been so severe and have so defied rectification that demolition has been the ultimate remedy [1.16]. Condensation is a natural phenomenon which occurs when warm moist air comes into contact with a cold surface, which cools the air below its saturation point, causing its water vapour to condense. This can happen on any cold surface within the building such as plastered wall or a pane of glass. In dwellings, condensation on glazings may obstruct the view through window and, if it becomes so excessive and no means for drainage is provided within the window frame, condensed water will run off causing damage to window frame, furniture and paintwork.

1.3.2 The mechanism of condensation

Water vapour is one of the constituents of the atmospheric air. Water vapour is invisible and only becomes noticeable when condensation forms on cold surfaces such as glass windows in buildings or when cold, dry air meets warm, moisture-laden air and fog results. Indirectly, humidity can be noticed when a black mould grows on the walls of an inadequately heated room within a building.

In many parts of the world where climates are warm and humidity levels are high, air becomes incapable of absorbing more moisture. Thus the human body cannot get rid of its internal heat by the evaporation of sweat, particularly if there is little air movement. The result is over-heating of the body and the sensation of a higher air temperature than the actual air temperature. With moisture contents between 40% and 70%, humidity is rarely noticed. Ideally, internal conditions should be maintained within these extremes. Lower humidity causes dryness of the throat and higher humidity cause feelings of oppression [1.17].

The ability of air to hold water vapour decreases as air temperature is lowered. When moist, warm air is cooled down by being in contact with cold air or any cold surface such as window glass, it becomes unable to carry its load of water vapour. Thus, it discards some of its moisture. As an example, in clear days surfaces lose heat by radiation to the clear sky and become cold especially after sunset. The air in contact to these surfaces also becomes cold and dumps part of its moisture on these surfaces as in dew on grass and tree leaves.

Single-glazed windows are considered the weakest thermal elements in building. In winter time, the temperature of the glass pane of the single-glazed window approaches the outside ambient temperature. The indoor air which is in contact to the glass surface discards some of its water vapour content forming condensation, e.g. tiny water droplets on glass surface.

1.3.3 Types of condensation in buildings

1.3.3.1 Surface condensation

Surface condensation occurs when warm, moisture-laden air comes into contact with a cold surface. The temperature of the air in contact falls down. If the air temperature is lowered to its dew-point or below that, condensation will occur on this surface. This condensation takes the form of tiny droplets of liquid water gathering on the surface. This type of condensation has a lot of effects on dwellers. It obstructs the view through

windows. If the amount of condensed water liquid is very high, it may run off causing damage to window wooden frames, wall paint and decorations, furniture, and so on. However, some windows have drainage holes which run the condensed water outside the building.

Surface condensation is much more evident, due to discoloration of decorations and the formation of mould growths on paint, wallpaper and textile surfaces. Such mould growth is likely whenever the relative humidity is frequently in excess of 80% [1.17]. But at least surface condensation can be easily seen and the physical condition causing it rectified.

1.3.3.2 Interstitial condensation

Interstitial condensation occurs within the thickness of a building component due to the difference in air pressure across the component. The internal air often has more moisture content, i.e. more humidity ratio than the external air especially in periods of cold weather. Therefore, the pressure of the internal air becomes higher. This pressure potential makes the internal air permeate within the structure towards the outer atmosphere. If this air meets a cold area within the structure, it discards some of its moisture content inside the structure.

Most buildings materials are to some extent permeable and allow the diffusion of the moisture-laden air through them. This air will cool as it moves through the structure and may eventually cool below its dew point. This scenario becomes very likely if the building structure is faced externally with an impermeable layer. This impermeable layer will resist vapour movement to the external atmosphere. As a result, condensation dampens the insulation of the structure and impairs its thermal properties. The moisture is also likely to render ineffective any insulation inside the component. This can have disastrous effects on the carefully calculated thermal efficiency of the building shell. It is likely, also, to further aggravate the condensation problem [1.17].

In this project the focus will be only on surface condensation on double glazed windows. Therefore, in the following sections there will be no mention to other types of buildings condensation. Moreover, only a temperate climate will be considered as it is the prevailing climate of the UK.

1.3.4 The causes of surface condensation

Condensation results from a series of relatively simple and well understood physical factors. Its occurrence should, therefore, be thoroughly predicted. The factors that effect the formation of condensation are as follows.

1.3.4.1 The effect of infiltrated external air

In cold weather, the temperature of the external air is usually so cold that its moisture content is very low even if its relative humidity is 100%. This phenomenon may be seen on a psychrometric chart. Thus, if very cold air infiltrates inside the building, the moisture increase within the building will be insignificant. Therefore, it is safe to say that this factor can be ignored in cold weather.

Another temporary phenomenon called "warm weather condensation" is worth mentioning. When there is a sudden change from cold to warm humid weather, there will be a short period when condensation can form on cold structural surfaces until they have had a chance to warm up. It usually affects high thermal capacity structures. Such structures are very slow to respond to the increase in temperature.

The amount of rainfall does not affect the risk of condensation. External humidity in temperate climates (with the exception of warm weather condensation) has little influence on internal condensation [1.17].

1.3.4.2 The effect of internal air

The internal humidity is the most important factor in condensation occurrence. Considerable amounts of water vapour are generated within dwellings by the occupants and their activities. It has been estimated [1.17] that four persons living in a house for 12 hours will, merely by the process of breathing, add 2.5 kg of water vapour to the internal air. An average person engaged in sedentary activities will exhale more than a litre of water vapour in 24 hours. More energetic activities can increase this amount by up to four times. Typical family activities, e.g. breathing, cooking, washing and drying clothes produce about 12 litres of water vapour per day. Flueless heating appliances (paraffin and gas heaters) that depend on combustion to produce their heat are particularly prolific producers of water vapour. Natural gas produces 1.5 kg of moisture for each m^3 burned, and paraffin produces 1.3 kg of moisture for each kg of paraffin.

In dwellings, kitchens and bathrooms are considered the most intensive moisture producers. To reduce the risk of condensation in dwellings, building professionals should provide means for preventing the moisture from spreading to other dwelling areas and to exhaust the water vapour near its source.

The most susceptible parts of a dwelling to condensation are those areas which are not heated or inadequately heated. Heating of a building is important in many respects. Firstly, internal warm air can carry more water vapour than cold air. Therefore water vapour which cold air cannot carry will be suspended in the warm air instead of being condensed on building furniture and structure. The moisture-laden air can then be removed by ventilation. Secondly, if heating of a building is supplied in consistent levels, it will keep the internal surfaces warm and above dew point. Intermittent heating, i.e. switching the heating systems off during periods of unoccupancy and sleeping times and switching them on during habitation hours will increase the condensation rate.

1.3.4.3 The effect of ventilation

In temperate climates, the outdoor air is likely to be at lower moisture content than the indoor air. Therefore, it is theoretically possible to avoid all condensation by adequate ventilation.

In the past, dwellings were naturally ventilated by means of less well-fitted doors and windows, suspended floors, flues or chimneys. New construction techniques, i.e. "build tight strategy", typically reduces natural ventilation. Opening windows and doors is being discouraged because of anticipated increased energy costs. In addition, occupants are sensitive to the discomfort of drafts created especially by open windows.

The paradox that faces building professionals nowadays is that, on the one hand, the greater the ventilation, the greater the heat necessary to replace that which is lost by ventilation, and consequently the greater the cost, especially with the presently high prices of fuel. On the other hand, the less the ventilation and the heat input to the building, the more likely the condensation occurrence.

Ventilation should be consistent throughout the whole building. In combination with that, windows should have ventilators. These ventilators provide a controlled amount of fresh air in small but adequate quantity which circulates around the window area keeping condensation at a minimum.

1.3.4.4 The effect of room surface temperature

Surface condensation will occur if the temperature of the surfaces of the internal space falls below the dew point of the neighbouring air. Therefore, internal surface temperature should be maintained within a few degrees below the internal air temperature. This is also a requirement for thermal comfort as for humans to be thermally comfortable surface temperature should never fall more than 5 °C below the air temperature [1.17].

To completely eliminate the risk of surface condensation, consistent, standard levels of temperature throughout the building and the internal air should be maintained. Also, the building shell has to have reasonable levels of thermal insulation. However, surface condensation may occur in areas where cold-bridging is possible across the structure of the building such as lintels over openings, walls and ceilings adjacent to balcony overhangs, edges of ground floors next to earth, etc. These areas may increase the overall U-value of a building. Due to the lower temperature resulting from cold-bridging at these areas, local condensation may occur.

Adequate insulation can minimise the risk of surface condensation by maintaining the surface temperature at a reasonable level. However, no amount of thermal insulation can make an unheated room warm. Insulation must always be complemented with a reasonable heating system if its effectiveness is to be realised.

1.3.5 Mould growth

The growth of mould is one of the inevitable consequences of condensation. Mould growth can occur if relative humidities remain consistently above 70%, even if there is no apparent liquid condensation. If the relative humidity exceeds 80%-90% for long periods mould growth is certain to occur [1.17].

Mould growth can be prevented by controlling the physical factors giving rise to condensation. However, direct chemical treatment, e.g. fungicidal washes and paints is required. Wallpaper adhesives may also be used to control mould growth. Mould treatment is expensive and cannot cure condensation problems without rectifying the causes resulting in these problems.

1.3.6 The avoidance of condensation

Condensation is very much related to the way in which buildings are heated, ventilated and insulated. By control of temperature and air movement, much of the inconvenience of condensation can be prevented. In any consideration of the thermal performance of a

building shell, it is essential to consider condensation as a very vital factor because, in extreme circumstances, it may cause structural collapse.

Condensation problem should be seriously addressed during the initial design of a dwelling by taking into consideration the following points:

- The provision of well insulated walls and roofs where building regulation standard U-value for walls should not exceed 0.5 W/m^2K [1.17]. If the thermal insulating levels required by the building regulations were met, it would be unlikely that surface condensation would occur in most normal building types.

- Intermittent heating should be avoided in houses with high thermal capacity walls. Despite the good thermal insulation properties of such walls, they require a long time to warm up to suitable temperatures. Buildings of high thermal capacity walls require a standard heating level throughout the heating period. If intermittent heating of a dwelling house is desirable then the structure should be of low thermal capacity or of medium to high thermal capacity with a low thermal capacity lining [1.17]. Walls with light weight capacity warm up more quickly and surface temperature soon rises above the dew-point.

- Adequate means for the removal of moisture from within the house by ventilation must be provided, especially in houses having no flues. Moist air should be removed at source, in kitchen, bathroom or shower and should not be allowed to move to cooler areas such as bedrooms. The air extraction can be done either by natural means through open windows or other vents, or mechanically by fitting an extraction fan.

1.4 Aim of the present project

The first step in analysing any surface condensation problem is to know the temperature of the surface being investigated. The temperature of the indoor pane of any multiple-

glazed window is normally assumed constant and referred to as the centre-glazing temperature. This assumption does not represent the real situation of the inner pane. It leads to erroneous assessment of condensation occurrence and quantity. It has been proven that there is a longitudinal temperature variation along the height of the inner pane of double glazed window. This stratification in temperature is the result of the heat transfer mechanism through windows. The aim of this project is to develop physical models for the temperature stratification along the height of double glazed windows. Based on these models, a spreadsheet-based software is developed to assess the frequency of condensation occurrence on any double glazed window.

The main objective of this research project is to provide building professionals with tools that enable them to calculate temperature along the inner pane height and to predict the condensation occurrence on double glazed windows. Furthermore, solutions are presented to help designers towards developing windows with suppressed condensation. The following work programme was undertaken as a means of achieving the above stated aims.

1. A rigorous literature review on the circulation of the infill gas within the cavity of double glazed window and its effect on the temperature distribution on window components.

2. A study of the effects of the edge-seal and frame conduction on double glazed window and its effect on condensation occurrence on windows. An experimental programme of the measurements of external and internal ambient temperatures, window glass temperatures, relative humidity, and wind speed, both in laboratory and in-situ, was undertaken in this respect.

3. Physical and mathematical model development and the use of software applications for analysing the temperature stratification along a window height was undertaken. The models were based on the experimental data obtained via activity undertaken in task 2 (see above).

4. The development of a three-dimensional model for analysing temperature distribution on the entire surface of the inner pane of double glazed windows.

5. The development of a model for assessing the nocturnal temperature drop inside a building subjected to a given daytime heating schedule.

6. The development of spreadsheet-based software for the estimation of the frequency of occurrence of condensation on double glazed windows.

The first, second, third and fourth tasks mentioned above will be addressed in Chapters 2, 4, 5 and 6 respectively. Chapter 3 provides a detailed background on the elementary theory of heat transfer from building surfaces in general and from double glazed windows in particular. Chapters 4, 5, 6 and 7 contribute to the end goal of developing a model for the assessment of frequency of condensation occurrence on double glazed windows.

References

1.1. ASHRAE handbook, 1985 Fundamentals, Section II, Chapter 8

1.2. K.C. Parsons, Human thermal environments: the effects of hot, moderate and cold environments on human health, comfort and performance, Taylor and Francis Ltd, London, UK, 1993

1.3. P. O. Fanger, Thermal comfort, McGraw-Hill Book Company, pp 244, New York, 1973

1.4. Pilkington Glass Ltd.: D. Button et al, Glass in building: A guide to modern architectural glass performance, Butterworth Archeticture, 1993

1.5. T. Muneer and B. Han, Use of CFD for thermal analysis of double glazings: computational methods and experimental measurements VII, 77-84, Eds: G. M. Carlomagno and C. A. Brebbia, Computational Mechanics Publications, UK, 1995

1.6. Department of Trade and Industry, Digest of the United Kingdom Energy Statistics-1997, HMSO, London, 1997.

1.7. O. Aschehoug and J. Baker, Frame and edge-seal technology - an international view, Proceedings of the Window Innovations'95 conference, Canada (5-6 June 1995)

1.8. B. Gerber, Tages-Anzeiger, Switzerland, "All Energy Technology Affects Our Climate - Not All to the Same Extent", Centre for the Analysis and Dissemination of Demonstrated Energy Technology, CADDET Energy Efficiency Newsletter, No. 2, pp 20-21, June 1995

1.9. B. Han, Investigation of thermal characteristics of multiple glazed windows, PhD Thesis, Napier University,1996

1.10. C. M. Harris, Noise control in buildings: a practical guide for architects and engineers, McGraw-Hill, Inc., New York,1994

1.11. D. J. Croome, Noise and the design of buildings and services, Construction Press, England, 1982

1.12. R. McMullan, Noise Control in Buildings, BSP Professional Books, Part 1, Noise, pp 11, UK, 1991

1.13. S. Carpenter, "New Technology, New Standards: Changing the Design of Canadian Windows", Conference Proceedings, Window Innovations'95, Toronto, Canada, pp 13-20, 5-6 Jun 1995

1.14. T. E. Johnson, Low-E Glazing Design Guide, Butterworth Architecture, USA, 1991

1.15. Glass Magazine, pp 70, December, 1988

1.16. A. Oliver, Dampness in Buildings, BSP Professional Books, London, England, 1988

1.17. P. Marsh, Thermal Insulation and Condensation, The Construction Press, New York, USA, 1979

2 Review of Previous Work

2.1 Introduction

This chapter reviews previous work on the following topics:

- The circulation of the infill gas within a cavity of a multiple glazed window and its effect on the temperature distribution on the window components [2.1].

- The effects of the edge-seal and frame of a multiple glazed window on its thermal performance [2.2-2.6].

- The study of the condensation phenomenon on multiple glazed windows and its frequency of occurrence [2.7-2.9].

In winter, due to the temperature difference between the inner and outer panes, the infill gas within a double glazed window enclosure flows upward near the indoor glazing and downward near the outdoor glazing. The descending gas becomes progressively colder. At the bottom of the cavity this cold gas turns and approaches the indoor glazing where it starts its ascent. Thus the glass near the bottom edge of the indoor glazing is cooled by cold infill gas and thus becomes susceptible to condensation. It has been proven by the present research work, both experimentally and analytically, that this circulation is responsible for the rise in the temperature along the height of the window's inner pane [2.10-2.12]. Wright and Sullivan [2.1] stated that the flow of the infill gas within the insulated glazing unit cavity contributes to the condensation problem at the bottom edge of the indoor glazing and have shown this to be the case by experimental results and numerical simulation [2.13].

None of the numerical methods currently in use for analysing frame and edge-seal heat loss, such as Refs. [2.14, 2.15], take account of infill gas convection and as such cannot be used to determine the minimum indoor pane temperature required to assess the

condensation occurrence on a window. Local variations in surface temperature can be found using very detailed numerical methods [2.13, 2.16] but this approach is expensive in terms of time, CPU time and hardware required.

Any model attempting to quantify local heat transfer rates in the bottom region of a double glazed window or any model intended to determine the temperature distribution across the face of the glazing must account for both the natural convection of the infill gas and conduction within the edge-seal, glass and frame components.

Wright and Sulivan [2.1] provide a numerical, two-dimensional conduction analysis for the frame and edge-seal which can be extended to account for infill gas motion. Their method requires one initial computational fluid dynamics (CFD) calculation to determine the infill gas flow pattern.

The contribution of the present research is that numerical models have been developed for the heat transfer at the bottom edge of a double glazed window. These models combine the effects of radiative energy exchange between the glass panes, natural convection due to circulating gas and conduction through the edge-seal and frame. This is in contrast to previous work which solely addressed the edge-seal conduction effects [2.3, 2.4].

2.2 Pilkington's method of condensation assessment

In the Environmental Advisory Service [2.7] provided by Pilkington Glass Limited, condensation prediction charts, as shown in Figs. 2.1-2.3 are used to determine whether or not condensation will occur on the inside surface of a window. These charts show the relationship between four parameters, i.e. internal temperature (T_i), external temperature (T_o), internal relative humidity (ϕ), and window thermal transmittance (U-value), at the condensation threshold. The condensation threshold represents the condition at which the window inside surface temperature is the same as the inside atmosphere dew point temperature. These charts are given for sheltered, normal, and severe conditions of the

outdoor exposure. Reference [2.7] also gives charts for tropical situations and for the vertical windows of refrigerated cabinets. Fig. 2.4 shows a condensation prediction diagram for inward heat flow for normal conditions. For the case of air-conditioned buildings in warm climates and for the windows of refrigerated cabinets, the outside pane of the window will be cooled at the bottom and may be subject to condensation.

To use the condensation prediction charts the temperature of the inside surface of the window indoor pane should be determined as follows.

When a steady thermal state is reached in a double glazed window, the heat flux through all the window components is same. For the entire window,

$$q = U(T_i - T_o) = \frac{(T_i - T_o)}{R_T} \qquad 2.1$$

where,

q	heat flux, W/m^2
R_T	overall thermal resistance, m^2K/W
T_i	internal ambient temperature, ^0C
T_o	external ambient temperature, ^0C
U	centre-glazing U-value, W/m^2K

Similar relationships can be applied to the window components to determine the particular surface temperatures (see Fig. 2.5).

$$t_4 = T_i - \frac{R_{si}(T_i - T_o)}{R_T} \qquad 2.2$$

where,

t_4	inner pane room-side temperature at centre-glazing level, ^0C
R_{si}	inside surface resistance, m^2K/W

For a double glazed window, the overall thermal resistance can be written as,

$$R_T = R_{so} + R_{g1} + R_a + R_{g2} + R_{si} \qquad 2.3$$

where,

R_a window cavity resistance, m^2K/W

R_{g1} outside pane thermal resistance, m^2K/W

R_{g2} inside pane thermal resistance, m^2K/W

R_{so} outside surface resistance, m^2K/W

R_{si} and R_{so} are calculated using Equation 2.4.

$$R_s = \frac{1}{\varepsilon \ h_r + h_c} \qquad 2.4$$

where,

ε surface emissivity

h_r radiation heat transfer coefficient, W/m^2K

h_c convection heat transfer coefficient, W/m^2K

R_s surface resistance, m^2K/W

For conventional glasses the emissivity, ε, may be taken as 0.9, but for special glasses may be much lower, of the order 0.1 [2.7]. The radiation coefficient, h_r, evaluates the exchange of energy by radiation between the surface and its surroundings. The radiation coefficient is calculated from the mean surface temperature T_s which is the mean of the surface temperature and the average temperature of its surroundings. The latter can usually be taken to be the same as the air temperature. Therefore, T_s for the inside and the outside surfaces are calculated from Equations 2.5 and 2.6.

$$T_{so} = \frac{1}{2}(T_o + t_1) \qquad 2.5$$

$$T_{si} = \frac{1}{2}(T_i + t_4) \qquad 2.6$$

where,

t_1 outer pane external temperature at centre-glazing level, ^0C

T_{si} inside mean surface temperature, ^0C

T_{so} outside mean surface temperature, ^0C

Once T_s is calculated h_r can be determined using Fig. 2.6. This figure is for a surface with unit emissivity and the value obtained must be multiplied by the emissivity of the surface.

The convection coefficient h_c relates to the heat transfer to or from the adjacent air. h_c for outdoor surfaces where there is appreciable air movement is obtained from Equation 2.7.

$$h_c = 5.8 + 4.1V_w \qquad 2.7$$

where V_w is the wind speed in metres per second. Equation 2.7 is recommended by CIBSE for wind speeds greater than 0.1 m/s. For indoor surfaces, where the only air movement is that due to convection currents, h_c is taken as 3.0 W/m^2K for vertical windows as recommended by CIBSE Guide [2.6].

Glass panes thermal resistances R_{g1} and R_{g2} can be calculated using Equation 2.8.

$$R_g = \frac{L_g}{k_g} \qquad 2.8$$

where k_g is the glass thermal conductivity and is taken as 1.0 W/mK for all building glasses. L_g is the thickness of the glass in metres.

The calculation procedure of R_a is the same as that of the surface resistance. The radiation and convection coefficients for the air space h_{ra} and h_{ca} respectively must firstly be determined and then substituted into Equation 2.4 to obtain R_a. Referring to Fig. 2.5, the mean of the air space surface temperatures is,

$$T_a = \frac{1}{2}(t_2 + t_3) \qquad 2.9$$

where,

t_2 outer pane cavity-side temperature at centre-glazing level, ^0C

t_3 inner pane cavity-side temperature at centre-glazing level, ^0C

The value of T_a obtained from Equation 2.9 can then be applied in Fig. 2.6 to obtain h_{ra}. The value for h_{ra} must be multiplied by the effective emissivity ε_{eff} of the two surfaces where,

$$\varepsilon_{eff} = \frac{1}{\frac{1}{\varepsilon_2} + \frac{1}{\varepsilon_3} - 1} \qquad 2.10$$

The convection coefficient of air space h_{ca} depends on the width and inclination of the air space, the temperature of its surfaces, and the direction of heat flow. Reference [2.7] gives figures to obtain h_{ca} values. The data given in these figures are for a mean air space temperature of 10 °C. They can be corrected for other temperatures using Equation 2.11, if the air space is narrow and the contribution of convection is consequently small, or using Equation 2.12, if the air space is wide and convection is important [2.7].

$$(h_{ca})_{T_a} = (h_{ca})_{10}[1 + 0.00306(T_a - 10)] \qquad 2.11$$

$$(h_{ca})_{T_a} = (h_{ca})_{10}[1 - 0.0028(T_a - 10)] \qquad 2.12$$

Equations 2.2-2.12 are recommended by Pilkington [2.7] for determination of the inside pane temperature, t_4, of a double glazed window. This temperature is then compared to the dew-point temperature of the inside air to decide whether or not condensation occurs on the surface of the inner pane. Thus if any three of the four parameters upon which condensation prediction charts are based are given, the fourth parameter value at which the threshold of condensation occurs can be determined.

This temperature, t_4, is sometimes called the centre-glass temperature and is used to represent the temperature of the whole inner pane. The present research work has shown, by measurements and calculations, that there is a temperature stratification on the inner pane and that the circulation of infill gas within the window cavity is the main factor responsible for this stratification. This result means that the assumption that the temperature of the whole inner pane can be taken as the centre-glass temperature is erroneous. Actually condensation will be initiated at the bottom edge of the inner glass, being the coldest part, and then extend upward as the inside relative humidity increases and/or the outside air temperature decreases.

2.3 ASHRAE procedure for U-value determination

Fenestration (any glazed aperture in a building envelope) usually consists of glazing material, frame and shading system. The total rate of heat transfer through a fenestration system can be calculated knowing the separate heat transfer contributions of the centre-glass, edge-seal, and frame. Using area-weighted U-values for each contribution, ASHRAE Fundamentals Handbook [2.6] provides Equation 2.13 for the calculation of the overall U-value of a fenestration.

$$U_o = (UA_{cg} + U_{eg}A_{eg} + U_fA_f) / A_{pf} \qquad 2.13$$

where,

A_{cg} projected area of glazing, m^2

A_{eg} projected area of edge-seal, m^2

A_f projected area of frame, m^2

A_{pf} projected area of the entire fenestration, m^2

U centre-glass U-value, W/m^2K

U_{eg} edge-of-glass U-value, W/m^2K

U_f frame U-value, W/m^2K

U_o overall U-value of the window, W/m^2K

The centre-glass U-value depends on the number of glazing panes, the gas-space dimensions, the orientation relative to vertical, the emittance of each surface, and the composition of the infill gas [2.6].

Spacers in multipane units greatly increase conductive heat transfer between the contacted inner and outer glazing. This phenomenon is called cold-bridging. It degrades the thermal performance of the glazing unit locally. Laboratory measurements have shown that the conductive region of edge-seal is limited to a 65 mm wide band around the perimeter of the glazing unit [2.6]. ASHRAE Fundamentals Handbook [2.6] provides Equation 2.14 for the calculation of the edge-of-glass U-value as a function of spacer type and centre-glass U-value.

$$U_{eg} = A + BU + CU^2 \qquad 2.14$$

where A, B, and C are correlation coefficients, which are listed in Table 2.1 for metal, insulating (including wood) and fused glass spacers, and a combination of insulating and metal spacers.

Table 2.1 Coefficients for edge-of-glass U-value. Ref. [2.6]

Spacer Type	A	B	C
Metal	1.266	0.842	-0.027
Insulating	0.681	0.682	0.043
Glass	0.897	0.774	0.010
Metal + Insulating	0.769	0.706	0.033

Approximate edge-of-glass U-values as a function of the centre-glass U-value for various types of spacers (e.g. aluminium spacers with sealants, insulating spacers including fibreglass, wood, and butyl) are quoted in Ref. [2.6].

Frame U-values for a variety of frame and spacer materials and glazing unit thickness are given in Ref. [2.6].

Estimating the rate of heat transfer through the frame [2.6] is complicated by:

1. the variety of fenestration products and frame configurations.
2. the different combinations of the materials used for frames.
3. the different sizes available in residential and commercial applications.
4. the glazing unit width and spacer type.

Equation 2.13 can be used to estimate the overall U-value of any window. This equation shows that there are significant effects of the edge-seal and frame on the heat flow through the window. Thermally poor edge-seals and frames may increase the heat loss through the window and impair its overall U-value and, moreover, reduce the temperature in the vicinity of the edge-seal substantially, thus increasing the possibility of condensation occurrence on the inner pane.

2.4 Edge-seals

The thermal performance of double glazed windows has recently seen dramatic improvements, with improved glass coatings and infill gases. Greater improvements can be achieved with the advent of evacuated glazing and the low pressure monolithic aerogel glazing with centre-glass U-values in the range of 0.3 - 0.8 W/m^2K [2.2]. These improvements should be accompanied by a parallel development in edge-seal and frame technology. Due to their cold bridge effect, thermally poor spacers can very markedly affect the performance of multiple glazed windows.

The most widely used spacers in multiple glazed units fall in one of the following classes:

1. aluminium spacer
2. steel spacer
3. metal spacer with thermal break
4. fibreglass / plastic spacer
5. butyl spacer
6. foam spacer

The products most commonly used in Europe are either hollow aluminium extrusions or roll-formed galvanised steel sections.

Aschehoug and Baker [2.2] measured the centre-glass and edge-seal U-values for different window configurations as shown in Tables 2.2 and 2.3. They found that as the centre-glass U-value decreases the edge-seal U-value also decreases but not at the same rate. This can be illustrated by considering a particular example. The edge-seal U-value for double glazed window with a metal spacer is 22% greater than the centre-glass, but for the quadruple glazing the edge is 187% greater than the centre.

Table 2.2 Typical centre-glass U-values for conventional high performance glazing. Ref. [2.2]

Glazing System	Centre-glass U-value (W/m^2K)
double glazing, air filled	2.78
double glazing, low-e, air filled	1.99
double glazing, low-e, argon filled	1.70
triple glazing, air filled	1.76
triple glazing, low-e, air filled	1.36
triple glazing, low-e, argon filled	1.19
quadruple glazing, low-e, krypton filled	0.62

Table 2.3 Typical edge-seal U-values for conventional high performance glazing. Ref. [2.2]

Glazing System	Metal Spacer Edge-glass U-value (W/m^2K)	Insulated Spacer Edge-glass U-value (W/m^2K)
double glazing, air filled	3.40	2.91
double glazing, low-e, air filled	2.83	2.21
double glazing, low-e, argon filled	2.62	1.97
triple glazing, air filled	2.67	2.02
triple glazing, low-e, air filled	2.36	1.69
triple glazing, low-e, argon filled	2.23	1.56
quadruple glazing, low-e, krypton filled	1.78	1.12

Aschehoug and Baker [2.2] also measured the frame U-values for different window configurations. Such experimental results are shown in Table 2.4. this table shows that the frame U-values are generally greater than the centre-glass U-values shown in Table 2.2.

Table 2.4 Typical frame U-values for conventional windows. Ref. [2.2]

Frame Material	Spacer Type	Frame Type/Number of Panes					
		Operable			Fixed		
		Single	Double	Triple	Single	Double	Triple
Aluminium	Aluminium	12.4	12.4	12.4	10.1	10.1	10.1
Aluminium with thermal break	Aluminium	5.4	5.4	5.4	6.6	6.6	6.6
	Insulated	-	4.9	4.9	-	5.2	5.2
Aluminium Clad Wood, Reinforced Vinyl	Aluminium	3.9	3.6	3.3	3.2	3	2.8
	Insulated	-	3.2	2.7	-	2.6	2.3
Wood, Vinyl	Aluminium	3.1	2.9	2.7	2.9	2.8	2.7
	Insulated	-	2.6	2.2	-	2.4	2.1
Fibreglass	Aluminium	2.7	2.5	2.3	2.6	2.3	2
	Insulated	-	2.2	1.8	-	2.1	1.6

Wakili and Frank [2.5] measured the equivalent thermal conductivity of different spacers where a number of identical spacers were used between two sheets of glass and tested in a hot-plate apparatus. Some results are shown in Table 2.5.

Table 2.5 Measured equivalent thermal conductivities for some commercially available spacers. Dimensions as reported in Ref. [2.2]

Spacer Type	Thermal Conductivity, W/mK
Aluminium 12 mm	1.35
Steel 20 mm	1.07
Stainless steel	0.37
ABS 15 mm + alufoil	0.52
Polycarbonate + alufoil	0.50
Butyl 12 mm	0.63
Foam 12 mm	0.20

Although the thermal conductivity of the aluminium spacer (best conductor) is much higher than the foam spacer (best insulator), the U-value improvement for the foam spacer over the aluminium spacer is in the order of 0.1-0.2 W/m^2K for most types of frames and glazings [2.2]. Using a more insulative spacer helps in increasing edge zone temperatures on the inside side, thus significantly reducing the risk of condensation.

The same procedure was used by Svendsen and Fritzel [2.3] who investigated the effect of different spacers on the total U-value of highly insulating windows by determining the thermal conductivity of each spacer by experiments and by calculations. The spacers under investigation, e.g. aluminium, stainless steel and silicon foam with metal foil have been tested with the same double glazed window (4+12argon+E4). The thermal conductivity of the edge-seal for each case was calculated using a computer program called FRAME [2.15] and these calculations were verified by means of measurements using a guarded hot-box thermal conductivity apparatus. During measurements, the temperature levels were held at 0 ^0C on the cold side and 20 ^0C on the warm side.

Temperatures along the warm side of the window, in the vicinity of the edge-seal, as shown in Fig. 2.7, were also measured. Equation 2.15 was then fitted to the data.

$$T(x) - T_{e,w} = Y_1\left[1 - \exp\left(-Y_2 x\right)\right] \qquad 2.15$$

where,

x	distance from edge-seal along the inner pane, m (see Fig. 2.7)
T(x)	temperature of glass pane at distance x, K
$T_{e,w}$	temperature of inner pane edge-seal, K
Y_1 and Y_2	constants

This model is based on the use of the temperature gradient on the glass from the edge towards the centre, because the heat flow in the glazing unit near the edge is a measure of the cold bridge effect of the spacer. The spacer and the sealants were considered to be of homogeneous material with an equivalent thermal conductivity. For the calculation it was assumed that the heat flow through the warm glass pane and the edge-seal are identical [2.3].

The linear heat flow through the edge was obtained using Equation 2.16.

$$q_e = k_g L_g \left.\frac{dT(x)}{dx}\right|_{x=0} \qquad 2.16$$

where,

q_e	linear heat flow through the window edge, W/m
$dT(x)/dx_{x=0}$	temperature gradient at edge-seal, K/m

Under the assumption that the edge-seal is homogenous and by knowing q_e, the thermal conductivity of the edge-seal can be obtained using Equation 2.17.

$$k_{edge} = \frac{q_e}{\Delta T_{edge}} \qquad 2.17$$

where,

k_{edge} thermal conductivity of the window edge, W/mK

ΔT_{edge} temperature difference across edge-seal, K (see Fig. 2.7)

The calculated values of thermal conductivity for the three spacers mentioned above were found to be in good agreement with the measured values. Svendsen and Fritzel's work showed that the temperature difference between a glazing edge zone and centre was reduced by using less thermally conductive spacers.

The thermal conductivity of edge-seals as determined by Svendsen and Fritzel [2.3] do not consider all modes of heat transfer involved within the window. Heat is transferred by radiation and also by convection of the surrounding air and of the infill gas within the window cavity. All these modes of heat transfer have been taken into consideration in the temperature distribution models developed later in this research work. Svendsen and Fritzel [2.3] did not investigate the problem of condensation as their concern was to study the effect of spacer type on the window overall U-value. However, it can be concluded that better spacers help increase the temperature on the bottom edge of the inside pane and hence reduce the risk of condensation.

With the aim of improving normal aluminium spacer bars to get better thermal properties for multiple glazed windows (lower overall U-values) and to reduce the surface condensation risk, Frank and Wakili [2.4] used hot box measurements and finite difference calculations to determine the thermal properties of different new spacers by determining the linear thermal transmittance coefficient ψ_g of each spacer. This approach is different from that used previously in Ref. [2.3] where the comparison between different spacers was in terms of the thermal conductivity. Frank and Wakili used a 2-D finite difference model to determine ψ_g for different frame and spacer bar types based on Equation 2.18.

$$U_o = \frac{U\,A_{cg} + U_f A_f + \Psi_g l_g}{A_{cg} + A_f} \qquad 2.18$$

where,

l_g length of inner perimeter of window frame, m

ψ_g linear thermal transmittance due to the combined thermal effects of the spacer, glazing and frame, W/mK

The frame and the centre-glass U-values are independent from each other and, therefore, can be measured or calculated separately.

The following cases were considered by Frank and Wakili [2.4] in their studies:

- three frame types, e.g. wood frame (U_f = 1.5 W/m^{2}K), PCV frame(U_f = 2.2 W/m^{2}K) and metal frame (U_f = 3.2 W/m^{2}K)
- three spacer bars, e.g. Aluminium spacer, stainless steel spacer and foam spacer
- normal and low E coated glass
- air and gas infill
- double and triple units

Tables 2.6-2.8 show the calculated linear thermal transmittance ψ_g obtained by Frank and Wakili [2.4] for the three different spacer bars tested.

Table 2.6 ψ_g-values for aluminium spacer in W/mK. Ref. [2.4]

Glazing U-value W/m^2K	Wood / PVC frame	Metal frame without thermal break	Metal frame with thermal break
DGW* > 2.7	0.04	0.06	0
DGW 2.2	0.05	0.07	0.01
DGW 1.6	0.06	0.08	0.02
DGW 1.0	0.07	0.09	0.03
TGW** > 2.1	0.04	0.06	0
TGW 1.6	0.05	0.07	0.01
TGW 1.0	0.06	0.08	0.02

* Double Glazed Window ** Triple Glazed Window

Table 2.7 ψ_g-values for stainless steel spacer in W/mK. Ref. [2.4]

Glazing U-value W/m^2K	Wood / PVC frame	Metal frame without thermal break	Metal frame with thermal break
DGW > 2.6	0.03	0.04	0
DGW 2.0	0.04	0.05	0.01
DGW 1.4	0.05	0.06	0.02
TGW > 2.0	0.03	0.04	0
TGW 1.4	0.04	0.05	0.01
TGW 0.7	0.05	0.06	0.02

Table 2.8 ψ_g -values for foam spacer in W/mK. Ref. [2.4]

Glazing U-value W/m^2K	Wood / PVC frame	Metal frame without thermal break	Metal frame with thermal break
DGW > 2.2	0.02	0.03	0
DGW 1.3	0.03	0.04	0.01
TGW > 1.7	0.02	0.03	0
TGW 0.8	0.03	0.04	0.01

Introducing new spacer materials such as silicon foam or thin stainless steel profiles can reduce ψ_g by up to 50% and therefore cause a rise of the surface temperatures of the glass edge which will reduce the risk of condensation [2.4]. Frank and Wakili mentioned that ψ_g could be subdivided into frame and glazing components and that the latter has a good linear dependency with the glazing U-value as shown in Fig. 2.8.

2.5 CIBSE approach to frequency of potential condensation

Table 2.9 lists the likely frequency of condensation occurrence for eight locations in the UK for a period of 20 years (1957-76). These locations are Belfast, Birmingham, Cardiff, Edinburgh, Glasgow, London, Manchester, and Plymouth.

The statistics in this table are based on the difference between the dew-point temperature in the middle of the day (mean of values at 09, 12, and 15 GMT) and the mean dry-bulb temperature of the preceding day (mean of hourly values from 00 to 23 GMT). The greatest temperature difference ranged from about 8 °C to about 11 °C at the eight places considered [2.8]. CIBSE Guide [2.8] assumes that the surface temperature of a heavyweight building during the preceding 24 hours to be the same as the mean outside air temperature. The statistics in Table 2.9, therefore, give a guide as to the likely frequency of occurrence of condensation following a rapid rise in atmospheric dew-point. As an example, this table shows that at Edinburgh there were 25 occasions where the daytime dew-point was in the range 5.0 to 5.9 °C higher than the mean dry-

bulb temperature of the preceding calendar day. The likely frequency of condensation occurrence at Edinburgh, during the period from (1957-76), was 934 times with an annual average frequency of 47 times.

CIBSE Guide has also addressed the response of the building walls to changes in the outside atmosphere temperature. Calculations based on a typical structure with brick walls 220 mm thick, normal timber floors, plasterboard ceilings, and a ventilation rate of one air-change per hour, show that if the outside dry-bulb temperature, following a period of steady temperature, rises at constant rate, the temperature of the inside surface of the walls will, after 12 hours, increase by less than one-quarter of the rise in the outside air temperature. Condensation will occur on the walls, but at only 20% of the possible rate because the low rate of ventilation limits the amount of water vapour available. Increasing the rate of ventilation will cause a corresponding increase in condensation.

The results listed in Table 2.9 for the frequency of condensation occurrence at different locations in the UK are based on the assumption that a heavyweight building, due to its thermal capacity, will maintain the same temperature as the mean temperature of the preceding day. When this temperature falls below the atmosphere dew-point, condensation will occur on the outside surface of the building. The CIBSE approach to the condensation problem does not take into consideration the condensation occurrence on the internal surfaces of a building which is most likely to be the case in the UK.

Table 2.9 Number of occasions in 20 years when dew-point temperature exceeds the preceding day's dry-bulb temperature by the amount indicated. Period (1957-67). Ref. [2.8]

Temperature Difference, °C	Belfast	Birmingham	Cardiff	Edinburgh	Glasgow	London	Manchester	Plymouth
0.0 - 0.9	446	431	520	400	151	355	289	654
1.0 - 1.9	296	259	355	248	108	261	206	359
2.0 - 2.9	139	159	154	140	59	159	118	153
3.0 - 3.9	88	76	89	72	43	52	54	57
4.0 - 4.9	45	40	40	34	21	45	19	36
5.0 - 5.9	27	29	17	25	14	18	14	13
6.0 - 6.9	8	10	6	5	6	11	5	7
7.0 - 7.9	5	6	2	9	2	3	1	2
8.0 - 8.9	2	0	1	0	1	3	2	0
9.0 - 9.9	0	0	0	0	2	1	0	1
10.0 - 10.9	1	2	0	0	0	1	0	0
11.0 - 11.9	0	0	0	1	0	0	0	0
Total Frequency	1057	1012	1164	934	407	909	708	1282
Annual Average Frequency	53	51	58	47	20	45	35	64

Table 2.9 Number of occasions in 20 years when dew-point temperature exceeds the preceding day's dry-bulb temperature by the amount indicated. Period (1957-67). Ref. [2.8]

Temperature Difference, °C	Belfast	Birmingham	Cardiff	Edinburgh	Glasgow	London	Manchester	Plymouth
0.0 - 0.9	446	431	520	400	151	355	289	654
1.0 - 1.9	296	259	355	248	108	261	206	359
2.0 - 2.9	139	159	154	140	59	159	118	153
3.0 - 3.9	88	76	89	72	43	52	54	57
4.0 - 4.9	45	40	40	34	21	45	19	36
5.0 - 5.9	27	29	17	25	14	18	14	13
6.0 - 6.9	8	10	6	5	6	11	5	7
7.0 - 7.9	5	6	2	9	2	3	1	2
8.0 - 8.9	2	0	1	0	1	3	2	0
9.0 - 9.9	0	0	0	0	2	1	0	1
10.0 - 10.9	1	2	0	0	0	1	0	0
11.0 - 11.9	0	0	0	1	0	0	0	0
Total Frequency	1057	1012	1164	934	407	909	708	1282
Annual Average Frequency	53	51	58	47	20	45	35	64

Normally, the dew-point inside the building is higher than that outside the building due to water generating activities inside the building. Furthermore, the dry-bulb temperature inside the building is higher than that outside the building (this is the design condition in the UK). Actually, it is very complex to study the condensation occurrence inside buildings due to the unavailability of models that give an assessment of the dry-bulb and dew-point temperatures of the air inside buildings. This task has been one of the objectives of this research work. Chapter 7 provides a model for the assessment of the internal air temperature at dawn providing that the outside air temperature is known.

Buildings consist of different fabrics, e.g. walls, floors, windows, etc. Each fabric reacts to the changes in the inside and outside conditions in a different manner due to the fabric's thermal resistance. Thermally, windows are considered the weakest fabrics in a building. Therefore, the inside surface of a window will suffer lower temperatures and hence will be more susceptible to condensation. The present research, however, has thoroughly investigated the frequency of condensation occurrence on double glazed windows in three locations in the UK, e.g. Edinburgh, Manchester, and London for a period of ten years (1980-89). This investigation was based on the models for calculating the temperature distribution on double glazed windows developed in Chapters 5 and 6 and the model for calculating the internal air temperature developed in Chapter 7.

References

2.1 J. L. Wright and H. F. Sullivan, A simplified method for the numerical condensation resistance analysis of windows, Proceedings of the Window Innovations'95 conference, pp 429-438, (5-6 June 1995), Toronto, Canada

2.2 O. Aschehoug and J. Baker, Frame and edge-seal technology - an international view, Proceedings of the Window Innovations'95 conference (5-6 June 1995), Toronto, Canada

2.3 S. Svendsen and P. Fritzel, Spacers for highly insulating windows, Proceedings of the Window Innovations'95 conference, pp 90-97, (5-6 June 1995), Toronto, Canada

2.4 T. Frank and K. G. Wakili, Linear thermal transmittance of different spacer bars, Proceedings of the Window Innovations'95 conference, pp 253-259, (5-6 June 1995), Toronto, Canada

2.5 K. G. Wakili and T. Frank, Thermal conductivity measurements on glass, sealants and spacer materials using a symmetrically arranged heat flow meter apparatus, Document T18/B8/CH1/93, IEA Solar heating and cooling programme Task 18, Switzerland, 1993

2.6 ASHRAE Handbook Fundamentals, American Society for Heating, Refrigeration, and Air Conditioning Engineers, Atlanta, USA, 1993

2.7 Pilkington Glass Limited, The Environmental Advisory Service, Calculating thermal transmittance, St. Helens, UK, 1981

2.8 CIBSE Guide A2, Chartered Institution of Building Service Engineers, London, 1982

2.9 Pilkington Glass Limited, Windows and Environment, Pilkington environmental advisory service, 1969

2.10 T Muneer, N Abodahab, and B Han, Gas flow in double glazing enclosures and its effect on longitudinal temperature variation, Proceedings of the Advances in Fluid Mechanics (AFM'96) Conference (New Orleans: USA, 11-13 June 1996). Computational Mechanics Publications (UK: Southampton, 1996)

2.11 N. Abodahab and T. Muneer, Free convection analysis of a window cavity and its longitudinal temperature profile, Energy Conversion and Management, Vol. 39, No. 1, London, England, 1997

2.12 T Muneer, N Abodahab, and A Gilchrist, Combined conduction, convection, and radiation heat transfer model for double glazed windows, Building Services Engineering Research & Technology (BSER&T), Vol. 18 No. 4, London, England, 1997

2.13 J. L. Wright and H. F. Sullivan, A 2-D numerical model for glazing system thermal analysis, ASHRAE Transactions, Vol. 101, Pt.1, 1995

2.14 ASHRAE, 1993 ASHRAE handbook - 1993 Fundamentals, Atlanta: American Society of Heating, Refrigeration and Air Conditioning Engineers, Inc.

2.15 Enermodal Engineering Ltd., Frame: a finite difference computer programme to evaluate thermal performance of window frame systems- version 2.0, 1989

2.16 D. Curcija and W. P. Goss, Two dimensional finite element model of heat transfer in complete fenestration systems, ASHRAE Transactions, Vol. 100, Pt. 2,1994

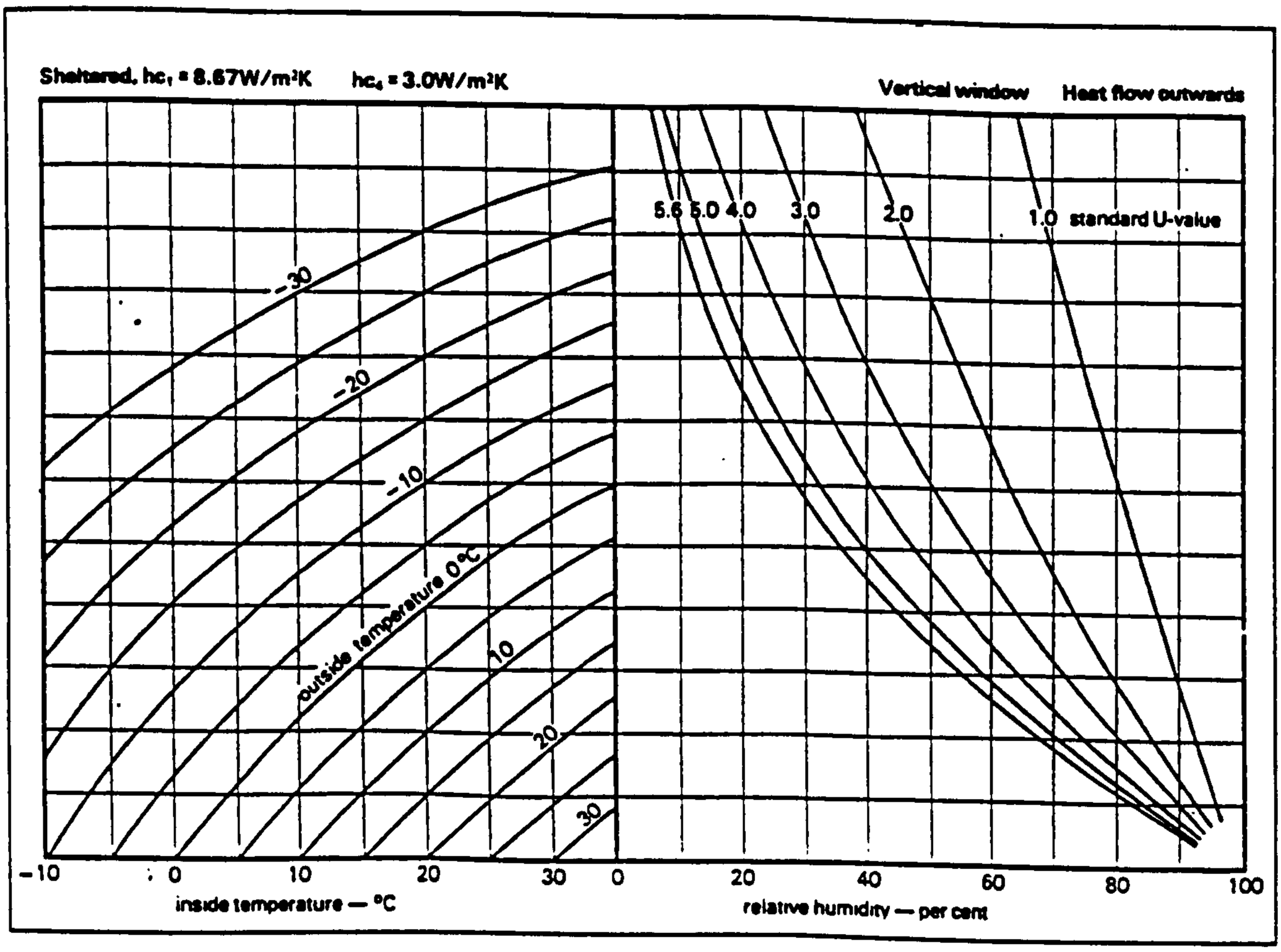

Figure 2.1 Condensation prediction diagram for sheltered exposure. Ref. [2.7]

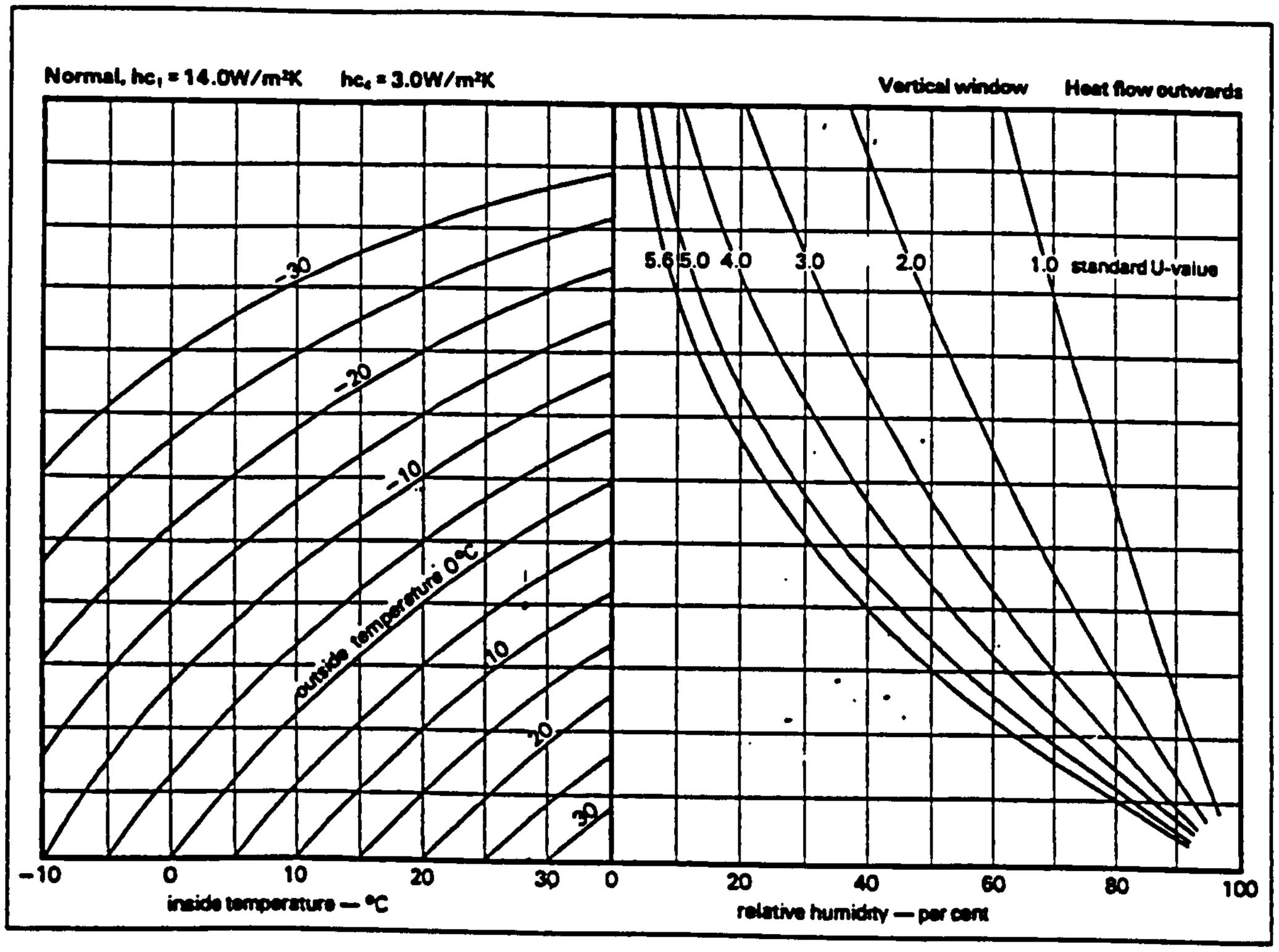

Figure 2.2 Condensation prediction diagram for normal exposure. Ref. [2.7]

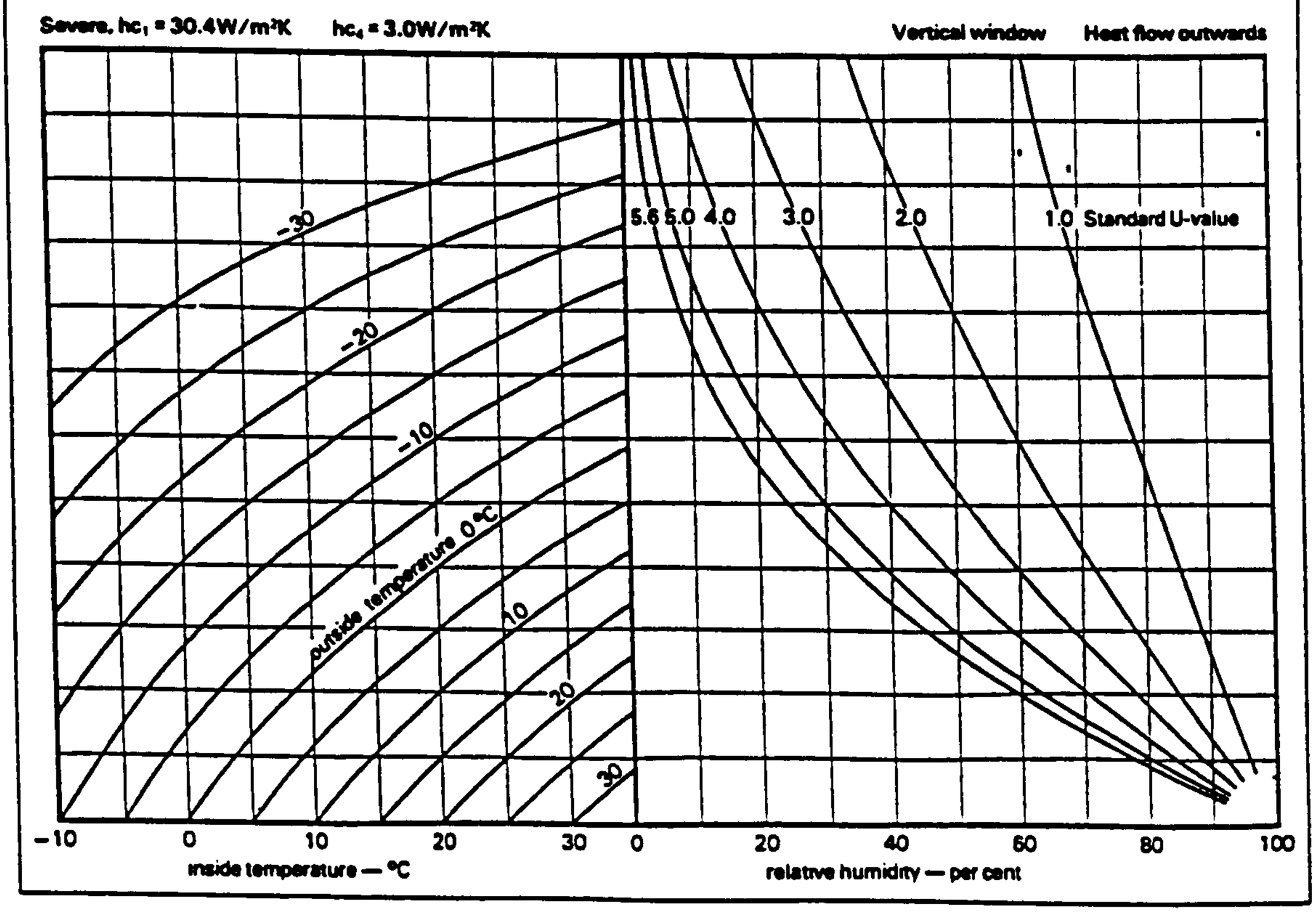

Figure 2.3 Condensation prediction diagram for severe exposure. Ref. [2.7]

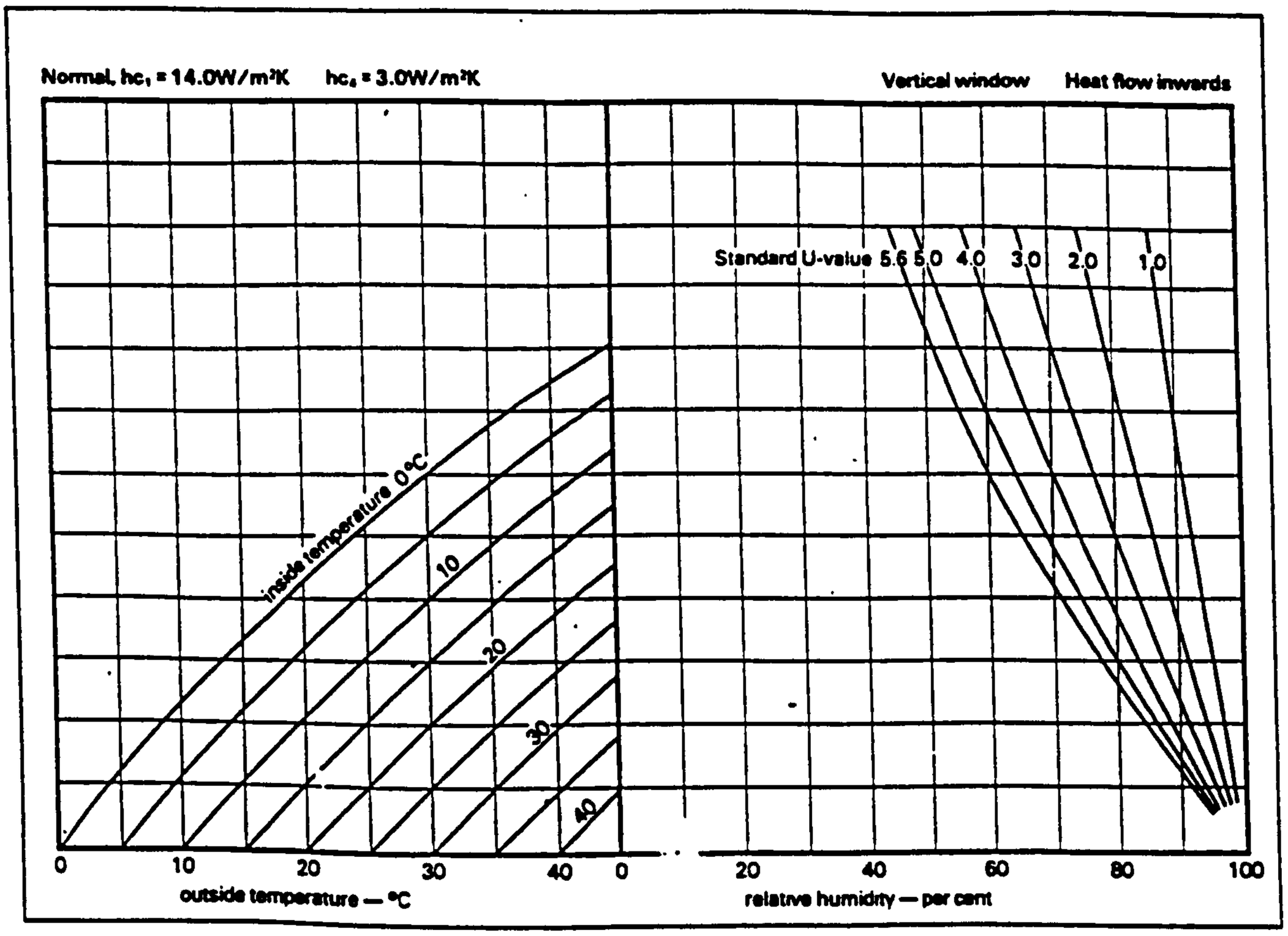

Figure 2.4 Condensation prediction diagram for inward heat flow. Ref. [2.7]

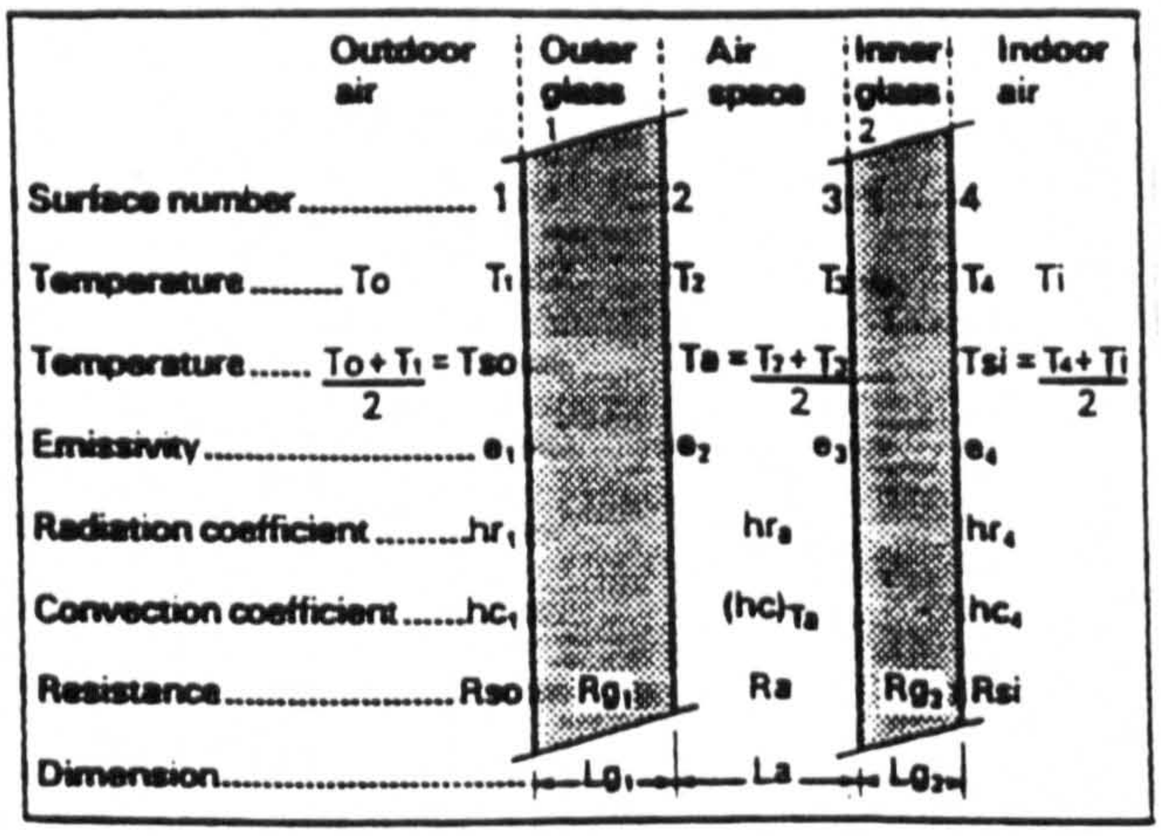

Figure 2.5 Pilkington's nomenclature. Ref. [2.7]

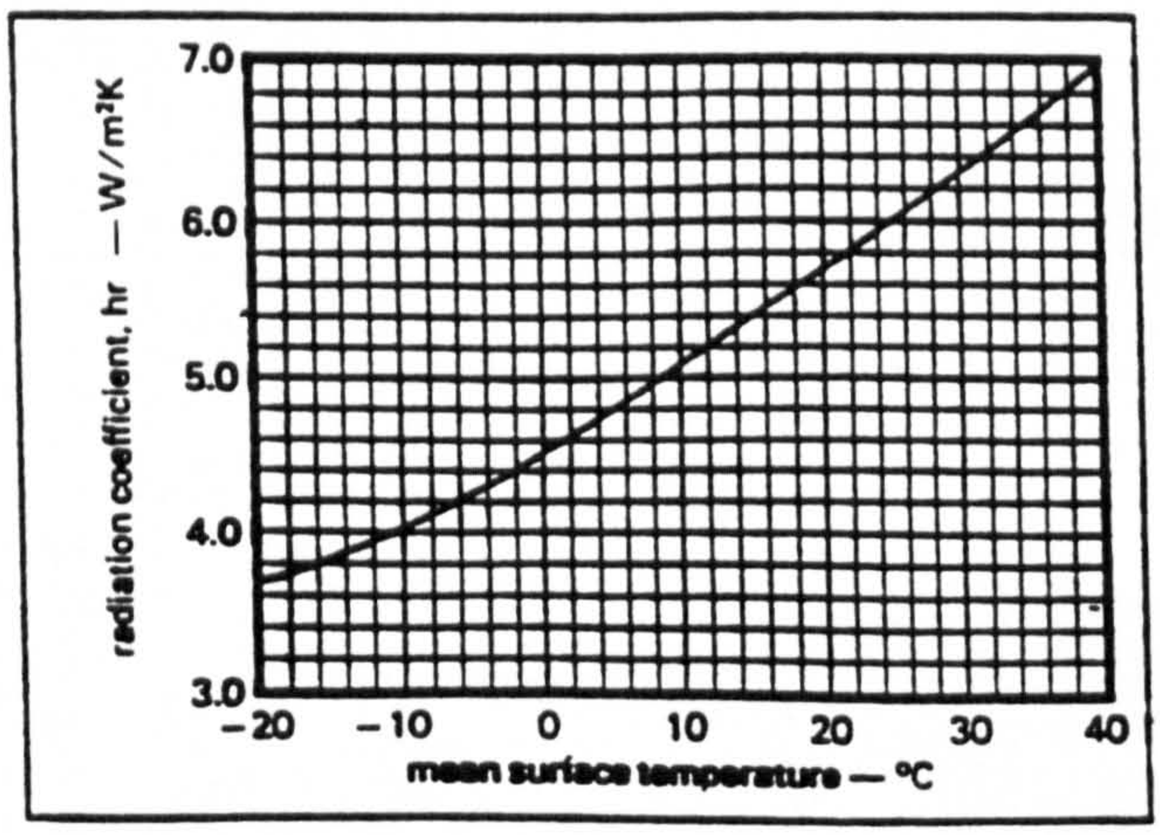

Figure 2.6 Radiation coefficient (emissivity = 1.0). Ref. [2.7]

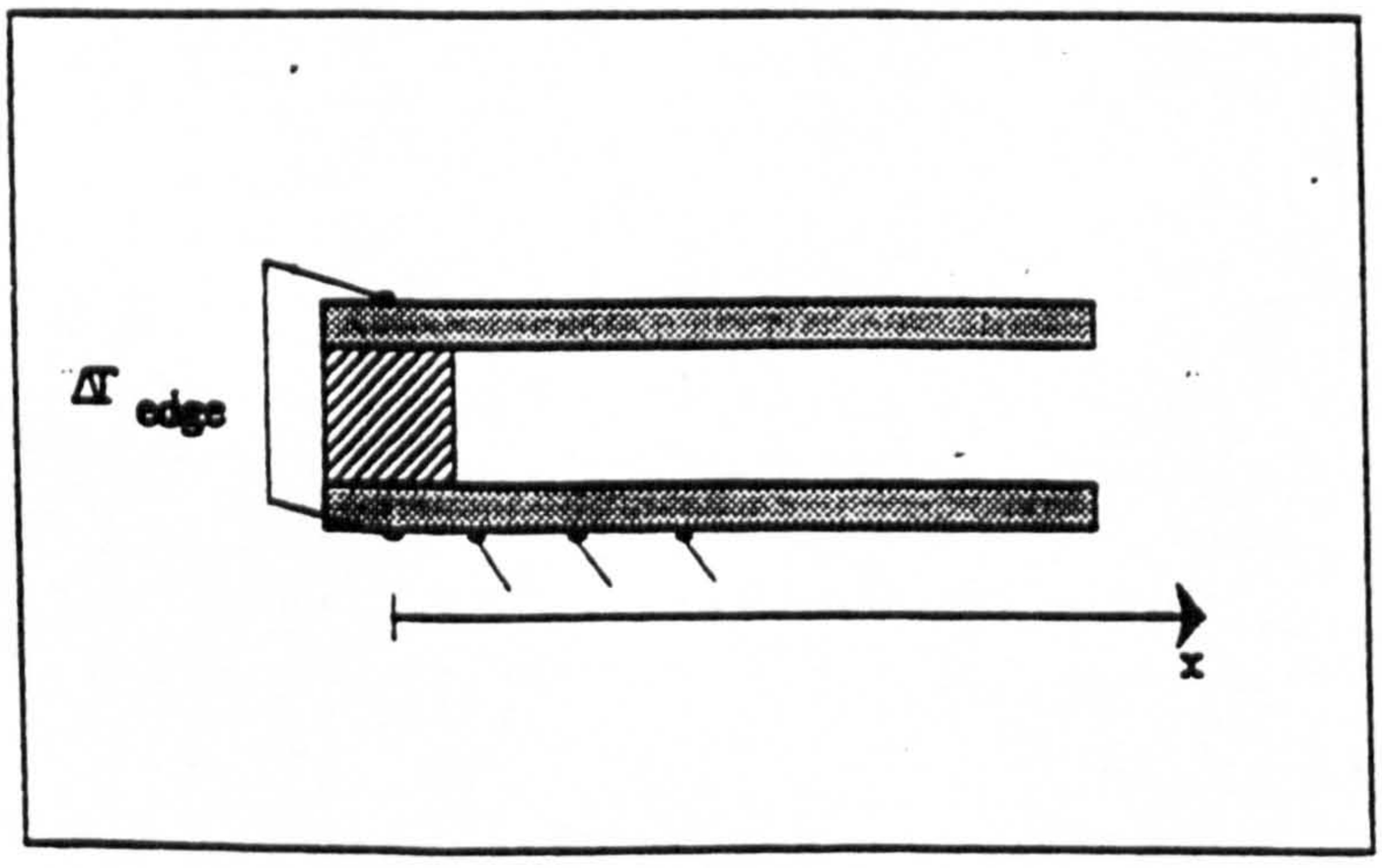

Figure 2.7 Window edge-seal arrangement used in Ref. [2.3]

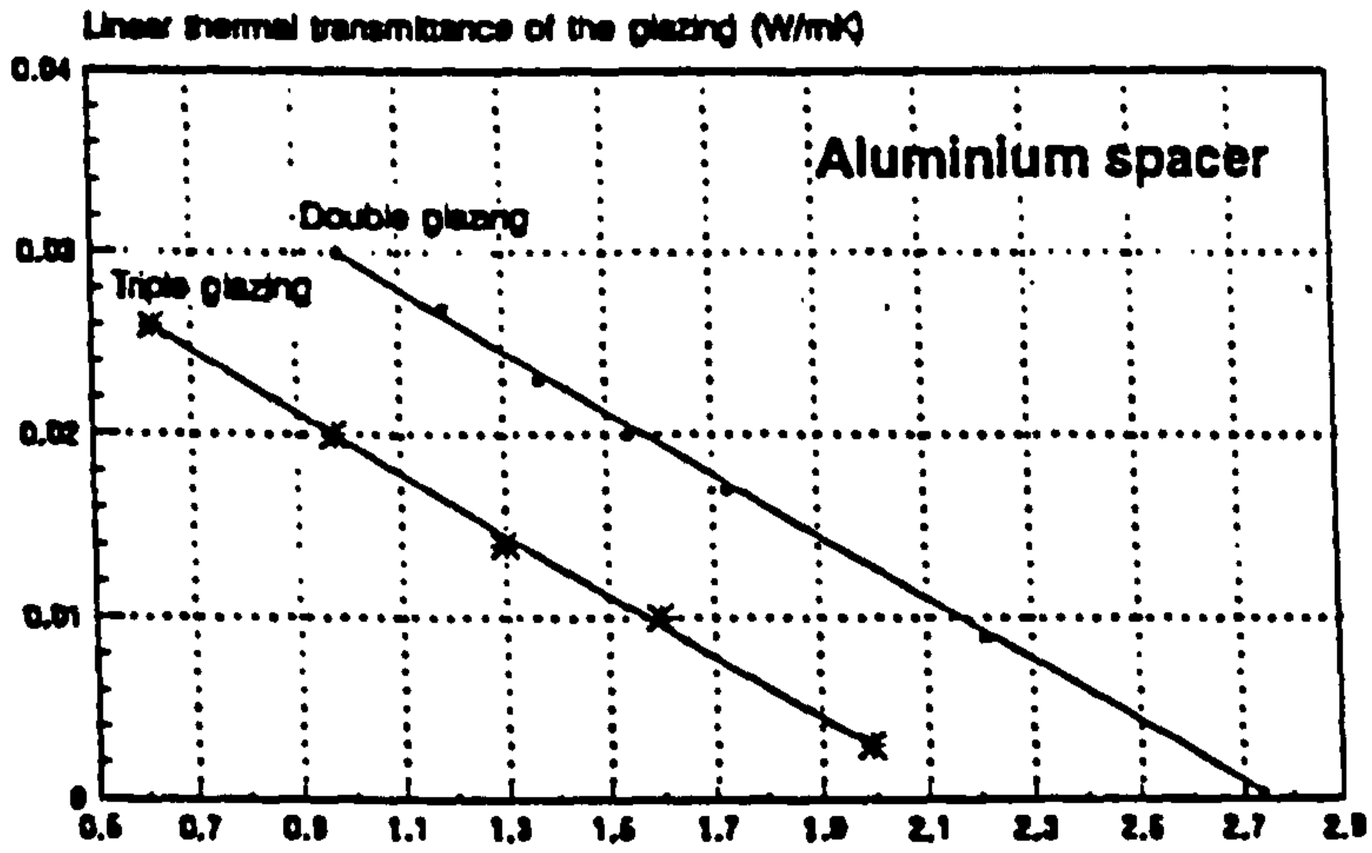

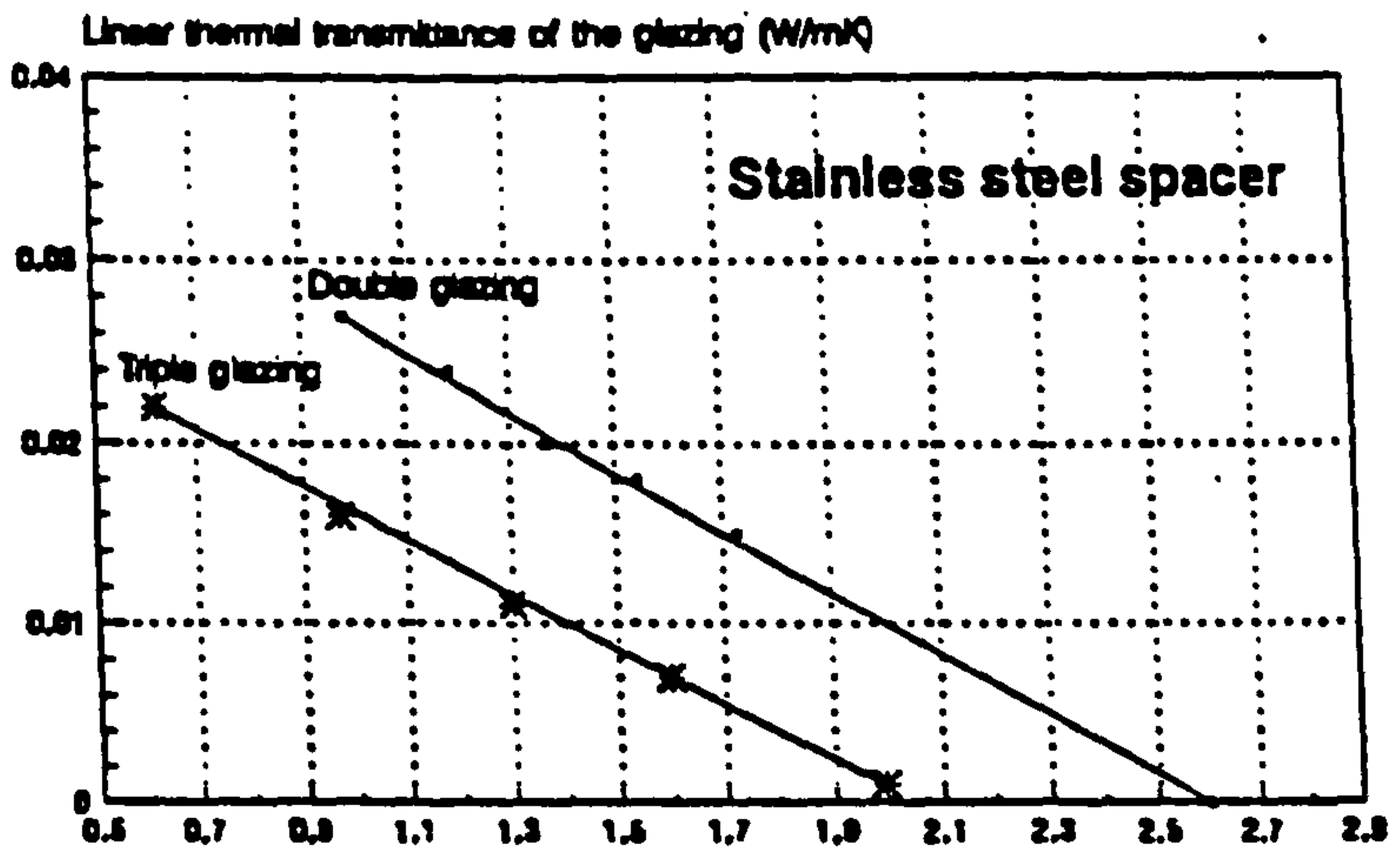

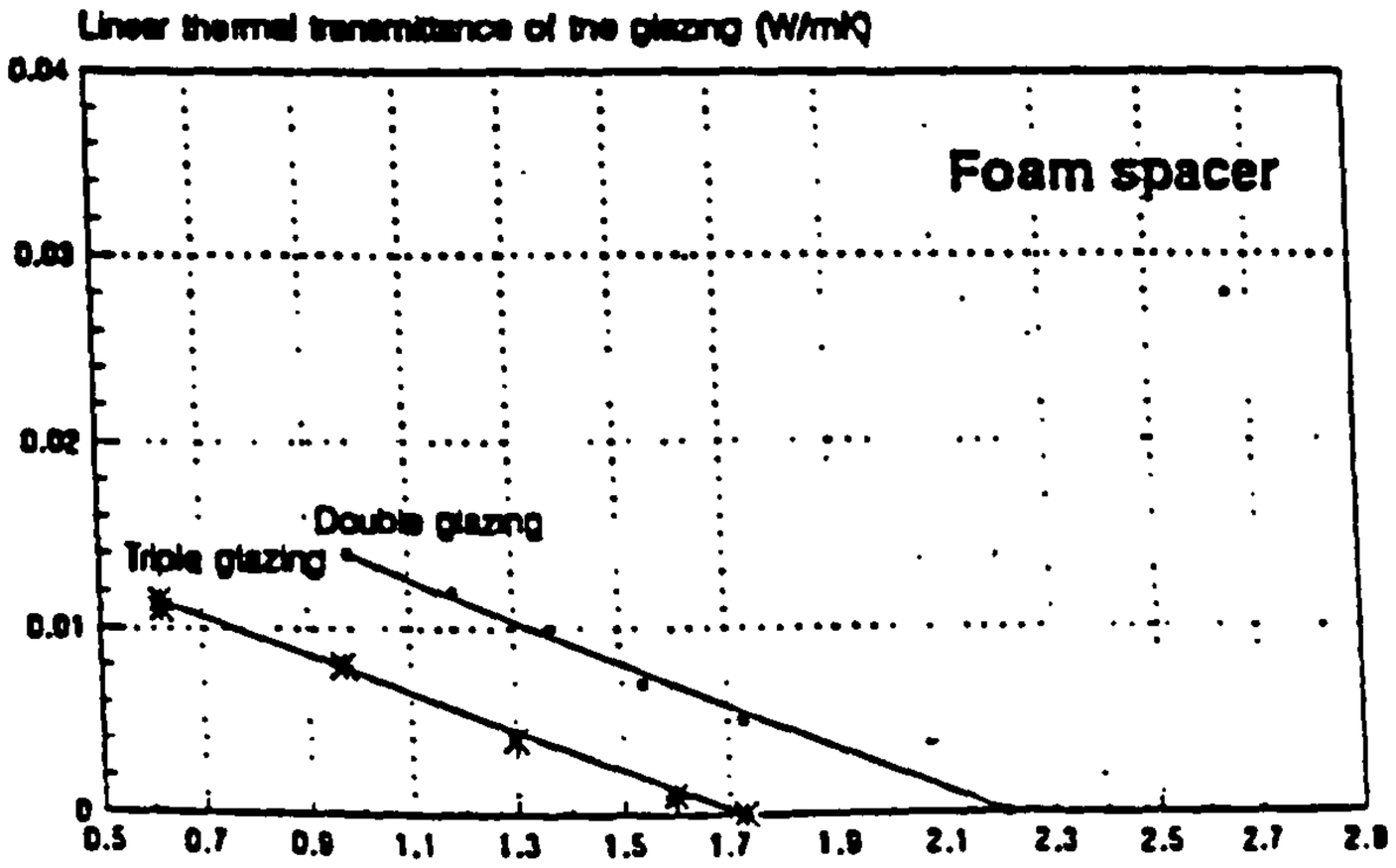

Figure 2.8 Linear thermal transmittance of the glazing. Ref. [2.4]

3 Thermal analysis of double glazed windows

3.1 Introduction

Double glazed windows were recognised at the beginning of this century as an essential requirement for energy conservation and thermal comfort within buildings. All research so far undertaken on double glazed windows has aimed to improve their thermal characteristics and hence reduce the overall heat loss from buildings. In previous studies [3.1, 3.2] it has been shown that 6% of the United Kingdom's energy consumption is due to domestic glazings. The reduction in heat loss through buildings results in lower energy consumption and hence reduced carbon dioxide emissions and greenhouse effect. Energy used in homes accounts for over a quarter of the UK's carbon dioxide emission [3.3].

Heat exchange between buildings and their surroundings occurs in two ways. Firstly, heat transfers to or from a building due to the temperature difference between the building and its surroundings. This exchange can take place by conduction, convection or radiation, individually or in combination. Secondly, heat transfers to or from a building due to air movement, e.g. infiltration or exfiltration.

This chapter will cover some of the theory of heat transfer from buildings. Heat loss through double glazed windows will be discussed in detail.

3.2 Building heat losses and gains

To calculate the steady state heat transfer through the fabric of a building, a simple theory can be used. Since winter conditions in the UK tend to govern building design, it is usual to denote the rate of heat transfer from a building to the outside as positive, i.e.

$$q_F = U_F A_F \Delta T \qquad 3.1$$

where,

q_F fabric heat loss, W

U_F fabric U-value, W/m^2K

A_F surface area of fabric, m^2

ΔT temperature difference between the inside and outside air, K

The thermal transmittance, U_F, is given by

$$\frac{1}{U_F} = \frac{1}{h_i} + \Sigma R + \frac{1}{h_o} \qquad 3.2$$

where,

h_i heat transfer coefficient for the fabric inside surface, W/m^2K

h_o heat transfer coefficient for the fabric outside surface, W/m^2K

ΣR sum of the resistances of the individual layers of the fabric, m^2K/W

The thermal transmittances for a wide range of building components are given in CIBSE guides [3.4, 3.5], e.g. windows, walls, roofs and floors.

In any building there is an infiltration and exfiltration of air due to unavoidable gaps in the construction. The rate of air movement into and out of any space within a building depends on the pressure differences, which in turn are affected by wind direction and speed around the building.

In the steady state, the mass flow rate of air out of any space, m, is equal to the mass flow rate into the space, i.e.

$$\dot{m} = \rho_i \dot{V}_i = \rho_o \dot{V}_o \qquad 3.3$$

3 Thermal analysis of double glazed windows

3.1 Introduction

Double glazed windows were recognised at the beginning of this century as an essential requirement for energy conservation and thermal comfort within buildings. All research so far undertaken on double glazed windows has aimed to improve their thermal characteristics and hence reduce the overall heat loss from buildings. In previous studies [3.1, 3.2] it has been shown that 6% of the United Kingdom's energy consumption is due to domestic glazings. The reduction in heat loss through buildings results in lower energy consumption and hence reduced carbon dioxide emissions and greenhouse effect. Energy used in homes accounts for over a quarter of the UK's carbon dioxide emission [3.3].

Heat exchange between buildings and their surroundings occurs in two ways. Firstly, heat transfers to or from a building due to the temperature difference between the building and its surroundings. This exchange can take place by conduction, convection or radiation, individually or in combination. Secondly, heat transfers to or from a building due to air movement, e.g. infiltration or exfiltration.

This chapter will cover some of the theory of heat transfer from buildings. Heat loss through double glazed windows will be discussed in detail.

3.2 Building heat losses and gains

To calculate the steady state heat transfer through the fabric of a building, a simple theory can be used. Since winter conditions in the UK tend to govern building design, it is usual to denote the rate of heat transfer from a building to the outside as positive, i.e.

$$q_F = U_F A_F \Delta T \qquad 3.1$$

where,

$\dot{m}$ air mass flow rate, kg/s

ρ_i density of air entering the building space, kg/m^3

ρ_o density of air exiting the building space, kg/m^3

$\dot{V}_i$ volume flow rate of air entering the building space, m^3/s

$\dot{V}_o$ volume flow rate of air exiting the building space, m^3/s

The term air change rate is frequently used in air movement calculations. It is expressed as,

$$n = 3600\frac{\dot{V}_i}{V} \qquad 3.4$$

where,

n air change rate per hour, $hour^{-1}$

V volume of the space, m^3

The net energy transfer due to air movement, or the ventilation energy transfer rate (q_v) in Watts is,

$$q_v = \dot{m}c_p(T_i - T_o) \qquad 3.5$$

where,

c_p air specific heat at constant pressure, J/kgK

T_i internal temperature, ^0C

T_o external temperature, ^0C

Over the temperature range from outside to inside, a constant value of c_p can be used.

In winter the air from outside is heated as it enters the space and then leaves the space at the room temperature, so the net energy transfer is known as the ventilation loss, q_v.

Combining Equations 3.3 and 3.4 and substituting into Equation 3.5 yields,

$$q_v = \frac{1}{3600} \rho_i c_p n V (T_i - T_o) \qquad 3.6$$

For atmospheric air over the normal inside temperature and humidity range, the mean value of the product $\rho_i c_p$ is approximately equal to 1200 J/m^{3}K. Hence as a good approximation for normal ventilation conditions, Equation 3.6 can be written as:

$$q_v = \frac{1}{3} n V \Delta t \qquad 3.7$$

where,

$\Delta t = T_i - T_o$

A certain number of air changes are required to maintain fresh, comfortable conditions inside any occupied space. In buildings which are mechanically ventilated or fully air-conditioned, air changes are more easily controlled [3.6].

3.3 Heat loss from windows

Heat loss from windows is quantified by the thermal transmittance or U-value. The U-value of a window is the overall heat transfer coefficient of the window and it is defined as the rate of loss of heat per square metre of the window area , under steady state conditions, for a temperature difference of one Kelvin between the inner and outer environments separated by the glazing. The total thermal transmittance of windows consists of three components arising from the glazing unit, frame, and the spacer between panes. These components can be measured or calculated separately. The

thermal transmittance of a window unit can be calculated using Equation 2.18 of Chapter 2.

In this chapter, only the glazing thermal transmittance (U_{cg}) will be discussed and will be referred to simply as (U-value).

Heat loss can also be quantified in terms of a thermal resistance (R-value). This is simply the inverse of the U-value,

$$\text{R-value} = \frac{1}{U} \quad (\text{m}^2\text{K/W}) \qquad 3.8$$

Table 3.1 gives U- and R-values for the double glazed widows tested in this study.

Table 3.1 U- and R-values for presently tested glazings

Trade Name	Glazing U-value	Glazing R-value
4-Air12-4	2.86	0.35
4-Ar12-4	2.72	0.37
4-Air12-E4	1.83	0.55
4-Ar12-E4	1.53	0.65
4E-Kr12-E4	1.14	0.88
4E-Xe10-E4	0.91	1.10

To understand the heat loss mechanism through windows, it is worthwhile to start by analysing the heat loss through a single-glazed window. Since, in general, winter conditions in the UK govern the design of windows it is usual to assume that heat is transferred from the building to the outside atmosphere. In a single-glazed window, there are three identifiable regions associated with the heat loss through a window, these are illustrated in Fig. 3.1.

A. Heat transfer to internal glass surface:

Heat is lost from the room to the internal glass surface whenever the glass surface is at a lower temperature than the internal air temperature and the room surface temperature. This heat is transferred in two ways:

- by exchange of long wavelength radiation between the glass surface and the room surfaces.
- By convection and/or conduction from the room air moving over the surface of the glass.

The greater heat loss is usually that due to radiation exchange unless the glass surface has a low emissivity coating.

B. Heat transfer through the glass

Heat transfer is by conduction. The resistance to heat transfer of glass is relatively low. This resistance can be calculated as follows,

$$R_g = \frac{L_g}{k_g} \qquad 3.9$$

where,

R_g glass thermal resistance, m^2K/W

L_g glass thickness, m

k_g glass thermal conductivity, normally taken as 1.0 W/mK

C. Heat transfer from the outer glass surface:

As with the inner glass surface, heat transfer from the outer glass surface is by long wavelength radiation exchange to the outside surroundings and by convection and/or

conduction to the air moving over the exterior surface of the glass . The heat transfer at this surface varies considerably and is climate dominated [3.7]. The long wavelength radiation exchange depends on the temperature of the surfaces of the outside surroundings and on the sky temperature. With clear skies, the sky temperature can be extremely low. This effect is demonstrated by the formation of dew and frost on surfaces exposed to clear skies due to their cooling below the ambient air temperature. The rate of heat transfer by convection/conduction is usually high due to the influence of wind, particularly on exposed sites. Wind driven rain will further increase the heat loss due to contact cooling and evaporation.

All present research work is targeted to the achievement of U-values of less than 0.35 W/m^2K for windows of less than 30 mm total thickness. Such values are equivalent to those generally required by legislation for wall installation [3.7].

An effective method for reducing window heat loss is to add a second pane of glass separated from the first pane by a sealed air space. The air gap and additional pane increase the thermal resistance of the window. Such windows are termed multiple glazed window. The sealed air gap provides a significant thermal resistance due to the low thermal conductivity of air compared with glass. The additional pane also provides an additional thermal resistance to long wavelength radiation exchange. Figure 3.2 illustrates the mechanism for heat loss through double glazed units.

The thermal transmittance, U-value, for multiple glazed windows can be calculated using the procedure outlined in the British Standards BS6993 [3.8]. The U-value obtained can then be substituted into Equation 3.1 to calculate the heat loss through the window.

The thermal transmittance (U-value) of the multiple glazed unit is given as [3.8]:

$$U = \frac{1}{\left[\frac{1}{h_o} + \frac{1}{h_t} + \frac{1}{h_i}\right]} \qquad 3.10$$

where,

h_t conductance of multiple glazed unit, W/m^2K

$$\frac{1}{h_t} = \sum^{N} \frac{1}{h_s} + d.r_g \qquad 3.11$$

where,

h_s infill gas heat transfer coefficient, W/m^2K

N number of window cavities

d total thickness of glass panes, m

r_g thermal resistivity of glass, m K/W

$$h_s = h_c + h_r \qquad 3.12$$

where,

h_c infill gas convection heat transfer coefficient, W/m^2K

h_r radiation heat transfer coefficient within the cavity, W/m^2K

The gas conductance (h_c) is given as:

$$h_c = \frac{Nu.k}{L} \qquad 3.13$$

where,

L cavity width, m

k infill gas thermal conductivity, W/mK

Nu Nusselt number

The radiation conductance (h_r) for each gas space is given as:

$$h_r = 4\sigma\left[\frac{1}{\varepsilon_1}+\frac{1}{\varepsilon_2}-1\right]^{-1} T_f^3 \qquad 3.14$$

where,

σ Stefan-Boltzmann constant, W/m^2K^4

ε_1 emissivity of the inner pane

ε_2 emissivity of the outer pane

T_f absolute temperature corresponding to the average of the mean pane temperatures, K

The effective emissivities of the surfaces bounding each enclosed gas space are required in order to calculate h_r. The effective emissivity is 0.845 for uncoated glass surfaces [3.8] and 0.12 for low emissivity coated glass surfaces [3.9].

The external heat transfer coefficient h_o varies around values of 12.5, 16.7 and 33.3 W/m^2K corresponding respectively to the three conditions; sheltered, normal and severe. Sheltered means up to the third floor of buildings in urban centres. Normal means most suburban and rural buildings or the fourth to eighth floors of buildings in urban centres. Severe means buildings on coastal or hill sites or above the fifth floor in suburban or rural areas or floors above the ninth in urban centres. Normally, the exterior heat transfer coefficient h_o is standardised to 16.7 W/m^2K for the purposes of comparison of glazing U-values for the vertical windows [3.8].

The internal heat transfer coefficient h_i is given by the expression,

$$h_i = h_{ri} + h_{ci} \qquad 3.15$$

where,

h_{ri} internal radiation heat transfer coefficient, W/m^2K

h_{ci} internal convection heat transfer coefficient, W/m^2K

The radiation heat transfer coefficient for normal glass surfaces is 5.3 W/m^2K [3.8]. If the interior surface of the glazing has a low hemispherical emissivity, the radiation coefficient h_{ri} is given by:

$$h_{ri} = 5.3 \times \frac{\varepsilon_h}{0.83} \qquad 3.16$$

where,

ε_h hemispherical emissivity of the coated surface

(the hemispherical emissivity of normal glass is 0.83)

The value of h_{ci} is 3.0 W/m^2K for natural convection at vertical surfaces [3.8]. When a fan blown heater is situated below or above a window, this value will be larger. For ordinary glass surfaces and natural convection:

$h_i = 5.3 + 3.0 = 8.3 \ W/m^2K$

This is a standardised value for the purpose of comparing glazing U-values.

Based on Computational Fluid Dynamic results, Muneer and Han [3.10] have developed Equation 3.17 which describes the convective heat transfer of the infill gas in a window cavity.

$$Nu = 0.3628\left(Gr \ \ Pr\right)^{0.2451} A_r^{-0.2783} \qquad 3.17$$

where,

Gr Grashoff number

Pr Prandtl number

A_r aspect ratio of the window cavity ($A_r = H_w/L$)

H_w window height, m

$$Gr = \frac{gL^3 \Delta T \rho^2}{T_f \mu^2} \qquad 3.18$$

$$\Pr = \frac{\mu c_p}{k} \qquad 3.19$$

where,

ΔT temperature difference between infill gas bounding surfaces, K

ρ infill gas density, kg/m^3

μ infill gas dynamic viscosity, kg/ms

c_p infill gas specific heat, J/kgK

g gravitational acceleration, m/s^2

The gas properties are determined at the film temperature, T_f, i.e. the mean of the gas bounding surfaces temperatures. If the Nusselt number is greater than unity this indicates that convection is occurring. If the value of the Nusselt number is less than unity this indicates that heat transfer is by conduction only and the Nusselt number is given the bounding value of unity. A typical glazing calculation is detailed below.

An argon filled double glazed window with a 12 mm gap and 0.4 m in height has one low emissivity coated pane. The internal and external ambient temperatures are 20 ^{0}C and 0 ^{0}C respectively. The thickness of each glass pane is 4 mm.

$T_f = 0.5 \times (20 + 0) + 273 = 283$ K

From Ref. [3.11] the following properties were obtained.

$\rho = 1.72$ kg/m^3

$\mu = 21.8 \times 10^{-6}$ kg/ms

$c_p = 0.52$ kJ/kgK

$k = 0.0168$ W/mK

$Pr = 0.677$

$A_r = H_w/L = 0.4 / 0.012 = 33.3$, $\Delta T = 20 - 0 = 20\ ^0C$

From Equation 3.18,

$$Gr = \frac{gL^3 \Delta T \rho^2}{T_f \mu^2} = [\ 9.81 \text{x}\ 0.012^3 \text{ x } 20 \text{ x} 1.72^2\ ] / [\ 283 \text{ x } (21.8 \text{ x } 10^{-6})^2\ ] = 7457.62$$

Using Equation 3.17, Nu can be calculated as follows,

$$Nu = 0.3628\left(Gr \quad Pr\right)^{0.2451} A_r^{-0.2783} = 0.3628(7457.62 \text{ x } 0.677)^{0.2451} \text{ x } 33.3^{-0.2783} = 7.78$$

From Equation 3.13, the gas conductance due to convection is obtained,

$$h_c = \frac{Nu.k}{L} = (7.78 \text{ x } 0.0168) / 0.012 = 10.89\ W/m^2K$$

Using Equation 3.14 to calculate h_r,

$$h_r = 4\sigma\left[\frac{1}{\varepsilon_1} + \frac{1}{\varepsilon_2} - 1\right]^{-1} T_f^3$$

$$= 4 \text{ x } (5.67 \text{ x } 10^{-8}) \text{ x } [(1 / 0.12) + (1 / 0.84) - 1)]^{-1} \text{ x } 283^3 = 0.60\ W/m^2K$$

From Equation 3.12,

$$h_s = h_c + h_r = 10.89 + 0.60 = 11.49\ W/m^2K$$

and from Equation 3.11,

$$\frac{1}{h_t} = \sum^{N} \frac{1}{h_s} + d.r = (1 / 11.49) + (0.008 \text{ x } 1) = 0.095 \text{ m}^2\text{K/W}$$

The British Standards recommend that h_i and h_o of normal multiple glazed window to be as follows,

$h_i = 8.3 \text{ W/m}^2\text{K}$

$h_o = 16.7 \text{ W/m}^2\text{K}$

Therefore, from Equation 3.10,

$$U = \frac{1}{\left[\frac{1}{h_o} + \frac{1}{h_t} + \frac{1}{h_i}\right]} = 1 / [(1 / 16.7) + 0.095 + (1 / 8.3)] = 3.63 \text{ W/m}^2\text{K}$$

Many other researchers have studied the natural convection phenomenon within enclosures and developed correlations for Nusselt number based on the enclosure width, i.e. the gap between the hot and cold walls. Some of these correlations are mentioned below,

Inaba [3.12]

$$\text{Nu} = 0.271 \, (H_w/L)^{-0.21} \, (\text{Ra} \sin Q)^{0.250} \qquad 3.20$$

where,

Q angle of the enclosure cavity from the horizontal, degree

Ra Rayleigh number

The above equation is only valid under the following conditions,

$5 \times 10^3 < Ra \sin Q < 1.2 \times 10^6$

$5 < H_w/L < 83$

El Sherbiny et al [3.13]

$$Nu = [\ 1,\ 0.288(Ra / A_r)^{1/4},\ 0.062\ Ra^{1/3}\ ]\ Max \qquad 3.21$$

The maximum of the three terms is to be used.

Raithby et al [3.14]

$$Nu = [\ 1,\ 0.75\ C_i\ \{(\cos F\ Ra) / A_r\}^{1/4},\ 0.29\ Ct\ (\cos F\ Ra)^{1/3}\ ]\ Max \qquad 3.22$$

The maximum of the three terms is to be used.

where,

F angle of the glass surface from the vertical, positive when the heated surface faces upward

and,

$-20 \text{ deg} < F < 20 \text{ deg}$

$C_i = 0.50/(1+(0.49/Pr)^{9/16})^{4/9}$

$C_t = [0.15, 0.14\ Pr^{0.084}]\ Min$

Wright [3.15]

$$Nu = \{Nu_1, Nu_2\}Max \qquad 3.23$$

where,

$Nu_1 = 0.0673838\ Ra^{1/3}$ $\quad 5x10^4 < Ra < 10^6$

$Nu_1 = 0.028154\ Ra^{0.4134}$ $\quad 10^4 < Ra < 5x10^4$

$Nu_1 = 1 + 1.7596678 \times 10^{-10}\ Ra^{2.2984}$ $\quad Ra < 10^4$

$Nu_2 = 0.242[Ra/A_r]^{0.272}$ $\quad$ for all values of Ra

Catton [3.16]

For aspect ratios in the range $1 < H_w/L < 10$, Catton [3.16] has suggested the following correlations (3.24 and 3.25).

$$Nu_L = 0.18\left(\frac{\mathrm{Pr}}{0.2+\mathrm{Pr}}Ra_L\right)^{0.29} \qquad 3.24$$

when,

$1 < H_w/L < 2$

$10^{-3} < \mathrm{Pr} < 10^5$

$$10^3 < \frac{Ra_L\ \mathrm{Pr}}{0.2+\mathrm{Pr}}$$

$$Nu_L = 0.22\left(\frac{\Pr}{0.2+\Pr} Ra_L\right)^{0.28}\left(\frac{H_w}{L}\right)^{-0.25} \qquad 3.25$$

when,

$2 < H_w/L < 10$

$\Pr < 10^5$

$10^3 < Ra_L < 10^{10}$

MacGregor and Emery [3.16]

For larger aspect ratios, MacGregor and Emery have proposed the following correlations (3.26 and 3.27).

$$Nu_L = 0.046 Ra_L^{1/3} \qquad 3.26$$

when,

$$1 < \frac{H_w}{L} < 40$$

$1 < \Pr < 20$

$10^6 < Pa_L < 10^9$

$$Nu_L = 0.42 Ra_L^{0.25}\ \Pr^{0.012}\left(\frac{H_w}{L}\right)^{-0.3} \qquad 3.27$$

when,

$$10 < \frac{H_w}{L} < 40$$

$$1 < Pr < 2x10^4$$

$$10^4 < Pa_L < 10^7$$

It must be borne in mind that h_c is an important parameter for the complete heat transfer network. Thus the minimisation of this parameter will yield beneficial savings in building energy consumption. Muneer and Han [3.10] developed design charts which are based on Equation 3.17. These design charts can be used to choose the thermally optimised multiple glazed window design by choosing the optimised h_c. They involve combinations of "hot" and "cold" temperature regimes encountered by the two glass surfaces of any window cavity, window height, gap width and for various gases presently used by manufacturers. They cover almost the whole range of windows used in industry.

3.4 The effect of window gap width on convection heat transfer coefficient

Significant improvement in energy efficiency may be achieved by increasing the air gap between two glazings. As illustrated by Muneer and Han's design charts [3.10], from the small enclosure width of 4 mm, where almost all the energy is transported via conduction, the coefficient drops sharply with the increasing gap width. This is due to the conduction heat transfer resistance being proportional to the thickness of the conducting material, the thicker the material is, the larger the resistance. Further increase of the gap width causes the decrease in h_c to be less rapid and eventually h_c becomes almost constant. Convection heat transfer is only slightly influenced by the gap width and is only affected by the temperature and the thermal property of the glass, so

that under fixed boundary conditions, although the gap width is increased, the convection heat transfer coefficient, h_c, is almost unchanged.

The limit gap width, between conduction and convection controlled heat transfer, is even more important than the optimum gap for a window designer. For a certain window, from the limit gap of conduction and convection to the optimum gap, there is only a small change in the convection coefficient but in the conduction regime, h_c is often very high. In choosing the optimum gap for a window design it would certainly be the best design thermally, but not necessarily the most economical. Knowing the limit gap would allow the most economical window to be designed without a great effect on its thermal performance. For instance, for an air filled window, under temperature conditions of 20 °C on the warm side and 0 °C on the cold side and with a 4 mm gap, which is in the conduction regime, the convection coefficient h_c is 6.25 $W/m^2 K$. When the gap is 12 mm, the value for h_c is about 2.20 $W/m^2 K$. For a 20 mm gap, which would be the optimum gap, the corresponding h_c is 1.90 W/m^2K. Therefore, from 4 mm to 12 mm, the gap has increased by 8 mm and the h_c decreased by 4.05 $W/m^2 K$, which is a 65% drop. From the limit gap of 12 mm to the optimum gap of 20 mm, the gap increased 8 mm and the h_c decreased 0.3 W/m^2K which is just a 14% drop. Obviously, the economically best window gap should lie between the limit gap and the thermally optimum gap.

3.5 The effect of infill gases on convection heat transfer coefficient

The use of inert gases can dramatically reduce the convective heat transfer coefficient. The optimum gap width (corresponding to minimum h_c) decreases with increasing infill gas molecular weight, M. The optimum gap width occurs at 8, 12, 16 and 20 mm for xenon, krypton, argon and air respectively [3.10]. This behaviour can be explained as follows. The buoyancy force, responsible for ensuing convection, is proportional to the density differential between the cold and hot gas, $(\rho_1-\rho_2)$, in the immediate neighbourhood of the cold and hot sides of the enclosure. Using the ideal gas relationship it may be shown that [3.1, 3.17 & 3.18],

$$Buoyancy\ \ Force\ = \rho_1 - \rho_2 = \frac{p}{\bar{R}}\left[\frac{1}{T_1} - \frac{1}{T_2}\right]M \qquad 3.28$$

where,

p gas pressure, Pa

$\bar{R}$ universal gas constant (= 8.3144 kJ/kmole K)

T_1 temperature of the hot side wall, K

T_2 temperature of the cold side wall, K

M gas molecular weight, kg/kmole

For fixed P and T values, the above relationship shows that the driving buoyancy force is directly proportional to the molecular weight of the gas. In a narrow gap (encountered in the conduction regime) the fluid layers are squeezed together and the interlayer shear force exceeds the driving buoyancy force. As the gap widens the shear force weakens up to the point where the hot and cold sides acquire distinct boundary layers. For a given gas this is the gap width at which minimum h_c exists. With a heavier gas the onset of convection, and the point where h_c is minimum, occurs at reduced gap width (larger buoyancy force).The above theory was originally postulated by Han [3.18]. It addresses the movement of the gas within narrow cavities. Analysis of heat transfer due to convection is, however, much more involved as the relevant transport properties have also to be taken into account.

3.6 The effect of window height on convection heat transfer coefficient

With increased enclosure height, h_c decreases. Muneer and Han [3.10] have shown that for an air filled window cavity (20 mm optimum gap) under temperature conditions of 20 °C on the warm side and 0 °C on the cold side, h_c for a one metre high window cavity is 1.64 W/m^2K and for a 0.6 metre high window, h_c is 1.90 W/m^2K, a 4% decrease. On the contrary, as expected, the height in the conduction regime makes almost no difference in the coefficient. This has also been shown by Muneer and Han's design

charts [3.10]. The decrease in h_c with height has also been addressed by El Sherbiny et al [3.13]. A window measurement carried out by Rayment et al [3.19] shed further light onto this finding.

3.7 The effect of temperature differential on convection heat transfer coefficient

By increasing the temperature difference, h_c increases and the optimum gap width decreases but in the conduction regime, h_c does not change. Muneer and Han [3.10] have also illustrated these results graphically. The decrease in the optimum gap occurs because when the temperature difference is increased the flow is in the form of two increasingly independent boundary layers and this enables convection to take over from conduction at a smaller gap width. This is also explained by Elder [3.20] and Gill [3.21]. The temperature levels have no measurable impact on h_c as long as the temperature differential remains constant [3.10].

3.8 The effect of low emissivity coatings on glazing U-value

A low emissivity (low-e) coating on the glass has the ability to reflect the long wavelength radiation emitted from the interior objects back to the building, thus conserving the building energy. It also provides the possibility of reducing the long wavelength radiation exchange between the panes. In air spaces with uncoated surfaces, the long wavelength radiation exchange between those enclosing glass surfaces is high, amounting to about 60% of the total heat exchange across the space. With one of the glass surfaces having a coating with emissivity less than 0.2 (compared with 0.88 for the uncoated glass surface), the radiation exchange is reduced by approximately 75% and consequently the U-value is reduced [3.7]. The term 'low-e' is taken to refer to coatings with an emissivity of 0.12 in the present project.

3.9 Model for calculation of glazing U-value

An Excel spreadsheet has been developed to calculate the glazing U-value for a double glazed window. The inputs to this model are the weather condition, the internal and external temperatures and the window specifications, e.g. window height, gap width, infill gas type, panes thickness and emissivity.

The calculation is initiated by assuming a U-value for the glazing unit under consideration. Then the centre glazing temperatures of the panes t_1, t_2, t_3 and t_4 (see Fig. 3.3) are calculated from the following equations:

$$t_1 = T_o + (1 / h_o)\, U\, [T_i - T_o] \qquad 3.29$$

$$t_2 = T_o + [R_{g1} + (1 / h_o)]\, U\, [T_i - T_o] \qquad 3.30$$

$$t_3 = T_i - [R_{g2} + (1 / h_i)]\, U\, [T_i - T_o] \qquad 3.31$$

$$t_4 = T_i - (1 / h_i)\, U\, [T_i - T_o] \qquad 3.32$$

The gas properties are determined at the film temperature (T_f) where,

$$T_f = \frac{1}{2}(t_2 + t_3) \qquad 3.33$$

The Nu and Gr numbers are then calculated using Equations 3.17 and 3.18 respectively. As mentioned previously, if Nu number is less than unity, it is taken as Nu = 1. Then h_t, h_c and h_r are calculated using Equations 3.11, 3.13 and 3.14 respectively. h_i and h_o are given the values 8.6 and 16.7 W/m^2K respectively. Finally, the U-value is calculated from Equation 3.10. The same process of calculation is repeated using the new U-value until successive calculated U-values differ by a sufficiently small amount. The last U-value obtained by this iteration is the required glazing U-value for the window. The

computer software Uval.xls (see Appendix H) includes the above model and is presently available on the accompanying floppy disk.

References

3.1. T. Muneer and B. Han, Use of CFD for thermal analysis of double glazings, Computational Methods and Experimental Measurements VII, 77-84, Eds: G. M. Carlomagno and C. A. Brebbia, Computational Mechanics Publications, UK, 1995

3.2. Department of Trade and Industry, Digest of the United Kingdom Energy Statistics-1993, HMSO, London, 1993

3.3. R. Jones, Minister of State for Construction and Planning and Energy Efficiency, Department of the Environment, Address to the "Energy Efficient Housing '96" delivered on 2 April 1996

3.4. CIBSE Guides A3 "Thermal properties of building structures", London, 1989

3.5. CIBSE Guide to Current Practice Volume A, London, 1986

3.6. T. D. Eastop and W. E. Watson, Mechanical services for buildings, Longman Group UK Limited, 1993

3.7. D. Button and B. Pye, Glass in building: A guide to modern architectural glass performance, Pilkington Glass Ltd., UK, 1993

3.8. BS6993 Part I, British Standards Institution, BS House, London, 1989

3.9. Personal communication with W.Davidson of Nor-Dan (UK) Ltd., Newmains, Lanarkshire, 1995

3.10. T. Muneer and B. Han, Design charts for multiple glazed windows, BSER&T 17, 4, pp 223-229, 1996

3.11. H. J. M. Hanley, R. D. McCarty and W. M. Harnes, The viscosity and thermal conductivity coefficients for dense gaseous and liquid argon, krypton, xenon, nitrogen and oxygen, J. Phys. Chem. Ref. Data, 3, 4, pp 979-1018, 1974

3.12. H. Inaba, Experimental study of natural convection in an inclined layer, Int. J. Heat Mass Transfer, 27, pp 1127-1139, 1984

3.13. S. M. ElSherbiny, K. G. T. Hollands and G. D. Raithby, Heat transfer by natural convection across vertical and inclined layers, Trans ASME J Heat Transfer, pp 96-102, February 1982

3.14. G. D. Raithby, K. G. T. Hollands and T. E. Unny, Analysis of heat transfer by natural convection across vertical fluid layers, Journal of Heat Transfer, Vol. 99, pp 287-293, May 1997

3.15. Reference Manual, Glazing System Thermal Analysis, VISION 3, Advanced Glazing System Laboratory, University of Waterloo

3.16. F. P. Incropera and D. P. DeWitt, Fundamentals of heat and mass transfer, New York, John Wiley, pp 542-544, 1990

3.17. T. Muneer, N. Abodahab and B. Han, Gas flow in double glazing enclosures and its effect on longitudinal temperature variation Proceedings of the Advances in Fluid Mechanics (AFM'96) conference, New Orleans, USA, (11-13 June 1996), Computational Mechanics Publications, UK, 1996

3.18. B. Han, Investigation of thermal characteristics of multiple glazed windows, PhD Thesis, Napier University,1996

3.19. R. Rayment, P. J. Fishwick, P. M. Rose and M. J. Seymour, A study of glazing heat losses and trickle ventilators, Building Research Establishment Occasional Paper, pp 38, October 1992

3.20. J. W. Elder, Laminar free convection in a vertical slot, Journal of Fluid Mechanics, Vol. 23, Part 1, pp 99-111, 1965

3.21. A. E. Gill, The boundary layer regime for convection in a rectangular cavity, Journal of Fluid Mechanics, Vol. 26, Part 3, pp 515-536, 1966

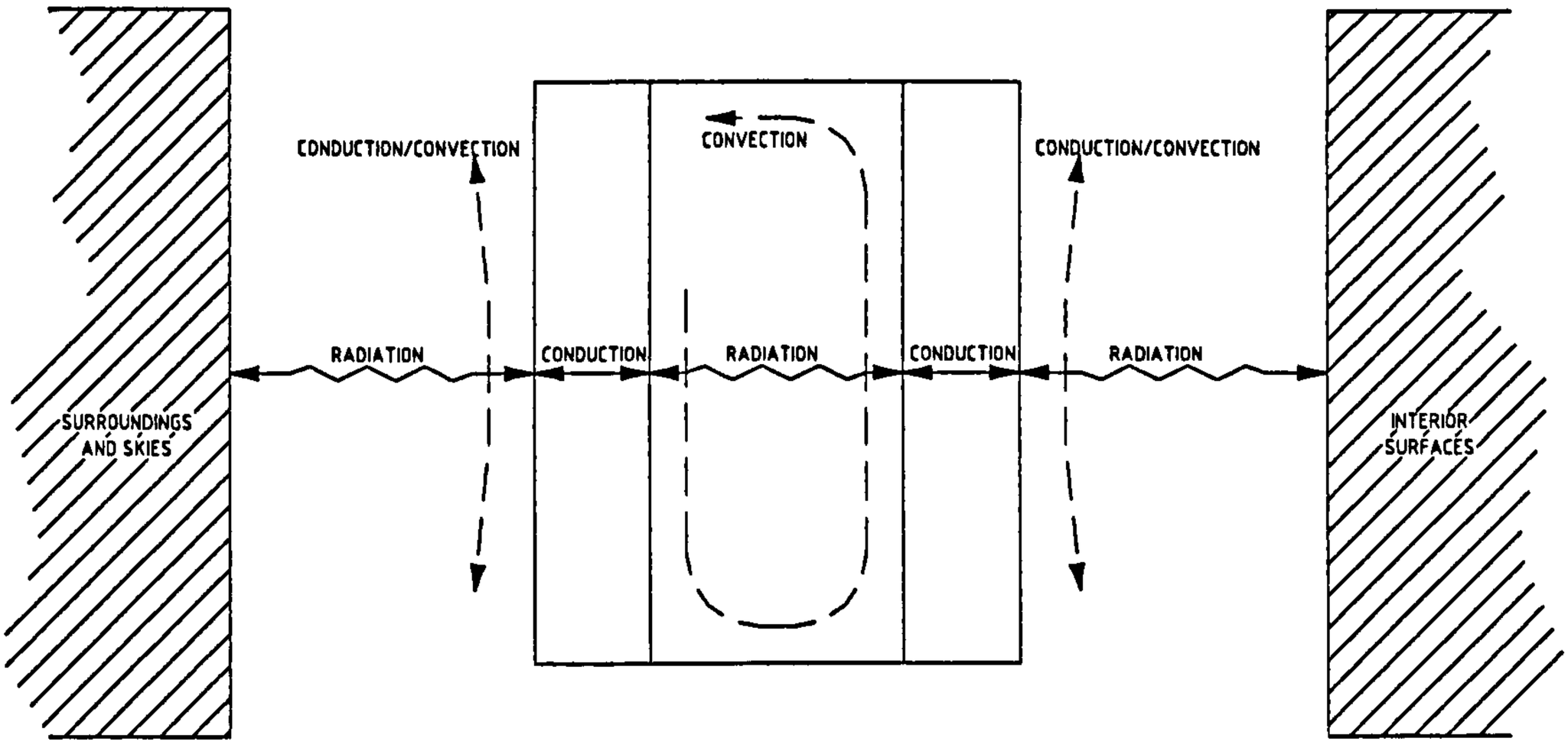

Figure 3.1 Mechanism for heat loss through single glazed units

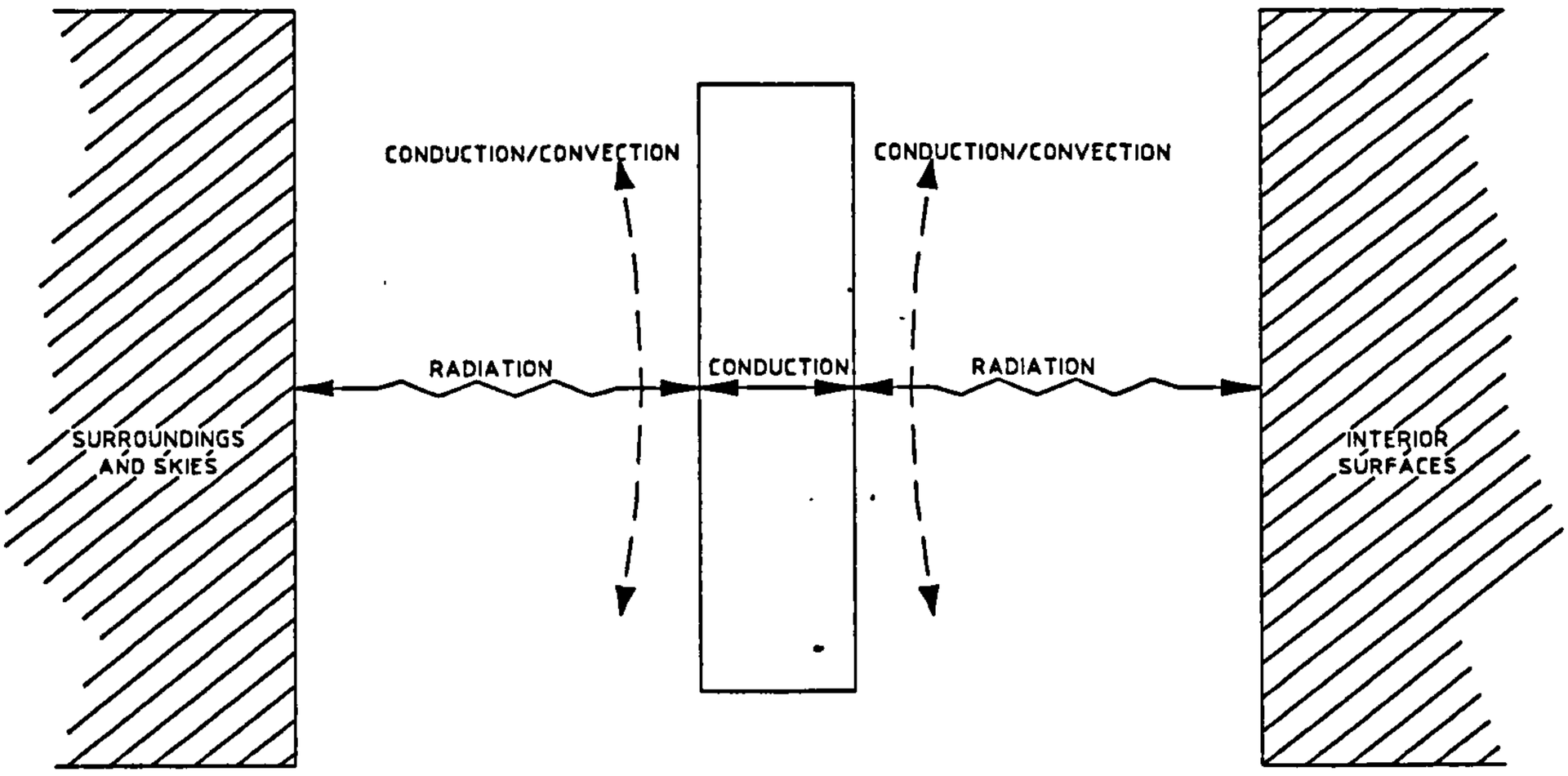

Figure 3.2 Mechanism for heat loss through double glazed units

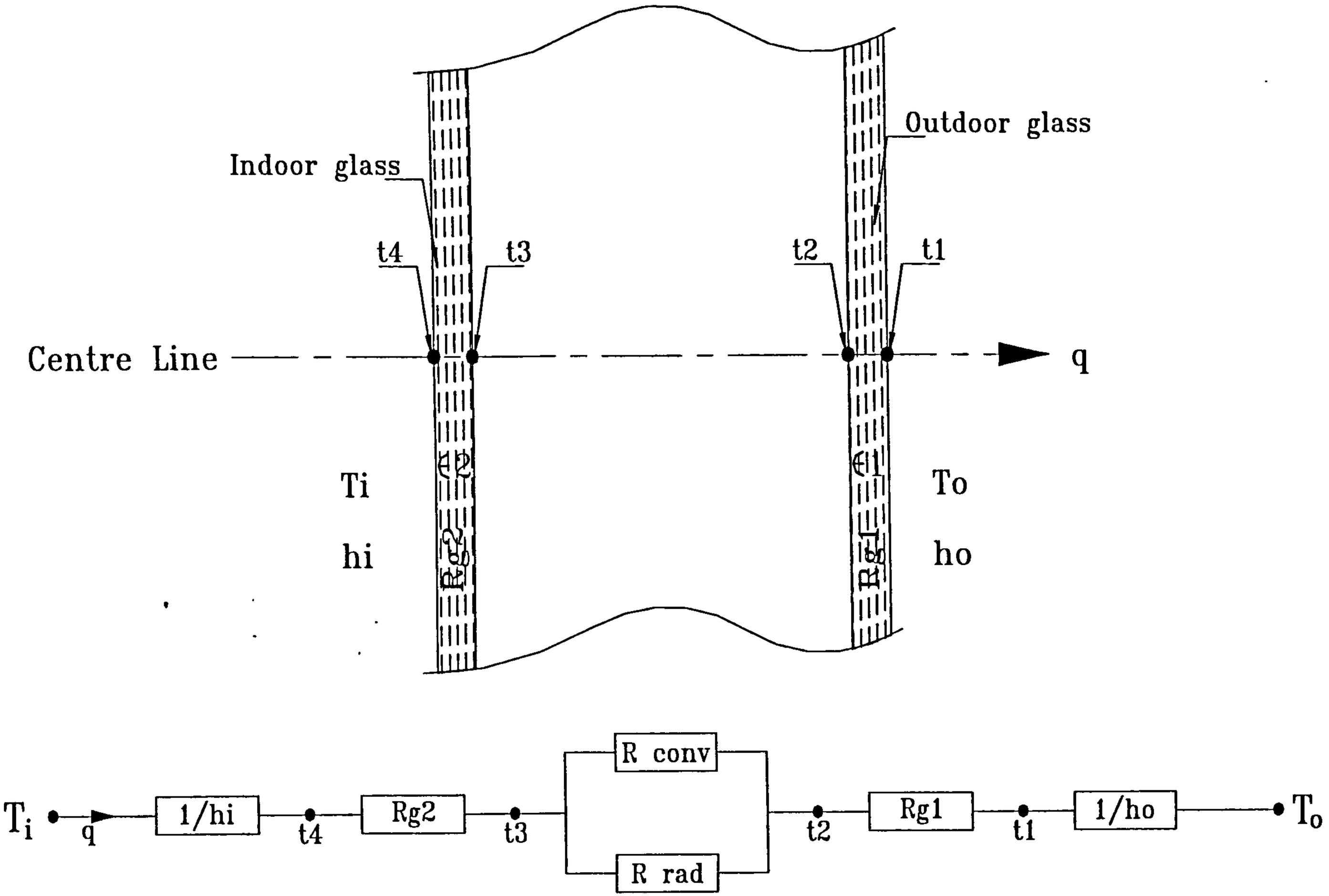

Figure 3.3 Centre - line thermal circuit for double - glazed window

4 Experimental Work

4.1 Introduction

Recently greatly improved performance has been demanded of the building fabric in general and of the window in particular. The need for improvement has been emphasised by sudden, large increases in the costs of fuels and by realisation of the need to conserve energy resources. Due to these requirements, window research has developed very rapidly over the last decade. Many organisations have been set up in the United Kingdom alone. The Glass & Glazing Federation, based in London [4.1], the Centre for Window and Cladding Technology [4.2] based in Bath, the Advanced Glazing Industry Club [4.3] based in Oxford, and Building Research Establishment based in Watford [4.4], are all engaged in window research. Almost all aspects of multiple glazed windows have been tested by building research institutes or university laboratories. For instance, heat loss through multiple glazed windows have been thoroughly measured and investigated by Muneer and Han [4.5]. Rayment et al [4.6], carried out a series of window tests which measured the effect on the heat loss of radiator positions (either under the window or on a side-wall), sill depth, curtains, double glazing and low-e glazing, trickle ventilators and window geometry.

A number of test facilities all over the world have been developed to carry out a variety of window measurements. The hot box [4.7] is a commonly used facility for measuring the heat transfer characteristics through window centre, edge-seal and frame. The hot box consists primarily of two parallel copper plates, positioned facing each other, that can be maintained at different but constant temperatures. Each plate is held at its desired temperatures by a constant temperature circulating bath that pumps a steady flow of water and glycol through a manifold of tubes attached to the back of the plate. It is thus possible to measure the heat transfer that occurs over the face of each of the guarded heater plates. Other systems are used to measure the solar radiation and daylight transmissivity, window air penetration, window resistance to wind load and rain

penetration, window hardness and resistance to human impact. Detailed information is provided in Refs. [4.8 - 4.12].

The objective of the present experimental work is to measure the temperature distribution on the inner pane of a double glazed window. This, in turn, will help in assessing the frequency of condensation occurrence usually encountered on the inner pane. The facility used in the present study to measure and investigate temperature distribution on a window inner pane consists of a specially built, well insulated test room with a controlled heater to simulate a real room under nocturnal winter conditions. A computerised data acquisition system is used to record the output from thermocouples, humidity probe and anemometer during the experiments.

To achieve the aims of the present research the experiments were divided into three parts. Each part was conducted to investigate one or more of the project aims. Measurements were taken during the winters of 1995 and 1996, i.e. at the end of the respective years. Eight window designs, representing the whole range of windows used in industry were tested. To eliminate solar effects on the experimental data, only night readings were considered for analysis.

The following sections discuss in detail the equipment, the measurement schedule and procedure and, finally, give the tests results and conclusions.

4.2 Test equipment

The first and third parts of the laboratory experiments were carried out in a well-insulated and temperature-controlled test room constructed on the roof of Napier University (Merchiston campus). Two data-scans 7220 and one squirrel (data logger) were used to monitor and log temperatures on the inner pane for windows under test, temperatures inside and outside the test room, and the external wind speed. The data-scans and squirrel continuously collected samples over 3-5 days, the data being collected during nocturnal periods to avoid heating up of the window glass due to solar

radiation absorption. The experimental data obtained was then passed directly onto a computer disk to be analysed using a spreadsheet.

The second part of the experiments was carried out in a residential house in Edinburgh. An occupied, single bedroom in this house was used for conducting the experiments. Ambient temperatures inside and outside the room were measured using calibrated thermocouples. A humidity probe was also fitted inside the room to measure the internal relative humidity. All measurements were recorded using three squirrels. The experimental data obtained by the squirrels was also conveyed onto computer disk to be analysed using a spreadsheet.

All the thermocouples used in the experiments were periodically calibrated. Test equipment will be discussed in detail in the following sections.

4.2.1 The test room

In order to carry out the proposed research programme and obtain good quality data, a small test room has been constructed in Edinburgh's urban area, on the roof of a five storey building (Napier University's Merchiston campus). The test room is well insulated and has two apertures of different areas (444 x 427 and 600 x 600 mm) to facilitate the investigation of different window designs. The test room was situated in the open air to simulate the window performance in in-situ conditions. The temperature inside the room was automatically controlled at 20 °C by using a temperature controller. The dimensions of the room are shown in Fig. 4.1a. A view of the test room is shown in Fig. 4.1b.

4.2.2 The experimental house

A detached house situated two miles from Edinburgh airport (Turnhouse) was selected for experiments. Being detached the house was ideal for considering only changes of the building internal temperature regardless of the heat transfer to or from neighbouring

houses which is the case for terraced houses. The house uses central heating system which works from 0600 hours until 0830 hours for the morning period and from 1600 hours until 2100 hours for the evening period. This heating routine allows the house to be nocturnally cooled by the effect of the external ambient environment. An occupied, single bedroom in this house was used for conducting the second part of the experiments. This bedroom is 2 m long, 2.5 m wide, and 2.5 m height.

4.2.3 The data-scan 7200

Two sets of data-scan 7200 series were used for data acquisition in the experiments conducted in the test room. Data-scan 7200 is one in a series of products by Measurement System Ltd., Berkshire, England. Each set of data-scan consists of a module which interfaces the sensors (thermocouples) to a computer placed inside the test room. Each module is a measurement processor which provides directly 16 analogue inputs. The measurement processors perform the measurement and the control of the data-scan system. Each measurement processor contains a powerful analogue to digital converter which can be programmed to provide either 16 or 14 bits of resolution and is sensitive to 0.625 μV [4.13, 4.14]. Each measurement processor module has two communication ports, an isolated RS232 port for communication with the host computer or any other local display terminals, and an isolated R485 network port for connecting up to 32 measurement modules over a network distributed up to 1.2 km. The isolated nature of these ports prevents ground problems and protects the network and the host computer in the event of high voltages entering the measurement modules. The power supply to the measurement modules is either 22 to 28V DC at 0.5A or 24 V AC RMS at 0.5 Amps maximum [4.13]. To maintain maximum noise rejection a switch is provided on every measurement processor module to match the module to the local mains frequency (50 Hz). An earthing stud is provided on each data-scan module to allow the metal case to be earthed. Before the computer can communicate via the RS232 interface, the correct baud rate has to be set up on the measurement processor module configuration switch. A baud rate of 9600 has been used in all the experiments.

4.2.4 The RS-Recorder

RS-Recorder is the software which was used to configure and monitor the data-scan module. It is a Microsoft Windows based data acquisition package and is able to monitor up to 64 independently configured channels, display and log their values to computer disk. RS-Recorder is able to update the display once a second. The package is split primarily into two suites of menus, one used to configure the data-scan, the other to scan and log the data.

Before using RS-Recorder, it is necessary to create a configuration file. This file defines the type and number of data-scan modules connected to the system, the set-up of each individual data-scan channel and the communications parameters associated with the data-scan. After creating a configuration file, RS-Recorder can be started for scanning and displaying data only or for scanning and logging the data to a disk. Scanning data can also be stopped and re-started any time. Data logged by RS-Recorder can be imported into either Lotus 123 or Microsoft Excel for analysing.

The RS-Recorder is supported with a Microsoft Windows based automatic installation program. At least 150K bytes of free disk must be available for the recorder program suite. Insufficient space causes the procedure to be aborted [4.15].

4.2.5 The data loggers

Data loggers, also called squirrels operate independently and unattended for long periods of time, in hostile and remote environments. Squirrel data loggers [4.16] combine sophisticated logging technology with a high degree of flexibility, featuring:

- a display for easy interaction
- simple programming by means of three push-buttons and the display
- dedicated inputs for easy plug-in sensor connection
- a dedicated analysis program for easy transfer and analysis of stored data

- compact size for easy portability
- robust, high quality build for durability
- battery powered for independent operation
- large memory size for long-term operation
- user programmable features for added flexibility, for example alarms
- useful combinations of inputs / measuring ranges for multi-purpose applications
- ability to interface with a wide range of sensors, meters and transducers
- ability to function both as a meter and as a data logger
- high accuracy and stability

Three data loggers were used in the present experiments. These are 1000, 1250, and 8-Bit. In the first part of the experiments, there was no need for using the squirrels because only 16 channels were needed and one data-scan 7200 was just adequate since it can supply up to 16 channels. However, the squirrels were needed in parts two and three of the experiments as the number of channels required could not be covered by the two data-scan modules available. Squirrels can accept a large range of inputs. In the present experiments, they were used in measuring humidity, temperature (K thermocouples), and wind velocity. The operation and set up procedures for these squirrels are given in Ref. [4.16].

4.2.6 The thermocouples

Thermocouples are the most widely used of all the temperature sensors due to their simplicity and reliability. In the present project, type K thermocouples have been used. Type K thermocouples are used extensively in science and industry because they have the best available combination of desired properties for a wide-range general purpose thermocouple. The specifications of type K thermocouples are as follows [4.17]:

Composition:	nickel-chromium alloy (Chromel) / nickel-aluminium alloy (Alumel)
Allowable environment:	oxidising, inert
Allowable temperature:	1260 °C

Limits of error [4.18]: 0-400 °C (±3 °C) 400-1100 °C (±0.75%)

Type K thermocouples were used to measure all temperatures involved in all the experiments, e.g. inside and outside the test room and the experimental house and temperatures on glazings surfaces. All the thermocouples used in the present experiments were carefully calibrated. The reference temperatures were measured via a scientific mercury-in-glass thermometer which, in turn, was checked for its accuracy against British Standard thermometers. One of these calibration results is shown in Table 4.1. As can be seen from this table, different fixed temperatures were used for calibration [4.18].

4.2.7 The humidity probe

There are a large number of techniques available for measurement of relative humidity. A brief description of these techniques which have been used or could be used in relative humidity measurements is given by Trechsel [4.19].

In the second part of experiments, the relative humidity inside the room was measured hourly by a Humitter 50U P1010040, manufactured by Vaesala of Germany. This relative humidity sensor is called an electrolytic hygrometer in which air is passed through a tube, where moisture is absorbed by a highly effective desiccant, usually phosphorous pentoxide, and electrolysed. The electric current required for electrolysis can be related to the humidity. This sensor is usually designed for use with moisture-air ratios in the range of 1 to 1000 ppm, but can be used with higher humidity [4.20]. This sensor specifications are as follows [4.19]:

Approximate temperature range	-100 to 30 ^{0}C
Approximate uncertainty	±5%
Response time	Fast
Primary output parameter	Current

4.2.8 The heating system

In order to simulate the temperature in a building room, a heated tank of water was used. The appropriately insulated water storage tank, with a built-in electric resistance heater, maintains the temperature of the water at 75 ^{0}C. The hot water tank was placed at the far end of the test room to avoid excessive hot spots in the neighbourhood of the window undergoing tests. The mass of water in the tank helps to stabilise the temperature inside the room which can be automatically controlled at 20 ^{0}C by a thermostat. A convection heater initially used proved to be unsuitable owing to the large temperature fluctuations it produced.

Table 4.1 Calibration results for the 56 thermocouples used in the present experiments

T/C* No.	55** °C	69.5 °C	90.5 °C	T/C No.	56.5 °C	68.5 °C	91°C
1	55.2	70	90.9	33	56.4	68.7	90.7
2	55.2	70	90.9	34	56.5	68.8	90.8
3	55.2	70.1	90.9	35	56.5	68.7	90.7
4	55.2	70	90.7	36	56.6	68.8	90.8
5	54.9	68.8	90.6	37	56.6	68.8	90.9
6	55	69.9	90.7	38	56.5	68.8	90.7
7	55	69.9	90.7	39	56.4	68.7	90.6
8	54.9	69.8	90.6	40	56.5	68.7	90.7
T/C* No.	**45 °C**	**58 °C**	**88°C**	**T/C* No.**	**49 °C**	**57.5 °C**	**81°C**
9	45.2	58.2	88.5	41	49.1	57.5	81.1
10	45	57.9	88.2	42	49.2	57.6	81.6
11	45.1	58.1	88.7	43	49.1	57.5	81.3
12	45.1	58.3	88.7	44	49.1	57.6	81.4
13	45.2	58.2	88.7	45	49.1	57.6	81.3
14	45.1	58.3	88.5	46	49	57.3	81.2
15	45.1	57.9	88.3	47	49	57.3	81.1
16	45	57.9	88.4	48	49	57.3	81.1
T/C* No.	**53.5 °C**	**77.5 °C**	**90°C**	**T/C* No.**	**51 °C**	**59.5 °C**	**90.5°C**
17	53.7	77.6	90.2	49	51.2	59.4	90.3
18	53.8	77.7	90.1	50	51.2	59.6	90.7
19	53.7	77.5	90.1	51	50.9	59.4	90.3
20	53.8	77.7	90.7	52	51.3	59.7	90.7
21	53.9	77.7	89.9	53	51	59.5	90.6
28	53.7	77.7	90.2	54	51	59.5	90.7
29	53.7	77.6	89.8	55	50.9	59.5	90.5
30	53.7	77.6	90.1	56	51	59.4	90.3
T/C* No.	**38.5 °C**	**64 °C**	**90.5 °C**				
22	38.3	63.7	89.7				
23	38.6	64.5	90.7				
24	38.5	64.5	90.7				
25	38.5	64.5	90.7				
26	38.5	64.5	90.7				
27	38.5	64.5	90.7				
31	38.5	64.3	90.6				
32	38.5	64.5	90.7				

*** Thermocouple**

**** Reference temperature measured via a scientific mercury-in-glass thermometer**

4.2.9 The anemometer

For the experiments undertaken in the residential house, an anemometer type A100, manufactured by Vector Instruments [4.21] was used. It consists of a wind vane, mounting arm and an indicator. The anemometer can measure wind speeds from 0 - 50 m/s. The anemometer calibration was performed against the air conditioning unit (AC573/00445 supplied by P. A. Hilton Limited). The supply voltage and current for the anemometer are respectively 12 V DC and 30 mA. The anemometer is a highly sensitive but robust transducer in which the rotational speed of a 3-cup rotor is measured by means of an electronic pulse generator and rate meter. An analogue DC voltage is obtained which is linear with respect to wind speed.

4.2.10 The window samples

The window samples used in the present work were supplied by the Nor-Dan company of Norway in the form of glazing units. Each glazing unit consists of two glass panes separated peripherally by an aluminium spacer and enclosing a gas within the cavity so formed. Different double glazed window designs have been tested. This range of windows covers most of the double glazed window designs which are used in industry.

Table 4.2 shows the specifications of the double glazed windows used, listed in descending order of their U-values. Reference to this table, it is clear that the windows may be divided into 2 broad groups, i.e. those which have a U-values below 2 W/m^2K and others with U-values around 2.8 W/m^2K. Thus it was decided to classify the first 2 windows as low-tech and the remaining ones as high-tech.

For all window samples, the glass thickness was 4mm, which is the most commonly used thickness. The window edge spacers are usually made of aluminium but are thermally broken to avoid excessive conduction heat transfer. A detailed cross section of double glazed window edge-seal is shown in Fig. 6.1 of Chapter 6.

Most gases used for filling multiple glazings are inert gases such as argon, krypton and xenon. They have the advantage of not reacting to form other compounds in normal conditions. They are harmless to human beings. However, krypton has a very low radioactivity level. Because the above inert gases are denser than air, they also reduce noise transmission.

Another window sample was constructed in the university laboratories as an innovative development [4.22]. It is now at a patent pending stage. This innovative window consists of two 600-mm square panes of glass separated by a wooden edge spacer. The 20 mm wide cavity formed by the two panes and the wooden spacer is filled with air. A 50-mm high glass baffle is placed mid-way in the cavity on the bottom spacer as shown in Fig. 4.2. This baffle plate helps in suppressing natural convection of infill gas within the window cavity, thus reducing the heat loss from the window or in other words, improving the window U-value

4.3 The measurement schedule and procedure

The measurements started in winter 1995, and ended in early 1997. Measurements were divided into three parts. The first part was conducted in the test room during winter 1995 where the temperature distribution along the vertical centreline of the inner pane for each window was measured. Eight windows were tested in this part of experiments, the six windows shown in Table 4.2 and the innovative window with and without the baffle. Each window in Table 4.2 was tested for an average period of two days. The innovative window 4-air20-4 with baffle was tested for seven days and without baffle for nine days. The second part was conducted in the experimental house during winter 1996 where internal air temperature and relative humidity of the house, the external ambient temperature and wind speed were measured hourly for a period of one month approximately. The third part was conducted in the test room during winter 1996 where the temperature distribution on the right-hand half of inner pane surface for only two

Table 4.2 Window configurations used in the present work

Window No.	Trade Name	Design Details	U_{ref}[1]
1	**4-Air12-4**	4-mm float glass + 12-mm Air gap + 4-mm float glass	2.86
2	**4-Ar12-4**	4-mm float glass + 12-mm Argon gap + 4-mm float glass	2.72
3	**4-Air12-E4**	4-mm float glass + 12-mm Air gap + 4-mm low emissivity coated glass	1.83
4	**4-Ar12-E4**	4-mm float glass + 12-mm Argon gap + 4-mm low emissivity coated glass	1.53
5	**4E-Kr12-E4**	4-mm low emissivity coated glass + 12-mm Krypton gap + 4-mm low emissivity coated glass	1.14
6	**4E-Xe10-E4**	4-mm low emissivity coated glass + 10-mm Xenon gap + 4-mm low emissivity coated glass	0.91

1. U_{ref} : The reference U-value, calculated at the glazing centre with T_i=20° and T_o =0 °C ($W/m^{2o}C$)[14]

window samples (numbers 1 and 6) in two dimensions, i.e. along the height and width of the inner pane was measured.

The detailed measurement schedule for the first part of the experiments is shown in Table 4.3 below.

Table 4.3 Measurement details for the first part of the experiments

Window Sample	Start of Experiment	End of Experiment
4E-xe10-E4	05/12/1995@ 16:32 HRS 12/12/1995 @ 16:48 HRS	06/12/1995@ 06:44 HRS 13/12/1995 @ 06:53 HRS
4E-kr12-E4	06/12/1995 @ 16:40 HRS 13/12/1995 @ 17:11 HRS	07/12/1995 @ 06:33 HRS 14/12/1995 @ 06:56 HRS
4-arg12-E4	07/12/1995 @ 15:50 HRS 14/12/1995 @ 16:41 HRS	08/12/1995 @ 06:36 HRS 15/12/1995 @ 05:44 HRS
4-arg12-4	08/12/1995 @ 16:10 HRS 16/12/1995 @ 15:28 HRS	09/12/1995 @ 06:50 HRS 18/12/1995 @ 05:49 HRS
4-air12-4	09/12/1995 @ 16:48 HRS 19/12/1995 @ 14:14 HRS	10/12/1995 @ 05:48 HRS 20/12/1995 @ 05:53 HRS
4-air12-E4	10/12/1995 @ 16:14 HRS 20/12/1995 @ 16:00 HRS	11/12/1995 @ 06:48 HRS 21/12/1995 @ 06:53 HRS
4-air20-4 without baffle	21/12/1995 @ 15:25 HRS	29/12/1995 @ 05:31 HRS
4-air20-4 with baffle	29/12/1995 @ 10:40 HRS	4/1/1996 @ 05:59 HRS

As this table shows, most window tests were conducted in winter time in order to obtain higher temperature gradients between the inside and outside environments. Greater temperature gradients are essential for obtaining better results for the temperature distribution on window inner panes.

The purpose of the first part of the experiments was to measure and investigate the temperature distribution along the vertical centreline of each window, and to use these

experimental data to develop a model that can be applied in calculating the temperature at any location along the vertical centreline of the inner pane.

To achieve good results from these experiments, the following procedure was followed:

A. The room heating system was adjusted to maintain the internal temperature of the test room at 20 ^{0}C during the experiment period.

B. All exposed surfaces of the window samples were carefully cleaned and dried.

C. Twelve positions were marked and numbered on the inner pane and two positions on the outer pane of each sample. Figure 4.3a shows the measurement positions on the inner pane of all the window samples. From this figure, it can be seen that more positions (finer mesh) were marked at the lower part of the inner pane because appreciable changes in temperature were expected. This region is of great concern in this project as condensation usually starts there. Less positions (coarser mesh) were marked for the remaining window height.

   Since, the outer pane was not the subject of attention in this work, and as it would be logical to assume that the forced convection on the outer pane would be significantly higher, only two thermocouples, one at the top and the other at the bottom end of the outer pane were used. These positions are shown in Fig. 4.3b. Future work may involve use of more thermocouples to measure the outer pane temperature in a finer grid.

D. The window to be tested was then installed in place.

E. Sixteen calibrated thermocouples were selected for measurements. They were tagged at both ends to facilitate their recognition and for the sake of querying abnormal readings. Tag numbers from 1 to 16 were given to the thermocouples as follows:

1 to 12	for interior pane longitudinal temperatures, starting from the bottom of the window glazing
13	for outside air temperature
14	for inside air temperature
15	for exterior pane bottom temperature
16	for exterior pane top temperature

F. Thermocouples 1 to 12 were attached to their corresponding marked positions on the inner pane. Thermocouple 13 was fitted outside the test room and its measuring point was placed 10 cm away from the outer pane centre. Thermocouple 14 was fitted inside the test room and positioned such that its measuring point was 10 cm away from the inner pane centre as shown in Fig. 4.3c. Thermocouples 15 and 16 were attached to their corresponding positions marked on the outer pane.

G. The other end of each thermocouple was connected to its corresponding data-scan channel which carry the same number as the thermocouple.

H. The data-scan was connected to the host computer. Before starting the RS-Recorder, a configuration file was created. This file defines the type and number of data-scan units connected to the system, the set-up of each individual data-scan channel and the communications parameters associated with the data-scan. After completing the configuration, the file was saved into the computer hard disk. Finally, the RS-Recorder might be started under two options. The first one is to start the RS-Recorder scanning the data-scan at the specified rate. The second option allows the user not only to scan the data-scan and display the data but to also log the data to disk in a suitable format for post analysis in a spreadsheet.

Measurements were carried out for each individual window sample over the periods shown in Table 4.3 above. The data-scan logged a set of data (16 readings) for each tested window every 10, 15, or 20 minutes. The experimental data for each window sample was saved in an Excel spreadsheet. In order to avoid solar radiation effects on

the instability of the temperatures obtained, only night readings (from 18:00 HRS till 06:00 HRS) were considered for analysis. An abstract from this experimental data for the window samples shown in Table 4.2 is given in Appendix A.

The second part of the experiments was undertaken in the house mentioned previously. Air temperature measurements were undertaken at the bedroom's mid-height at four locations using four calibrated thermocouples. Four readings for external air temperature were also undertaken. The humidity probe was fitted inside the room. The anemometer was also installed outside the house. Measurements were recorded hourly for the period from November 18, 1996 to January 4, 1997, this being the coldest period in Edinburgh. The purpose of these experiments was to assist the development of a model that can be used in assessing the frequency of condensation occurrence on double glazed windows.

The procedure followed to perform these experiments was as follows:

A. Three data loggers, also called squirrels, were set up to be used in the acquisition of the experimental data. The operation and set up procedure for these squirrels is given in the working instructions [4.16]. These squirrels were as follow:

   a) Data logger 1000
   b) Data logger 1250
   c) Data logger 8-Bit

B. Four calibrated thermocouples were installed at bedroom's mid-height at four different locations to measure four internal ambient temperature readings inside the bedroom. These thermocouples were connected to data logger (a).

C. Another four calibrated thermocouples were used outside the bedroom to measure four external ambient temperature readings. These thermocouples were also connected to data logger (a) .

D. The humidity probe was installed inside the bedroom to measure the internal relative humidity and connected to data logger (b).

E. The anemometer was installed outside the house, 5 m above the ground. Its supply current was provided form the house mains. The anemometer was connected to data logger (c) which records the analogue DC voltage output from the anemometer. This reading can be multiplied by a factor to obtain wind speeds in m/s.

The three data loggers were set up to record hourly measurements for internal ambient temperature (4 readings), external ambient temperature (4 readings), internal relative humidity (1 reading), and wind speed (1 reading). Thus for every hour, a set of 10 readings was recorded by the three data loggers.

The experimental data were then conveyed from the data loggers to computer hard disk and saved as an Excel spreadsheet. Because condensation normally occurs on windows in the early morning hours, being the coldest period of the day, only measurements for the period from midnight to 6 a.m. were used for analysis. An abstract of this experimental data is shown in Appendix B.

Visual observations for the condensation occurring on the window of the experimental room were recorded. The condensed water usually forms a pattern that is broad at the bottom edge of the glazing and has narrow webs at both sides of the glazing. The height of the bottom pattern from the edge-seal was measured daily at 06:00 hours. Table 4.4 shows these measured results.

The third part of the experiments was undertaken in the test room during winter 1996. This part was an extension of the experiments performed in the first part. Measurements of the temperature distribution on the inner pane in two dimensions, i.e. along the height and width of the inner pane were undertaken. Only the two extreme windows in Table 4.2, i.e. numbers 1 and 6 were tested. The purpose of these experiments was to investigate the effects of the side and top edge spacers on the temperature distribution of

Table 4.4 Condensation height measured on the double-glazed window of the experimental room at 06:00 hours

Date	Condensation height, mm
22/12/1996	90
23/12/1996	47
24/12/1996	24
25/12/1996	22
26/12/1996	14
27/12/1996	20
28/12/1996	0
29/12/1996	21
30/12/1996	18
31/12/1996	14
01/01/1997	5
02/01/1997	20
03/01/1997	18
04/01/1997	38

the inner pane and to try to develop a three dimensional model that can be used in assessment of the temperature of the inner pane at any location.

The procedure followed in conducting these experiments was the same as that mentioned above for the first part of experiments. In this part the surface of the inner pane for each window was divided into zones. Each zone was represented by a node as shown in Fig. 4.4. From this figure it can be seen that because of symmetry only the right half of the inner pane was considered which was divided into 48 nodes numbered as shown in Fig. 4.4. Calibrated thermocouples were attached at these nodes and two other thermocouples were used to measure the external and internal ambient air temperatures. For all these thermocouples (50 thermocouples) used in measurements, two data-scan modules providing 32 channels and three data loggers providing 18

channels were needed. The two data-scan modules were connected to the computer located in the test room. Each window was tested for two days. Every five minutes 50 measurements were taken by the two data-scan modules and the data logger. The experimental data collected was saved into the computer hard disk as Excel spreadsheets. An abstract of this data is shown in Appendix C.

4.4 Test results

First part of the experiments:

Figure 4.5 shows a plot of one set of measured data for window number 5 (see Table 4.2). It shows that the temperature along the vertical centreline of the window inner pane increases as the height increases. It also shows that there is a decrease in temperature both at the bottom and top edges of the window. The same result was obtained from all window samples. However, the variation of temperature along the height differs from one window to the other. Figure 4.6 shows a comparison between the top and bottom temperatures of the outer pane for the same window. As can be seen from Fig. 4.6, the temperatures of the positions under consideration show near uniformity. However, for obtaining a complete picture future work may involve use of more thermocouples to measure the outer pane temperature in a finer grid.

Second part of the experiments:

From the experimental data of this part, values of T_i at 0600 hours are plotted against their corresponding values of T_o. One such plot is shown in Fig. 4.7. The choice of the hour was made due to the fact that this represents the time at which T_o acquires the minimum value and before the bedroom heater is switched on.

The measured values of relative humidity have been plotted for all days. Figure 4.8 shows one such plot for ten nights data. Only relative humidity values from mid-night

until 06:00 hours, i.e. the period of nocturnal cooling down of the bedroom have been plotted.

Third part of the experiments:

Figures 4.9a and 4.9b show one set of the measured data for window samples 1 and 6 respectively. These figures give the temperature distribution on the right-hand half of the surface of the inner pane. It can be seen from Figs. 4.9a and 4.9b that the temperature of the inner pane increases with window height. This increase is on average of 2.5 ^{0}C for window number 1 and 3.8 ^{0}C for window number 6. However, there is a slight drop in temperatures at the top and bottom edges. It can also be seen from these figures that the pane temperatures changes are very slightly in the horizontal direction with a slight drop at the edge.

4.5 Results and discussion

4.5.1 Figure 4.5 demonstrates the interplay of the two factors which determine the longitudinal temperature variation on the inner pane of a double glazed window. These are:

(a) The circulation of gas within the enclosure, alternating between the hot and cold sides. This is the dominant factor and it is responsible for the rise in the temperature along the height. The infill gas in the sealed space flows upward near the indoor glazing and downward near the outdoor glazing. The descending gas becomes progressively colder. At the bottom of the cavity this cold gas turns and comes into contact with the bottom of the indoor glazing. This has also been demonstrated by Frank and Wakili [4.23]. The effect of the circulating gas on the temperature of the edge-seal of double glazed windows has been also addressed by Wright and Sullivan [4.24]. This phenomenon will be studied in detail in Chapter 5.

(b) The conduction effects due to the metallic spacer which acts as a thermal bridge between the cold external environment and the warm internal environment. The cold bridging effect of the spacer is the reason for the temperature drop at the bottom and top edges of the glazing. In Chapter 6, a two-dimensional model that involves cold bridging effects of the edge-seal on the temperature distribution of inner pane surface has been developed.

In order to compare the temperature variation in diverse window configurations with disparate geometry, internal temperature and external weather conditions, two dimensionless parameters T* and Y* are introduced.

$$T^* = \frac{t_i - T_o}{T_i - T_o} \qquad 4.1$$

$$Y^* = \frac{Y}{H} \qquad 4.2$$

where,

H	height of the arbitrary point from the window bottom edge, m
T*	dimensionless temperature
t_i	temperature of the inner glass pane at an arbitrary point, ^{0}C
T_i	the internal ambient temperature, ^{0}C
T_o	the external ambient temperature, ^{0}C
Y*	dimensionless height

Figure 4.10 shows the T* band-width containing two-thirds of the entire data set (mean ± standard deviation) for window number 5. This plot shows significant scatter of data, primarily resulting from varying external weather conditions, i.e. rainy or dry, calm or windy, overcast or clear conditions. Figure 4.11 shows the complete range of T* obtained from the experimental data of the window samples. This figure shows only the temperature stratification along the inner glazing height, i.e. the bottom and top edges effects on temperature were ignored by discarding one measurement at the top and 2

measurements at the bottom. Since the focus of attention was the bottom end of the window, more thermocouples were attached at that region. It was found that no general statistical analysis could be undertaken for the modelling of the temperature profile along these lines , i.e. relating T* to Y*. Rather a semi-analytical physical model was developed which proved to be extremely fruitful. This model is explained in Chapter 5.

From Fig. 4.5, it can be seen that the temperature variation between the highest and lowest temperatures that occur on the centreline of the inner pane surface of window number 5 is about 4.5 °C. This variation increases with decreasing U-value. This observation can be explained as follows. The indoor centre-glazing temperature increases and the outdoor pane temperature decreases with the decrease of U-value due to increased cavity thermal resistance. As mentioned previously in section 4.5.1 (a), the descending in-fill gas would approach the temperature of the cold outer glazing. Thus, the bottom temperature of the inner pane also decreases with a lowered U-value. Therefore, the temperature variation will increase quite rapidly due to the combined effect of the elevated indoor glazing top temperature and lowered bottom temperature of the inner pane. This argument is strengthened by the modelling results in Chapter 6.

4.5.2 Figure 4.7 gives a relationship between T_i and T_o for the bedroom during the night-time cooling down period, i.e. when there are no solar effects, the heating system is switched off and the house is cooled down by the external environment. By knowing the external ambient temperature T_o, the internal ambient temperature T_i can be obtained using the regressed Equation 4.3,

$$T_i = 0.58T_o + 11.3 \qquad 4.3$$

The above relationship is valid only for the experimental room under discussion. However, relation such as Equation 4.3 may be easily derived for any given enclosure. Statistical t-test analysis has been applied to these data to check the confidence of this relationship.

$$t = \sqrt{n_d - 2}\left\{R / \sqrt{1 - R^2}\right\} \qquad 4.4$$

where,

n_d number of days for which data was collected (n = 35)

R correlation coefficient (R = 0.74)

t t-test statistic

The value of t was calculated from Equation 4.4 and found to be 6.23. This value suggests a strong relationship between T_i and T_o.

Building services professionals in the United Kingdom are showing an increased interest in the use of night-time natural ventilation for cooling as part of the current trend towards low energy building designs. Night ventilation in an occupied office can reduce the day time dry resultant temperature by up to 4 °C at the start of occupation compared with an office without night ventilation [4.25]. Thus the type of model, represented by Equation 4.3, can also be a useful tool for nocturnally cooled building design.

4.5.3 It can be seen from Fig. 4.8 that the relative humidity changes slightly within the cooling down period. This change is however, of a minor order night upon night. This is due to the thermal capacity of the building structure which dampens the influence of the changing weather over a short period of time.

4.5.4 The temperature distributions shown in Figs. 4.9a and 4.9b represent only one set of the measured data for window samples 1 and 6 respectively. From these figures, it is clear that the temperature of the inner pane increases with the increase of window height. As it can be seen from these two figures, there is an average increase of 2.5 ^{0}C between the highest and lowest temperatures along any vertical line in the case of window number 1 and of 3.8 ^{0}C in the case of window number 6. This confirms the phenomenon discussed earlier in point 'a' of section 4.5.1. It can also be seen from these figures that there is a slight drop in temperatures at the top and bottom edges which illustrates the cold-bridge effect of the edge-seal mentioned earlier in point 'b' of section

4.5.1. Figures 4.9a and 4.9b also show that the pane temperatures change very slightly in the horizontal direction with a slight drop at the side edges.

To examine the results stated earlier in this section, infra-red photographs were taken for the air-filled double glazed window of the experimental house and these are shown in Fig. 4.12. These figures show clearly the temperature distribution on the complete window. It is quite clear that the temperature drops towards the edge-seal.

References

4.1. Glass & Glazing Federation, London, UK

4.2. Centre for Window and Cladding Technology, CWCT Service Ltd, University of Bath, Claverton Down, Bath, UK

4.3. Advanced Glazing Industry Club, Advanced Glazing Technology Group, School of Engineering, Oxford Brookes University, Gipsy Lane, Headington, Oxford, UK

4.4. Building Research Establishment, Garston, Watford, UK

4.5. T. Muneer and B. Han, Heat transfer characteristics of multiple glazed windows: measured and modelled results, Proc. of the NORTHSUN'94 International conf., pp 389-394, Glasgow, [Eds: K MacGregor and C Porteous], Sept. 1994

4.6. R. Rayment, P. J. Fishwick, P. M. Rose and M. J. Seymour, A Study of Glazing Heat Losses and Trickle Ventilators, Building Research Establishment Occasional Paper, October 1992

4.7. H. F. Sullivan, J. L. Wright, Guarded Heater Plate Measurements in Support of Warm-Edge Technology, Proceedings of "Window Innovation'95, 1995

4.8. J. H. Klems, Method of Measuring Night-Time U-values Using the Mobile Window Thermal Test Facility, ASHRAE Transaction, Part 2, pp 619-629, 1992

4.9. D. I. Milburn, K. G. T. Hollands, The Measurement of Solar Optical Properties of Glazing Materials, Proceedings of Window Innovation'95, 1995

4.10. Department of Energy Efficiency, National Board for Industrial and Technical Development, NUTEK, Sweden, Technology Procurement of Energy-Efficient Window, 1991

4.11. B. D. Hunn, M. M. Grasso, A. M. Rewerts, M. A. Beaydry, An innovative shading fabric for improved daylighting and solar gain control, Proceedings of Window Innovation'95, 1995

4.12. D. Button and B. Pye, Glass in building: A guide to modern architectural glass performance, Pilkington Glass Ltd., UK, 1993

4.13. Datascan Installation and User Guide, Datascan Technology, Measurement Systems Ltd., UK, 1995

4.14. RS-Datascan 7200 User Manual, Datascan Technology, Measurement Systems Ltd., UK, 1995

4.15. RS-Recorder User Manual, Measurement Systems Ltd., UK, 1995

4.16. Grant Working Instructions, Grant Instruments (Cambridge) Limited, Barrington, Cambridge, UK

4.17. J.V. Nicholas and D. R. White, Traceable temperatures, DSIR Science Information Division, Wellington, 1982

4.18. BS 1041: Part 4, Guide to the selection and use of thermocouples, 1992

4.19. Heinz R. Trechsel, Moisture control in buildings, ASTM, 1994.

4.20. Handbook of Fundamentals, Chapter 13, ASHRAE, Atlanta, GA, 1989

4.21. Vector Instruments Shortform Catalogue, Rhyl, Clwyd, UK

4.22. Multi-glazed window unit, British patent application No. 9517511.3, 25 August 1995

4.23. Frank T and Wakili K Linear Transmittance of different spacer bars Proceedings of the Window Innovations' 95 Conference, Toronto, 5 and 6 June 1995

4.24. J. L. Wright and H.F. Sullivan, A Simplified Method for the Numerical Condensation Analysis of windows, Window Innovations'95, pp 429-438, 1995

4.25. B. Webb and P. Concannon, In the cool of the night, Building Services Journal, CIBSE, December 1996.

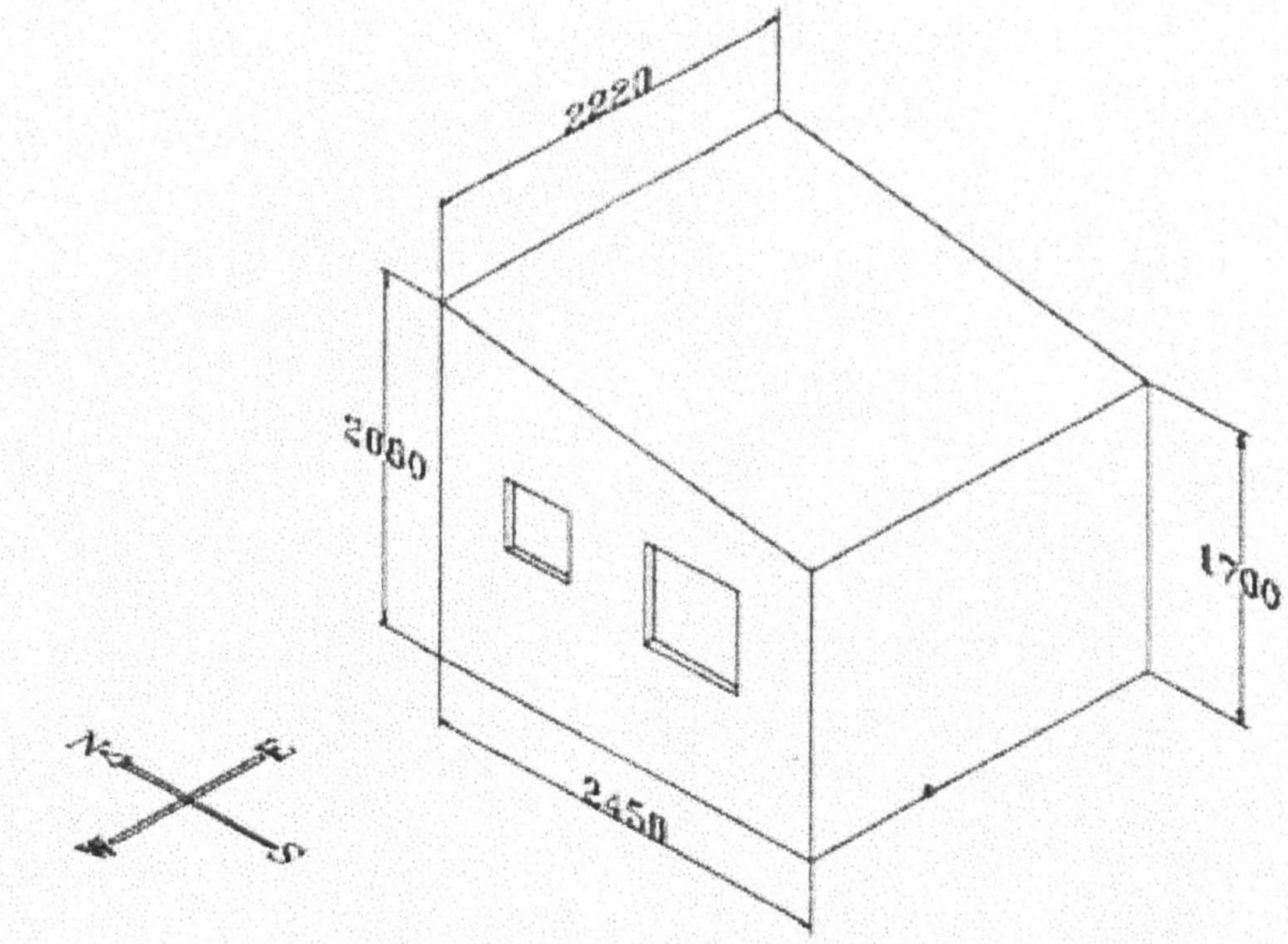

Figure 4.1a Dimensions of the test room

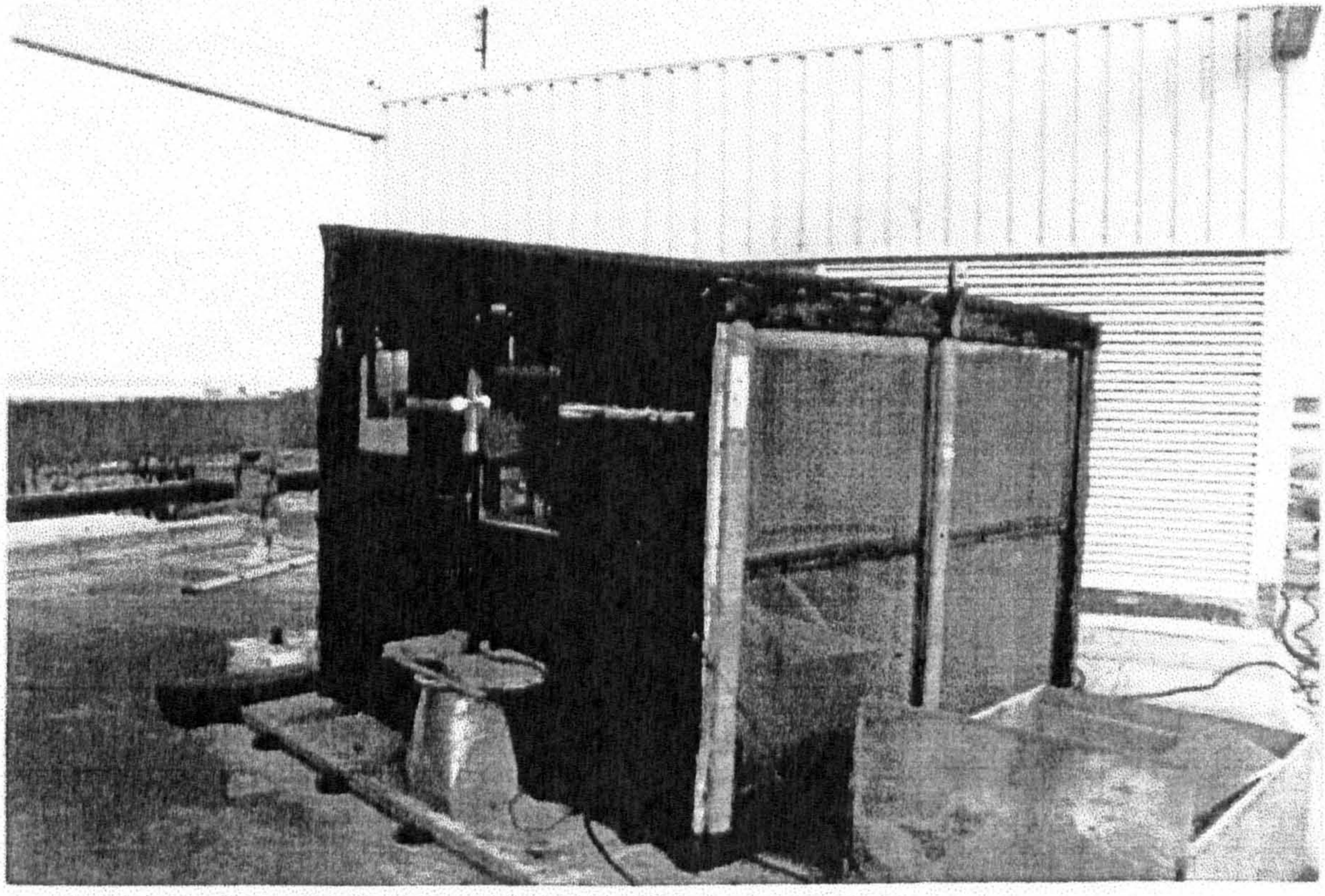

Figure 4.1b View of the test room

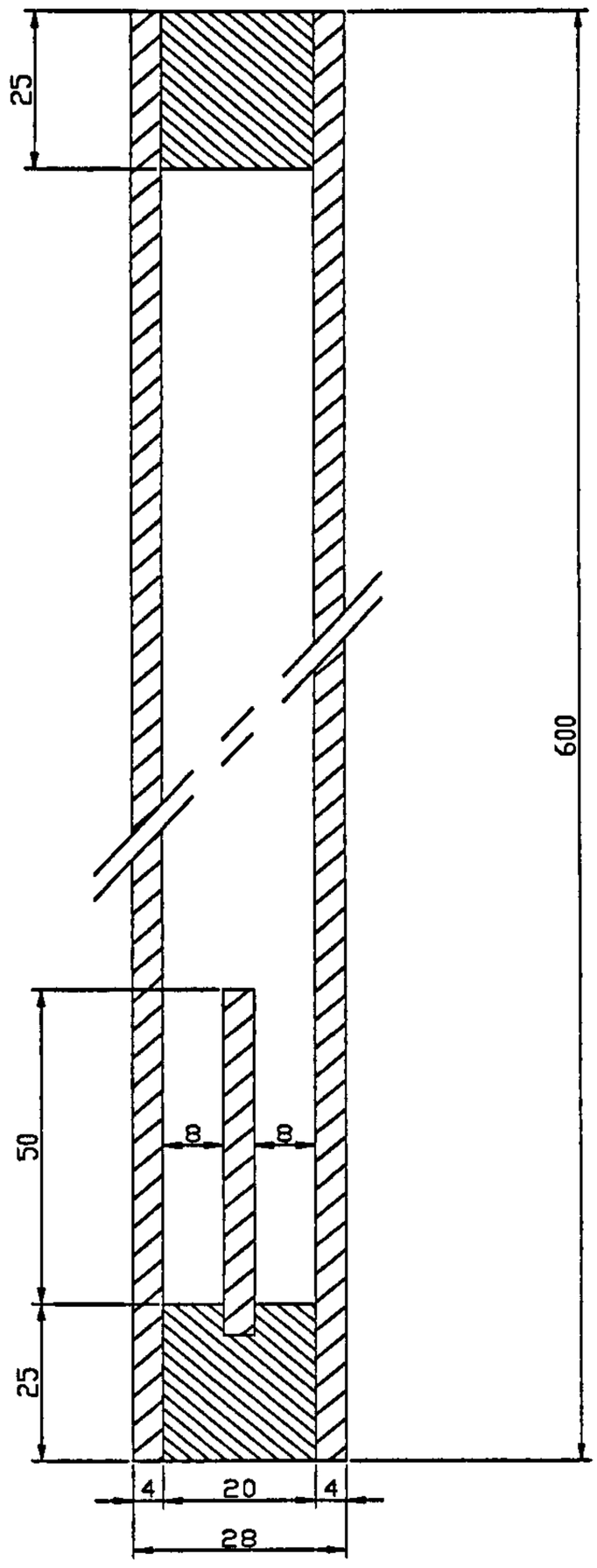

Figure 4.2 The cross section of a window with a 50mm high baffle plate.

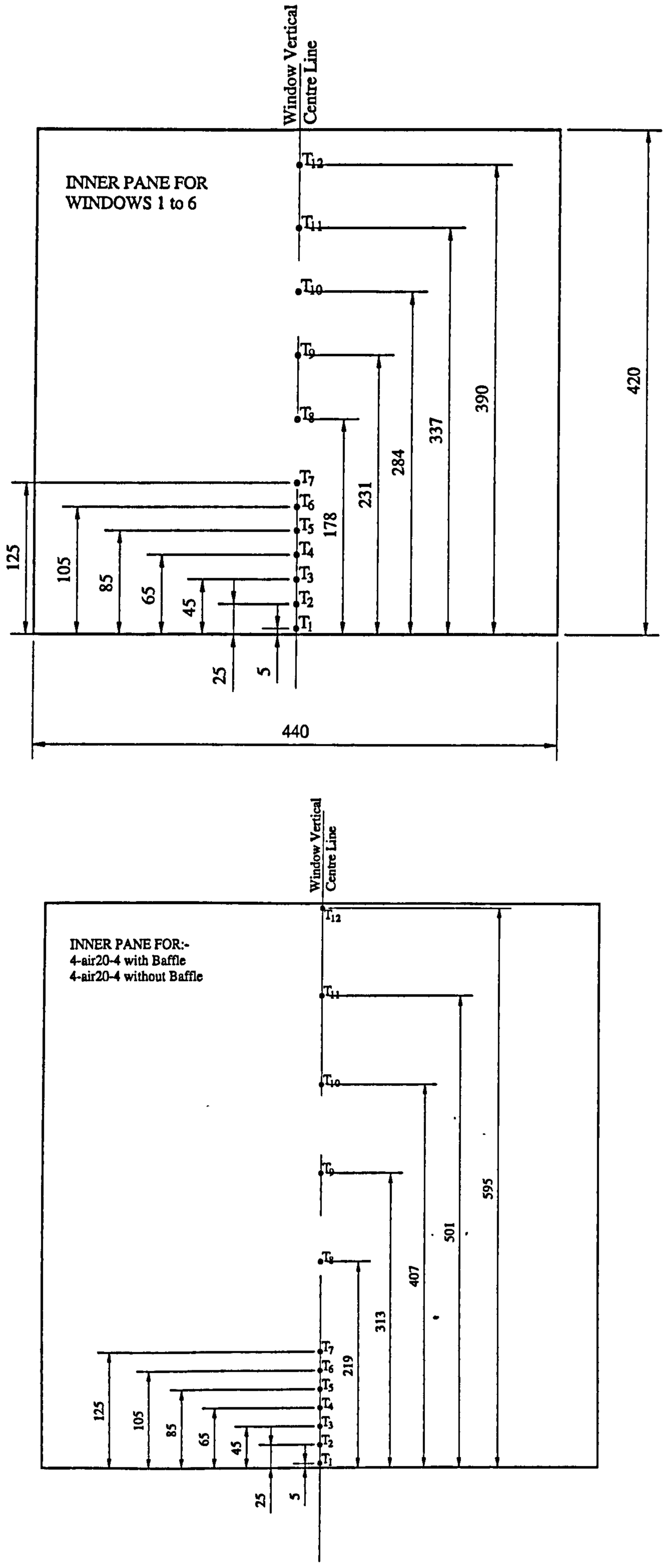

Figure 4.3a Measurement positions on the inner pane of the window samples

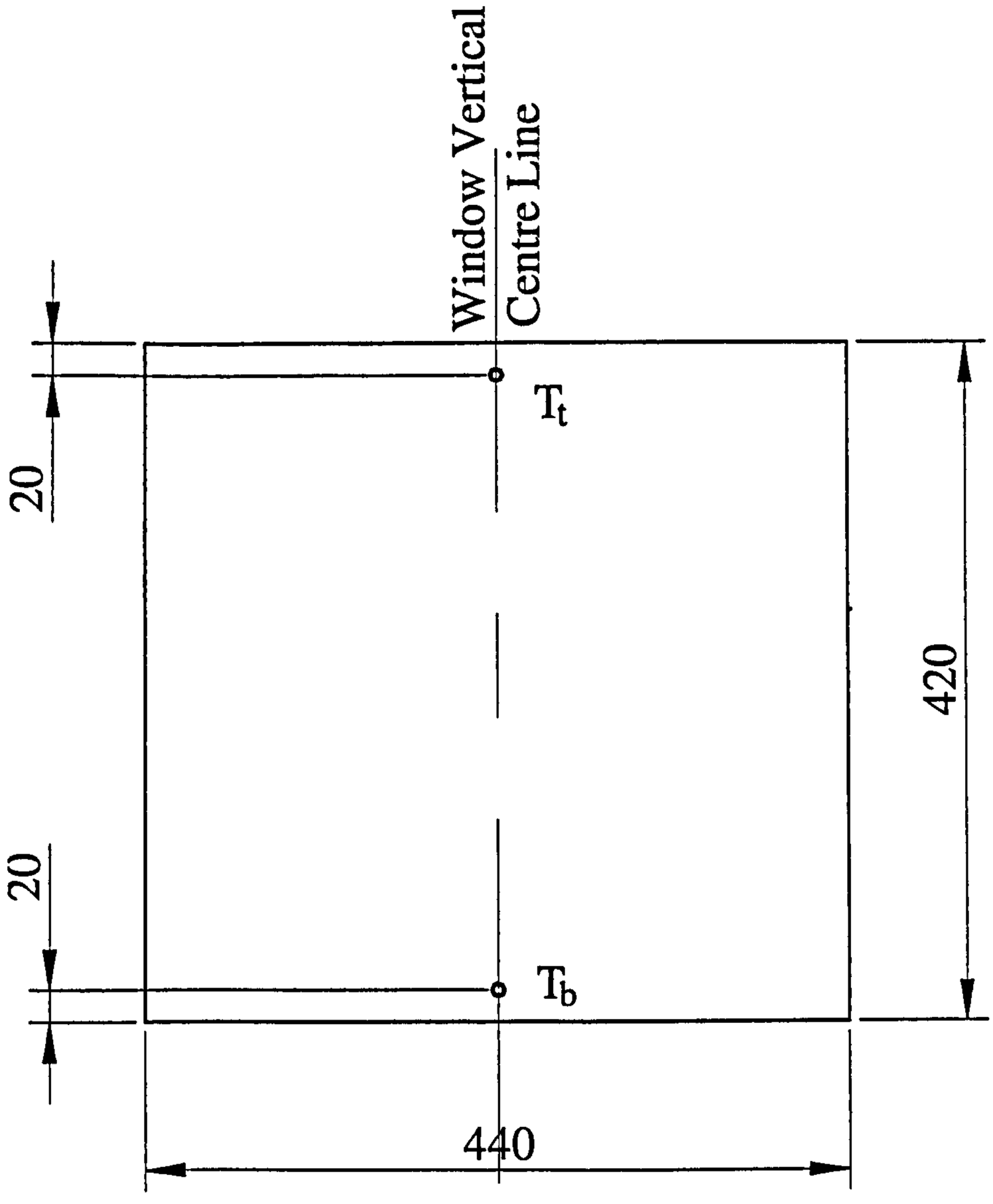

Figure 4.3b Measurement positions on the outer pane of the window samples

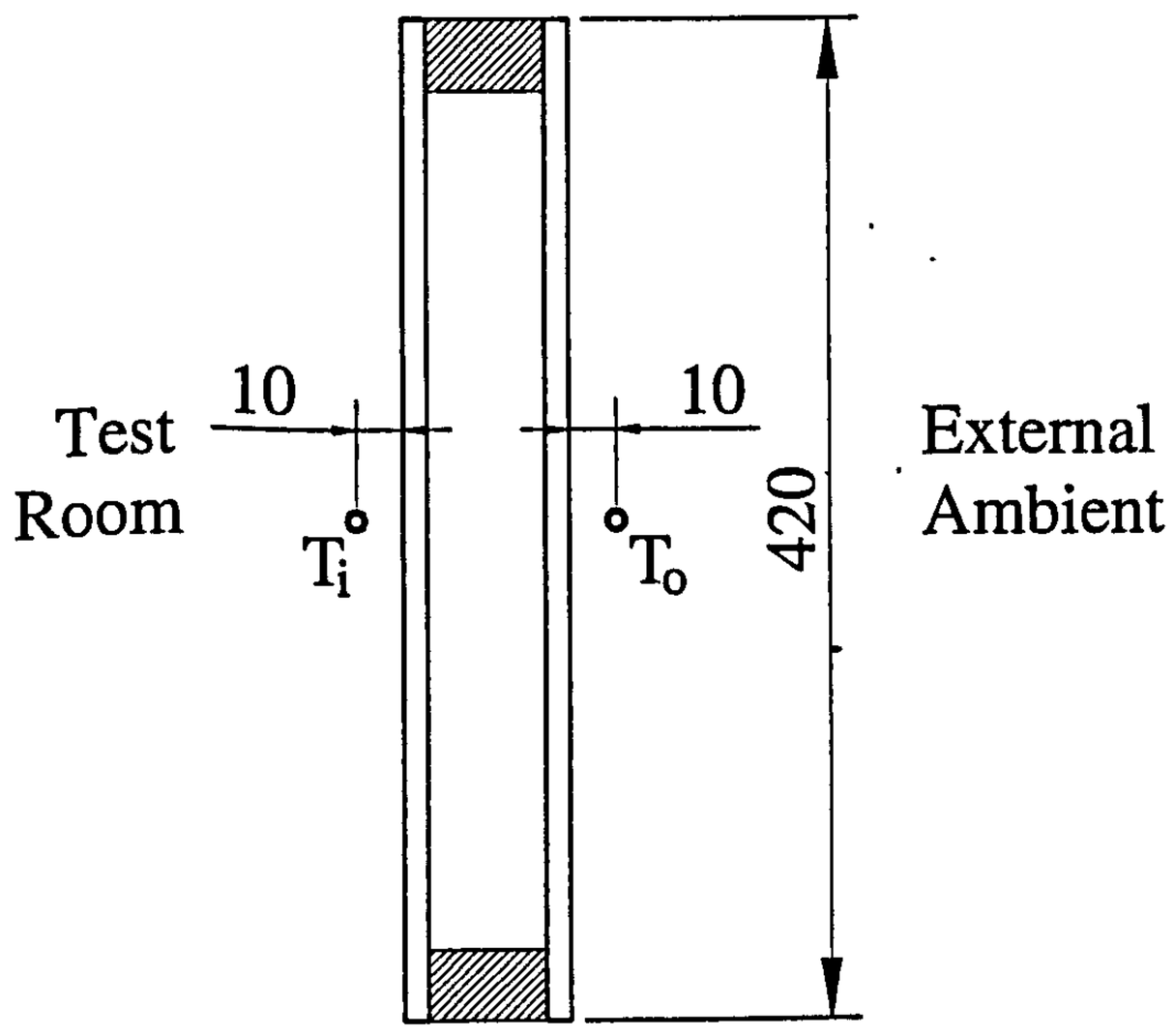

Figure 4.3c Measurement positions for internal and external air temperatures

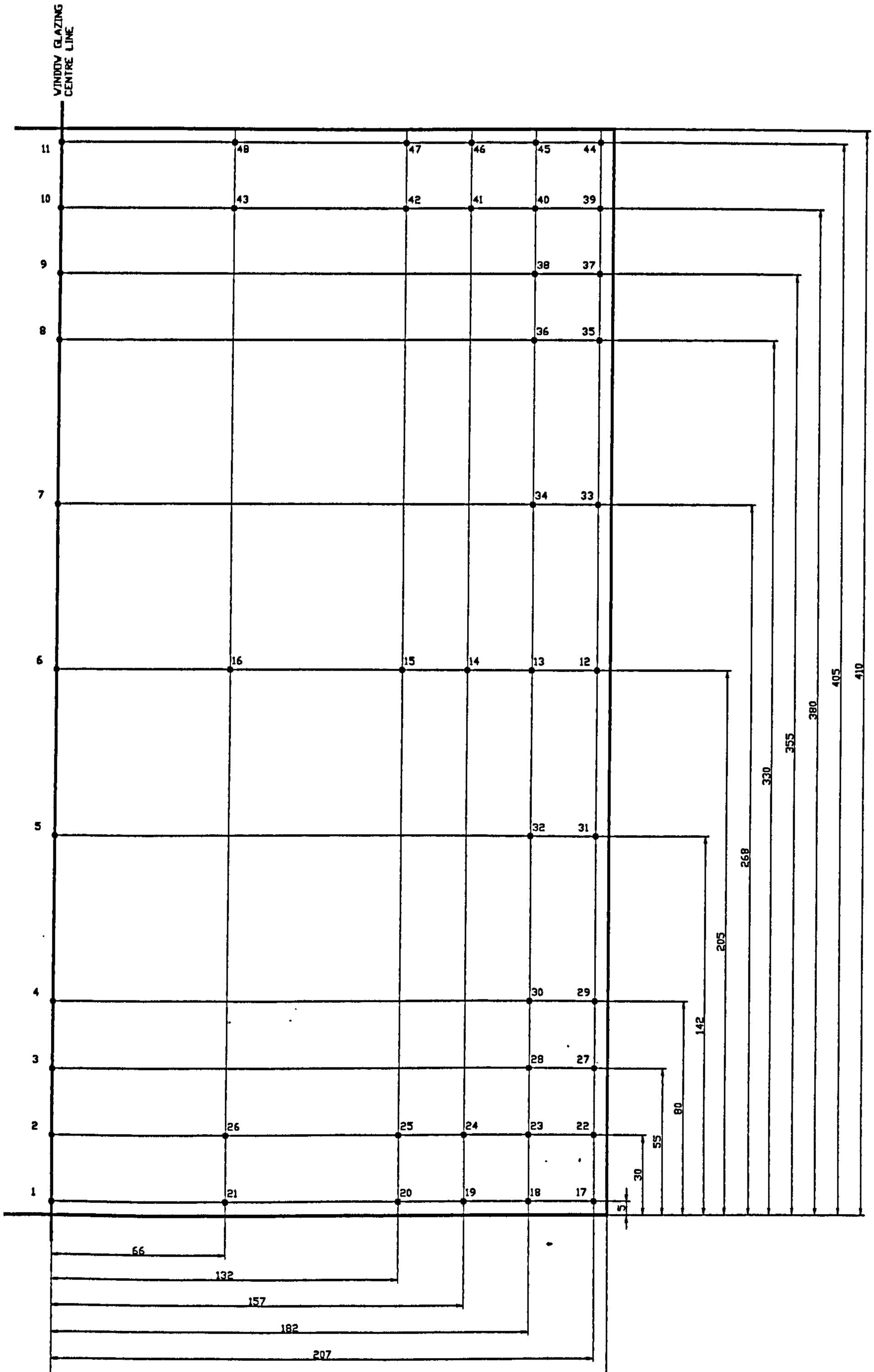

Figure 4.4 Locations for measurement on inner pane of double glazed window

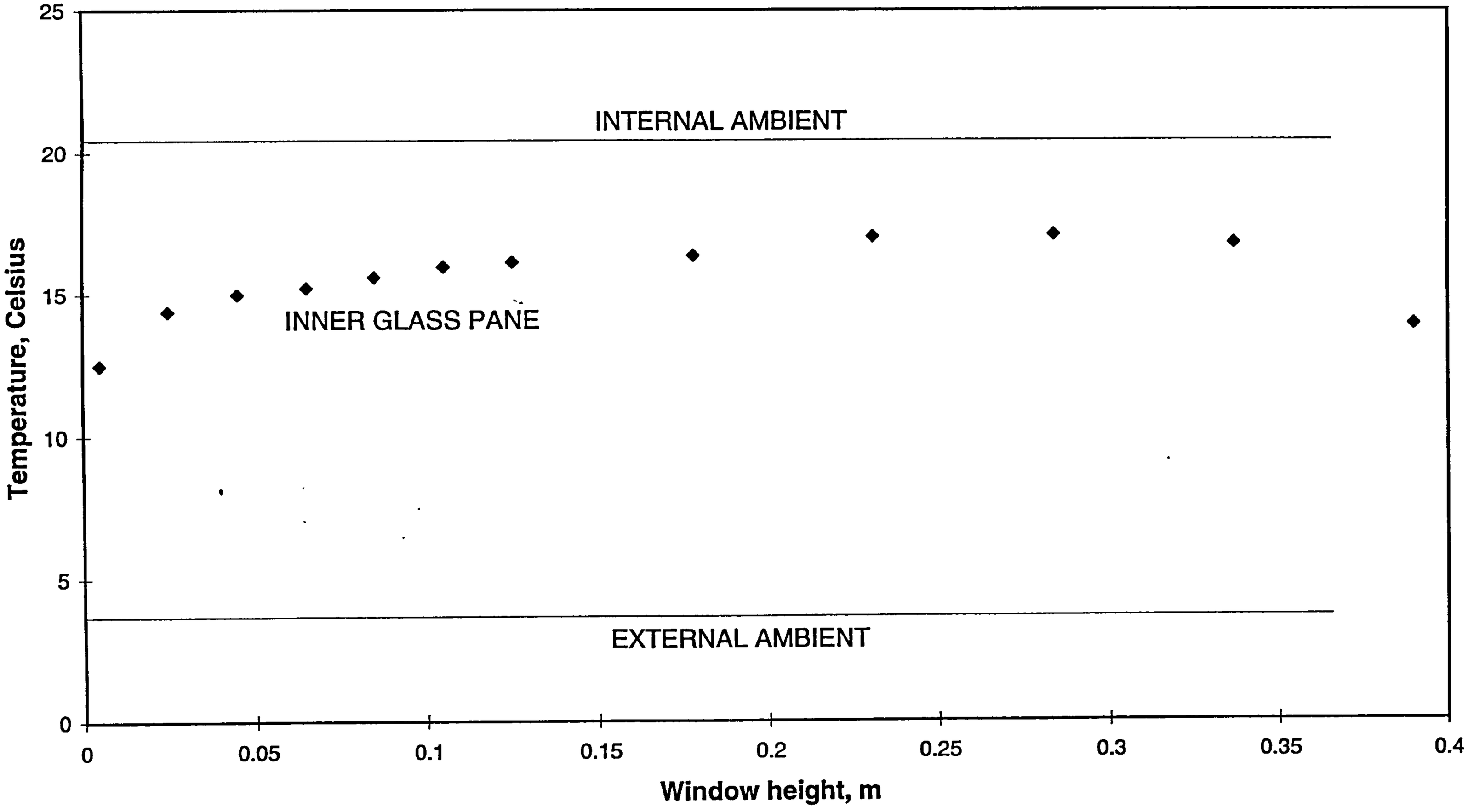

Figure 4.5 Temperature variation along window height - Krypton infill

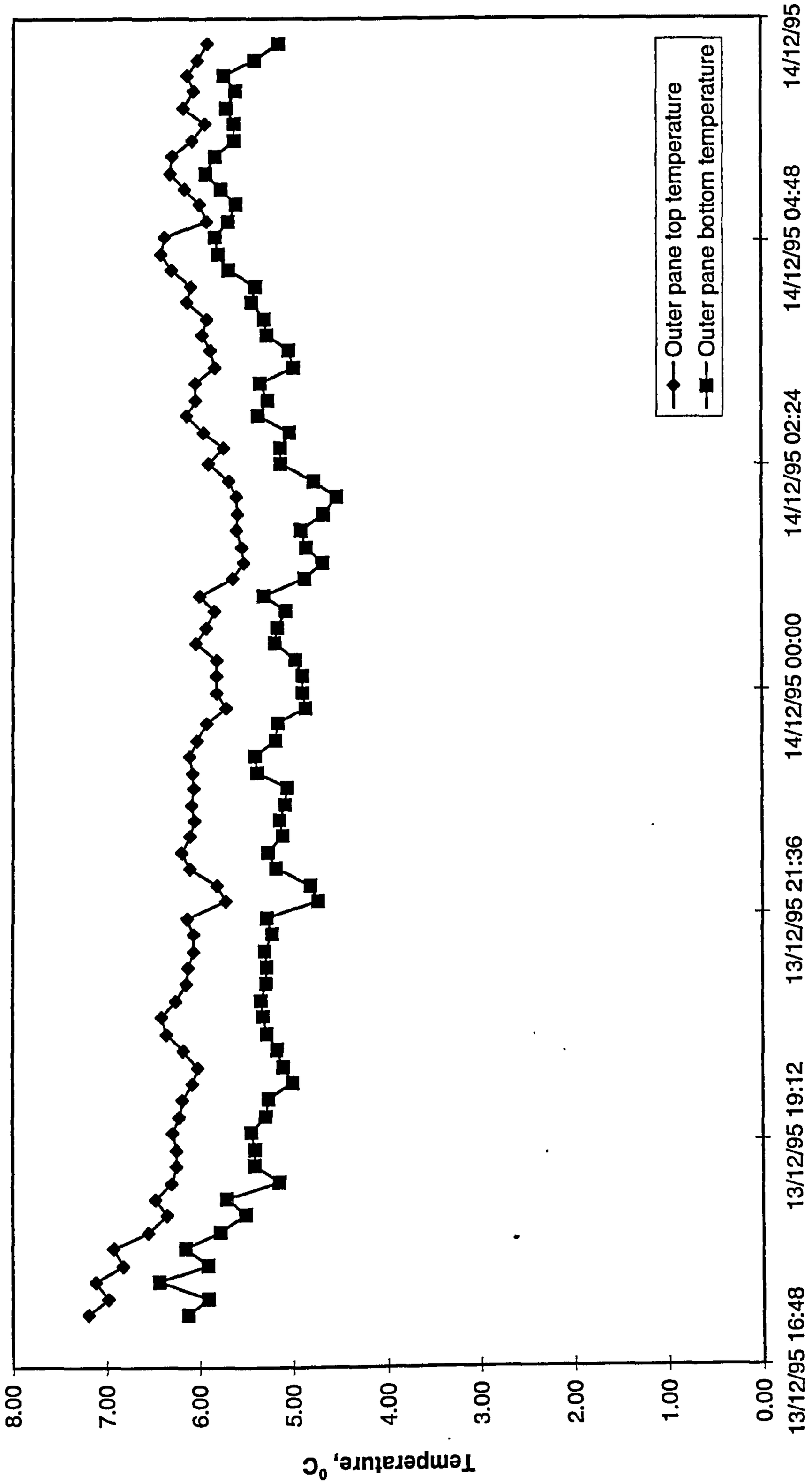

Figure 4.6 Temperature distribution on the outer pane of 4E-kr12-E4

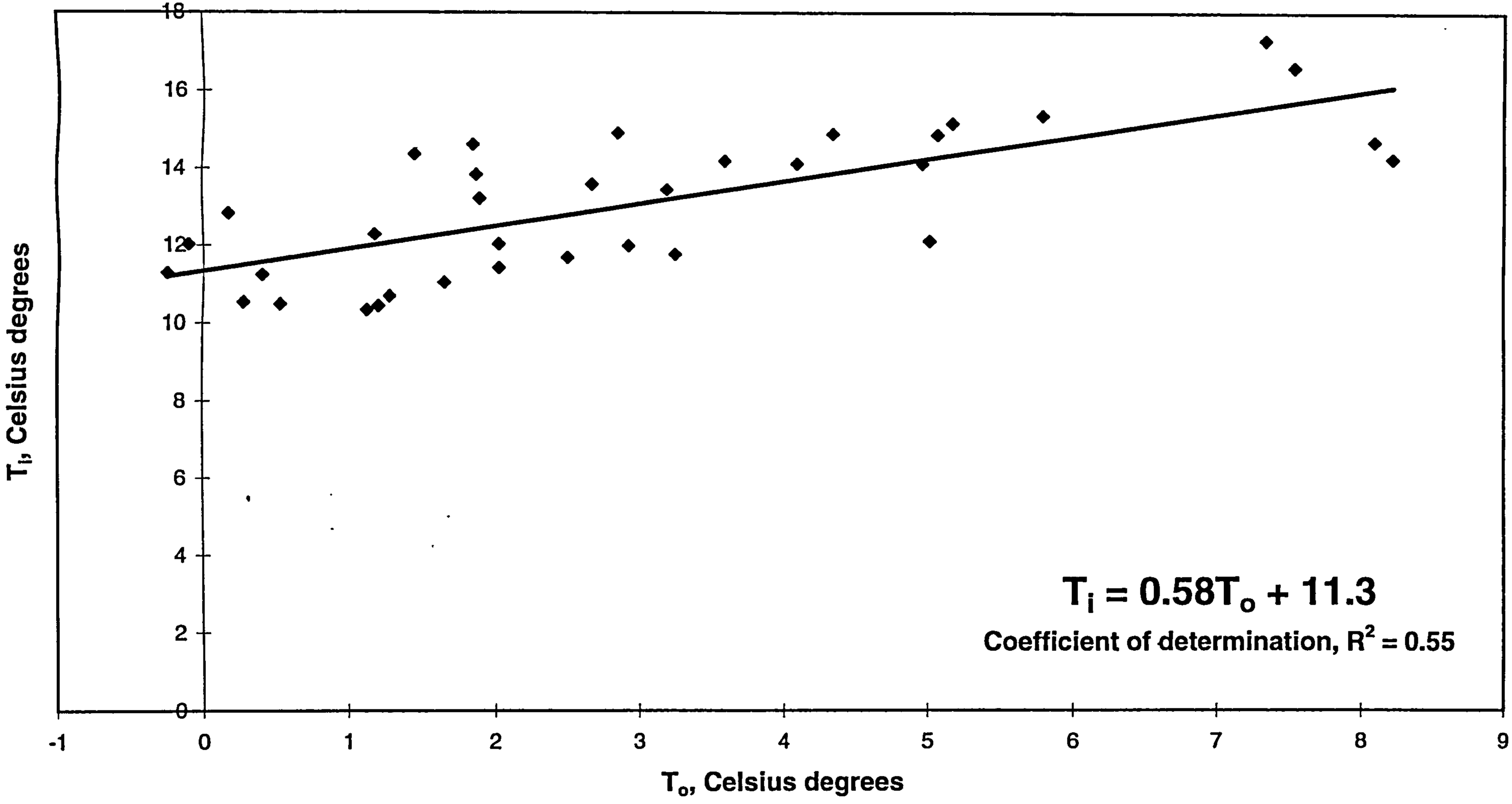

Figure 4.7 Nocturnal cooling performance of an occupied bedroom

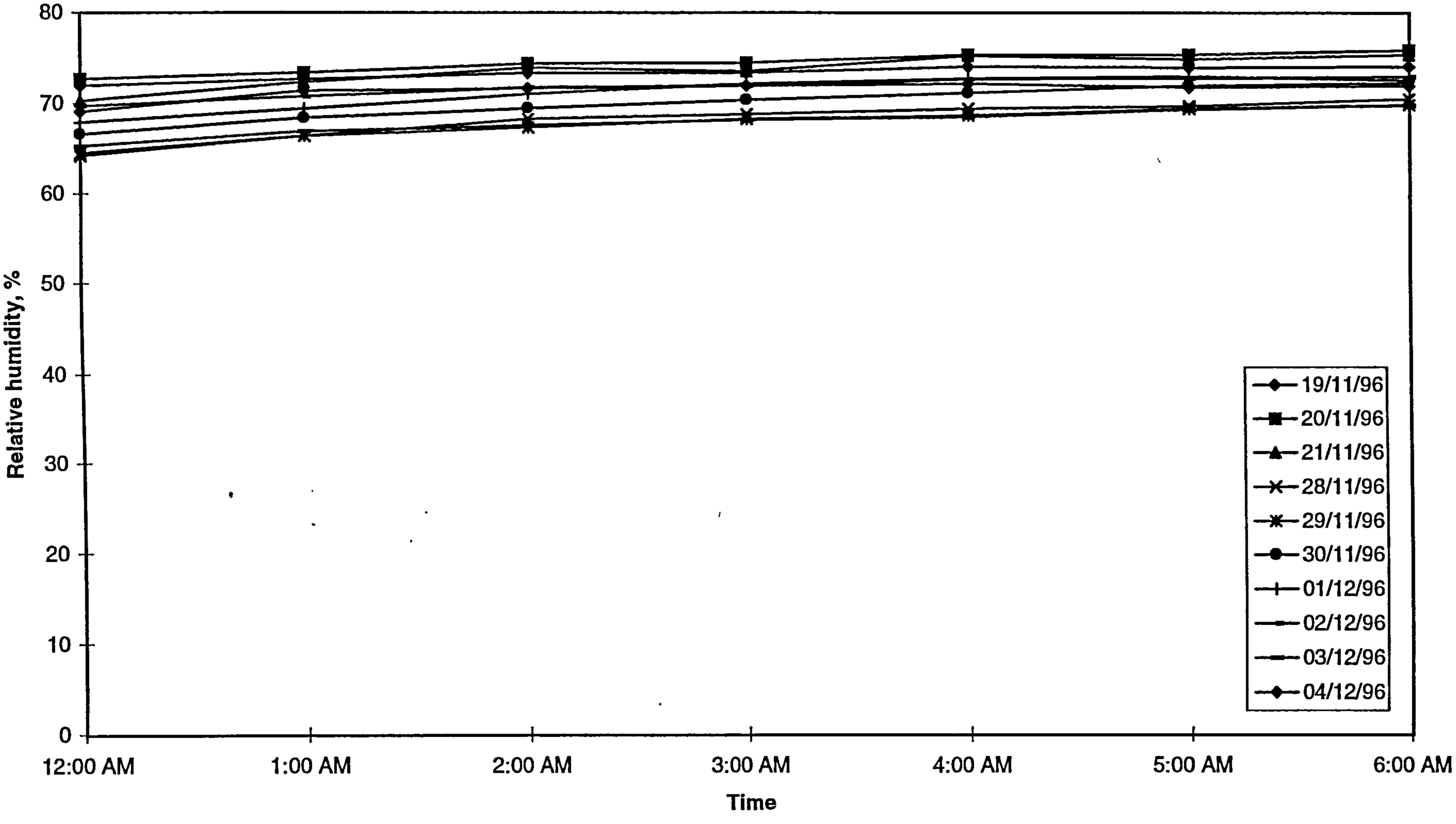

Figure 4.8 Nocturnal relative humidity for a single occupant bedroom

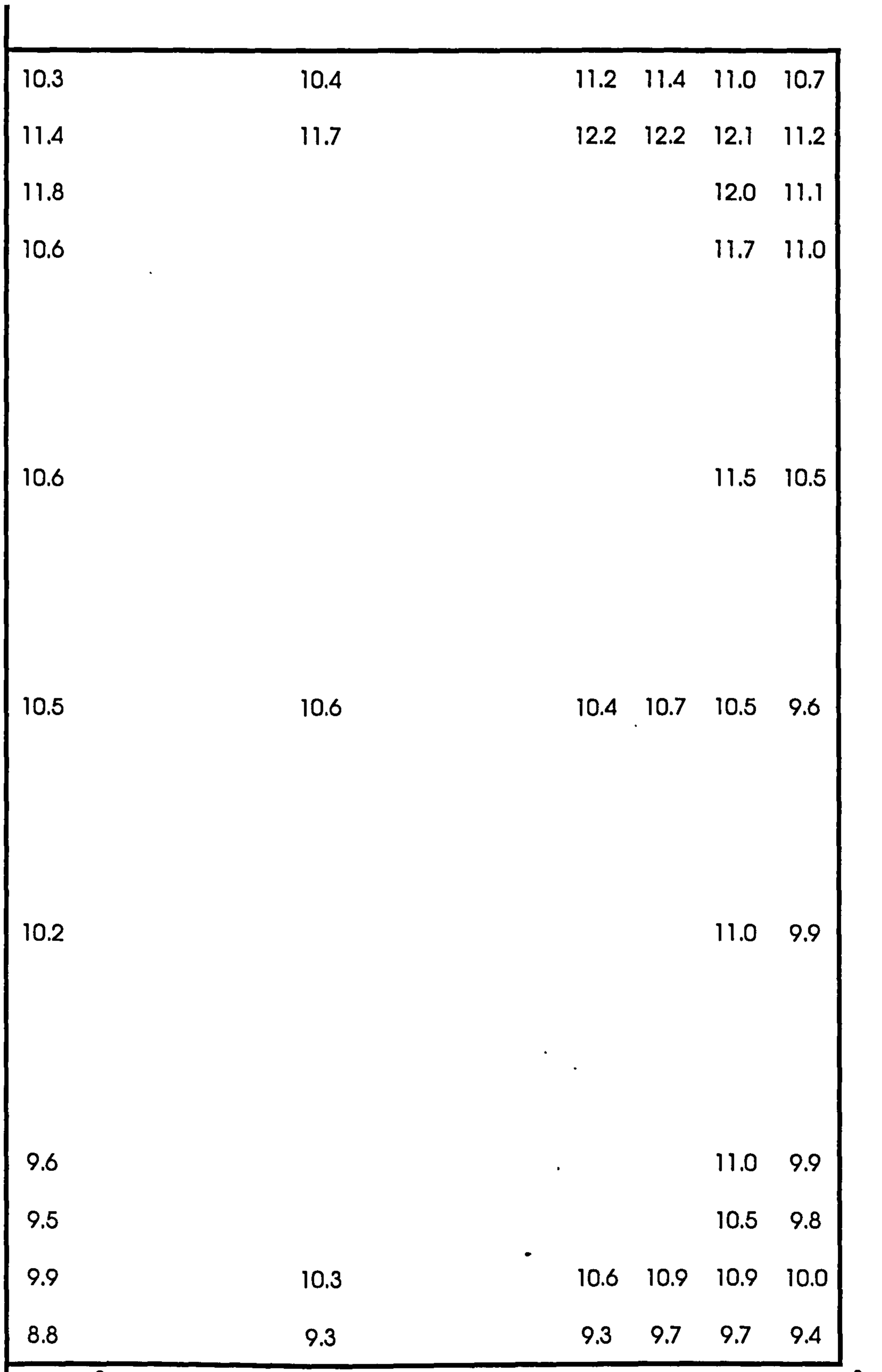

Figure 4.9a Temperature distribution for 4+Air12+4 inner pane (experimental data)

14.3	15.5	16.3	16.5	16.2	15.3
17.8	18.2	18.8	18.7	18.3	15.8
18.7				18.5	15.8
18.0				18.3	15.6
18.2				18.0	15.2
18.5	18.3	18.2	18.0	17.2	14.3
18.2				17.5	14.7
17.4				17.8	15.1
17.0				17.2	14.7
16.6	16.9	17.1	17.3	16.9	15.2
14.4	14.4	14.6	14.8	14.6	14.0
$T_i = 22°C$					$T_o = 7°C$

Figure 4.9b Temperature distribution for 4E+Xe10+E4 inner pane (experimental data)

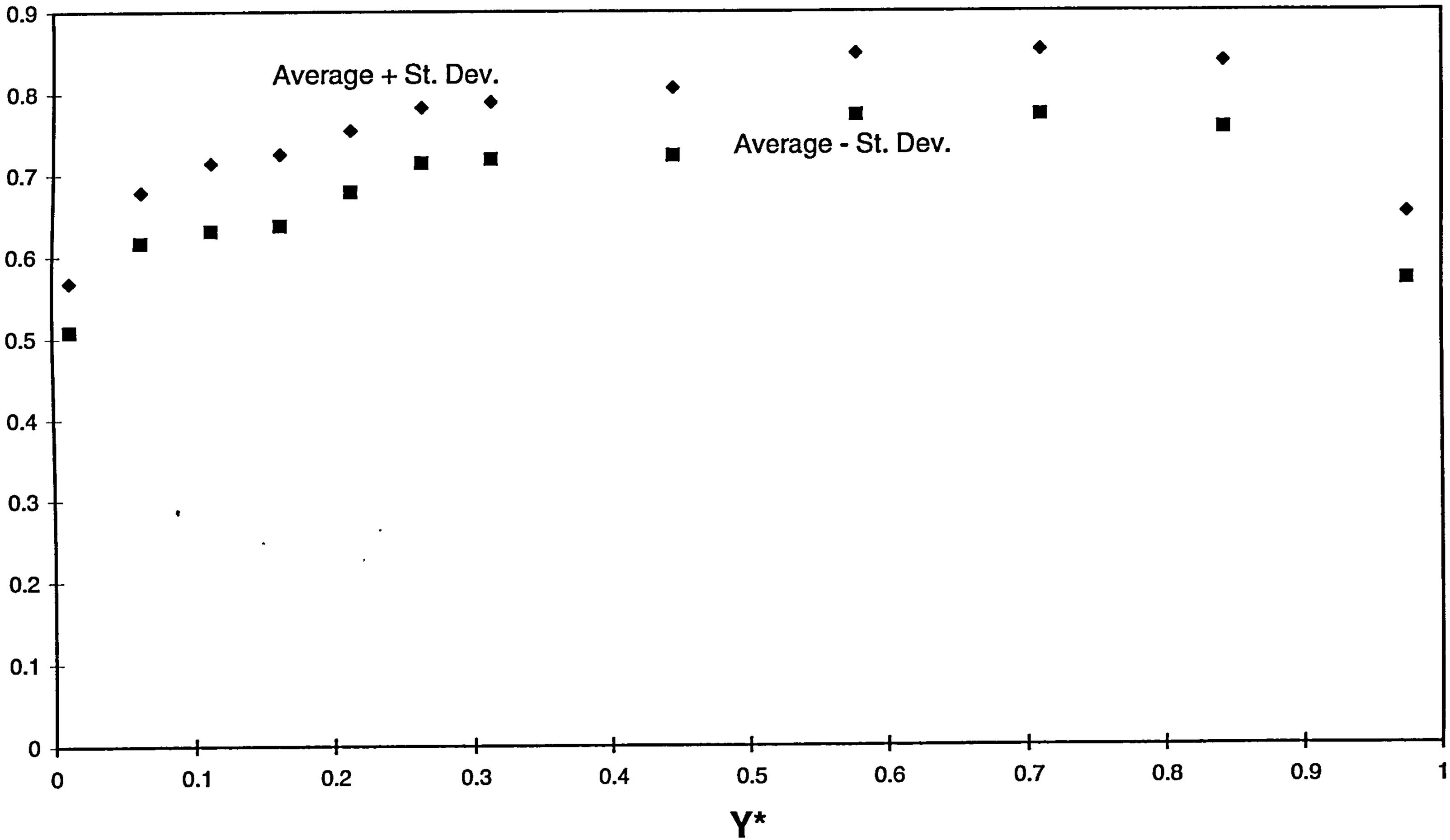

Figure 4.10 Dimensionless temperature variation against dimensionless window height -krypton infill

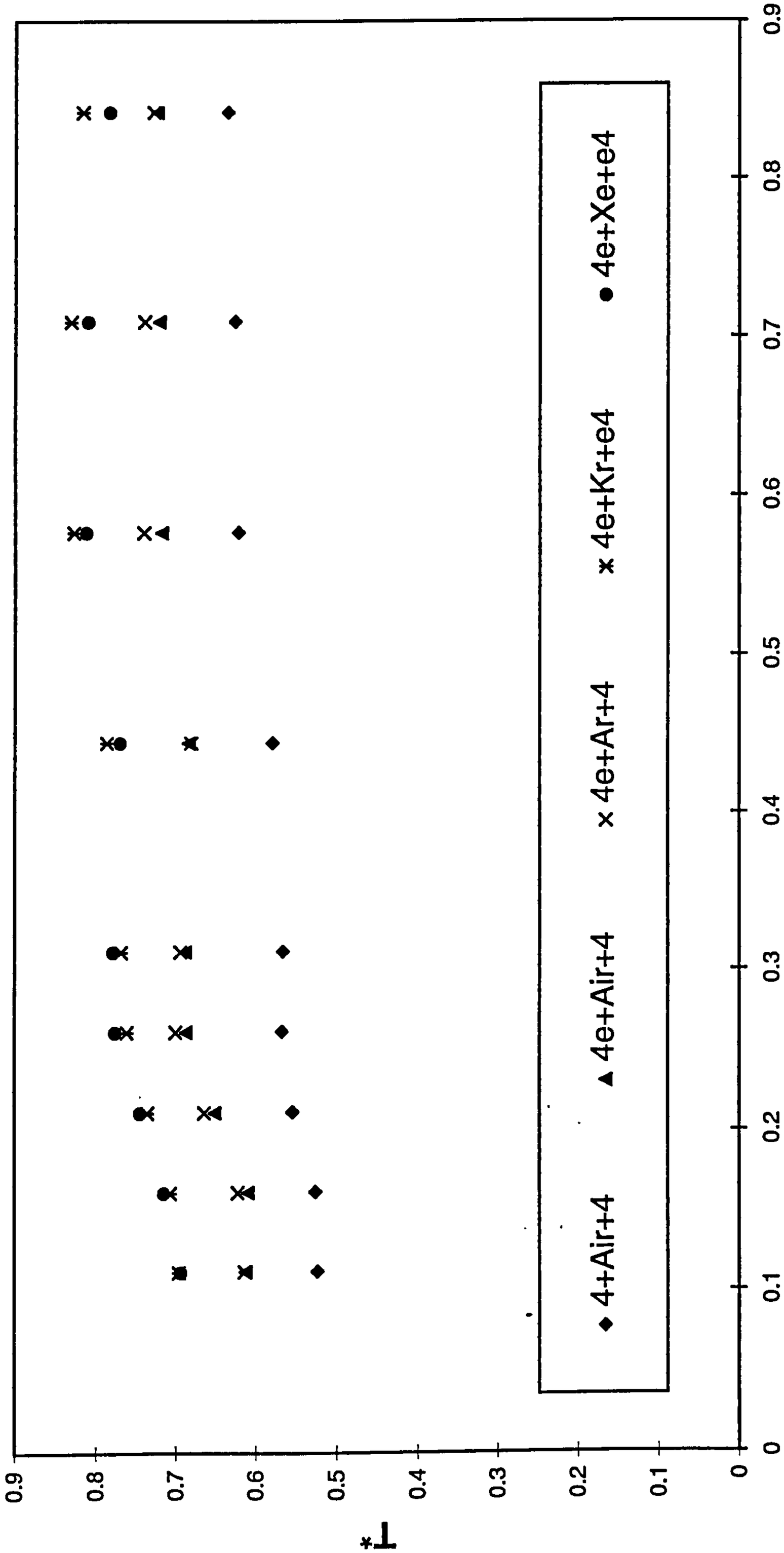

Figure 4.11 Dimensionless temperature variaton against dimensionless height for five window configurations

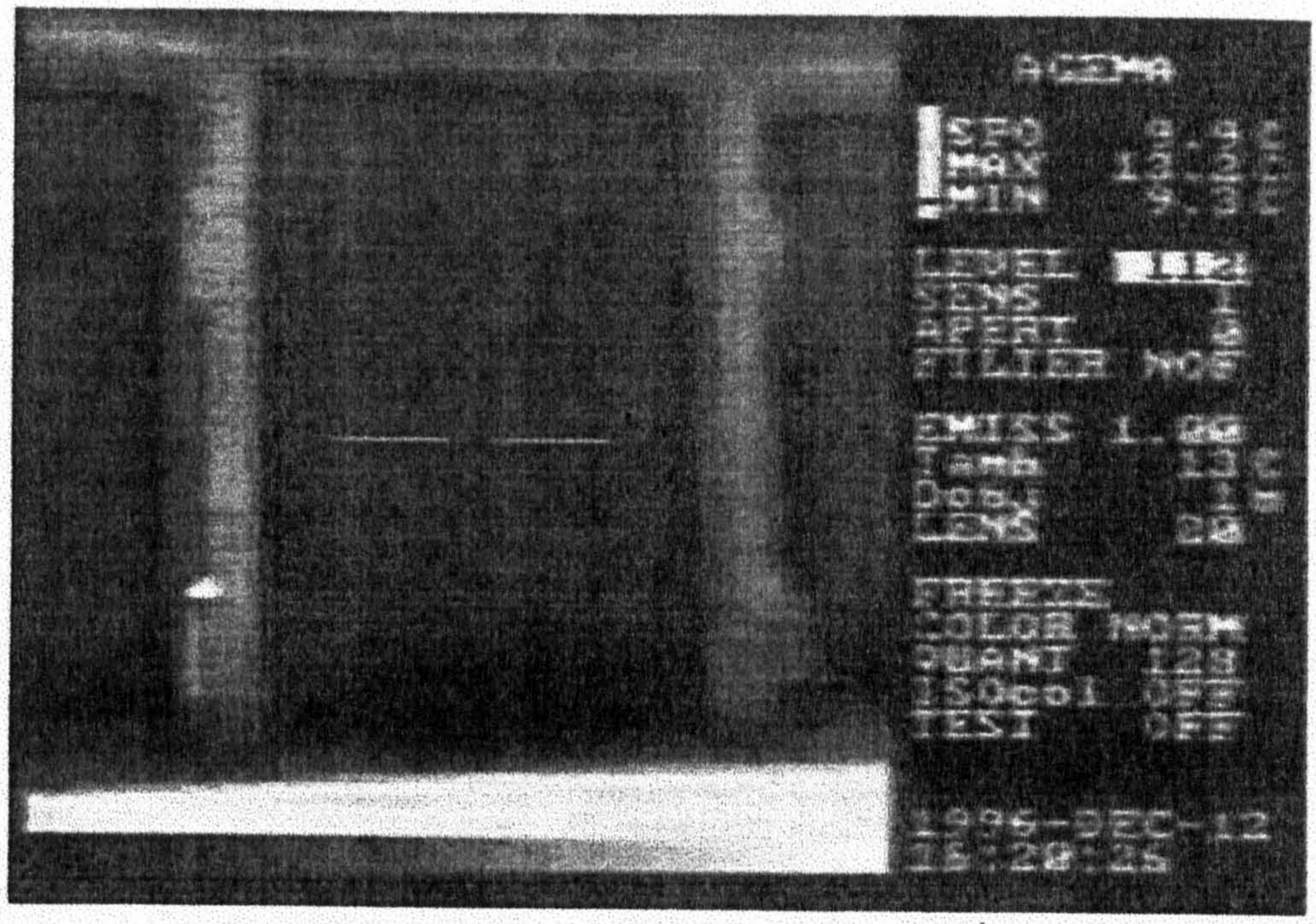

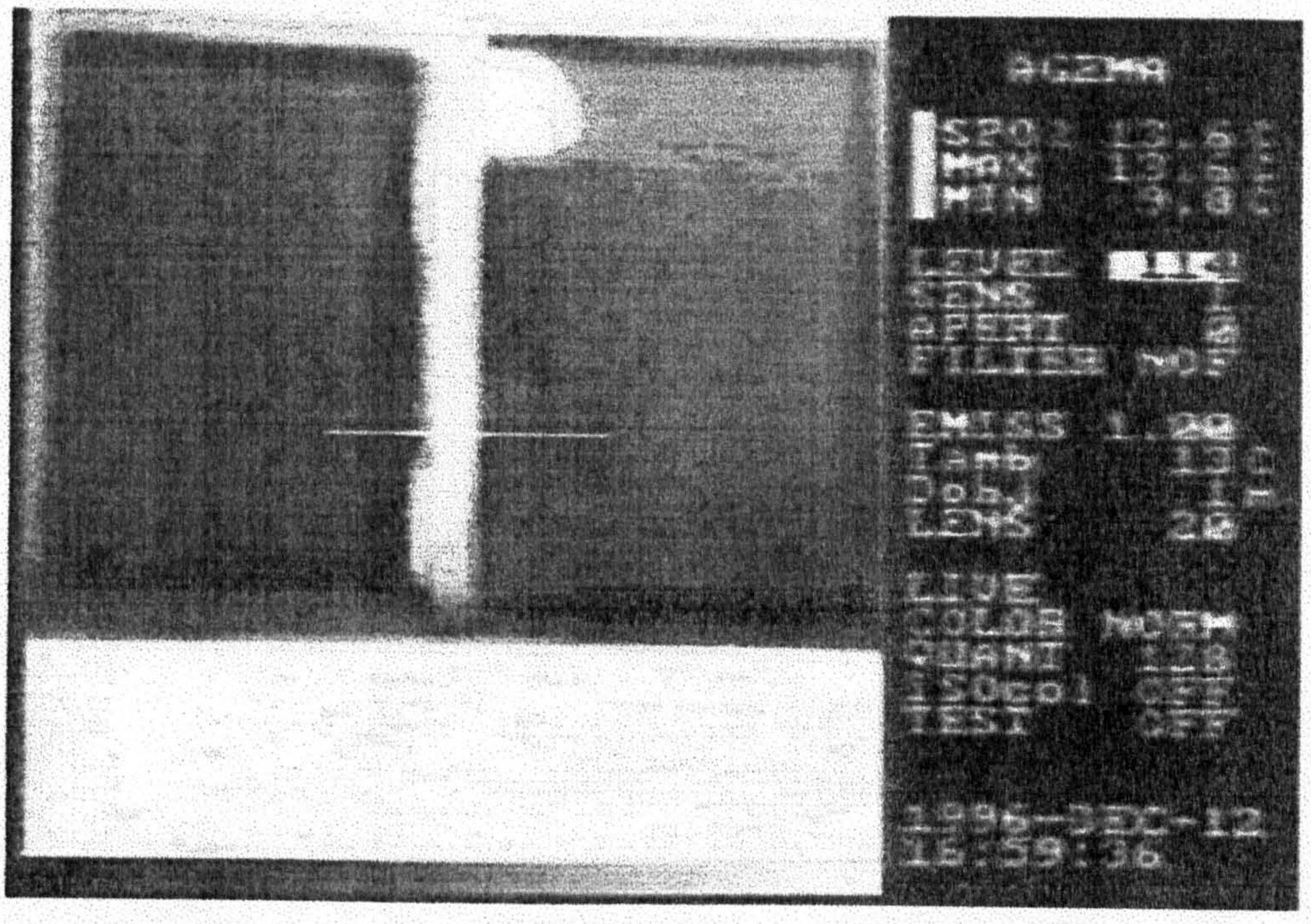

Figure 4.12 Infrared thermograph showing temperature distribution for an air-filled double glazed window (In-situ experiments): Top picture – Zoom view, Bottom picture – Normal view

5 Natural convection analysis of a window cavity and its longitudinal temperature profile

5.1 Introduction

Condensation prediction charts are widely used to predict the conditions under which condensation will occur [5.1, 5.2]. These charts, shown in Figs. 2.1-2.4 of Chapter 2, are based on four parameters:

- *inside air temperature*
- *outside air temperature*
- indoor relative humidity
- U-value of the glazing

These charts are plotted under the assumption that the inner glass pane is at a uniform temperature. By knowing any three of the above parameters, the fourth can be found. The interior glass pane temperature is normally assumed to be equal to the centre-glazing temperature. This assumption ignores the effect of infill gas convection within the window cavity and its impact on the temperature distribution of the inner glass pane. The present work shows the invalidity of this assumption and demonstrates the temperature stratification along the height of the inner pane. This stratification dictates that the lowest temperature of the interior glass is at its lower edge where condensation will be initiated. Therefore, the assumption of isothermal interior glass gives incorrect conclusions for the occurrence of condensation.

In the present work, measurements and modelling techniques have been used to study the longitudinal temperature variation of double glazed windows. It has been shown that the temperature variation is primarily due to the buoyancy driven flow of gas within the sealed enclosure. The present work provides a physical model which can be used to calculate, with a significant level of accuracy, the temperatures along the height of

double glazed windows. This method may be a prerequisite for the quantification of condensation so commonly encountered in the European and North American climates.

5.2 Review of experimental work

As mentioned previously in Chapter 4, centreline longitudinal temperature measurements at a minimum of 12 points were undertaken on several window configurations, i.e. a combination of varying glass coatings and infill gases. Table 4.2 provides the design details of the windows under investigation. For each case fifteen-minute averages of longitudinal temperatures were recorded using an electronic data logger.

The total number of readings for each window, recorded during a winter period, were in excess of 600. To exclude the solar effects on the measured data, only those taken during night were considered as shown in Appendix A. Figure 5.1 shows the temperature measurement schematic for a krypton window with two low-emissivity glass panes. This window has a glazing U-value of 1.14 W/m^2-K (see Table 4.2). Figure 5.1 demonstrates the effect of the infill gas circulation on the longitudinal temperature variation. This is the dominant factor and it is responsible for the rise in the temperature along the height as the cold air moves up the heated glass. Figure 5.1 also demonstrates the cold-bridge effect of the edge-seal which lowers the glass temperatures at its top and bottom edges. This will be discussed in detail in the next chapter.

In order to compare the temperature variation in different window configurations, with disparate geometry and with different internal and external conditions, two dimensionless parameters (T* and Y*) have been introduced. T* and Y* are given by Equations 4.1 and 4.2 of Chapter 4.

An Excel-spreadsheet has been used to analyse the experimental data. At each time of measuring, i.e. at each 15 minutes, 12 temperature readings were recorded for the 12 vertical locations on the interior glass pane. Furthermore, 2 internal ambient

temperatures and 2 external ambient temperatures were also recorded and the average values obtained. Thus at each measuring time, 12 centreline longitudinal temperatures and the averaged internal and external temperatures were recorded as shown in Appendix A. T* and Y* were calculated using Equations 4.1 and 4.2. Figure 5.2 shows the T* band-width containing two-thirds of the entire data set (mean ± standard deviation) for the xenon-infill double glazed window. This plot shows significant scatter of data, primarily resulting from varying external weather conditions. Figure 4.11 of Chapter 4 shows the complete range of T* obtained in the present investigation for the windows tested. It was apparent that no general statistical analysis could be undertaken for the prediction of the temperature profiles , i.e. relating T* to Y*. However, a semi-analytical physical model was derived which proved to be extremely fruitful. This is explained in the following section.

5.3 Physical Model

The assumption that a vertical wall is isothermal would be a good approximation in cases where the vertical wall is massive and highly conducting. The physical situation of a heated glass wall is neither isothermal nor constant heat flux, however, the latter condition is closer to reality for heat transfer through a double glazing system. For gaseous fluids such as those used in window enclosures, Bejan [5.3] has used scaling law analysis to show that,

$$\delta_t \sim H\,[Ra^*_H\ Pr]^{-1/5} \qquad 5.1$$

and,

$$\Delta T \sim [q / k]\ H\,[Ra^*_H\ Pr]^{-1/5} \qquad 5.2$$

where the expression for uniform heat flux Rayleigh number is,

$$Ra^*_H = g\,\beta\,H^4\,q / \alpha\,\nu\,k \qquad 5.3$$

where,

α infill gas thermal diffusivity, m^2/s

β infill gas volumetric thermal expansion coefficient ($1 / T_f$), K^{-1}

ΔT differential temperature (t_i . T_f), ^oC

δt thermal boundary layer thickness, m

g gravitational acceleration, m/s^2

H height along the interior glass, taken from the bottom edge of the glass, m

k infill gas thermal conductivity, W/mK

ν infill gas kinematic viscosity (μ / ρ), m^2/s

Pr Prandtl number

q heat flux, W/m^2

Ra^*_H constant heat flux Rayleigh number

t_i temperature of the inner glass pane at an arbitrary point, ^0C

All physical properties Pr, α, ν, and k are evaluated at the enclosure film temperature T_f which may be approximated as the average between the centre-glazing temperatures of the hot and cold glass panes t_3 and t_2 shown in Fig. 3.3 of Chapter 3. These, in turn, may be obtained from Equations 5.4 and 5.5 [5.4] using values of internal convection (h_i) and external convection (h_o) coefficients given in Ref.[5.5-5.7],

$$t_3 = T_i - (R_{g2} + \frac{1}{h_i})q \qquad 5.4$$

$$t_2 = T_o + (R_{g1} + \frac{1}{h_o})q \qquad 5.5$$

where,

$$q = U_{ref} (T_i - T_o) \qquad 5.6$$

h_i = 8.3 W/m^{2}K and h_o = 16.7 W/m^{2}K [5.5-5.7]. U_{ref} is the reference U-value of any given window which is the glazing U-value calculated at T_i = 20 °C and T_o = 0 °C. Table 4.2 gives the reference U-values (U_{ref}) for all windows under test.

R_{g1} and R_{g2} are respectively the exterior and interior glass resistances (R_{g1} = R_{g2} = 1.0 m^{2}K/W).

The film temperature of the infill gas is assumed as the average of t_2 and t_3,

$$T_f = \frac{1}{2}(t_2 + t_3) \qquad 5.7$$

A generalised form of Equation 5.4 is presently proposed as,

$$\Delta T = c[q/k]\, H\, [Ra^*_H\, Pr]^m \qquad 5.8$$

where c and m are constants.

The model represented by Equation 5.8 has been further refined using a new dimensionless group. Presently, this dimensionless group has been named as the 'Napier Number' after the well known Scottish mathematician John Napier who invented logarithms in 1614 at the site of the present work.

$$\text{Napier Number } Na = \Delta T\, k / (q\, H) \qquad 5.9$$

Thus Equation 5.8 becomes,

$$Na = c\, [Ra^*_H\, Pr]^m \qquad 5.10$$

The logarithmic form of Equation 5.10 is

$$\text{Log Na} = \text{Log c} + \text{m Log } [Ra^*_H \text{ Pr}] \qquad 5.11$$

Equation 5.11 is a linear relationship where m is the slope and Log c is the intercept.

Using Excel-spreadsheets, the experimental data for each window has been processed to determine the linear relationship between the two dimensionless groups Na and $[Ra^*_H$ Pr]. These data have been used to calculate Na and $[Ra^*_H$ Pr] for each window and for each location of temperature measurement at each recorded time. Then, Log Na values were plotted against their corresponding Log $[Ra^*_H$ Pr] values. All windows show linear trends in the form of Equation 5.11. Equation 5.10 has been fitted for each window individually using Excel Solver facility to find the optimum values for m and c. Table 5.1 shows values of m and c for each window under investigation. For each measured temperature of each window, a corresponding temperature has been computed using Equation 5.10 and values of m and c shown in Table 5.1. To statistically compare the computed temperatures with their corresponding measured temperatures, values of the mean bias error (MBE) and the root mean square errors (RMSE) have been calculated for each window as shown in Table 5.1. MBE and RMSE were calculated using the following formulae.

$$\text{MBE} = \frac{\sum(\text{Tmeasured} - \text{Tcomputed})}{\text{No of data points}}$$

$$\text{RMSE} = \sqrt{\frac{\sum(\text{Tmeasured} - \text{Tcomputed})^2}{\text{No of data points}}}$$

The MBE's show a remarkably good performance with the maximum of the average deviations being under a third of a degree Celsius. The RMSE's are also low with the maximum value not exceeding three-quarter of a degree Celsius. These values indicate that the computed temperatures are in good agreement with the measured temperatures.

In order to obtain generalised values of c and m considering all the windows, Log Na values have been plotted against their corresponding Log $(Ra^*_H$ Pr) values for 'low' and

'high-tech' windows. Each group was dealt with separately. These are shown in Figs. 5.3 and 5.4 respectively. From these figures, it is clear that despite the scatter of the data points, there is a definite trend. Similar plots were made considering all the windows (low and high-tech). Figure 5.5 represents the result.

Table 5.1 Values of c and m (Equation 5. 10) and error analysis for temperature estimation

Window Configuration	Classification	c	m	MBE	RMSE
4-Air12-4	Low-tech	0.3	-0.19	0.16	0.43
4-Ar12-4	Low-tech	0.43	-0.24	-0.04	0.48
4-Air12-E4	High-tech	1.06	-0.22	0.338	0.73
4-Ar12-E4	High-tech	0.91	-0.22	0.31	0.72
4E-Kr12-E4	High-tech	0.57	-0.18	0.004	0.66
4E-Xe10-E4	High-tech	0.61	-0.19	-0.1	0.53
Theoretical value, Ref. [5.3]	High-tech	-	-0.2	-	-

It is apparent from Table 5.1 that the slopes of all lines (m values) are nearly the same and also in close agreement with Bejan [5.3]. However the y-intercepts of the above models are different. The present work has shown that c is uniquely related to the U-value of any given window. With a view to produce a generalised model, c is proposed as,

$$c = c_o + c_1 U_{ref} \qquad 5.12$$

where c_o and c_1 are constants.

Table 4.2 gives the reference U-values (U_{ref}) for all windows under test. These values are given by Muneer and Han [5.8].

Substituting Equation 5.12 into Equation 5.10 gives,

$$Na = (c_o + c_1 U_{ref}) (Ra^*_H Pr)^m \qquad 5.13$$

Equation 5.13 was fitted for c_o, c_1, and m for all windows taken together using the present measurements. Excel Solver was used to fit this equation. The following values have been obtained:

$c_o = 1.1563$

$c_1 = -0.31$

$m = -0.2$

Substituting Equations 5.3 and 5.9 into Equation 5.13 and rearranging yields,

$$t_i = T_f + (q H / k) (c_o + c_1 U_{ref}) ([g \beta H^4 q Pr] / [\alpha \nu k])^m \qquad 5.14$$

This equation represents the physical model which can be used to compute the longitudinal temperature variation of the inner glass pane of any double glazed window. The analysis may easily be extended for multiple glazings. The computer software LongTemp.xls (see Appendix I) includes the above model and is presently available on the accompanying floppy disk.

The following example shows such calculation for a particular case. For an argon filled double glazed window with a 12 mm gap, 1.0 m height, and 2.72 W/m^2K U_{ref}, the temperature at a height of 0.5 m from the edge-seal along the vertical centreline of the inner pane can be computed as follows. Assume that the internal and external ambient temperatures are 20 ^0C and 0 ^0C respectively, $R_{g1} = R_{g2} = 1.0$ m^2 K/W, $h_i = 8.3$ W/m^2K and $h_o = 16.7$ W/m^2K.

From Equation 5.6, $q = 54.4$ W/m^2

From Equation 5.5, $t_2 = 3.48\ ^0C$

From Equation 5.4, $t_3 = 13.23\ ^0C$

From Equation 5.7, $T_f = 281.5$ K and $\beta = \frac{1}{281.5} = 0.003552\ K^{-1}$

From Ref. [5.9] the following properties were obtained:

$\rho = 1.73\ kg/m^3$

$\mu = 21.7466 \times 10^{-6}$ kg/m.s

$C_p = 0.521778$ kJ/kg.K

$k = 0.016753$ W/m.K

$\nu = 12.57575 \times 10^{-6}\ m^2/s$

$\alpha = 1.86 \times 10^{-5}\ m^2/s$

Pr=0.677

The required temperature is calculated using the model represented by Equation 5.14 where H = 0.5 m,

$$t_i = (281.5\text{-}273.15) + \frac{54.4 \times 0.5}{0.01753} \times (1.1563 - 0.31 \times 2.72)$$

$$\times \left(\frac{9.81 \times 0.003552 \times 0.5^4 \times 54.4 \times 0.677}{1.86 \times 10^{-5} \times 12.57575 \times 10^{-6} \times 0.016753}\right)^{-0.2} = 16.98\ ^oC$$

5.4 Results and Discussion

The semi-analytical model presented by Equation 5.14 was used to compute the longitudinal temperatures for each of the six windows under investigation using the weather data obtained from the present measurements and the values of c_o, c_1 and m listed above. Typical results of the model evaluation are shown in Fig. 5.6. Statistical error analysis was also undertaken by pooling data from all windows. The resulting MBE of 0.01 °C and RMSE of 1.2 °C shows the significant promise of the model. Figure 5.7 shows the variation of the measured and computed temperatures against the window height for some windows. It also shows the temperature used by Pilkington

[5.1] which does not vary with the window height. From these figures, it is clear that the longitudinal temperature increases with the window height. This proves the dominant influence of natural convection within the window cavity. The drops in temperature at the bottom and top of the window are due to edge spacer effects.

The glass vertical temperature variation is of importance regarding condensation. Conventionally, the procedure to estimate window glass temperature was as follows. The centre-glazing temperature, t_4, shown in Fig. 3.3 is calculated using 3.32. As can be seen U-value, h_i, T_i and T_o are required to calculate t_4. The temperature of the inner pane is normally assumed constant and equals t_4 as per the Pilkington's procedure [5.1]. This procedure, however, falls short of the true representation as demonstrated via Fig. 5.7. The unvarying temperature used by Pilkington gives erroneous estimates for condensation prediction because condensation will occur at the bottom edge of the glass at a temperature lower than that suggested by Pilkington.

It has been shown herein that the temperature at any given point on the interior glass pane may be estimated provided H, T_o , T_i , and U_{ref} are known. Figure 5.8 shows an information flow diagram for such computations.

5.5 Conclusions

The proposed model will be of good use for the precise quantification of the condensation problem so commonly encountered in dwellings. To date the developments on this front have been the use of a crude model [5.1, 5.2, 5.10, 5.11] which assumes a uniform temperature of the inner glass pane. Such models require four physical parameters T_i, T_o, indoor humidity and the centre-glazing U-value to ascertain the risk of condensation using the condensation prediction charts shown in Figs. 2.1-2.4. It has been shown herein, via measurements, that the above isothermal assumption is invalid. Common experience also shows that condensation always initiates at the bottom edge of windows and it progresses upwards with the drop in external temperature and/or the increase in the indoor relative humidity.

References

5.1. D. Button et al, Glass in Building: A guide to modern architectural glass performance, Pilkington Glass Ltd., Butterworth Architecture, London, 1993

5.2. P. March, Thermal Insulation and Condensation, The Construction Press, London, 1979

5.3. A. Bejan, Convection Heat Transfer, Wiley, New York, 1984.

5.4. Pilkington Glass Limited, Calculating thermal transmittance, The environmental advisory service, St. Helens, UK, 1981

5.5. CIBSE Guide A, Charted Institution of Building Service Engineers, London, 1982

5.6. BS6993 Part I, British Standard Institute, London, 1989

5.7. T. Muneer and B. Han, Design charts for multiple glazed windows, BSER&T 17, 4, 223-229, 1996

5.8. T. Muneer and B. Han, Use of CFD for thermal analysis of double glazings, Computational Methods and Experimental Measurements VII, 77-84, Eds: G. M. Carlomagno and C. A. Brebbia, Computational Mechanics Publications, Southampton, 1995

5.9. H. J. M. Hanley, R.D. McCarty and W. M. Harnes, The viscosity and thermal conductivity coefficients for dense gaseous and liquid argon, krypton, xenon, Nitrogen and Oxygen, J. Phys. Chem. Ref. Data, 3, 4, 979-1018, 1974

5.10. D. A. Button and R. Dunning, Fenestration 2000, Pilkington Glass Ltd., St. Helens, UK, 1989

5.11. T. E. Johnston, Low-E Glazing design Guide, Butterworth Architecture, London, 1991

5.12. CIBSE Guide A2, Chartered Institution of Building Service Engineers, London, 1982

5.13. ASHRAE Guide: Fundamentals, American Society Heating, Refrigerating, and Air-conditioning Engineers, Atlanta, 1993

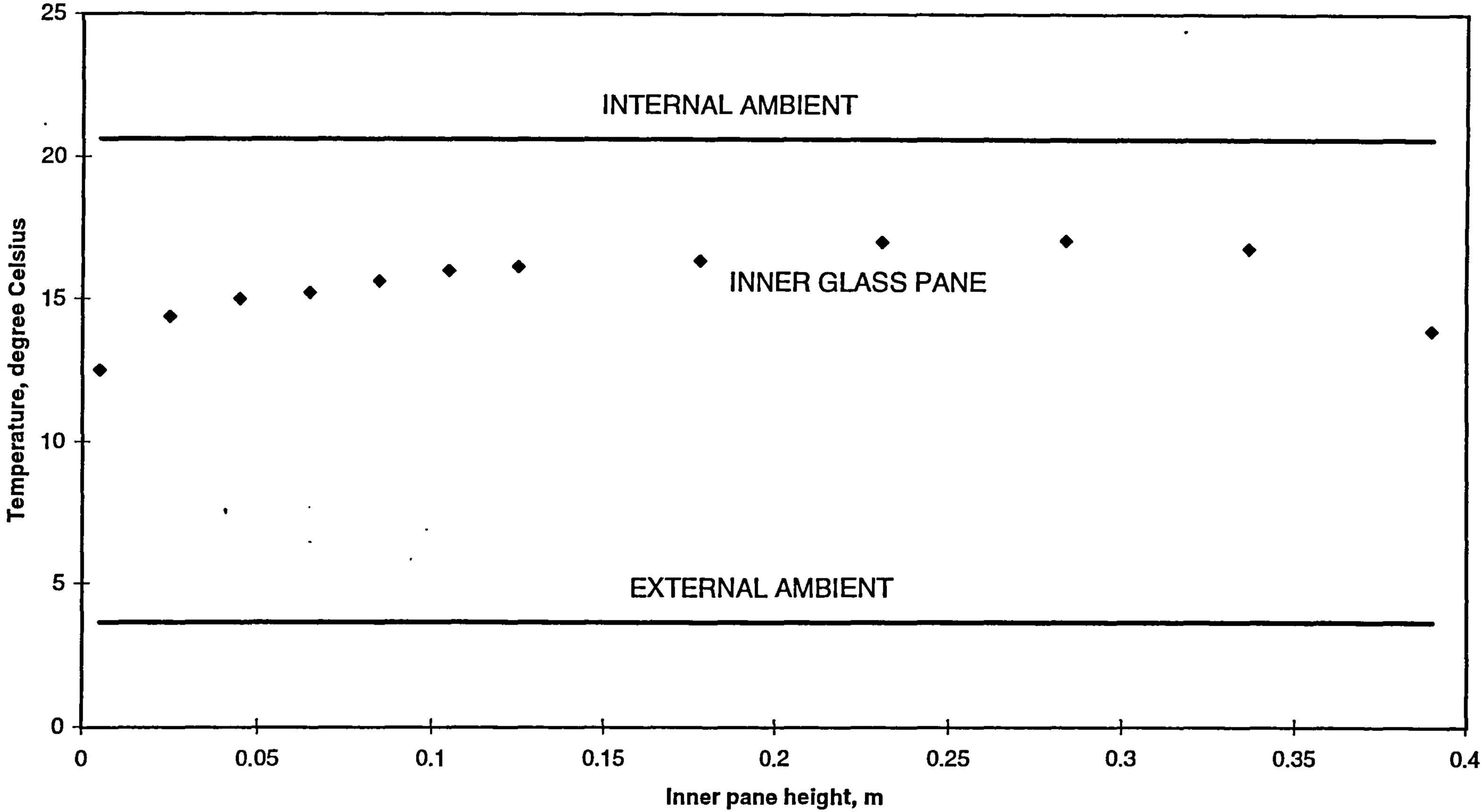

Figure 5.1 Temperature variation along the inner pane height - Krypton infill

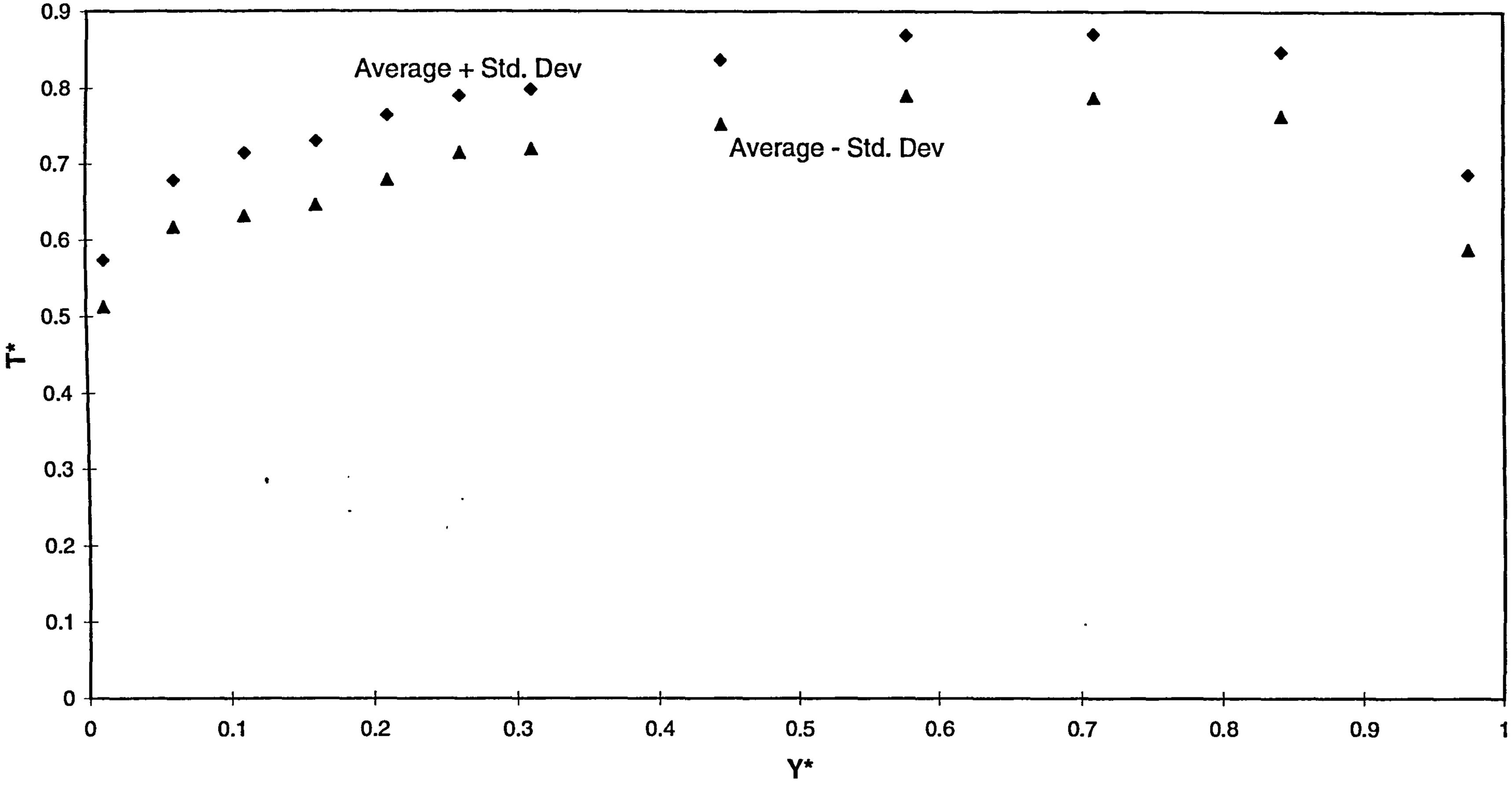

Figure 5.2 Dimensionless temperature variation against dimensionless window height - xenon infill

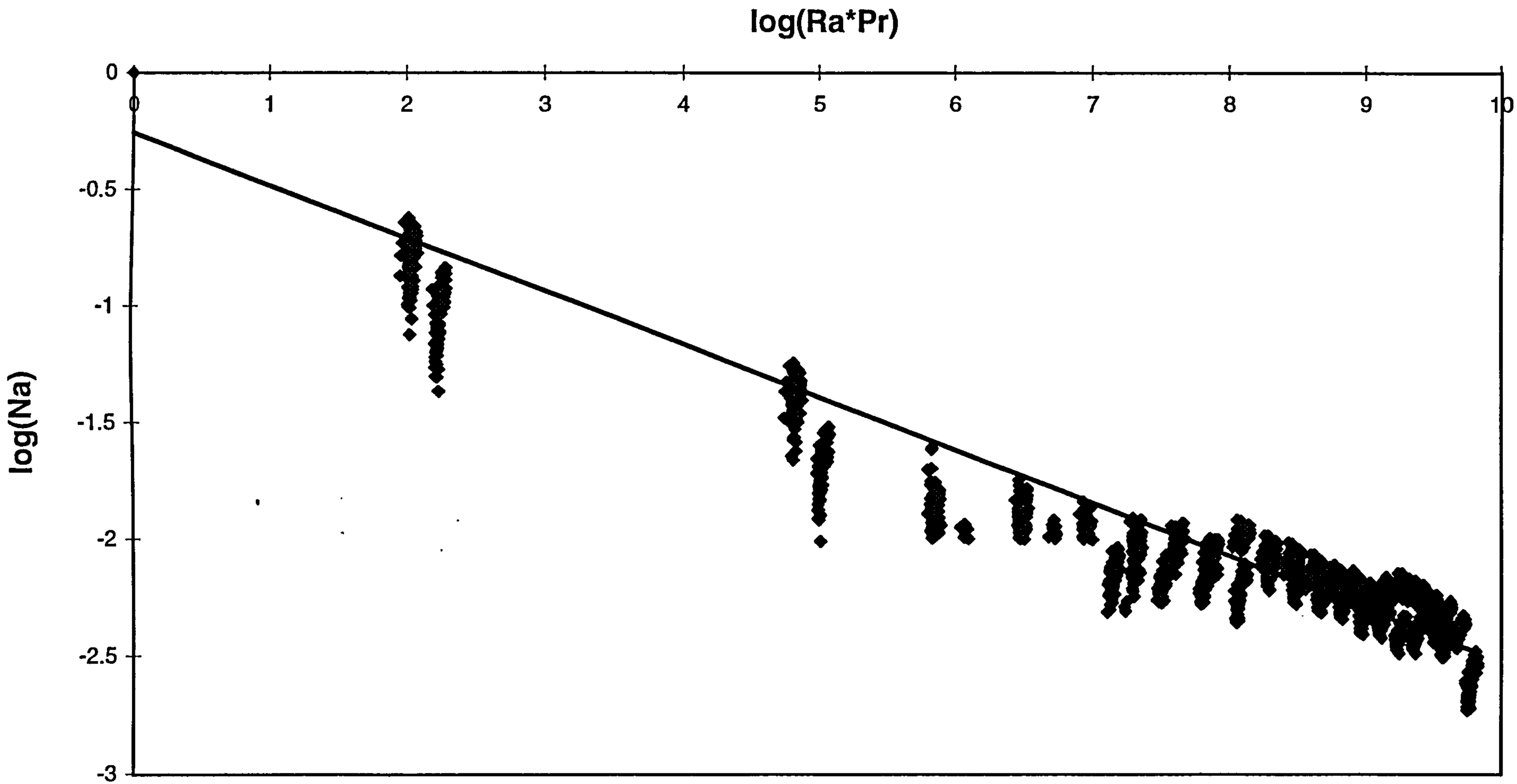

Figure 5.3 Napier number versus (Ra*Pr) for the 4-Air12-4 and 4-Ar12-4 windows

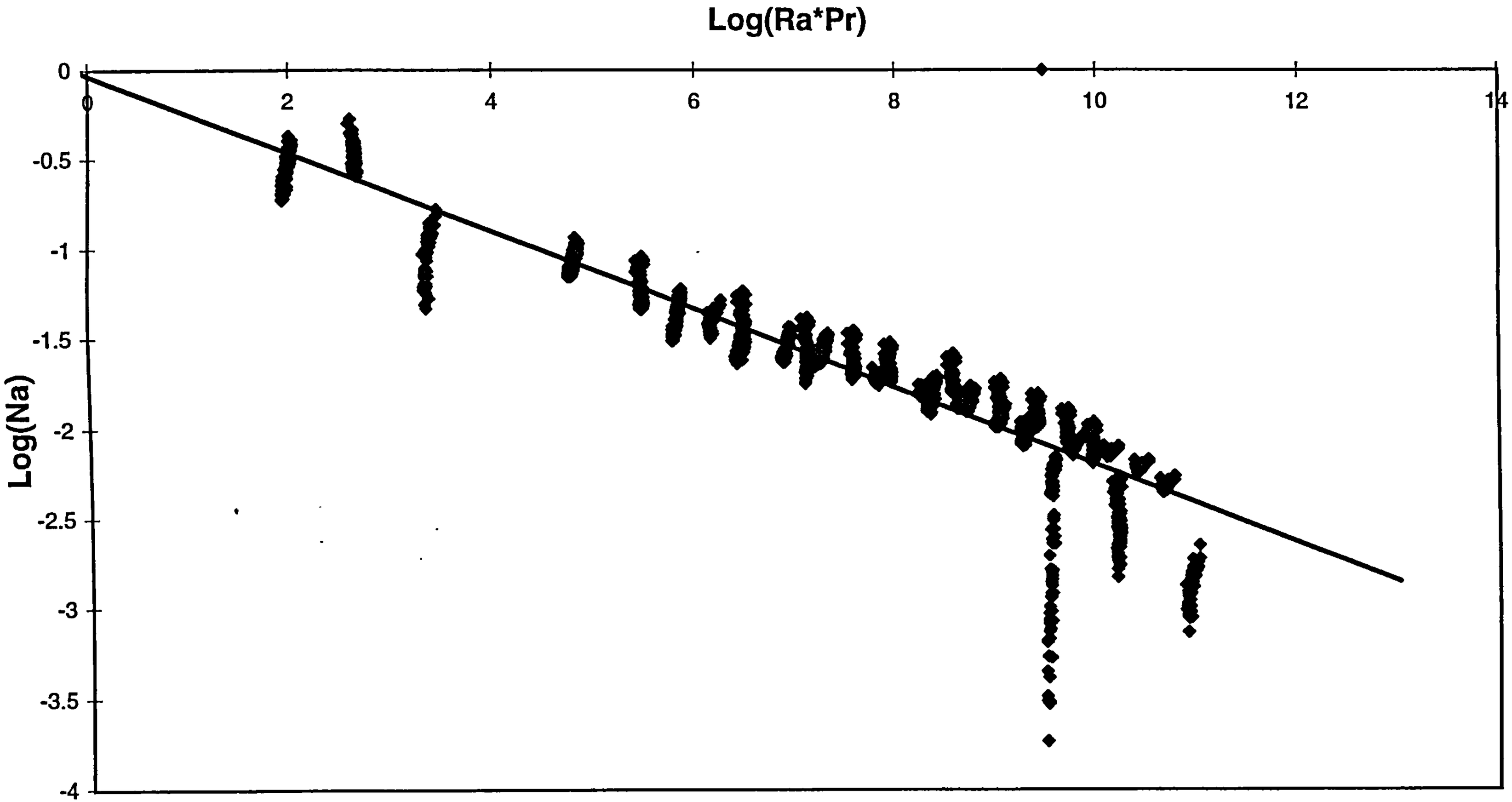

Figure 5.4 Napier number versus (Ra*Pr) for the 4E-Xe10-E4, 4E-Kr12-E4, 4-Air12-E4 and 4-Ar12-E4 windows

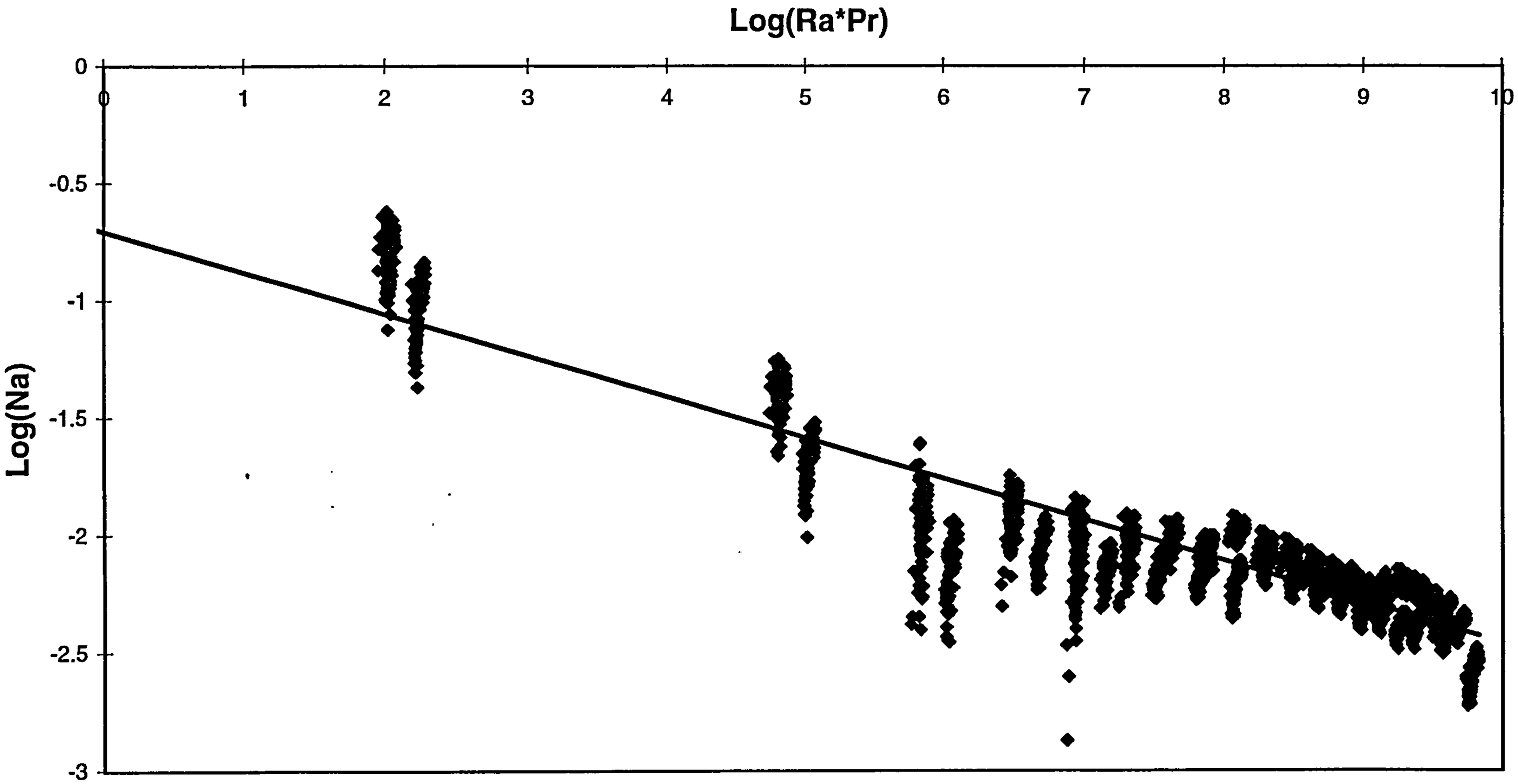

Figure 5.5 Napier number versus (Ra*Pr) for all the windows

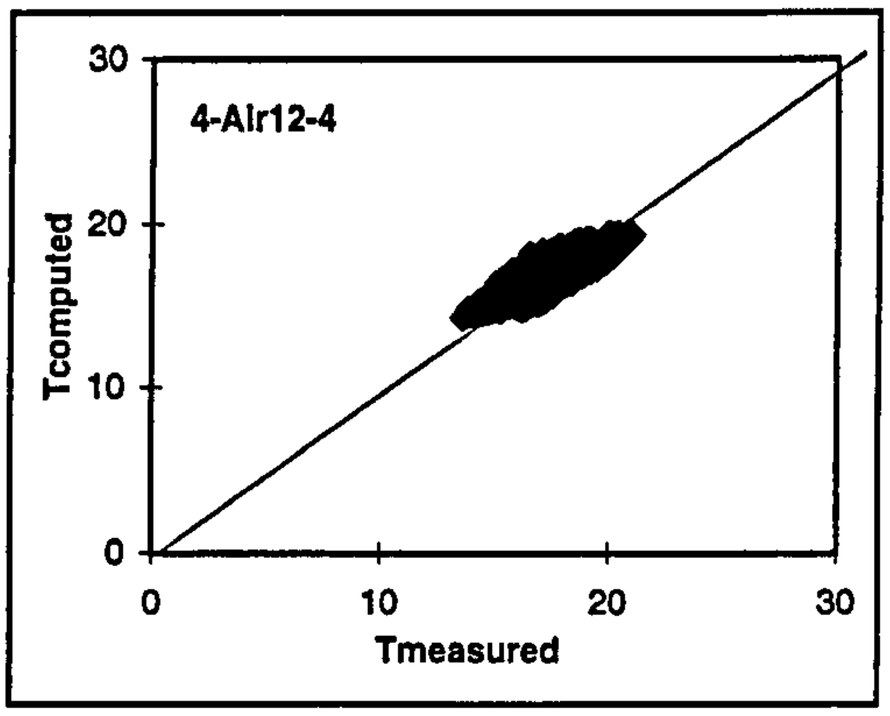

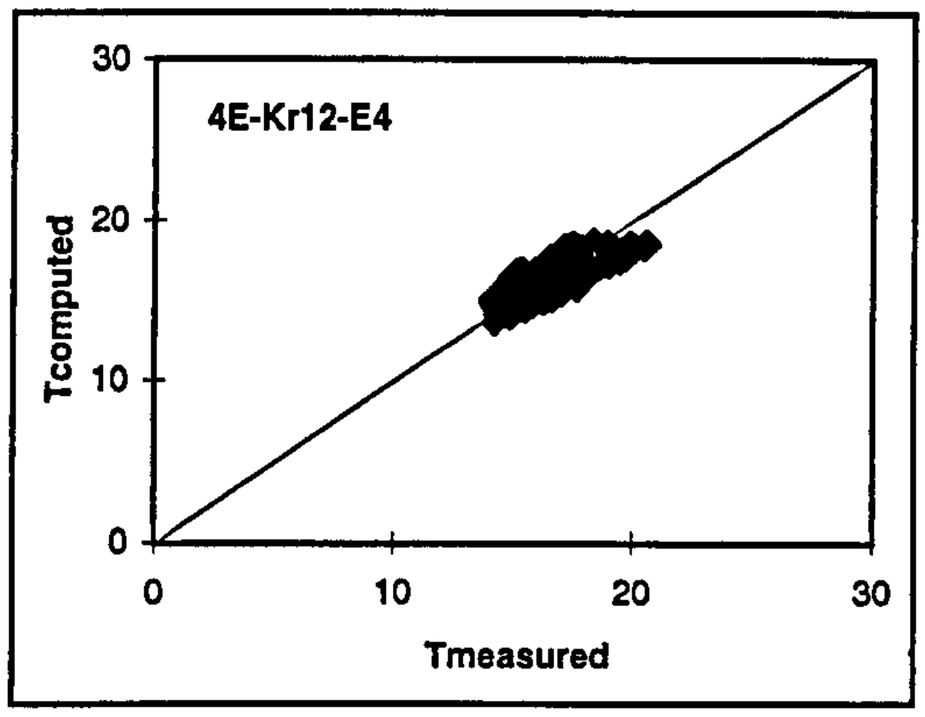

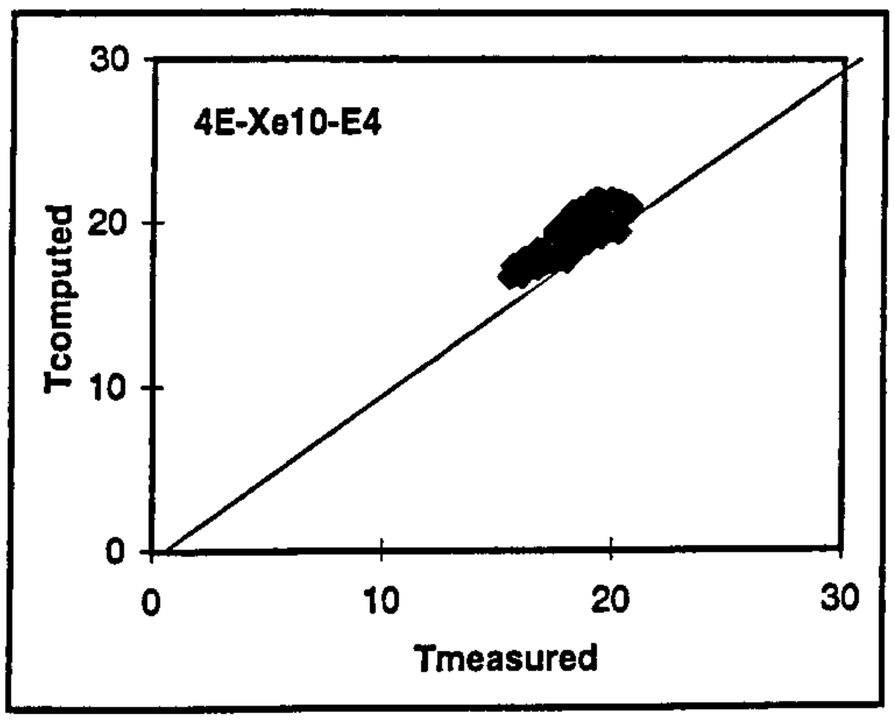

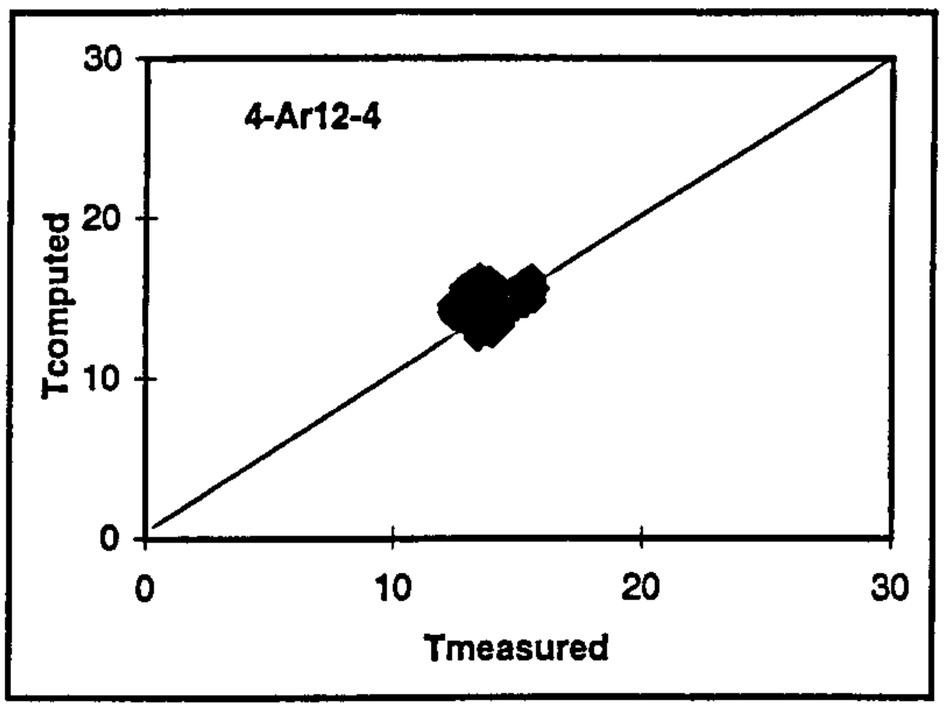

Figure 5.6 Evaluation of the model for longitudinal temperature estimation

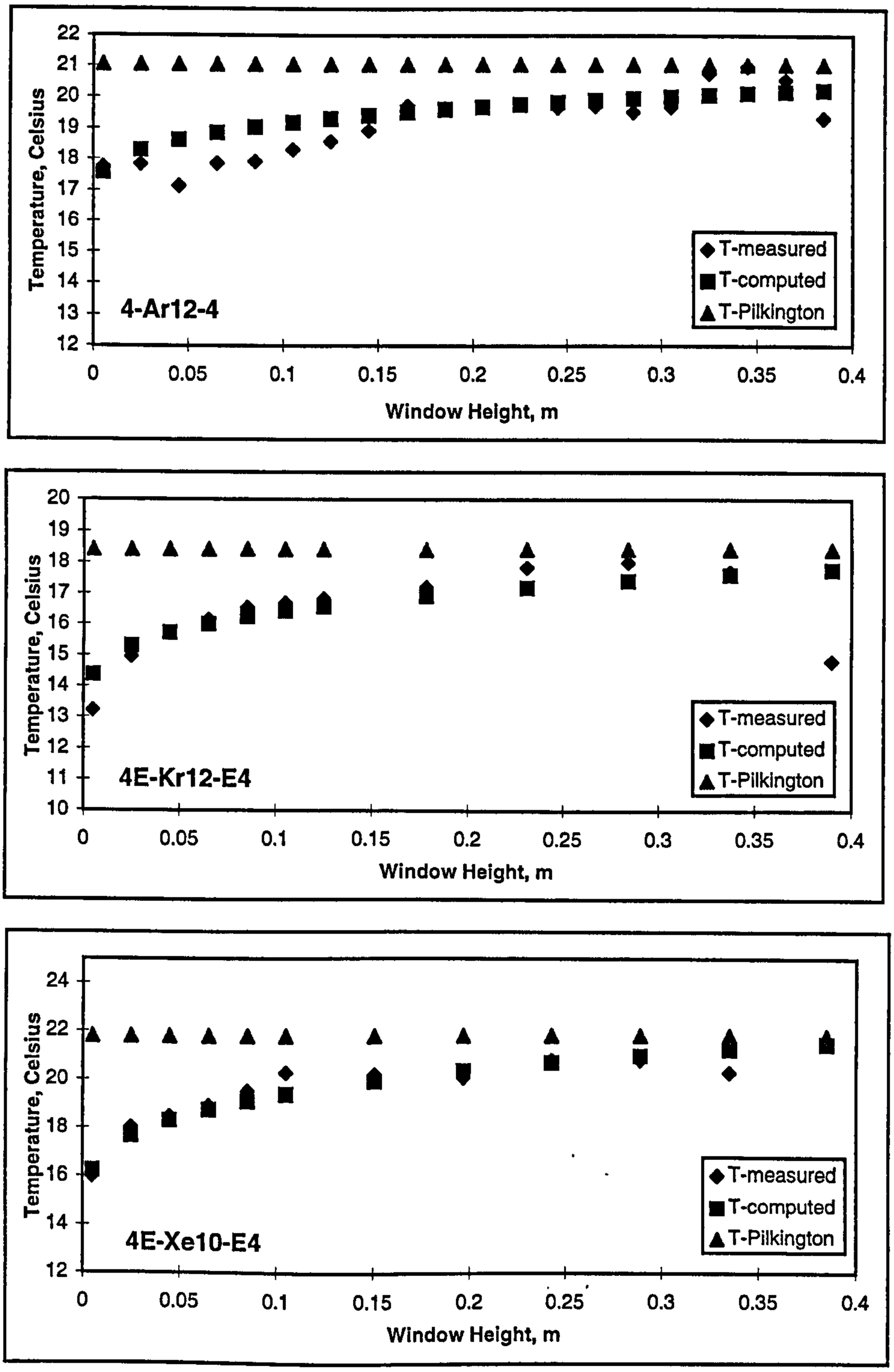

Figure 5.7 Measured and computed temperature variation for three window configurations

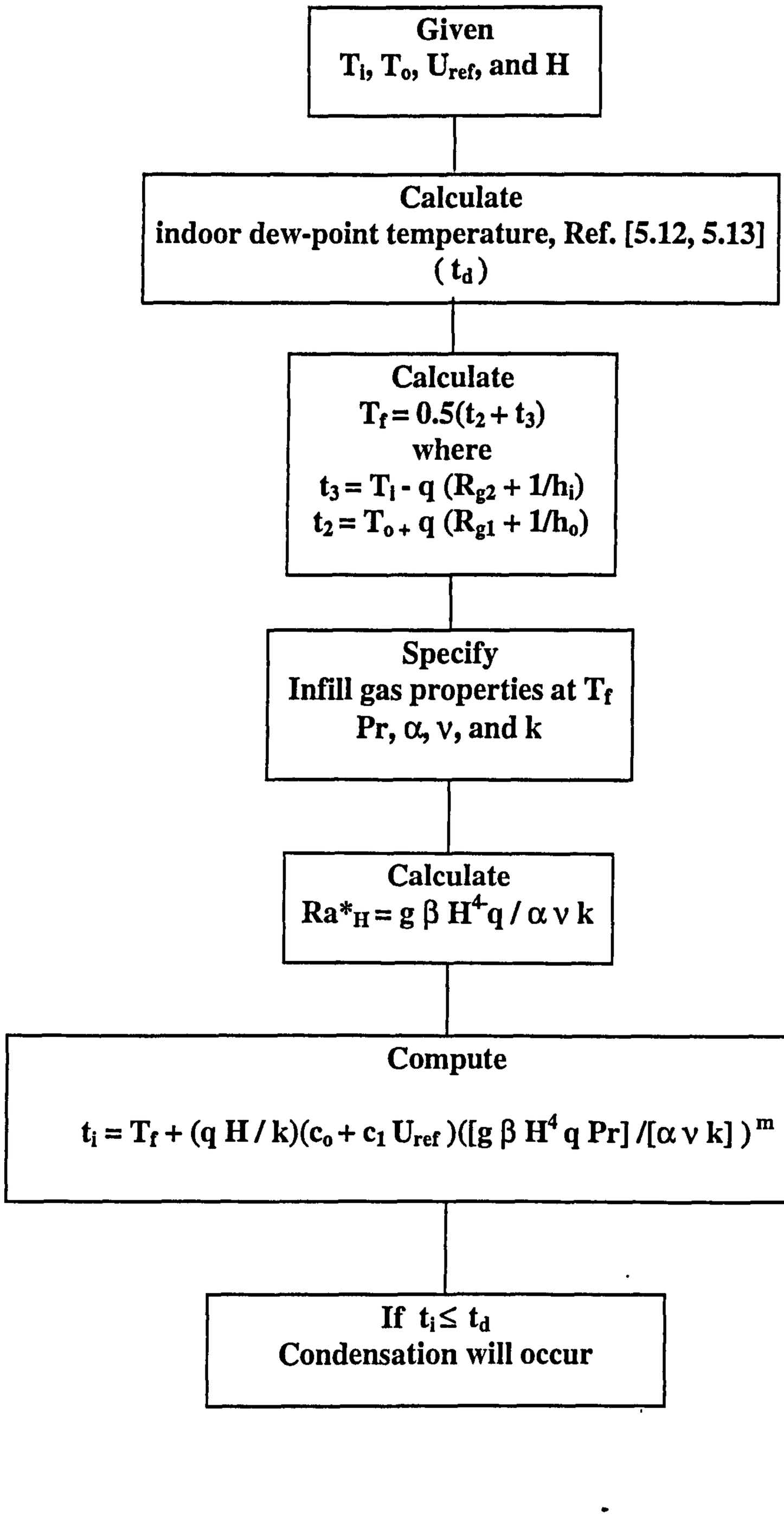

Figure 5.8 Flow diagram to assess condensation occurrence on double-glazed windows

6 Combined conduction, convection, and radiation heat transfer model for double glazed windows

6.1 Introduction

Modern double glazed windows use hermetically sealed, insulative glazing units, which consist of two panes of glass separated by an edge-seal. The edge-seal isolates the space between the two glass panes and consequently creates an insulative cavity suitable for the use of low emissivity coatings and/or low conductivity infill gases, e.g. dry air (dew point < -40 °C), argon, krypton, or xenon.

The thermal transmittance of a complete double glazed window depends on three components, the glazing unit, the edge-seal (spacer), and the frame. Double glazed windows containing high performance glass require a compatible high insulation in their edge spacer and frame. If this is not achieved, then the insulation benefits of the glass can be significantly diminished. Whilst a conventional double glazed window with low-e and argon infill gas achieves U-values between 1.3 and 1.8 W/m^2K, poorly insulated frames of wood, plastic, aluminium or steel may give U-values ranging from 2.8 to 7.0 W/m^2K [6.1]. The thermal effect of the edge-seal for different conditions of exposure, e.g. sheltered, normal, and severe may be calculated from tables given in [6.2]. This value can be used in calculating the overall U-value of the window by using Equation 3.8 of Chapter 3.

The edge-seal considered in this analysis consists of an aluminium spacer, desiccant, polyisobutylene, and polysulphide as shown in Fig. 6.1. The presence of the aluminium spacer creates a thermal short circuit at the window edge-seal. This increases the overall U-value of the window and lowers the local temperatures at the edge region, often causing condensation on the glass.

Window condensation in dwellings and offices can be very troublesome. To evaluate the risk of condensation in buildings, analytical and numerical models have been developed to calculate the longitudinal temperature distribution of the indoor glazing. It has been shown herein that the above mentioned temperature variation is primarily due to the buoyancy driven flow of gas within the sealed enclosure. However, the window edge-seal and frame have a considerable effect on the temperature distribution and also on the U-value of the window. In this chapter measurements and a two-dimensional numerical solution technique have been used to study the cold bridge effects of a windows edge-seal and frame on the temperature distribution along the height of the inner glazing. This analysis provides a method for assessing the frequency of condensation occurrence on double glazed windows so commonly encountered in the European and North American climates.

To determine if condensation will occur on a window, one needs to compute the minimum indoor pane temperature and this can be done by using the two-dimensional numerical model developed in this chapter. It will be shown that the point of occurrence of the minimum temperature is the bottom edge of the glazing. It will also be demonstrated that the convection flow of the infill gas is a major contributor to the reduction in temperature at the bottom edge. However, the edge-seal and the frame also have a considerable effect.

The experimental data used in this analysis was the same data as used in the previous chapter. These experimental data are shown in Appendix A. In the following section, a two-dimensional numerical model for the temperature distribution on the bottom part of the window inner glazing has been developed. This model takes into consideration all modes of heat transfer, i.e. convection, radiation, and conduction encountered at the bottom edge of the indoor glazing. The results of the analytical work will be compared with the experimental data to check the validity of this model.

6.2 The 2-D numerical model

Figure 6.1 shows a cross-section of a typical double glazed window. A list of the windows investigated is given in Table 4.2 of Chapter 4. This cross section shows the details of the design of the window glazing unit and frame. It also shows the thermal nodal arrangement used in the analysis. For simplicity of analysis the edge-seal, i.e. aluminium spacer, polyisobutylene, and polysulphide, are assumed to have rectangular shapes.

Following the recommended practice [6.3] for the region of influence of the edge-seal, heat transfer at only the bottom part of the glazing up to a height of 35 mm above the edge-seal was considered. A two-dimensional analysis utilising a numerical solution technique has been used. The finite-difference technique is used to approximate differential increments in the temperature and space co-ordinates. The edge-seal, inner glass pane, and frame were divided into 14 elements in the x and y directions as shown in Fig. 6.1. The nodes of these elements are 1-7 and a-g. The object is to compute the temperature of these nodal points. The Gauss-Seidel iteration [6.4] technique was used to obtain an efficient solution.

The steady state temperature T_i of any node i (see Fig. 6.2) may be obtained in terms of the resistances and temperatures of the adjoining nodes T_j as,

$$T_i = \frac{q_i + \sum_j (T_j / R_{ij})}{\sum_j (1 / R_{ij})} \qquad 6.1$$

where q_i is the heat delivered to node i by heat generation, radiation, etc. The R_{ij} can comprise of conduction, convection and radiation elements. Since the experimental data was obtained during night time only, it was assumed that there was no heat generation within the nodes (nocturnal conditions) and accordingly the value of q_i was taken as zero in the present analysis.

Figure 6.3 shows the complete thermal network for the nodal arrangement shown in Fig. 6.1. For the ease of analysis and identification the resistances between the nodes are numbered as shown in Fig. 6.3 . Table 6.1 presents the calculation scheme and numerical values of the resistances of Fig. 6.3. A cavity width of 12 mm has been used for all windows with the only exception being the xenon window for which the cavity width was 10 mm. The following points were used in the calculation of the resistances listed in Table 6.1.

A- The physical situation of the heated glass wall is quite involved. To be precise, it is neither isothermal nor constant heat flux, however, present measurements have shown it to be closer to the latter. The heat transfer per unit area of the glazing unit (W/m^2) was assumed constant and computed as

$$q = U_{ref}(T_i - T_o) \qquad 6.2$$

where T_i is the internal ambient temperature (°C), T_o is the external ambient temperature (°C), and U_{ref} is the reference U-value (W/m^2K), calculated at the glazing centre with $T_i = 20$ °C and $T_o = 0$ °C

B- Figure 3.3 of Chapter 3 shows the centreline thermal circuit for a double glazed window. Temperatures t_1, t_2, t_3, and t_4 are designated for the glazing surfaces as indicated. t_2 and t_3 can be calculated using Equations 3.30 and 3.31 respectively [6.5], where R_{g1} and R_{g2} are respectively the outdoor and indoor glass thermal resistances ($R_{g1} = R_{g2} = 0.004$ K/W)

The temperature t_2 of the outdoor glazing was assumed constant over the entire height of the glass. The outer pane was not the subject of attention in this work, therefore, only two thermocouples, one at the top and the other at the bottom end of the outer pane were used. Figure 6.4 shows the variation of these two temperatures (measured on window number 2) with time. As it is apparent from Fig. 6.4, the

differences between the top and bottom temperatures are very small. However, future work may involve use of more thermocouples to measure the outer pane temperature in a finer grid.

C- The rate of heat transfer by conduction through any medium is given by Fourier's law.

$$q = kA\frac{\Delta T}{\Delta x} \qquad 6.3$$

where,

A material cross sectional area perpendicular to the direction of heat flow, m^2

k thermal conductivity of the material, W/mK

ΔT differential temperature across material thickness, °C

Δx material thickness, m

The thermal conduction resistance can be derived from Fourier's law as follows.

$$R_{cond} = \frac{\Delta x}{kA} \qquad 6.4$$

Although the thermal conductivities of materials vary with temperature, over a temperature range of up to 200 °C the variation is insignificant and constant values may be assumed in order to simplify the analysis [6.4]. The thermal conductivity of each window component is given in Table 6.2 below.

Table 6.2 Thermal conductivities of window components

Material	Thermal conductivity (k), W/mK
Float Glass	1.0
Wood	0.13
Aluminium	220
Desiccant	0.12
Polysulphide	0.19
Polyisobutylene	0.2

D- As explained previously in Chapter 3, heat transfer from the building interior surfaces, e.g. internal walls, furniture, etc., to the internal pane of the double glazed window is by radiation and convection. The thermal resistances of convection and radiation may be combined together and represented by one resistance called the internal surface resistance. Heat is also lost from the outer pane in the same way, i.e. by convection and by radiation to the exterior surroundings. The combined resistance, in this case, is called the external surface resistance.

The glazings surface radiative heat transfer resistance depends upon the temperature of the radiative glass, its shape and emissivity. It also depends on the shape and emissivity of the other surface to which the glazing radiates, e.g. the building's interior surfaces in the case of the internal pane and the exterior surroundings in the case of the outer pane.

The glazings surface convective heat transfer resistance depends upon the direction of the heat flow , i.e. upward, downward, or horizontal, the direction of the wind speed across the surface.

Values of the inside surface resistance R_{si} vary but standard values are given in Refs. [6.6, 6.7]. For a vertical double glazed window with high emissivity factor ($\varepsilon_1 = \varepsilon_2 = 0.88$), R_{si} equals 0.12 [6.6-6.8]. Thus the inside surface transfer

coefficient h_i which represents both convection and radiation encountered at the internal surface of the double glazed window's inner pane is the inverse of R_{si} and equals 8.3 W/m^2K.

Values of the external surface resistance R_{so} are also given in Refs. [6.6, 6.7]. For double glazed windows, values of R_{so} depend upon the emissivities of the external surface of the outer pane and the type of the outside atmosphere to which the glazing is exposed, i.e. sheltered, normal, or severe.

Presently measurements for window samples were undertaken in the test room which was built on the fifth floor of Napier University building. Therefore, the exposure conditions can be assumed normal. The emissivity of the external surface of the outer pane for all windows was taken as 0.88 and the wind speed was assumed 3 m/s. Under these assumptions, the external surface resistance used in this analysis was taken as 0.06 m^2k/W [6.6]. Thus the glazing outside surface heat transfer coefficient h_o which represents both convection and radiation encountered at the external surface of the double glazed window's outer pane is the inverse of R_{so} and equals 16.7 W/m^2K.

For outdoor horizontal planes, the external surface heat transfer coefficient h_o was taken as 25 W/m^2K [6.6, 6.7].

E- For the elements 3, 4, 5 and 6 shown in Fig. 6.1, the net radiative heat transfer from an element to the outer glass pane can be calculated using the following basic formula.

$$q_r = \frac{\sigma(T_1^4 - T_2^4)}{\frac{1-\varepsilon_1}{\varepsilon_1 A_1} + \frac{1}{A_1 F_{12}} + \frac{1-\varepsilon_2}{\varepsilon_2 A_2}} \qquad 6.5$$

Using this formula, the radiation resistance can be written as follows,

$$R_{rad} = (T_1 - T_2)/q_r \qquad 6.6$$

Thus,

$$R_{rad} = \frac{\frac{1-\varepsilon_n}{\varepsilon_n A_n} + \frac{1}{A_n F_{no}} + \frac{1-\varepsilon_1}{\varepsilon_1 A_o}}{\sigma(T_n^2 + t_2^2)(T_n + t_2)} \qquad 6.7$$

where,

A_n	node surface area with unit depth, m^2
A_o	surface area of the outer pane with unit depth, m^2
ε_1	outdoor glass emissivity
ε_n	nodal surface emissivity
F_{no}	view factor of the nodal element with respect to the outer glass pane
R_{rad}	radiation resistance, m^2K/W
σ	Stefan-Boltzmann constant ($\sigma = 5.678 \times 10^{-08}$ W/m^2K^4)
T_n	node temperature, where n represents node number (3, 4, 5, or 6)

Emissivity is a surface radiative property defined as the ratio of the radiation emitted by the surface to the radiation emitted by a blackbody at the same temperature. The emissivity depends strongly on the nature of the surface, which can be influenced by the method of fabrication, thermal cycling, and chemical reaction with its environment. More literature regarding the complications of the surface emissivity is given in Refs. [6.9, 6.10]. In the present analysis, the emissivities of the inner and outer glass surfaces which face each other are taken as 0.88 for float glass and 0.12 for glass with a low emissivity coating of Tin-oxide [6.3].

The view factor F_{no} is defined as the fraction of the radiation leaving surface (n) which is intercepted by surface(o). The view factor F_{no} used in Equation 6.7

represents the fraction of radiation that leaves the surface of the nodal element and is intercepted by the surface of the outer inner pane that faces it. As can be seen from Fig. 6.1, the surface area of each nodal element for a depth unit (2-D analysis) is (0.007 x 1 = 0.007 m^2). This area is very small compared to the area of the outer pane which is (0.42 x 1 = 0.42 m^2). Nodal elements 3-6 also exchange radiation with the surfaces of the edge-seal surrounding the cavity. This part of radiation is very minor and can be ignored. Therefore, F_{no} can be assumed to be unity.

Equation 6.7 is used only for nodes 3, 4, 5, and 6 because the other nodes 1 and 2 are obstructed by the window edge-seal as shown in Fig. 6.1.

The infill gas is assumed to be a non-participating medium which means that it neither emits, absorbs, nor scatters radiation. Therefore, it has no effect on the long wavelength radiation exchange between the glass panes. A vacuum meets these requirements exactly and most gases meet them to an excellent approximation [6.11]. All the radiative surfaces are assumed grey, diffuse and opaque to infrared radiation [6.11].

F- Heat transfer from the nodal elements 3, 4, 5 and 6 also occurs by the virtue of natural convection to the infill gas. It has been shown by the experiments and Computational Fluid Dynamics (CFD) that with the exception of very narrow double glazing cavities, the gas movement within the enclosure may be closely approximated as channel flow [6.8]. For the cavity width presently being considered in this work, it was shown in Ref. [6.8] that the infill gas forms an inactive core which separates the boundary layers on either sides of the vertical cavity walls. Based on the above, it is therefore appropriate to select the model given by Equation 6.8 for natural convection across a uniformly heated vertical plate [6.11].

$$\Delta T_X = 1.15\left(\frac{x}{H_w}\right)^{0.2} \Delta T_{H_w/2} \qquad 6.8$$

where,

$$\Delta T_{H_w/2} = t_3 - T_f \qquad 6.9$$

and,

$$T_f = \frac{t_2 + t_3}{2} \qquad 6.10$$

where,

$\Delta T_{H_w/2}$ temperature difference between the centre-glazing and the core of the infill gas (= t_3 - T_f), °C

ΔT_X temperature difference at any height (x) between a given node and the core of the infill gas (= T_n - T_f), °C

t_2 outer pane cavity-side temperature at centre-glazing level, °C

t_3 inner pane cavity-side temperature at centre-glazing level, °C

T_f infill gas film temperature, °C

The convection resistance between the inner glass and the infill gas can be written as,

$$R_{conv} = \frac{\Delta T_X}{qA} = 1.15\left(\frac{x}{H_w}\right)^{0.2} \frac{\Delta T_{H_w/2}}{qA} \qquad 6.11$$

Table 6.3 shows the procedure followed in this analysis to calculate R_{conv} using Equation 6.11 for nodes 3, 4, 5, and 6 for window No. 2 (see Table 4.2). Only one set of the experimental data of window No. 2 has been used herein.

Table 6.3 Calculation of R_{conv} for window No. 2, (U_{ref}=2.72, T_i=0 °C, T_o=20 °C)

Node No.	x (m)	L (m)	$\Delta T_{L/2}$ (°C)	ΔT_X (°C)	q (W/m^2)	A (m^2)	R_{conv} (K/W)
3	0.0035	0.4	4.88	2.18	54.4	0.007	5.71
4	0.0105	0.4	4.88	2.71	54.4	0.007	7.11
5	0.0175	0.4	4.88	3.00	54.4	0.007	7.88
6	0.0245	0.4	4.88	3.21	54.4	0.007	8.42

In Table 6.3, x is the vertical height of the node measured from the bottom edge-seal surface in metres. The height of window L is 0.4 m. $\Delta T_{L/2}$ represents the difference between the inner pane temperature and the infill gas film temperature at the window mid-height. In this example t_3 = 13.23 °C (Equation 3.31) and T_f = 8.35 °C (Equation 6.10). Therefore, $\Delta T_{L/2}$ = 4.88 °C. The value of q is (2.72 x (20-0) = 54.4 W/m^2) as calculated using Equation 6.2. The surface area A of each node for a depth unit is (0.007x1 = 0.007 m^2).

G- The temperatures for node 7 and other nodes up to the centre of the window were calculated using the convection model developed in the previous chapter. This model can be applied with a significant level of accuracy to compute the temperature distribution along the entire window height except in the edge region. It can be represented as follows,

$$t_7 = T_f + (q\,H / k)\,(c_o + c_1\,U_{ref})\,([g\,\beta\,H^4\,q\,Pr] / [\alpha\,\nu\,k])^{m} \qquad 6.12$$

Calculation of such temperatures was mentioned previously in Chapter 5.

H- Due to the massive wooden frame underneath the window unit, the heat transfer by conduction from the window to the wooden frame can be neglected. Thus the wooden surface under the glazing unit, plane B-B in Fig. 6.1, is assumed to be insulated.

The detailed resistance network of Fig. 6.3 is reducible to the simplified network shown in Fig. 6.5. The values of the resistances of Fig. 6.5 are given in Table 6.4. The radiative resistances associated with nodes 3, 4, 5, and 6 are provided in terms of unknown nodal temperatures. The numerical values for the above resistances are generated iteratively during the process of obtaining a solution.

Based on the above relationships (Equations 6.1-6.12), the set of equations which enables the estimation of the desired nodal temperatures is given in Equation 6.13. Conductances are used rather than resistances to facilitate writing the nodal equations ($C = R^{-1}$),

$$T_a = (C_{1a}T_1 + C_{ad}T_d + C_{ab}T_b) / C_t \quad \text{and} \quad C_t = C_{1a} + C_{ad} + C_{ab} \qquad 6.13a$$

$$T_b = (C_{ab}T_a + C_{be}T_e + C_{bc}T_c) / C_t \quad \text{and} \quad C_t = C_{ab} + C_{be} + C_{bc} \qquad 6.13b$$

$$T_c = (C_{bc}T_b + C_{cf}T_f + C_{co}T_o) / C_t \quad \text{and} \quad C_t = C_{bc} + C_{cf} + C_{co} \qquad 6.13c$$

$$T_d = (C_{2d}T_2 + C_dt_c + C_{de}T_e + C_{ad}T_a) / C_t \quad \text{and} \quad C_t = C_{2d} + C_d + C_{de} + C_{ad} \qquad 6.13d$$

$$T_e = (C_{de}T_d + C_et_2 + C_{ef}T_f + C_{be}T_f) / C_t \quad \text{and} \quad C_t = C_{de} + C_e + C_{ef} + C_{be} \qquad 6.13e$$

$$T_f = (C_{ef}T_e + C_{fg}T_g + C_{fo}T_o + C_{cf}T_c) / C_t \quad \text{and} \quad C_t = C_{ef} + C_{fg} + C_{fo} + C_{cf} \qquad 6.13f$$

$$T_g = (C_gt_2 + C_{gy}T_o + C_{gx}T_o + C_{fg}T_f) / C_t \quad \text{and} \quad C_t = C_g + C_{gy} + C_{gx} + C_{fg} \qquad 6.13g$$

$$T_1 = (C_{1i}T_i + C_{12}T_2 + C_{1a}T_a) / C_t \quad \text{and} \quad C_t = C_{1i} + C_{12} + C_{1a} \qquad 6.13h$$

$$T_2 = (C_{2i}T_i + C_{23}T_3 + C_{2d}T_d + C_{12}T_1) / C_t \quad \text{and} \quad C_t = C_{2i} + C_{23} + C_{2d} + C_{12} \qquad 6.13i$$

$$T_3 = (C_{3i}T_i + C_{34}T_4 + C_{3r}t_2 + C_{3c}t_c) / C_t \quad \text{and} \quad C_t = C_{3i} + C_{34} + C_{3r} + C_{3c} \qquad 6.13j$$

$$T_4 = (C_{4i}T_i + C_{45}T_5 + C_{4r}t_2 + C_{4c}t_c) / C_t \quad \text{and} \quad C_t = C_{4i} + C_{45} + C_{4r} + C_{4c} \qquad 6.13k$$

$$T_5 = (C_{5i}T_i + C_{56}T_6 + C_{5r}t_2 + C_{5c}t_c) / C_t \quad \text{and} \quad C_t = C_{5i} + C_{56} + C_{5r} + C_{5c} \qquad 6.13l$$

$$T_6 = (C_{6i}T_i + C_{67}T_7 + C_{6r}t_2 + C_{6c}t_c)/C_t \quad \text{and} \quad C_t = C_{6i}+C_{67}+C_{6r}+C_{6c} \qquad 6.13m$$

To initiate the Gauss-Seidel iteration, an initial set of values for T_1, T_2, T_3, T_4, T_5, T_6, T_a, T_b, T_c, T_d, T_e, T_f, and T_g was assumed. New values of the above nodal temperatures were calculated using Equation 6.13. The process was repeated until all nodal temperatures converged to within 0.01 ^{0}C.

6.3 Results and Discussion

Abstracts from the experimental data for all the windows under investigation are presented in Appendix A. The experimental data for each window consists of sets of 14 values (12 temperatures along the height of the inner pane, the internal ambient temperature and the external ambient temperature). These sets were measured at different intervals of times.

For each window a Microsoft Excel spreadsheet was used to solve for the thirteen nodal temperatures represented by Equations 6.13. The internal and external ambient temperatures in each experimental set and the values of all the resistances mentioned in Table 6.4 were substituted in Equations 6.13. An initial set of temperatures T_1 to T_g was assumed to initiate the solution process. New values of the nodal temperatures T_1 to T_g were calculated according to Equations 6.13. This process was repeated until successive values differed by a sufficiently small amount. In terms of the Excel spreadsheet, a test was inserted to stop the calculations when $|T_{n+1} - T_n| \leq 0.01$ °C. Obviously, the smaller this value, the greater calculation time required to obtain the desired result. The final converged solution has been checked by performing an energy balance for each node.

The computer software Conduct.xls (see Appendix J) includes the above model and is presently available on the accompanying floppy disk.

For window No. 2 (U_{ref} = 2.72, T_i = 0 °C, T_o = 20 °C), see Table 6.3, the temperatures of all the thirteen nodes were obtained by using Conduct.xls. After 28 iterations, the final converged solution was found to be as follows:

T_1 = 9.53 °C	T_2 = 9.08 °C	T_3 = 9.70 °C	T_4 = 10.05 °C
T_5 = 10.16 °C	T_6 = 10.06 °C	T_a = 8.22 °C	T_b = 6.54 °C
T_c = 1.09 °C	T_d = 8.31 °C	T_e = 6.41 °C	T_f = 0.85 °C
T_g = 0.52 °C			

An energy balance was performed for each node to check for the correctness of the solution obtained. For each node, the sum of the input energies should equal the sum of the output energies. Table 6.5 shows the absolute value of the difference between the input and output energies for each node. This value should approach zero. This procedure was repeated for all windows under investigation. For each window a converged solution was obtained for each set of experimental data as described above.

Table 6.5 Energy balance calculations

Node Number	$\left\lvert Input\ Energy\ \ Rate - Output\ Energy\ \ Rate \right\rvert$, Watt
1	1.61×10^{-6}
2	9.9×10^{-7}
3	6.4×10^{-7}
4	3.6×10^{-7}
5	1.5×10^{-7}
6	3.82×10^{-6}
a	1.3×10^{-5}
b	3.2×10^{-5}
c	29×10^{-5}
d	3.6×10^{-5}
e	1.8×10^{-5}
f	28×10^{-5}
g	5.55×10^{-17}

Table 6.6 shows the number of data sets of computed temperatures obtained by the above procedure for each window. Each of these computed data sets were then compared with the corresponding measured data sets.

Both computed and measured temperatures for each individual tested window have been plotted against the height of the window. Two such plots are shown in Figs. 6.6 and 6.7 which show good agreement. To demonstrate the results of the model developed presently and the previous model developed earlier in Chapter 5, only window heights up to 0.35 m were used in Figs. 6.6 and 6.7. The present model enables the estimation of the nodal temperatures 1-6 which requires a predetermined value for the temperature of node 7 (seed nodal temperature). Hence the need for the model presented in the previous chapter for initiating computations for nodes 1-6. Details of this computation is given in

Table 6.6 Number of converged solution for each window

Window Number (See Table 4.2 of Chapter 4)	Number of computed data sets
1	114
2	69
3	50
4	50
5	79
6	55

section 6.2.7 above. The temperature of node 7 is thus fixed and predetermined before the present analysis is undertaken. It is worth mentioning that the previous chapter dealt with the temperature distribution along the entire window height except for the edge region. In contrast, the aim of the present analysis is to calculate temperature distributions in the edge region where convection as well as conduction effects occur.

The contribution of the present analysis is that a holistic model has been developed for the heat transfer at the bottom edge of a double glazed window. This model combines the effects of radiative exchange between the glass panes, natural convection due to the circulating gas and conduction through the spacer. This is in contrast to previous work which solely addressed the spacer conduction effects [6.12].

The validity of the present combined heat transfer model for the bottom part of the window is demonstrated by the comparison shown in Fig. 6.8 where the computed temperatures are plotted against the corresponding measurements for window No. 2 (Table 4.2). The values of the mean biased error (MBE) and the root mean square errors (RMSE) for each window are shown in Table 6.7.

To evaluate the contribution of the metallic spacer in lowering the bottom edge temperatures, the edge-seal (Fig. 6.1) has been replaced by an infinite resistance in the model and the calculations repeated again for all windows using this imaginary

resistance. This procedure eliminates the conduction effects. Table 6.8 shows a comparison of the temperature difference between the centre-glazing and the bottom node (node 3) for the two scenarios, i.e. an aluminium and a perfectly insulated spacer, respectively shown in columns 4 and 5. Column 4 shows an increasing trend for the above temperature differential. This has also been demonstrated by Frank and Wakili [6.13]. This phenomenon can be explained as follows. The indoor centre-glazing temperature t_3 increases and the outdoor pane temperature t_2 decreases with the decrease of U-value due to increased cavity thermal resistance. This conclusion can be verified by Equations 3.30 and 3.31. As mentioned previously, the descending infill gas would approach the temperature of the cold outer glazing. Thus T_3, the bottom temperature of the inner pane also decreases with a lowered U-value. Therefore, the temperature differential (t_3-T_3) will increase quite rapidly due to the combined effect of the elevated t_3 and lowered T_3. Reference is now made to column 5 of Table 6.8. Once again an increasing differential between t_3 and T_3 is noticeable between cases 1 and 2, and between cases 3 and 4. The above two comparisons demonstrate the effect of higher resistance to the heat flow due to convection. The temperature differential (t_3-T_3) also increases from case 1 to 3 and from case 2 to 4 due to the increased radiative resistance between the respective cases. The situation in cases 5 and 6 is very involved. Several counteracting influences may be identified. Firstly, the descending colder gas gets cooler with decreasing U-value, thus tending to bring down T_3. Secondly, the node 3 looses less heat by radiation and therefore tends to improve T_3. Thirdly, (t_3-T_3) decreases due to increased thermal contact between these nodes for heavier, inert gases as shown by Muneer and Han [6.8, 6.14, 6.15].

For any given case, a comparison between columns 4 and 5 illustrates the effect of the conductivity of the edge-seal. Column 5 provides the values of (t_3-T_3) for a hypothetical situation wherein the aluminium spacer resistance is replaced with an infinite resistance. Cases 1 and 6 lie at the extreme ends of the comparative exercise. It is clear that for an air-filled window (case 1) the edge conductivity has a minor influence, e.g. its relative weighting is only 17%. However, for the low emissivity xenon windows the spacer

conduction is the major contributor in reducing the edge temperature. The relative weighting of the edge effect in this case is 60%.

6.4 Three-dimensional model

The analysis considered in section 6.2 involves heat flow in two directions only, e.g. D1 and D2 as shown in Fig. 6.9. In this figure, D1 represents the vertical direction which lies in the plane of the inner pane surface (y-axis), D2 represents the direction perpendicular to the plane of the inner pane surface (z-axis), and D3 represents the horizontal direction which lies in the plane of the inner pane surface (x-axis). The previous analysis has provided a 2-D model which can calculate the temperature distribution along the vertical centreline of the window indoor pane (along D1). This model has been expanded to include heat flow in a third direction, D3. The development of a 3-D model is needed to investigate the effect of the edge-seal at both sides and top of the glazing on the temperature distribution of the indoor pane. This gives a complete picture of the temperature distribution on the entire surface of the indoor pane of a double glazed window. To develop a 3-D model, experimental and analytical work has been carried out as described below.

Temperature measurements were taken for two windows, i.e. 4-air12-4 and 4E-xenon10-E4. These windows were selected because they have the lowest and highest thermal performance respectively. Temperatures of 48 nodes on the surface of the inner pane of each window and the internal and external ambient temperatures were measured as explained in Chapter 4. Each window was tested for two days during which measurements were recorded every five minutes. Abstracts from the experimental data for both windows are shown in Appendix C. Figure 6.10 shows the temperature distribution of one set of these measurements on the inner glazing surface of the 4-air12-4 sample.

The finite-difference technique was used for obtaining numerical solutions for this 3-D problem. Due to symmetry, only the right-hand half of the inner pane surface was

considered. It was divided into 169 zones (finite elements). Each zone was represented by a node. These nodes were labelled with three-digit numbers as shown in Fig. 6.11. The Gauss-Seidel iteration [6.4] technique was used to obtain an efficient solution for this nodal arrangement as in the case of the 2-D analysis discussed earlier in section 6.2.

The boundary conditions for this problem were considered as follows. In direction D1, the pane bottom temperature T_3 (mentioned in section 6.2 above) was assumed to be the boundary condition in this direction, both at the top and at the bottom boundaries. This assumption is justified in view of the large conductance of the metallic spacer. Further, references are made to Fig. 4.5 of Chapter 4 which shows the validity of this assumption. In direction D2, the boundaries are the infill gas at one side and the room environment at the other side. In direction D3, T_3 is assumed as the boundary condition at the right-hand side and the glazing centreline temperatures calculated previously as the boundary condition at the left-hand side. This assumption is justified in view of the large conductance of the metallic spacer. The centreline temperatures T_{000} and T_{010} shown in Fig. 6.11, were calculated by interpolation between T_3 and T_4 for T_{000} and between T_6 and T_7 for T_{010}. The remaining centreline temperatures, e.g. T_{020}-T_{160} were calculated by using the model developed previously in Chapter 5 (Equation 6.12 above).

After defining the boundary conditions for this problem, the analytical procedure used in section 6.2 was followed. The steady state temperature of each node was obtained in terms of the resistances and temperatures of the adjoining nodes using Equation 6.1.

The conduction and radiation resistances for all nodes were calculated using Equations 6.4 and 6.7 respectively. For the first and second rows of nodes (Fig. 6.11), the convection resistance between any node and the circulating infill gas was calculated using Equation 6.11, where x = 0.005 m for the first row of nodes and x = 0.030 m for the second row of nodes. For the remaining nodes, the model developed by Muneer and Han [6.8] was used to calculate the convection resistance. This model (Equation 6.14) was explained previously in Chapter 3.

$$Nu = 0.3628(Gr\ Pr)^{0.2451}\ {}_{A}{}^{-0.2783} \qquad 6.14$$

The combined convection and radiation resistance between the window inner pane surface and the internal environment was taken as ($R_{si} = 0.12$).

Therefore, the temperatures of the nodes can be written as follows.

The temperature equation of node (001),

$$T_{001} = 0.0084\ T_{000} + 0.003276\ T_{011} + 0.002352\ T_{002} + 0.0546\ T_3 + 1.36x10^{-11}\ (T_{001}^2 + t_2^2)\ (T_{001} + t_2)\ t_2 + 0.000573\ q\ T_f / \Delta T_{L/2} + 0.002266\ T_i / (0.0084 + 0.003276 + 0.002352 + 0.0546 + 1.3\ 6x10^{-11}\ (T_{001}^2 + t_2^2)\ (T_{001} + t_2) + 0.000573\ q\ / \Delta T_{L/2} + 0.002266)$$

Nodes (002-008) are identical, therefore, their temperature equations will take the same form as node (002),

$$T_{002} = 0.002352\ T_{001} + 0.0042\ T_{012} + 0.002352\ T_{003} + 0.07\ T_3 + 1.75x10^{-11}\ (T_{002}^2 + t_2^2)\ (T_{002} + t_2)\ t_2 + 0.000735\ q\ T_f / \Delta T_{L/2} + 0.002905\ T_i\ / (0.002352 + 0.0042 + 0.002352\ + 0.07\ + 1.75x10^{-11}\ (T_{002}^2 + t_2^2)\ (T_{002} + t_2) + 0.000735\ q\ / \Delta T_{L/2} + 0.002905)$$

The temperature equation of node (009),

$$T_{009} = 0.002352\ T_{008} + 0.002352\ T_{019} + 0.0392\ T_3 + 0.0392\ T_3 + 9.8x10^{-12}\ (T_{009}^2 + t_2^2)\ (T_{009} + t_2)\ t_2 + 0.000411\ q\ T_f / \Delta T_{L/2} + 0.001627\ T_i / (0.002352 + 0.002352 + 0.0392 + 0.0392 + 9.8x10^{-12}\ (T_{009}^2 + t_2^2)\ (T_{009} + t_2) + 0.000411\ q\ / \Delta T_{L/2} + 0.001627)$$

The temperature equation of node (011),

$$T_{011} = 0.015\,T_{010} + 0.003276\,T_{021} + 0.0042\,T_{012} + 0.003276\,T_{001} + 2.43\text{x}10^{-11}\,(T_{011}^2 + t_2^2)\,(T_{011} + t_2)\,t_2 + 0.000715\,q\,T_f / \Delta T_{L/2} + 0.004046\,T_i / (0.015 + 0.003276 + 0.0042 + 0.003276 + 2.43\text{x}10^{-11}\,(T_{011}^2 + t_2^2)\,(T_{011} + t_2) + 0.000715\,q / \Delta T_{L/2} + 0.004046)$$

Nodes (012-018) are identical, therefore, their temperature equations will take the same form as node (012),

$$T_{012} = 0.0042\,T_{011} + 0.0042\,T_{022} + 0.0042\,T_{013} + 0.0042\,T_{002} + 3.12\text{x}10^{-11}\,(T_{012}^2 + t_2^2)\,(T_{012} + t_2)\,t_2 + 0.000917\,q\,T_f / \Delta T_{L/2} + 0.005188\,T_i / (0.0042 + 0.0042 + 0.0042 + 0.0042 + 3.12\text{x}10^{-11}\,(T_{012}^2 + t_2^2)\,(T_{012} + t_2) + 0.000917\,q / \Delta T_{L/2} + 0.005188)$$

The temperature equation of node (019),

$$T_{009} = 0.0042\,T_{018} + 0.002352\,T_{029} + 0.07\,T_3 + 0.002352\,T_{009} + 1.75\text{x}10^{-11}\,(T_{019}^2 + t_2^2)\,(T_{019} + t_2)\,t_2 + 0.000513\,q\,T_f / \Delta T_{L/2} + 0.002905\,T_i / (0.0042 + 0.002352 + 0.07 + 0.002352 + 1.75\text{x}10^{-11}\,(T_{019}^2 + t_2^2)\,(T_{019} + t_2) + 0.000513\,q / \Delta T_{L/2} + 0.002905)$$

Nodes (021, 031, 041, 051, 061, 071, 081, 091, 101, 111, 121, 131, 141, 151 and 161) are identical, therefore, their temperature equations will take the same form as node (021),

$$T_{021} = 0.015\,T_{020} + 0.003276\,T_{031} + 0.0042\,T_{022} + 0.003276\,T_{011} + 2.43\text{x}10^{-11}\,(T_{021}^2 + t_2^2)\,(T_{021} + t_2)\,t_2 + 0.000488\,h_c\,T_f + 0.004046\,T_i / (0.015 + 0.003276 + 0.0042 + 0.003276 + 2.43\text{x}10^{-11}\,(T_{021}^2 + t_2^2)\,(T_{021} + t_2)\,t_2 + 0.000488\,h_c + 0.004046)$$

Nodes (029, 039, 049, 059, 069, 079, 089, 099, 109, 119, 129, 139, 149, 159 and 169) are identical, therefore, their temperature equations will take the same form as node (029),

$$T_{029} = 0.0042\ T_{028} + 0.002352\ T_{039} + 0.07\ T_3 + 0.002352\ T_{019} + 1.75\text{x}10^{-11}\ (T_{029}^2 + t_2^2)\ (T_{029} + t_2)\ t_2 + 0.00035\ h_c\ T_f + 0.002905\ T_i\ /\ (0.0042 + 0.002352 + 0.07 + 0.002352 + 1.75\text{x}10^{-11}\ (T_{029}^2 + t_2^2)\ (T_{029} + t_2) + 0.00035\ h_c + 0.002905)$$

The remaining nodes are identical, therefore, their temperature equations will take the same form as node (022),

$$T_{022} = 0.0042\ T_{021} + 0.0042\ T_{032} + 0.0042\ T_{023} + 0.0042\ T_{012} + 3.12\text{x}10^{-11}\ (T_{022}^2 + t_2^2)\ (T_{022} + t_2)\ t_2 + 0.000625\ h_c\ T_f + 0.005188\ T_i\ /\ (4\ \text{x}\ 0.0042 + 3.12\text{x}10^{-11}\ (T_{022}^2 + t_2^2)\ (T_{022} + t_2) + 0.000625\ h_c + 0.005188)$$

These 153 equations were inserted in an Excel spreadsheet. An initial set of values for all nodal temperatures was assumed to initiate the Gauss-Seidel iteration. New values of the above nodal temperatures were calculated using the same equations. The process was repeated until all nodal temperatures converged to within a small amount of 0.01 °C.

These calculations were repeated for both window samples (4-air12-4 and 4E-xenon10-E4). For the 4-air12-4 window, for example, the above calculations were repeated 132 times which is the number of the measured sets of temperatures. Each time the internal and external air temperatures for each individual measured set were input in the spread sheet and a converged solution was obtained. Figure 6.12 shows the calculated converged temperatures which correspond to the measured temperatures shown in Fig. 6.10. It can be seen from Fig. 6.10 that despite the presence of some faulty readings due to measurement errors, the temperature of the inner pane increases with the window

height. This increase is on average 2.5 °C. However, there is a slight drop in temperature at the top edge which illustrates the cold-bridge effect of the seal-edge. It can also be seen from Fig. 6.10 that the pane temperatures change very slightly in the horizontal direction D3 with a slight drop at the side edges. The calculated temperatures show the same behaviour as the measured temperatures with an average increase of 2 °C over the window height as shown in Fig. 6.12. Generally, the calculated temperatures were found to be lower than the corresponding measured temperatures. To evaluate this model statistically, the RMSE and MBE for the measured and calculated temperatures shown in Figs. 6.10 and 6.12 were calculated and found to be 1.8 and 1.6 °C respectively.

6.5 Conclusions

The analysis given in this chapter provides a 2-D numerical model to obtain the longitudinal temperature distribution for the bottom part of double glazed windows. The drop of temperature at the bottom is attributed to the convection of the cavity gas, the radiation heat exchange and the cold bridge effects of the spacer and frame. It has been shown that the cavity gas convection is an important factor in the reduction of the bottom edge temperature. Cold bridging is also a significant factor for the conductive loss of heat at the edge surface. However, the present analysis has shown that the relative weighting for the conductive loss is only 17% for air filled windows. However, for the high-tech windows with low emissivity coating and heavier infill gases the edge effects dominate the temperature distribution.

To investigate the temperature distribution of the entire inner pane taking into account the effects of the circulating gas and the cold-bridging along the glazing edges, the two-dimensional model was extended in the direction D3 (Fig. 6.9) to obtain a three-dimensional temperature representation. The results of the three-dimensional model were not encouraging as the measured and computed temperatures were not in close concordance. The temperature, T_3, calculated from the two-dimensional model was taken as the boundary condition for all the glass edges in order to facilitate the calculation process. This imposed boundary condition may be the reason for results of a

poor quality. However, the three-dimensional model does show the impact of the edge-seal on the temperature distribution and also emphasises the effect of the infill gas circulation. Further work may involve the use of CFD technique to simulate the window in a more holistic manner.

References

6.1 D. Button and B. Pye, Glass in building: A guide to modern architectural glass performance, Pilkington Glass Ltd., UK, 1993

6.2 ISO 6946 Thermal insulation calculation methods, Part 1, Steady state thermal properties of building components and building elements, 1983

6.3 T. E. Johnson,. Low-E glazing design guide, Butterworth Architecture, London, 1991

6.4 J. P. Holman, Heat transfer, pp 99-105, McGraw Hill, New York, 1990

6.5 Calculating thermal transmittance, Pilkington Glass Limited environmental advisory service, St. Helens, UK, 1981

6.6 CIBSE Guide A3, Thermal properties of building structures, London, 1989

6.7 BS6993 Part I, British Standard Institute, London, 1989

6.8 T. Muneer and B. Han, Design charts for multiple glazed windows, BSER&T 17, 4, pp 223-229, 1996

6.9 G.G. Gubareff et al, Thermal radiation properties survey, 2nd ed., Honeywell Research centre, Minneapolis, 1960

6.10 W. D. Wood et al, Thermal radiative properties, Plenum Press, New York, 1964

6.11 F. P. Incropera and D. P. DeWitt, Fundamentals of heat and mass transfer, pp 542-544, John Wiley, New York, 1990

6.12 S. Svendsen and P. Fritzel, Spacers for highly insulated windows Proceedings of the Window Innovations' 95 Conference, pp 90-97, Toronto, 5 and 6 June 1995

6.13 T. Frank and K. Wakili, Linear Transmittance of different spacer bars, Proceedings of the Window Innovations' 95 Conference, pp 253-259, Toronto, 5 and 6 June 1995

6.14 T. Muneer and B. Han, Simplified theory for free convection in enclosures - application to an industrial problem, Energy Conversion & Management (Elsevier Science) 37, 9, 1996

6.15 T. Muneer and B. Han, Use of CFD for thermal analysis of double glazings, Computational Methods and Experimental Measurements VII, 77-84, Eds: G. M. Carlomagno and C. A. Brebbia. Computational Mechanics Publications, Southampton, UK, 1995

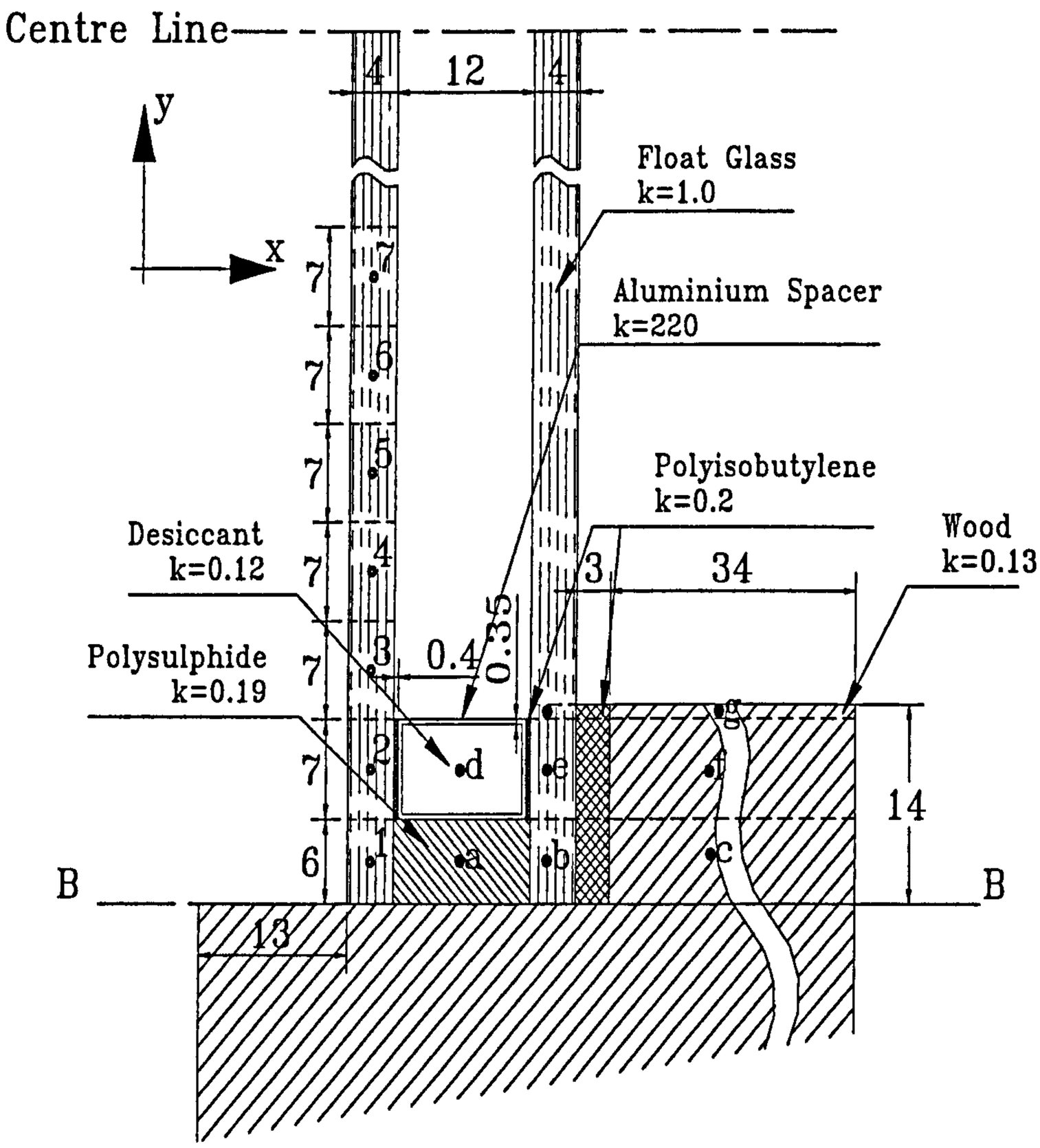

Figure 6.1 Design Schematic and nodal arrangement of windows under investigation (k values given in W/m K; glazing height 400mm; cavity gap 10mm for xenon and 12mm for all other infill gases)

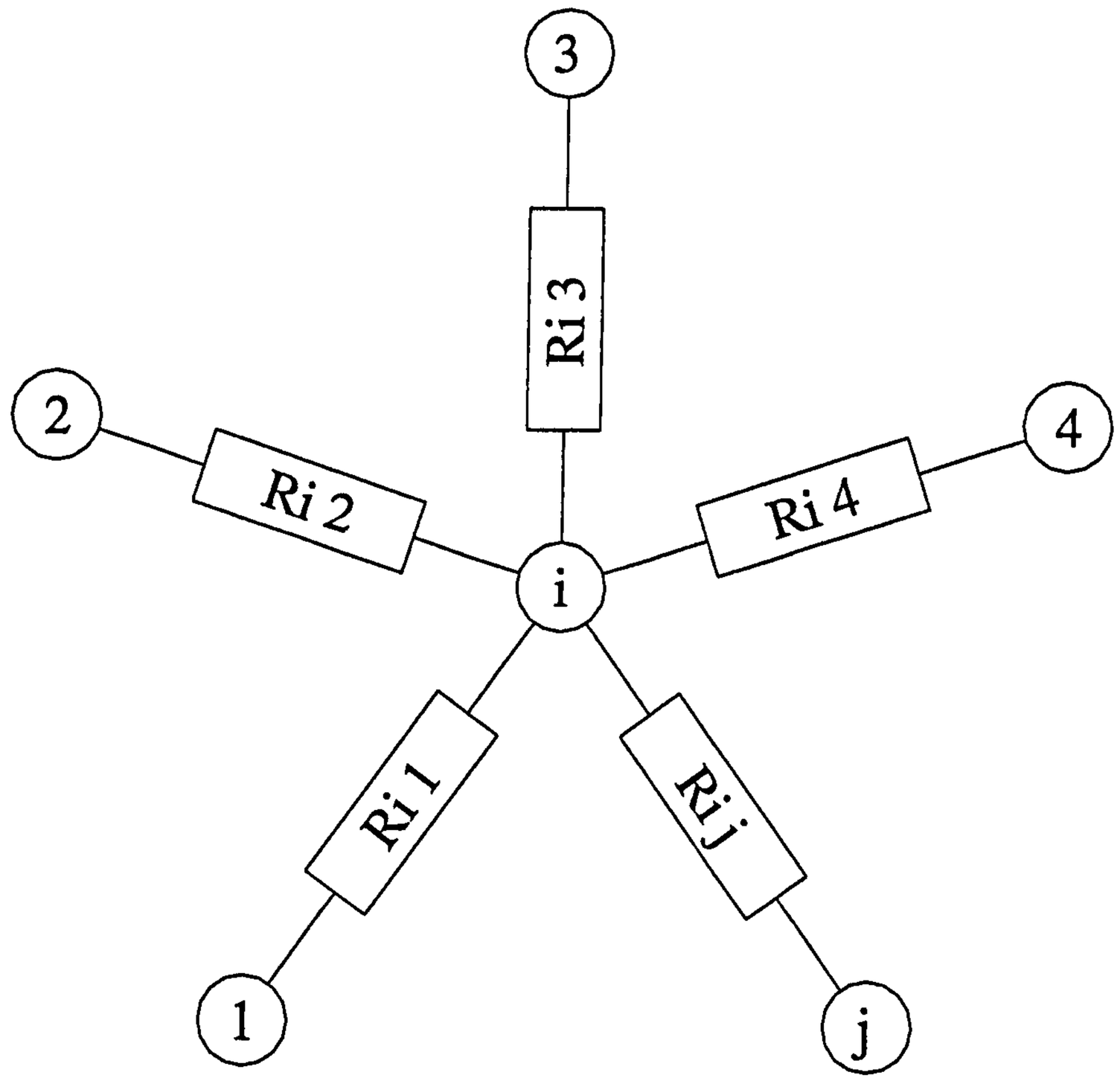

Figure 6.2 General Node

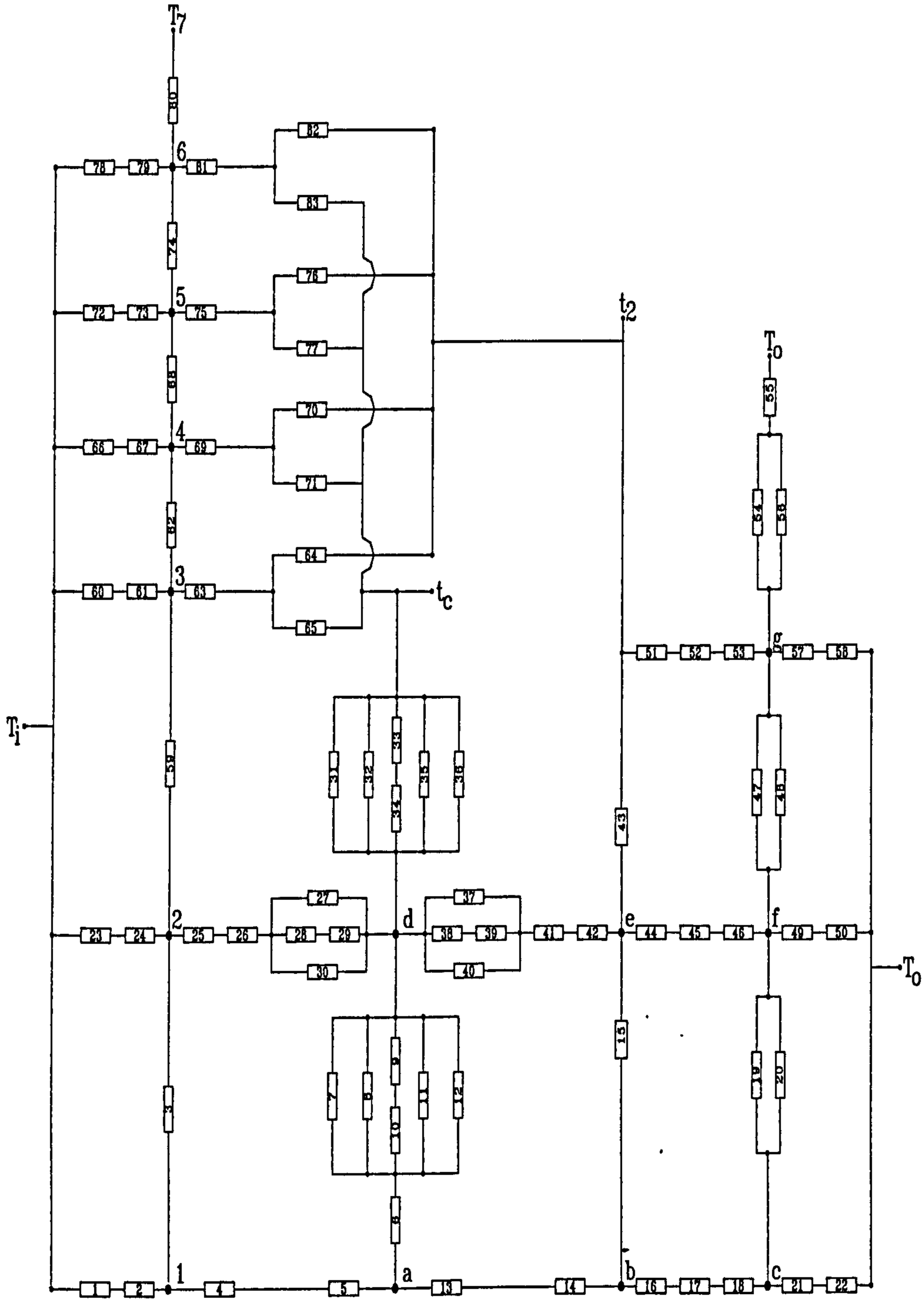

Figure 6.3 Thermal resistance network

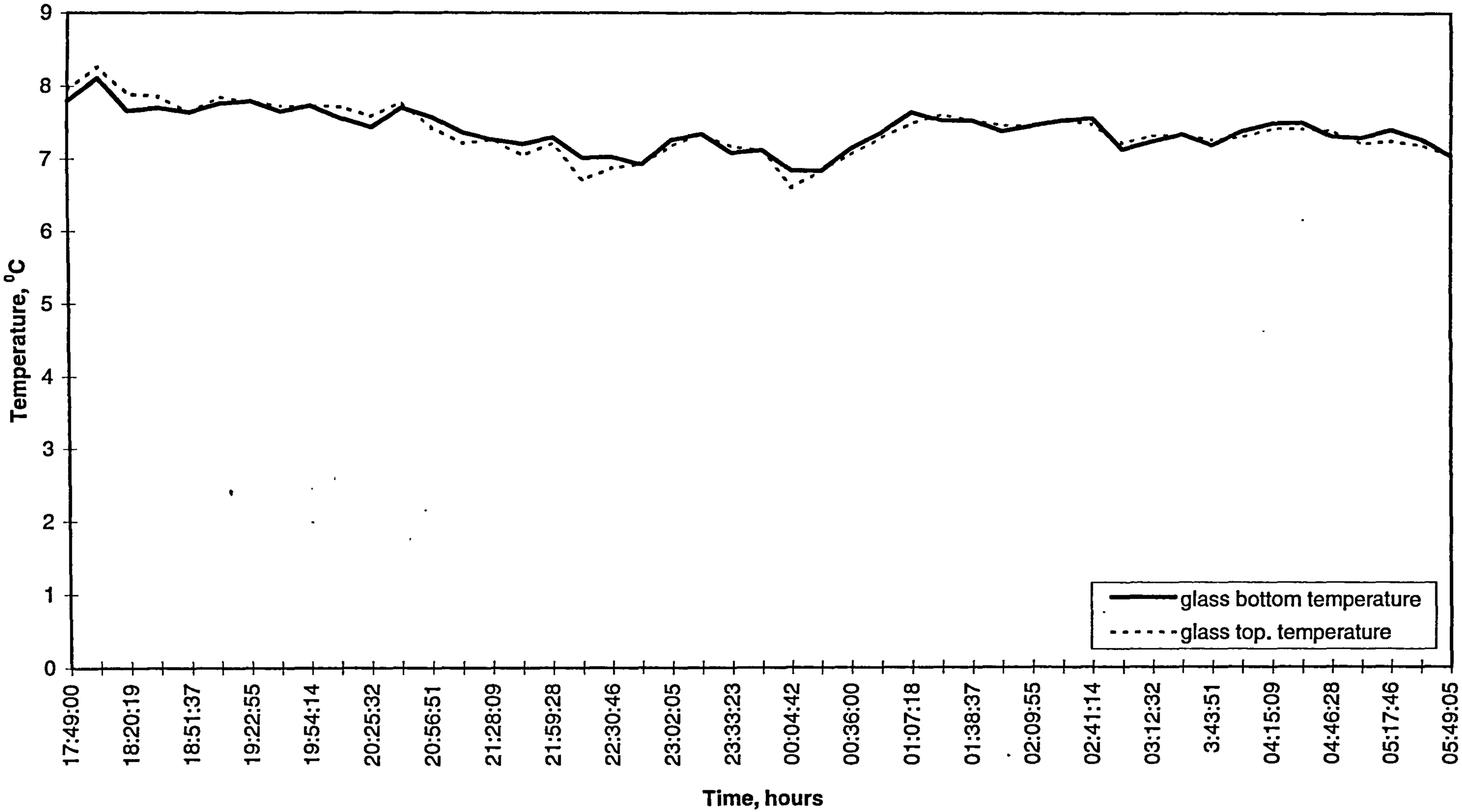

Figure 6.4 Temperatures measured on the outer pane of a 4-argon12-4 window for one night

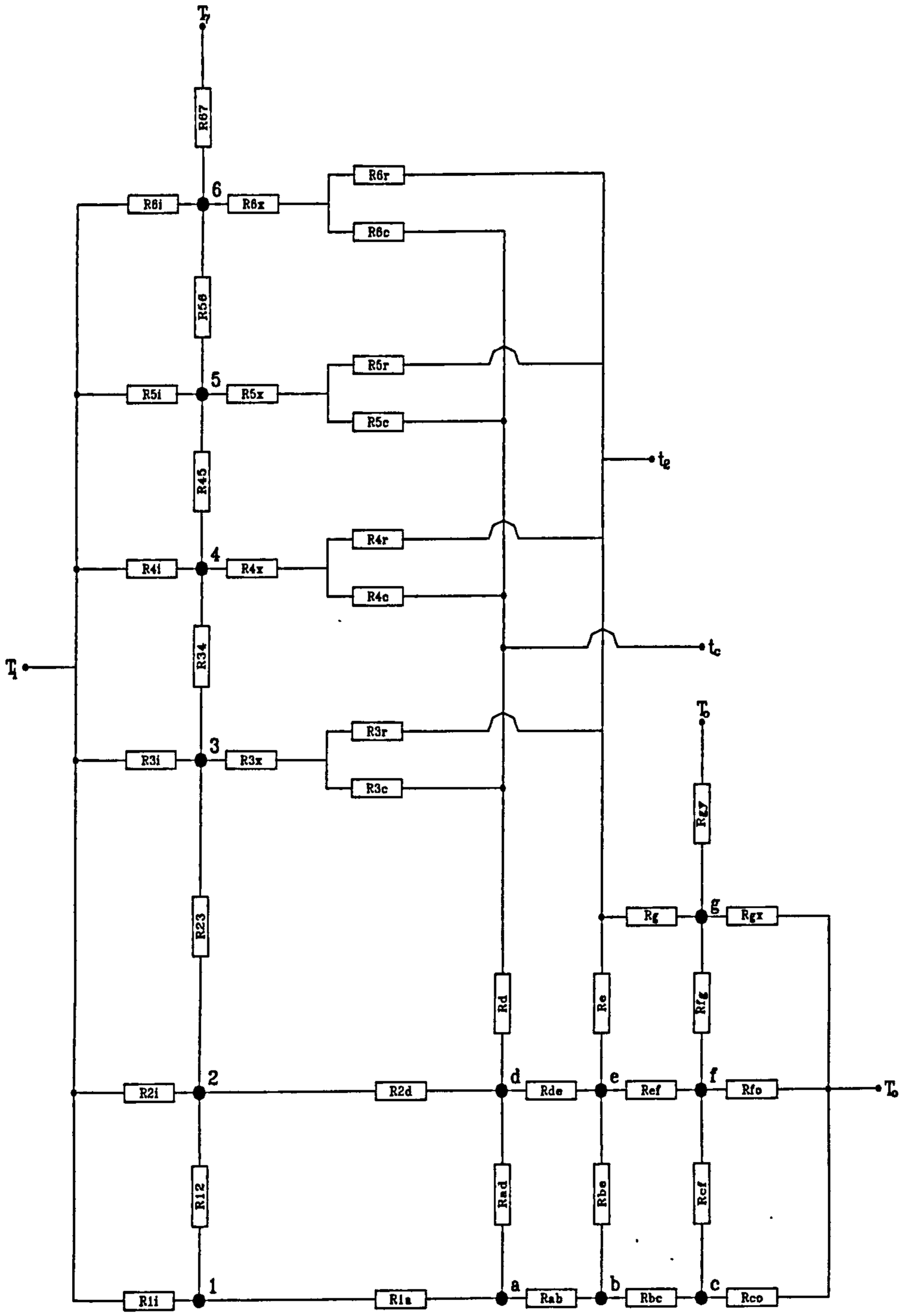

Figure 6.5 Simplified thermal resistance network

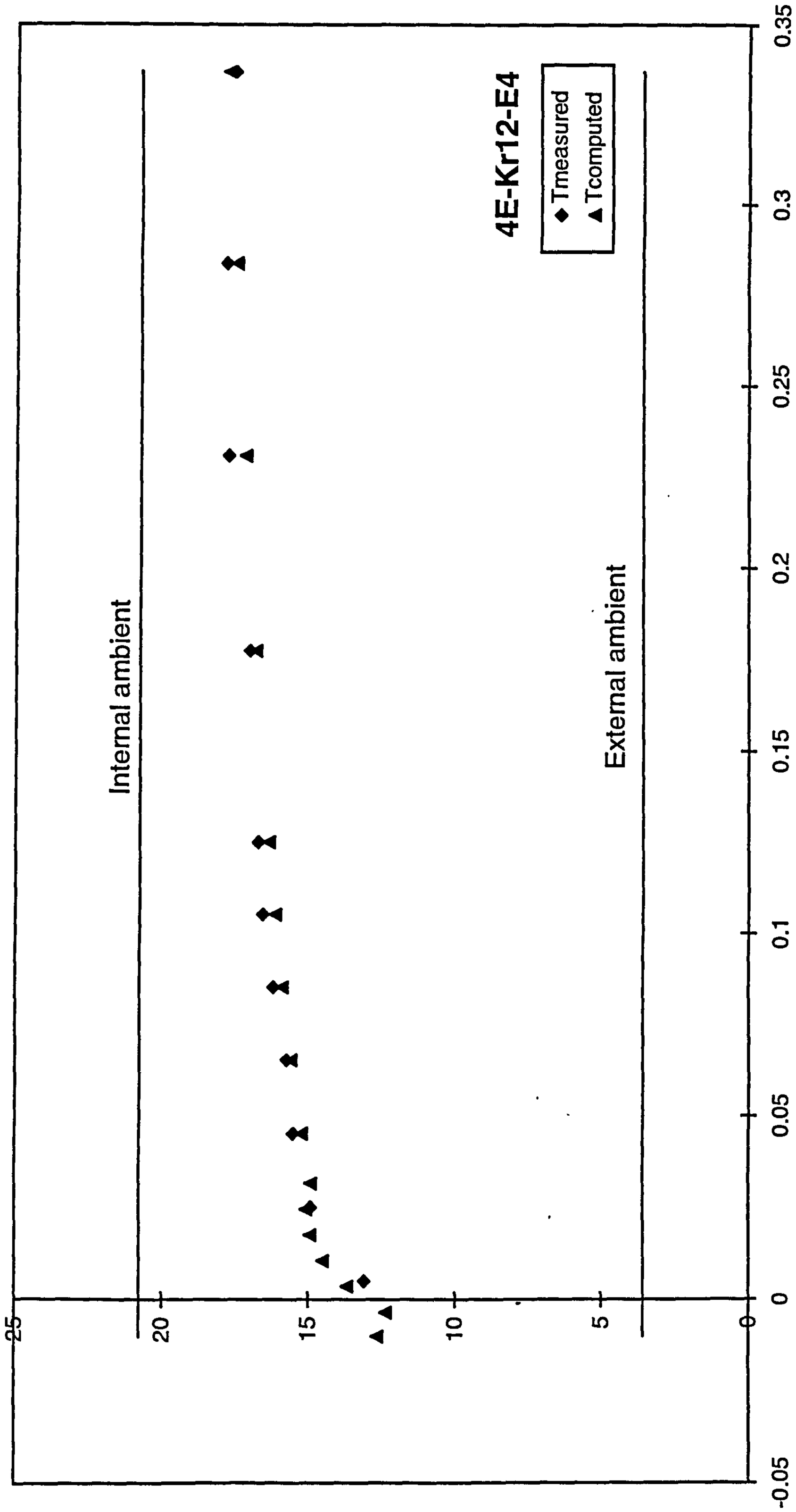

Figure 6.6 Measured and computed temperatures against window height

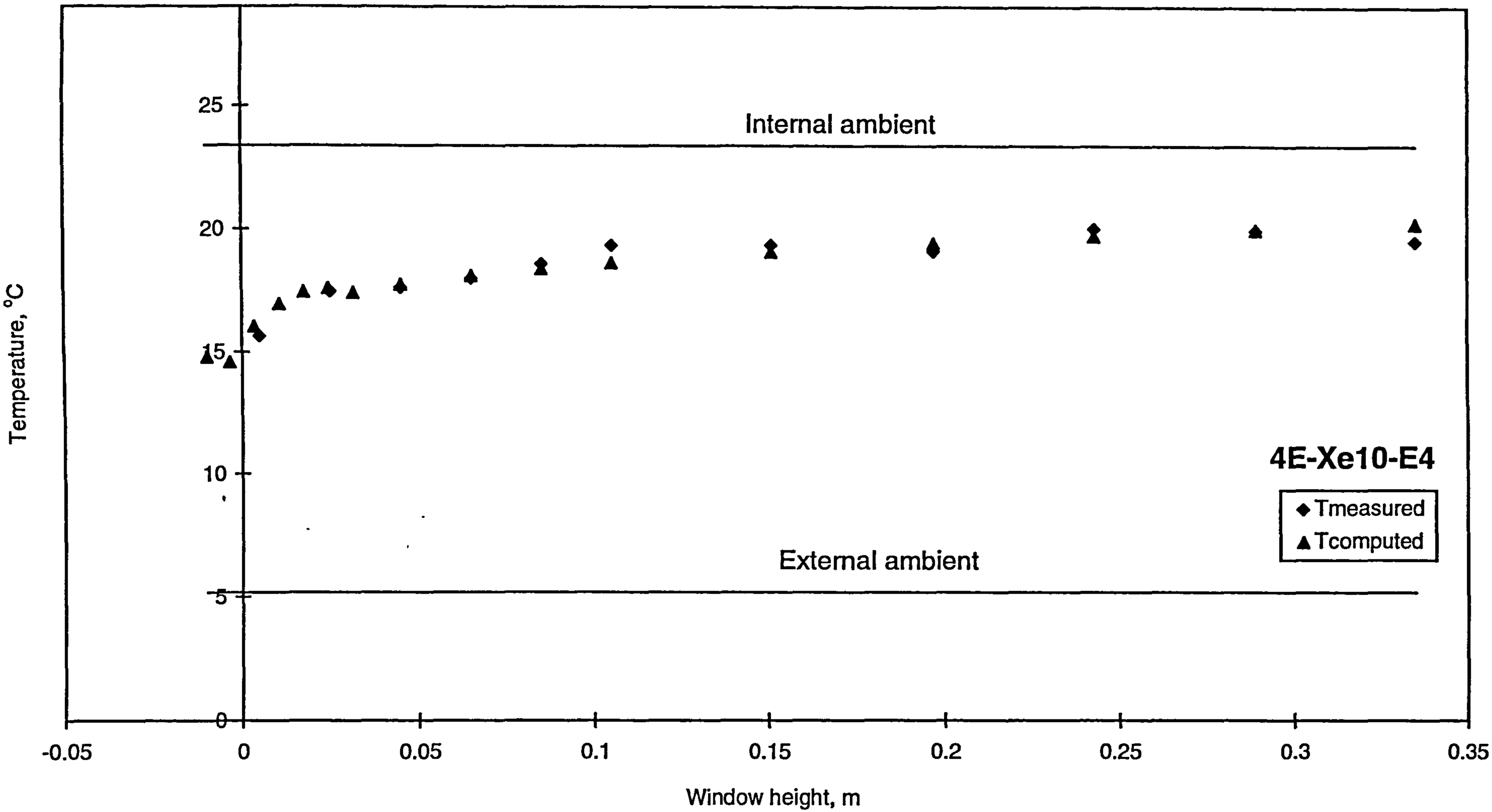

Figure 6.7 Measured and computed temperatures against window height

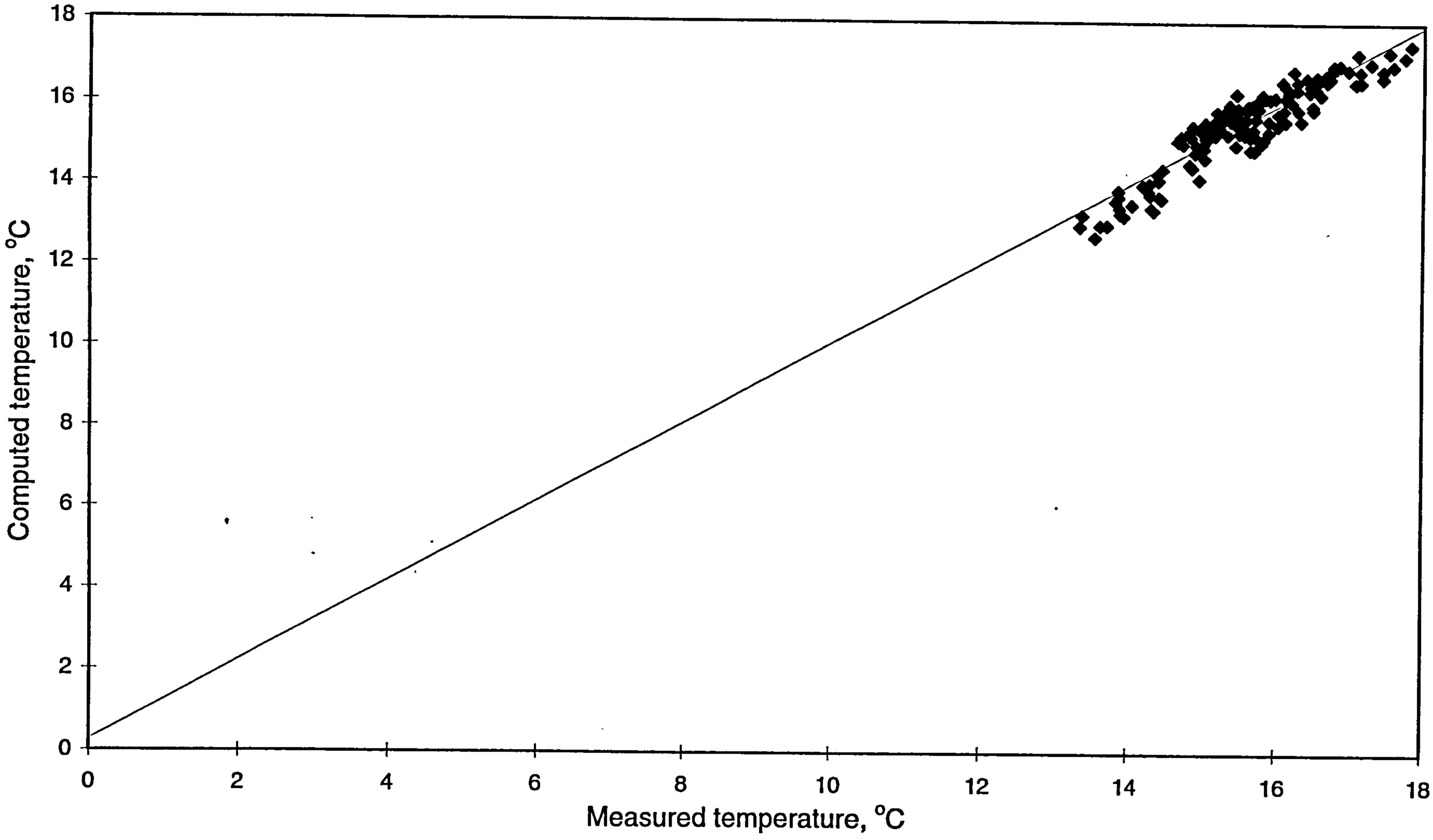

Figure 6.8 Evaluation of the model for 4-Argon12-4 window for nodes 1 and 2

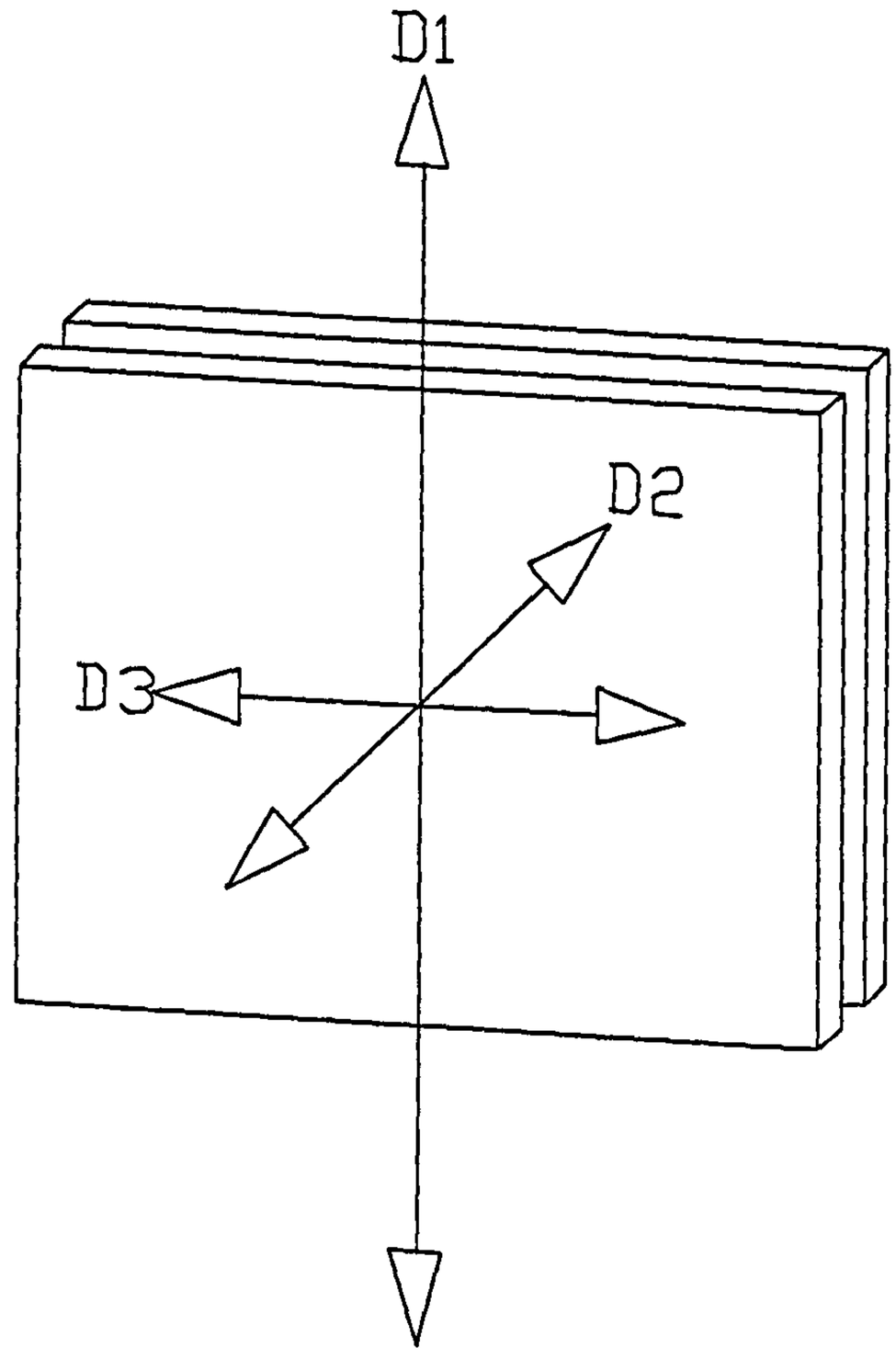

Figure 6.9 Directional representation

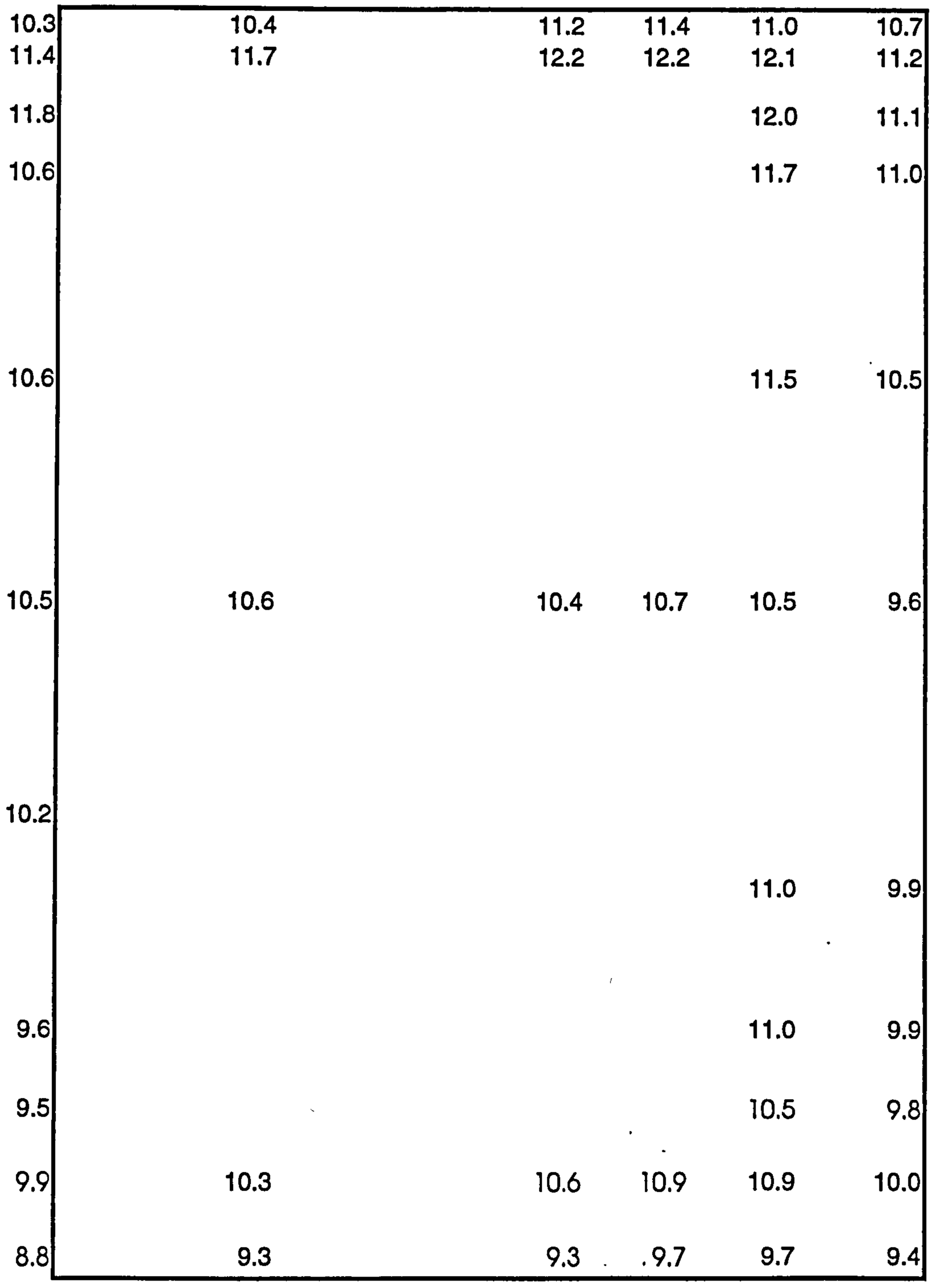

Figure 6.10 Distribution of measured temperatures on the right-hand half of a 4-air12-4 window (refer to Fig. 6.12 for nodal positions)

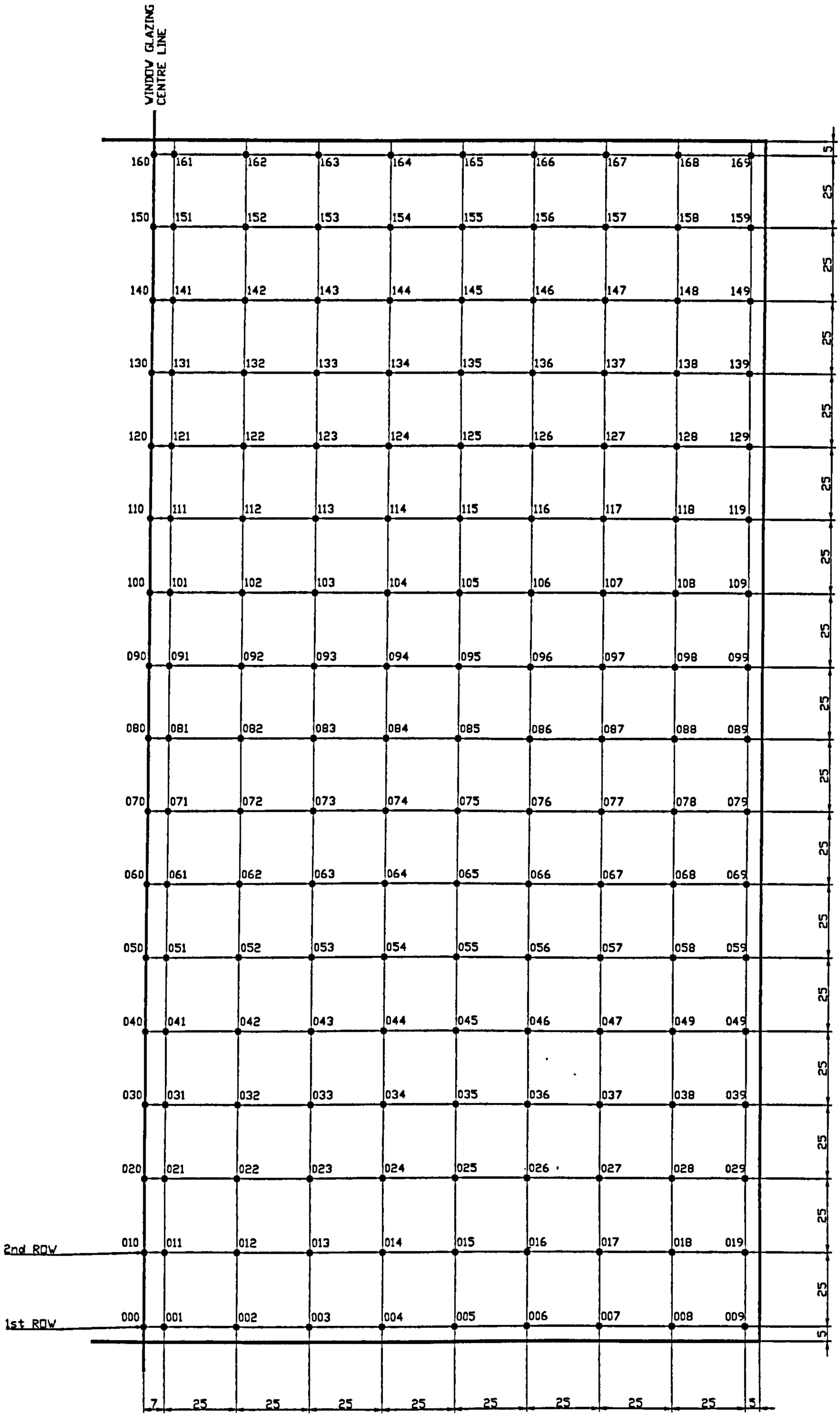

Figure 6.11 Nodal arrangement for window inner pane (right half only)

9.2		8.3	8.3	8.3	8.3	8.1
9.2		10.1	10.1	10.1	9.7	8.3
9.1					10.1	8.3
9.1					10.1	8.3
9.0					10.2	8.3
8.9		10.7	10.7	10.6	10.2	8.3
8.8					10.2	8.3
8.6					10.1	8.3
8.5					9.9	8.3
8.3		8.9	8.9	8.9	8.8	8.1
8.0		8.1	8.1	8.1	8.1	8.0

Figure 6.12 Distribution of calculated temperatures on the right-hand half of a 4-air12-4 window (refer to Fig. 6.12 for nodal positions)

Table 6.1 Calculation scheme and numerical values of resistances shown in Figure 6.3

Resistance No.	Resistance Value, W/K
1	= 1/(8.3 x 0.006) = 20.08
2,4,14,16	= 0.002/(1 x 0.006) = 0.333
23,60,66,72,78	= 1/(8.3 x 0.007) = 17.212
24,25,42,44,61,63, 67,69,73,75,79,81	= 0.002/(1 x 0.007) = 0.286
3,15	= 0.0065/(1 x 0.004) = 1.625
59,62,68,74,80	= 0.007/(1 x 0.004) = 1.75
43	= 0.004/(1 x 0.004) = 1
5,13	= 0.006/(0.19 x 0.006) = 5.263
7,12,31,36	= 0.0035/(0.2 x 0.0004) = 43.75
8,11,32,35	= 0.0035/(220 x 0.00035) = 0.0455
10,33	= 0.00035/(220 x 0.0105) = 0.000152
9,34	= 0.00315/(0.12 x 0.0105) = 2.5
6	= 0.003/(0.19 x 0.012) = 1.316
26,41	= 0.0004/(0.2 x 0.007) = 0.286
27,30,37,40	= 0.0056/(220 x 0.00035) = 0.0727
28,39	= 0.00035/(220 x 0.0063) = 0.000253
29,38	= 0.00525/(0.12 x 0.0063) = 6.944
17	= 0.003/(0.2 x 0.006) = 2.5
45	= 0.003/(0.2 x 0.007) = 2.143
18,21	= 0.017/(0.13 x 0.006) = 21.795
46,49	= 0.017/(0.13 x 0.007) = 18.681
22	= 1/(16.7 x 0.006) = 9.98
50	= 1/(16.7 x 0.007) = 8.554
53,57	= 0.017/(0.13 x 0.001) = 130.77
58	= 1/(16.7 x 0.001) = 59.88
51	= 0.002/(1 x 0.001) = 2
52	= 0.003/(0.2 x 0.001) = 15
19	= 0.0065/(0.2 x 0.003) = 10.833
20	= 0.0065/(0.13 x 0.034) = 1.471
47	= 0.004/(0.2 x 0.003) = 6.667
48	= 0.004/(0.13 x 0.034) = 0.905
54	= 0.0005/(0.2 x 0.003) = 0.833
56	= 0.0005/(0.13 x 0.034) = 0.113
55	= 1/(25 x 0.037) = 1.081
64	$= \frac{\frac{1-0.88}{0.88x0.007}+\frac{1}{1x0.007}+\frac{1-0.88}{0.88x0.4}}{5.678X10^{-08}(T_3^2+t_2^2)(T_3+t_2)} = \frac{162.68}{5.678X10^{-8}(T_3^2+t_2^2)(T_3+t_2)}$
65	$= 1.15(\frac{0.0035}{0.4})^{0.2}(t_c-t_3)\Big/[0.007xU(T_i-T_o)]$
70	$= 162.68/[5.678X10^{-08}(T_4^2+t_2^2)(T_4+t_2)]$
71	$= 1.15(\frac{0.0105}{0.4})^{0.2}(t_c-t_4)\Big/[0.007xU(T_i-T_o)]$
76	$= 162.68/[5.678X10^{-08}(T_5^2+t_2^2)(T_5+t_2)]$
77	$= 1.15(\frac{0.0175}{0.4})^{0.2}(t_c-t_5)\Big/[0.007xU(T_i-T_o)]$
82	$= 162.68/(5.678X10^{-08}(T_6^2+t_2^2)(T_6+t_2))$
83	$= 1.15(\frac{0.0245}{0.4})^{0.2}(t_c-t_6)\Big/[0.007xU(T_i-T_o)]$

Table 6.4 Calculation scheme and numerical values of resistances shown in Figure 6.6

Resistance No.	Resistance Value[1], K/W
R_{1i}	$=R_1+R_2=20.413$
R_{12}	$=R_3=1.625$
R_{1a}	$=R_4+R_5=5.596$
R_{ab}	$=R_{13}+R_{14}=5.596$
R_{ad}	$=R_6+1(1/R_7+1/R_8+1/(R_9+R_{10})+1/R_{11}+1/R_{12})=1.34$
R_{bc}	$=R_{16}+R_{17}+R_{18}=24.628$
R_{be}	$=R_{15}=1.625$
R_{co}	$=R_{21}+R_{22}=31.775$
R_{cf}	$=R_{19}.R_{20}/(R_{19}+R_{20})=1.295$
R_{2i}	$=R_{23}+R_{24}=17.498$
R_{23}	$=R_{59}=1.75$
R_{2d}	$=R_{25}+R_{26}+1/(1/R_{27}+1/(R_{28}+R_{29})+1/R_{30})=0.609$
R_d	$=1(1/R_{31}+1/R_{32}+1/(R_{33}+R_{34})+1/R_{35}+1/R_{36})=0.0225$
R_{de}	$=R_{41}+R_{42}+1/(1/R_{37}+1/(R_{38}+R_{39})+1/R_{40})=0.609$
R_e	$=R_{43}=1$
R_{ef}	$=R_{44}+R_{45}+R_{46}=21.11$
R_{fo}	$=R_{49}+R_{50}=27.235$
R_{fg}	$=R_{47}.R_{48}/(R_{47}+R_{48})=0.797$
R_g	$=R_{51}+R_{52}+R_{53}=147.77$
R_{gy}	$=1/(1/R_{54}+1/R_{56})+R_{55}=1.181$
R_{gx}	$=R_{57}+R_{58}=190.65$
R_{3i}	$=R_{60}+R_{61}=17.5$
R_{34}	$=R_{62}=1.75$
R_{3x}	$=R_{63}=0.286$
R_{3r}	$=R_{64}$
R_{3c}	$=R_{65}$
R_{4i}	$=R_{66}+R_{67}=17.5$
R_{45}	$=R_{68}=1.75$
R_{4x}	$=R_{69}=0.286$
R_{4r}	$=R_{70}$
R_{4c}	$=R_{71}$
R_{5i}	$=R_{72}+R_{73}=17.5$
R_{56}	$=R_{74}=1.75$
R_{5x}	$=R_{75}=0.286$
R_{5r}	$=R_{76}$
R_{5c}	$=R_{77}$
R_{6i}	$=R_{78}+R_{79}=17.5$
R_{67}	$=R_{80}=1.75$
R_{6x}	$=R_{81}=0.286$
R_{6r}	$=R_{82}$
R_{6c}	$=R_{83}$

1. All resistances' values are listed in Table 6.1

Table 6.7 MBE and RMSE values for windows under test

Case No.	Trade Name	MBE*	RMSE**
1	**4-Air12-4**	0.71	0.84
2	**4-Ar12-4**	0.075	0.41
3	**4-Air12-E4**	0.57	0.66
4	**4-Ar12-E4**	0.49	0.67
5	**4E-Kr12-E4**	-0.67	0.89
6	**4E-Xe10-E4**	-0.48	0.73

* Mean Biased Error **Root Mean Square Error

Table 6.8 Cold bridge effects on (t_3-T_3)

Case No.	Window Type	U-value[A] (W/m^2K)	(t_3-T_3)[B] Conduction, Convection, radiation[C]	(t_3-T_3) Convection, Radiation[D] Only
1	**4+Air12+4**	2.86	3.3	2.7
2	**4+Arg12+4**	2.72	3.4	2.9
3	**4+Air12+E4**	1.83	5.0	3.9
4	**4+Arg12+E4**	1.53	5.5	4.3
5	**4E+Kr12+E4**	1.14	5.4	2.5
6	**4E+Xe10+E4**	0.91	5.8	2.4

A. Internal & external ambient temperatures are assumed 20, 0°C respectively.
B. (t_3-T_3) is the temperature difference between centre-glazing and node 3.
C. Temperature values calculated by the numerical model. All heat transfer modes are involved.
D. Temperature values calculated by the numerical model. Cold bridge effects are excluded by replacing the Aluminium spacer by an infinite resistance.

7 Frequency of condensation occurrence on double glazed windows

7.1 Introduction

Condensation might be described as the modern disease of buildings [7.1]. A few years ago it was hardly ever mentioned. People's requirements for better standards of thermal comfort have led them to change the way of heating and ventilating their houses. This benign change has been accompanied with an inadvertent increase in condensation levels within buildings. For this reason, condensation has become a very important issue in building design.

Condensation is a natural phenomenon which occurs when moist air is cooled to a certain temperature causing the water vapour in the air to change its state to liquid water. The causes and avoidance of condensation in buildings have been discussed in detail in Chapter 1.

All building types are prone to condensation provided the conditions necessary for its formation are present. Some specialised buildings, e.g. industrial sector buildings suffer from condensation , but always in a way which can be expected due to the activities taking place in the buildings. In this chapter, surface condensation on double glazed windows in dwellings is investigated.

Some of the important factors which may increase the incidence of condensation in dwellings are:

- A significant number of dwellings in the United Kingdom remain unoccupied throughout the working day. For economical reasons therefore these houses will remain unheated during day time. When occupants return in the early evening, they switch on heating appliances, but simultaneously generate moisture by means of

cooking, washing, bathing, and also due to their very presence indoors. Some surfaces may take longer to warm up than the indoor air and condensation may occur on them.

- For economical reasons, only some areas in the house are appropriately heated such as the living room. The movement of air through the house may result in warm moist air from living rooms, showers, bathrooms and kitchens being carried to unheated or inadequately heated areas, particularly the bedrooms, with the resultant effect of condensation on windows, walls and fabrics. In some cases this effect may be so severe that it may trigger mould growth.
- The increase in the noisiness of our environment and the demand for thermal comfort has led occupants to seal windows and other openings. This has resulted in ventilation being reduced to a level whereby moisture removal has become an acute problem in modern buildings.

Condensation problem should be seriously addressed during the initial design of a dwelling by taking into consideration the following points:

- The provision of well insulated walls and roofs where building regulation standard U-value for walls should not exceed 0.5 W/m^2K [7.2].
- Intermittent heating should be avoided in houses with high thermal capacity walls. Despite the good thermal insulation properties of such walls, they require a long time to warm up to suitable temperatures. Buildings with high thermal capacity walls require a standard heating level throughout the heating period. If intermittent heating of a dwelling house is desirable then the structure should be of low thermal capacity or of medium to high thermal capacity with a low thermal capacity lining [7.2]. Walls with low thermal capacity warm up more quickly and surface temperatures soon rise above the dew-point temperature.
- Adequate means for the removal of moisture from within the house by ventilation must be provided, especially in houses having no flues. Moist air should be removed at source, in the kitchen, the bathroom or the shower and should not be allowed to move to cooler areas such as bedrooms. The air extraction can be done either by

natural means through open windows or other vents, or mechanically by fitting an extraction fan.

Condensation is very much related to the way in which buildings are heated, ventilated and insulated. By the control of temperatures in dwellings and air movement by ventilation, much of the inconvenience of condensation can be prevented. In any consideration of the thermal performance of the building shell, it is essential to consider condensation as a very vital factor because it could cause structural collapse in extreme circumstances.

In this chapter a model has been developed to calculate the variation of the nocturnal building temperature provided the external temperature is known. Further, spreadsheet based software has been developed to assess the potential frequency of condensation which may occur on any double glazed window predominantly during the early hours of morning. This phenomenon is well known within the United Kingdom [7.2]. The present model has been applied for three locations in the UK, e.g. Edinburgh, Manchester, and London using meteorological data available for these locations for a period of ten years.

The present model, although concerned only with surface condensation on double glazed windows, may be of interest for all research related to energy use in buildings.

7.2 Review of experimental work

A detached house situated two miles from Edinburgh airport (Turnhouse) was selected for experiments. Being detached, the house was ideal for considering only changes of the building internal temperature regardless of the heat transfer to or from neighbouring houses which is the case for terraced houses.

The house uses a central heating system which works from 0630 hours until 0830 hours for the morning period and from 1600 hours until 2100 hours for the evening period.

This heating routine allows the house to be nocturnally cooled by the effect of the external ambient environment. An occupied, single bedroom in this house was used for conducting experiments. Air temperature measurements using thermocouples were undertaken at the bedroom's mid-height at four locations indoors and also externally using four probes. Averaged indoor and outdoor temperatures were thus obtained. A humidity probe was also fitted inside the room to measure the internal relative humidity. Measurements were recorded every hour for the period from 18 November 1996 to 4 January 1997, this being the coldest period in Edinburgh. Full details of the experimental work has been described previously in Chapter 4. An abstract from this experimental data is given in Appendix B.

7.3 Assessment of the nocturnal cooling rate of occupied bedrooms

Condensation on any internal surface will occur when its temperature falls below the dew-point of the indoor air. Glazings, in general, are thermally the weakest elements and more susceptible to condensation than other surfaces in any building. Therefore it is logical to evaluate the condensation occurrence on glazings. In Europe and North America double glazed windows have become the de facto standard for window designs. The present analysis includes double glazed windows of various designs, i.e. using infill gas and/or low emissivity coated glass. The analysis may be extended to deal with multiple-glazed units, single-glazed windows, or other surfaces such as walls.

To determine the potential frequency of condensation occurrence on a building window glazing the internal air temperature, T_i and relative humidity, ϕ should be known.

Steady state heat transfer through the fabric of a building can never be reached. Basic changes in external conditions are caused by the normal daily cycle. Furthermore, weather changes can also cause variations in external conditions from day to day or even within a shorter period of time [7.3]. Therefore, the thermal analysis of a building is very complex.

To simplify the study of the thermal analysis of a building, two approaches can be used. The first approach is to assume that the building consists of two unit masses separated by an air gap. The heat transfers from the internal mass to the air gap then to the outer mass and finally to the external environment. This route of heat transfer is reversed if the temperature of the external environment exceeds that of the building. This approach can be used only for houses with air cavity walls.

The second approach, which has been applied in the present study, assumes that the complete building is a single unit that losses heat to the external environment during the cooling down period. This assumption is valid as the thermal resistance of the external air film on the building surface is high compared with the internal thermal resistances within the building. Thus the heat transfer from the building to its surroundings is controlled by the surface heat transfer. This implies that the structure is at a mean temperature equal to the internal air temperature with no significant temperature variations within the structure as cooling down occurs. In practice there is an interaction between the elements of the building and the air within the building, as well as temperature variation within the structure itself.

From Newton cooling law,

$$hA_b(T_i - T_o) = -\rho \ Vc\frac{dt}{d\tau} \qquad 7.1$$

Rearranging this equation and integrating gives,

$$\int \frac{dt}{(T_i - T_o)} = -\frac{hA_b}{\rho Vc}\int d\tau \qquad 7.2$$

Solving Equation 7.2 yields,

$$\ln\ (T_i - T_o) = -\left(\frac{hA_b}{\rho\, Vc}\right)\tau \qquad 7.3$$

where,

A_b	building surface area, m^2
c	building specific heat, J/kg K
h	heat transfer coefficient from the building surface to external air, W/m^2K
ln	natural logarithm
ρ	building density, kg/m^3
T_i	building lump temperature at a certain time, °C
τ	time, seconds
T_o	external air temperature at a certain time, °C
V	building volume, m^3

Suitable mean values of density and specific heat for the whole building have been assumed. Since the air within the building is assumed to be of negligible thermal capacity compared to that of the solid structure the volume, V, is that of the building material only.

The term ($\rho Vc/hA_b$) in Equation 7.3 is called the time constant. A large time constant means that the building requires a longer time to cool down or heat up between specific temperatures. In other words, the building has a thermal capacity (ρVc) which is much greater than the heat transfer rate per unit temperature difference between the building and its surroundings (hA_b).

During the unheated period, the building structure cools down due to the influence of the external environment. The temperature of the building structure, in general, can be affected by the external air temperature, T_o, the long wavelength radiation loss to the clear sky, wind speed, wind direction, infiltration and/or ventilation.

From the experimental data shown in Appendix B and using Equation 7.3, ln (T_i-T_o) is plotted against the time (τ) for each day as shown in Figures (7.1-7.5). These figures show that there is a linear relationship between ln (T_i-T_o) and (τ). Each day has been

represented by a line whose slope gives an indication of the cooling rate of the building at that day. The slopes of these lines are listed in Table 7.1.

Table 7.1 Daily cooling rates of the experimental building

Date	Slope, sec^{-1}	Date	Slope, sec^{-1}	Date	Slope, sec^{-1}
19/11/96	-1.598E-05	08/12/96	-2.347E-05	21/12/96	-1.525E-05
20/11/96	-1.057E-05	09/12/96	-1.476E-05	22/12/96	-1.525E-05
21/11/96	-1.987E-05	10/12/96	-1.476E-05	23/12/96	-1.310E-05
28/11/96	-1.952E-05	11/12/96	-1.593E-05	24/12/96	-1.469E-05
29/11/96	-6.121E-06	13/12/96	-1.098E-04	25/12/96	-1.504E-05
30/11/96	-1.751E-05	14/12/96	-6.581E-05	26/12/96	-5.852E-06
01/12/96	-3.267E-05	15/12/96	-7.948E-06	28/12/96	-1.593E-05
02/12/96	-1.633E-05	16/12/96	-8.010E-06	29/12/96	-1.407E-05
03/12/96	-1.538E-05	17/12/96	-6.928E-06	30/12/96	-2.121E-05
04/12/96	-1.651E-05	18/12/96	-1.111E-05	31/12/96	-9.046E-06
07/12/96	-2.417E-05	19/12/96	-5.657E-06	01/01/97	-1.915E-05

As can be seen from Table 7.1, slopes are not the same. This means that the cooling rate for the building is different from day to day. This can be attributed to various factors which participate in cooling of the building, e.g. cloud cover, wind speed, wind direction, infiltration and/or ventilation.

A study of the influence of the cloud cover and wind speed on the building's cooling rate has been carried out based on the available experimental data. Due to the insufficiency of these data, no relationships could be derived. However, cloud cover effects on the cooling rate of the building were apparent, i.e. the lower the cloud cover value, the higher the cooling rate.

The building's time constant on any day can be calculated from the slope of its corresponding line as shown below.

From Table 7.1, the slope of the line corresponding to the day 28/11/96 = -1.952×10^{-5} sec^{-1}

The time constant for the experimental house on that day, therefore, is the reciprocal of the absolute value of the slope = 51220 sec = 14.28 hours.

From the data for the experimental house, values of T_i at 0600 hours are plotted against the corresponding values of T_o. One such plot is shown in Fig. 7.6. This figure shows a reasonably linear relationship between T_i and T_o The choice of the given hour was made due to the fact that this represents the time at which T_o acquires the minimum value and the bedroom heater is switched on.

Thus by knowing the external ambient temperature, T_o the internal ambient temperature, T_i can be obtained using the regressed equation given in Equation 7.4,

$$T_i = 0.58T_o + 11.3 \qquad 7.4$$

The above relationship is valid only for the experimental room under discussion. However, relation such as Equation 7.4 may be easily derived for any given enclosure. Webb and Concannon [7.4] have also obtained a relationship similar to the one shown in Fig. 7.6.

Statistical t-test analysis has been applied to these data to check the confidence of this relationship,

$$t = \sqrt{n_d - 2}\left\{R / \sqrt{1 - R^2}\right\} \qquad 7.5$$

where, n_d is the number of days for which data was collected (n_d = 35) and R is the correlation coefficient (R = 0.74). Substituting values of n and R in Equation 7.5 gives a value of t = 6.34. This indicates a high confidence of association.

Building services professionals in the United Kingdom are showing an increased interest in the use of night-time natural ventilation for cooling as part of the current trend towards low energy building designs. Night ventilation of an office building can reduce the day time dry resultant temperature by up to 4 °C at the start of occupation compared with an office without night ventilation [7.4]. Thus the above model, represented by Equation 7.4, can also be a useful tool for nocturnally cooled building design.

7.4 Assessment of the internal humidity

As mentioned previously, the assessment of the potential frequency of condensation occurrence on any building's window requires the determination of T_i and ϕ. These two properties enable the determination of the indoor dew-point temperature by using the principles of psychrometery.

Relative humidities within a single occupancy bedroom were measured hourly for the entire test period referred to above. The measured values of relative humidity, shown in Appendix B, have been plotted for as shown in Figures 7.7-7.10. It can be seen from these figures that the relative humidity changes slightly within the cooling down period. This change is however, of a minor order night upon night. This is due to the thermal capacity of the building structure which dampens the influence of the changing weather over a short period of time. Thus as a starting point an average value of 70% for the indoor relative humidity can be assumed for the present analysis.

7.5 Computation of the internal dew point temperature

This analysis is based upon the standard procedure given in ASHRAE [7.5]. Providing the temperature of the indoor air (dry bulb air temperature) is known, which can be calculated from Equation 7.4, the water vapour saturation pressure, P_{ws}, may be obtained from thermodynamic property tables or calculated from the following formula for the temperature range of 0 to 200°C,

$$\ln (P_{ws}) = (k_1 / T_i) + k_2 + k_3 T_i + k_4 T_i^{\,2} + k_5 T_i^{\,3} + k_6 \ln (T_i) \qquad 7.6$$

where,

$k_1 = -5.8002206 \times 10^{+03}$

$k_2 = -5.516256$

$k_3 = -4.8640239 \times 10^{-02}$

$k_4 = 4.1764768 \times 10^{-05}$

$k_5 = -1.4452093 \times 10^{-08}$

$k_6 = 6.5459673$

The actual partial pressure of water vapour, P_w, may be calculated from,

$$P_w = \phi P_{ws} \qquad 7.7$$

where,

ϕ relative humidity

Therefore, the indoor air dew point temperature, t_d, for the range of 0 to 93 °C may be obtained from,

$$t_d = k_7 + k_8\theta + k_9\theta^2 + k_{10}\theta^3 + k_{11}(P_w)^{0.1984} \qquad 7.8$$

Where,

$\theta = \ln (P_w)$

$k_7 = 6.54$

$k_8 = 14.526$

$k_9 = 0.7389$

$k_{10} = 0.09486$

$k_{11} = 0.4569$

7.6 Estimation of the inner glazing temperature

Based on the studies reported in previous chapters, it has been shown that a significant temperature stratification occurs along the window height at the inner pane of any double glazed window [7.6]. This longitudinal stratification occurs due to the circulating infill gas within the window cavity. The infill gas travels downwards along the outer glass pane, approaches the bottom part of the cavity, changes direction and absorbs heat from the warmer inner pane during its upward flow.

The natural convection of the infill gas within the cavity and the cold bridging effects ally to make the bottom edge the coolest part of the internal glazing. Thus condensation will initiate at the bottom edge of the glazing if the temperature at the edge reaches the room dew point temperature.

The temperature of the inner glazing bottom edge has been calculated for each of the six window designs used in the present study. Table 4.2 lists the design features of the windows under investigation. This study has been extended to investigate the condensation occurrence frequency in three locations in the United Kingdom, e.g. Edinburgh, Manchester, and London.

The calculation was initiated by determining the internal and external centre-glazing temperatures,

$$t_3 = T_i - (R_{g2} + \frac{1}{h_i})q \qquad 7.9$$

$$t_2 = T_o + (R_{g1} + \frac{1}{h_o})q \qquad 7.10$$

where,

$$q = U_{ref}\,(T_i - T_o), \qquad 7.11$$

$h_i = 8.3$ W/m^{2}K and $h_o = 16.7$ W/m^{2}K [7.7].

The film temperature of the infill gas is assumed as the average of t_2 and t_3,

$$T_f = \frac{1}{2}(t_2 + t_3) \qquad 7.12$$

The transport properties for the infill gas, e.g. β, ν, α, Pr and k corresponding to the film temperature are then specified and used to calculate the Rayleigh number,

$$Ra^*_H = g\,\beta\,H^4\,q\,/\,\alpha\,\nu\,k \qquad 7.13$$

The model given in Chapter 6 has been used to calculate the very bottom temperature of the inner glazing (t_g). Firstly, the temperature of the node 7, shown in Fig. 6.1, was calculated using the convection model developed in Chapter 5,

$$t_7 = T_f + (\,q.H\,/\,k\,)\,(c_o + c_1.U_{ref}\,)\,(Ra^*_H.Pr)^m \qquad 7.14$$

Secondly, the temperature of node 3, t_g, shown in Fig. 6.1, which is the bottom most node on the inner glazing is determined by using the set of Equations 6.13. Node 3 temperature may be considered as the required inner glazing temperature for condensation studies.

7.7 Determination of the frequency of occurrence of condensation

By comparing the internal air dew point temperature, t_d, with the bottom edge inner glazing temperature, t_g, an assessment of the occurrence of condensation may be made. Thus,

If $t_g \leq t_d$ condensation will occur on the glazing bottom edge.

The potential frequency of condensation occurrence has been investigated for three locations in the United Kingdom, e.g. Edinburgh, Manchester, and London. Recent meteorological data for each of these three locations for a period of ten years (1980-89) have been used in the present analysis.

The Microsoft Excel spreadsheet package has been used in the present work. The spreadsheet Condense.xls (see Appendix K) incorporates the steps mentioned in sections 7.3 to 7.7 above. In the spreadsheet, these steps have been repeated for each hour. The four early morning hours of each day, e.g. 03:00, 04:00, 05:00, and 06:00 hours have been considered. These hours are considered the coldest period of the day. Therefore, the number of calculations for each location for the period of 10 years will be:

For leap years 1980, 1984, and 1988

The number of calculations = {3x366x4} = 4392

For years 1981, 1982, 1983, 1985, 1986, 1987, and 1989

The number of calculations = {7x365x4} = 10220

Therefore, the total number of calculations for each location during 10 years

= 4392+10220 = 14612. This is repeated for each window design.

What follows shows the algorithmic flow that the spreadsheet Condense.xls (see Appendix K) performs in order to decide whether a certain window in a certain location at a certain external ambient temperature will suffer condensation or not.

Given data

Location: Edinburgh

Window design: 4-Air12-4 (See Table 4.2 for window specifications)

External Ambient temperature (T_o): -2 °C

Calculation flow

Determine the internal air temperature from Equation 7.4, T_i = 10.2 °C

Determine the internal air dew point temperature (Equations 7.6-7.8), t_d = 5.0 °C

Determine the internal and external centre-glazing temperatures (Equations 7.9 and 7.10), t_3 = 5.84 °C, t_2 = 0.22 °C

Determine the infill gas film temperature (Equation 7.12), T_f =276.18 K

Specify the infill gas transport properties at T_f,

$\beta = 0.003621\ K^{-1}$

$\nu = 13.07354 \times 10^{-6}\ m^2/s$

$\alpha = 1.89 \times 10^{-5}\ m^2/s$

Pr = 0.714

k = 0.024293 W/mK

Determine Rayleigh number at node 7 where H = 0.0315 m (Equation 7.13),

Ra^*_H = 202708.8

Determine the node 7 temperature (Equation 7.14), t_7 = 4.16 °C

Determine the node 3 temperature (Equations 6.13), t_g = 3.8 °C

$t_g < t_d$. Therefore, condensation will occur.

For a different window design 4E-Xe10-E4 (see Table 4.2 for window specifications) located in Edinburgh with an external ambient temperature T_o = -2 °C, the calculation method is as above but results in the node 3 temperature, t_g, being 5.28 °C and $t_g > t_d$, hence no condensation.

These two examples show that in addition to their high thermal performance, high-tech windows can effectively suppress condensation.

7.8 Results and discussion

Meteorological data for Edinburgh, Manchester, and London for a period of ten years, i.e. from 1/1/1980 to 31/12/1989 have been obtained from the UK Meteorological

Office based in Bracknell. These data have been analysed for the potential frequency of condensation occurrence on the double glazed window designs listed in Table 4.2. Tables 7.3 -7.9 show the results of the present exercise. It is obvious that the potential frequency of condensation occurrence increases for cooler locations, i.e. for the same window design the highest potential frequency of condensation occurs in Edinburgh and the lowest in London. The results show that for the base case (window No. 1 in Table 4.2) the average potential frequency of condensation for Edinburgh is over twice that for London.

For obvious reasons the annual average of condensation occurrence for any given location decreases with a reduction in the U-value. This study quantifies the influence of the modern super-insulated windows on the potential frequency of condensation occurrence. For example a comparison of Tables 7.3 and 7.8 shows that condensation occurrence will decrease by about 40-50% if less efficient glazings (e.g. window No. 1) are replaced by the most efficient windows (e.g. window No. 6). The only question that may arise is whether it is economical to install xenon-infill windows. These windows are thermally efficient but more expensive owing to the high production cost of this gas [7.8]. It is not easy to assess the relevant value analysis as it involves the estimation of the damage and discomfort related to condensation, e.g. damage to furniture, paintwork, building fabrics, and window elements. The above mentioned value analysis also involves the psychological effects condensation has on occupants which are difficult to quantify.

As mentioned previously, the circulating infill gas within the enclosure is responsible for the lowered temperature of the bottom part of the inner glass pane. The identification of this phenomenon has led to an innovative development [7.9] which is now at a patent pending stage (window No. 7). This innovation uses the introduction of a 50-mm high glass baffle, placed mid-way in the cavity on the bottom spacer. This baffle plate constricts the descending cold air next the outer glass pane from hitting the bottom part of the inner glass. This helps in keeping the temperature at the bottom part of the inner glass at a higher value than would otherwise be the case. Table 7.9 shows that the

innovative window No. 7 is least susceptible to condensation occurrence. This design can be successfully introduced into window manufacturing. In high-tech windows, installing a baffle will further suppress the occurrence of condensation.

7.9 Conclusions

It is common experience that within dwellings condensation occurs on glazing surfaces during the early hours of the morning. Condensation initiates at the coldest part of the glazing which is the bottom edge. It, then, propagates upwards as the external temperature and/or the internal humidity increases. Figures 7.11a and b show two photographs for a double glazed window in one of the bedrooms of the experimental house. These photographs were taken during the early morning of one the 1996 winter days. The room was occupied with one adult person the night before. Both photographs show many water droplets forming at the bottom edge of the window. It can be seen that condensation occurred also on the side edges of the window due to cold bridging by the edge spacer. Some photographs had been taken for another bedroom in one of the Napier University flats (Morrison Circus accommodation flats) as shown in Figs. 7.12a and b. They also show the same kind of pattern. To quantify this problem a simplified model for assessing the nocturnal temperature drop inside a building subjected to a daytime heating schedule has been provided. This model requires the knowledge of a single weather parameter, i.e. the external temperature at dawn.

A Microsoft Excel based spreadsheet for calculating the potential frequency of condensation occurrence on double glazed windows has been developed herein. This software requires the external ambient temperature and the window U-value. Hourly weather data from three UK locations for a period of ten years were analysed using this software. The results show that the potential frequency of condensation occurrence for Edinburgh is over twice that for London. This study also quantifies the influence of the modern super-insulated windows on the occurrence of condensation. Compared with an air-filled, float-glass window, a xenon window using low emissivity coating will reduce the probability of condensation occurrence by half. The potential of using an innovative

window, one which employs a short baffle to suppress convection within the sealed cavity, has also been demonstrated.

References

7.1. A. Oliver, Dampness in Buildings, Blackwell Science Ltd, UK, 1997

7.2. D. J. Croome and A. F. C. Sherratt, Condensation in Buildings, Applied Science Publishers Ltd, England, 1972

7.3. T. D. Eastop and W.E. Watson, Mechanical services for buildings, Longman scientific technical, England, 1992

7.4. B. Webb and P. Concannon, In the cool of the night, Building Services Journal, December 1996

7.5. ASHRAE Handbook Fundamentals, American Society for Heating, Refrigeration and Air Conditioning Engineers, Atlanta, USA, 1993

7.6. N. Abodahab and T. Muneer, Free convection analysis of a window cavity and its longitudinal temperature profile, Energy Conversion and Management, Vol. 39, No. 1, 1998

7.7. CIBSE Guide A, Chartered Institution of Building Service Engineers, England, 1982

7.8. Fernie and T. Muneer, Monetary, energy and environmental implications for infill gases used in high-performance windows, Chartered Institution of Building Service Engineers, Vol. 17, No. 1, England, 1996

7.9. T. Muneer, N. Abodahab and B. Han, Gas flow in double glazing enclosures and its effect on longitudinal temperature variation, Proceedings of the Advances in Fluid Mechanics (AFM'96) Conference, New Orleans, USA, Computational Mechanics Publications, Southampton, UK, 11-13 June 1996

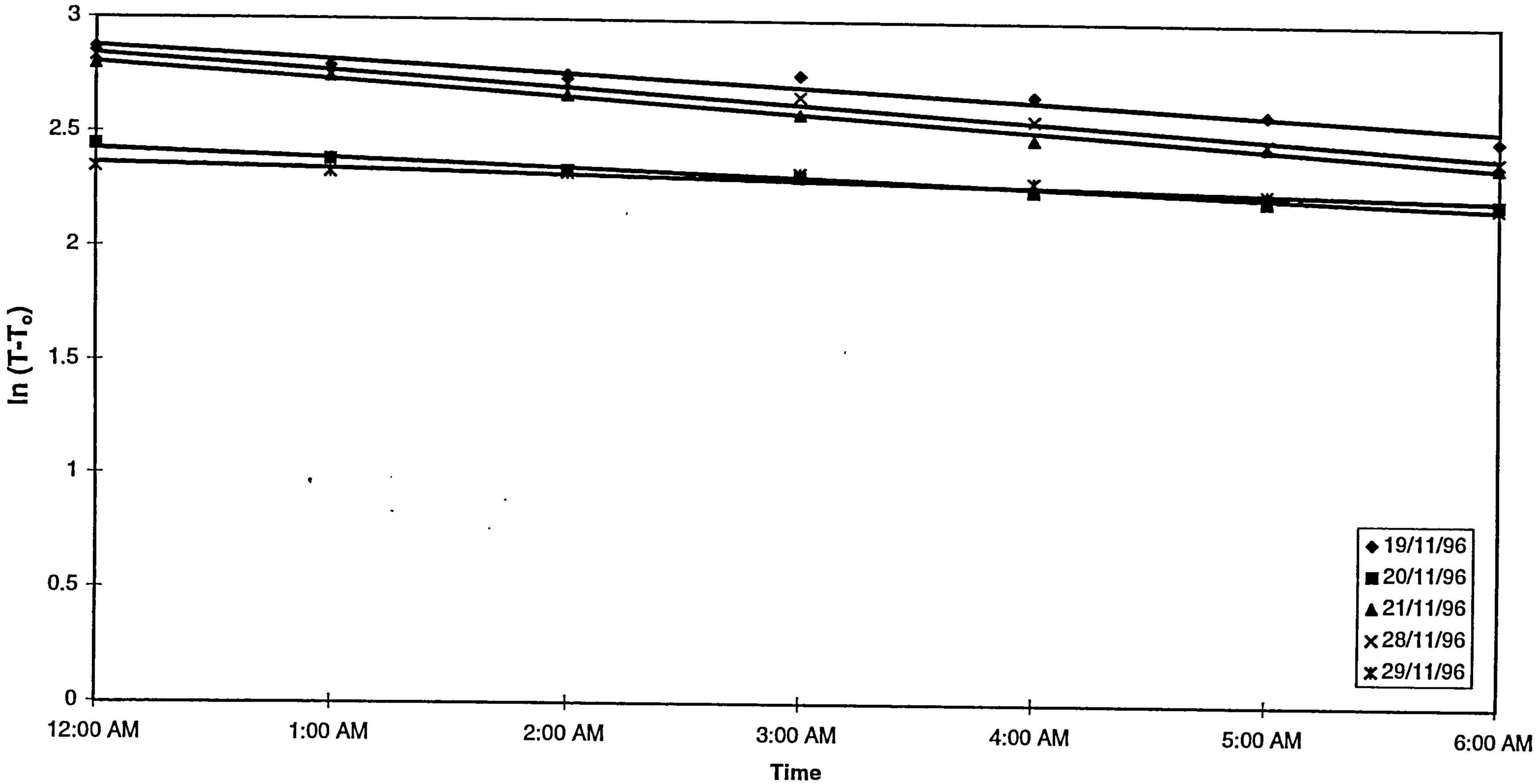

Figure 7.1 Building's cooling rate for certain days

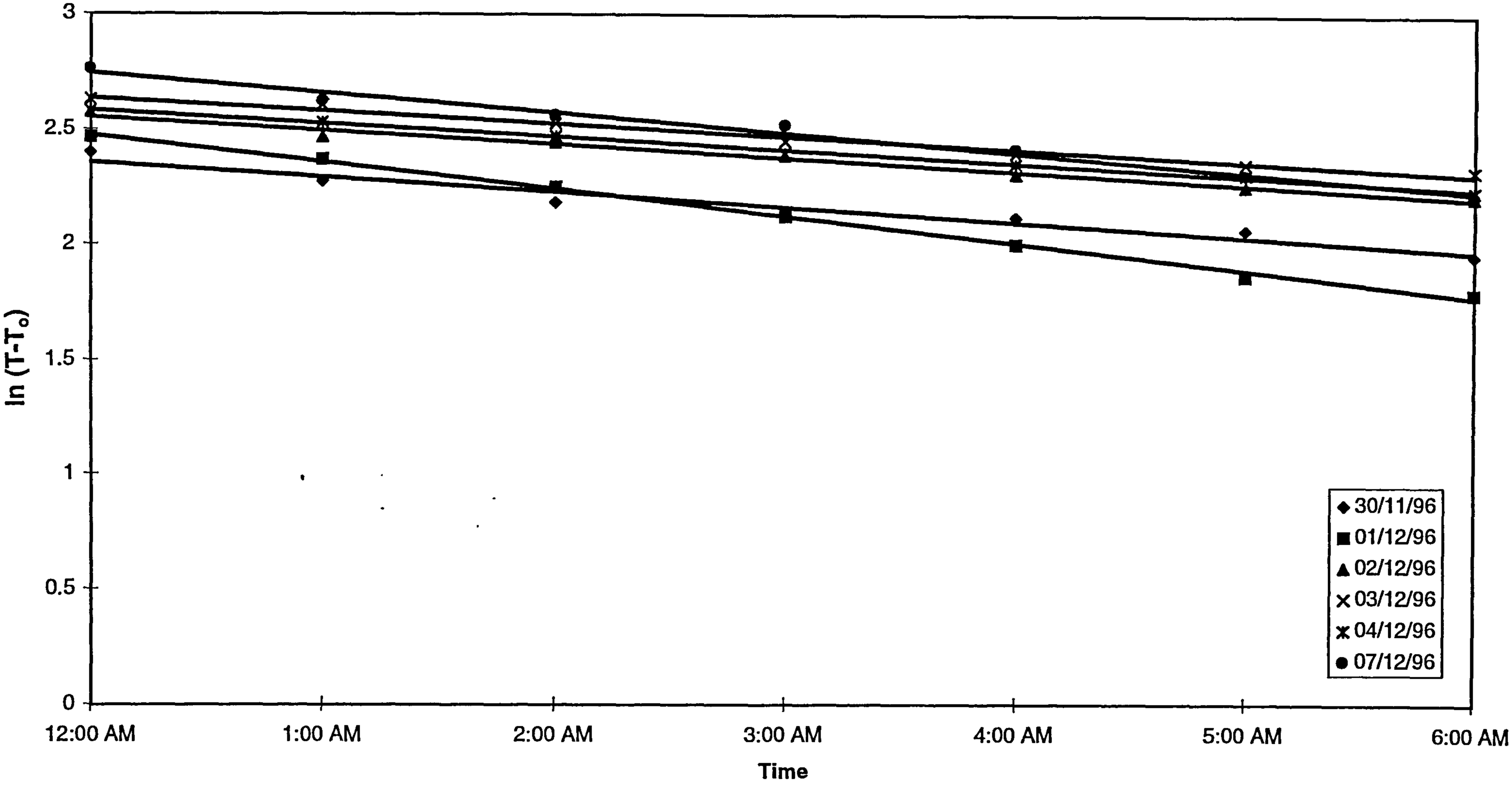

Figure 7.2 Building's cooling rate for certain days

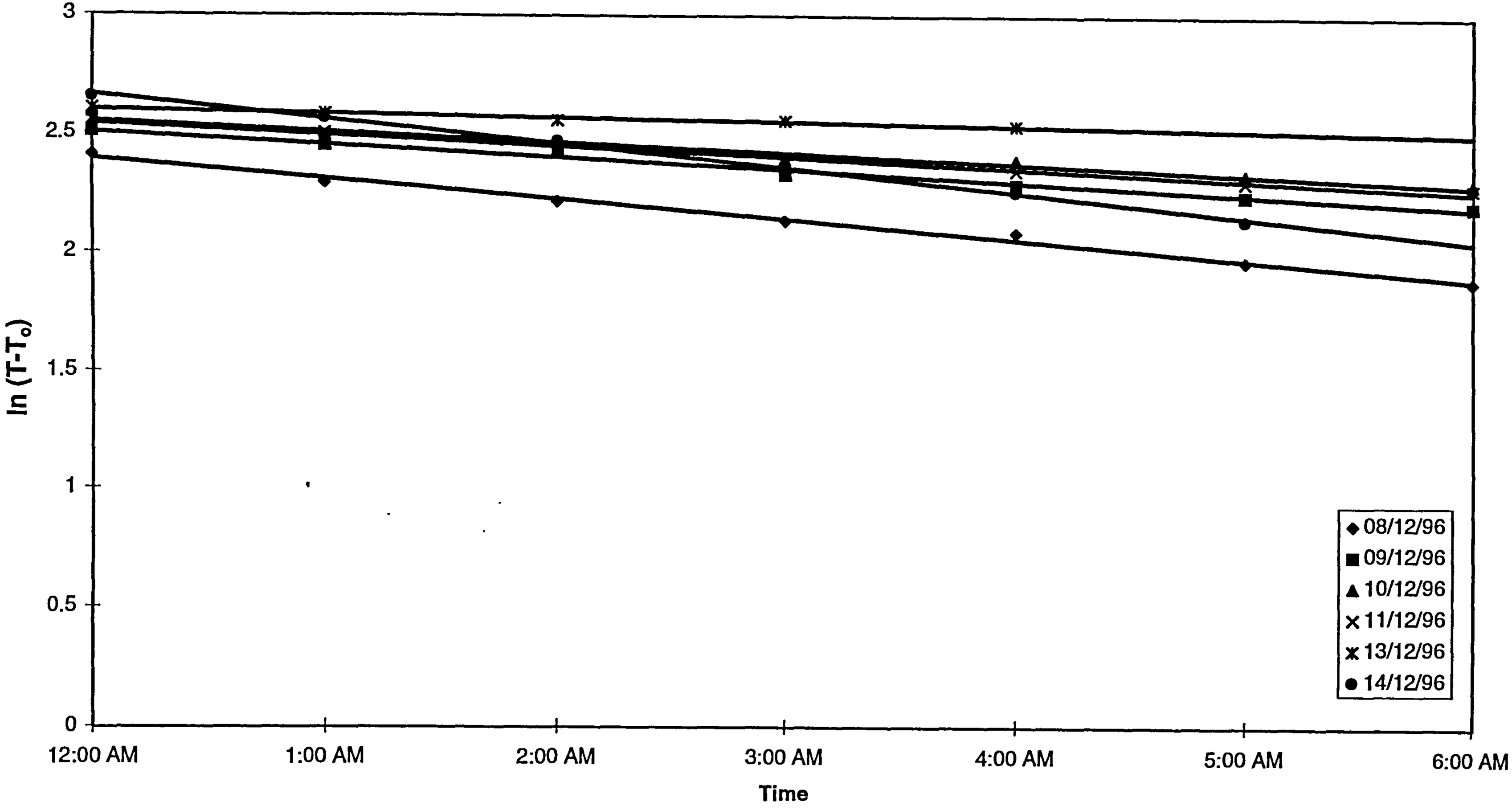

Figure 7.3 Building's cooling rate for certain days

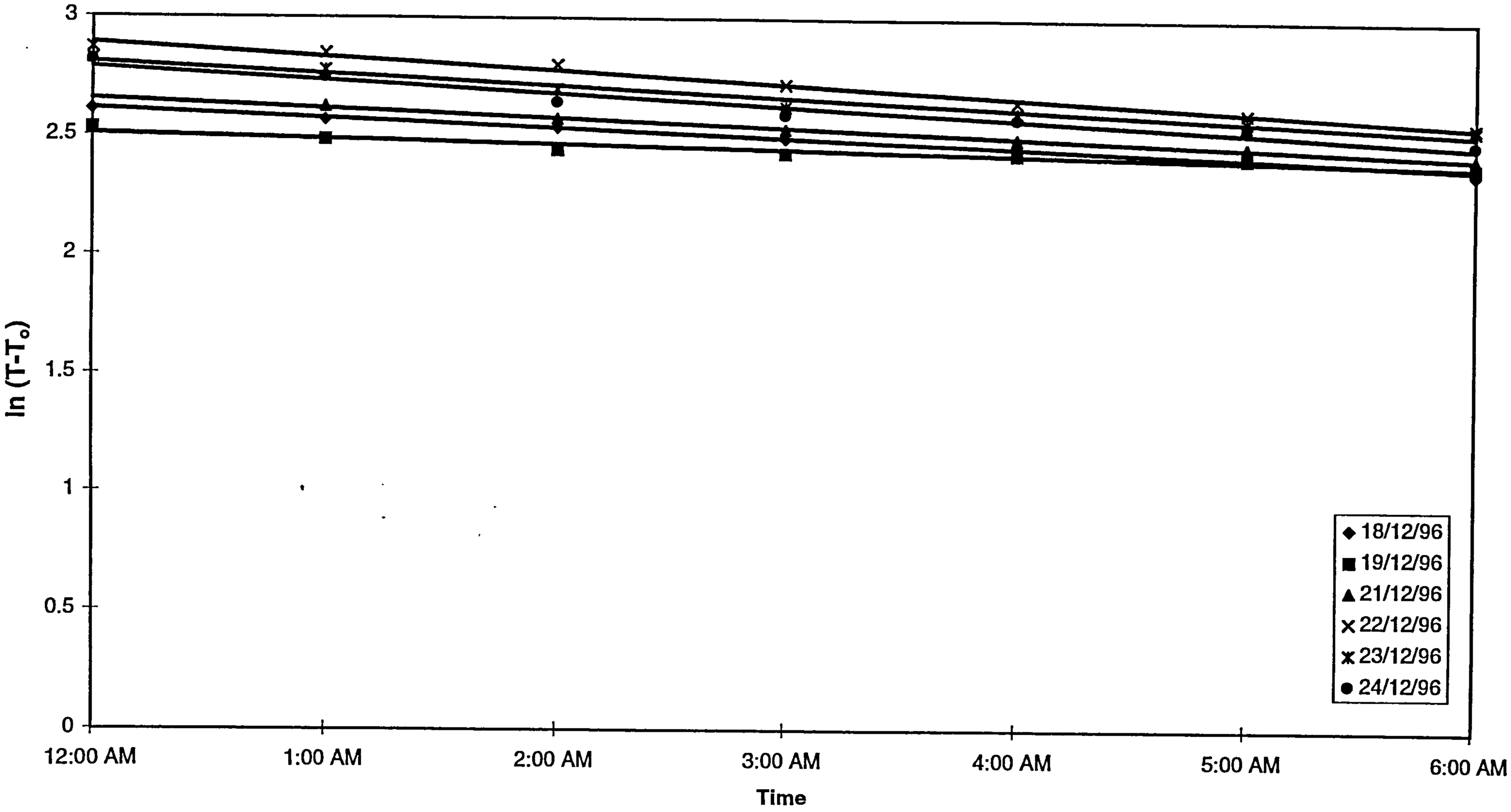

Figure 7.4 Building's cooling rate for certain days

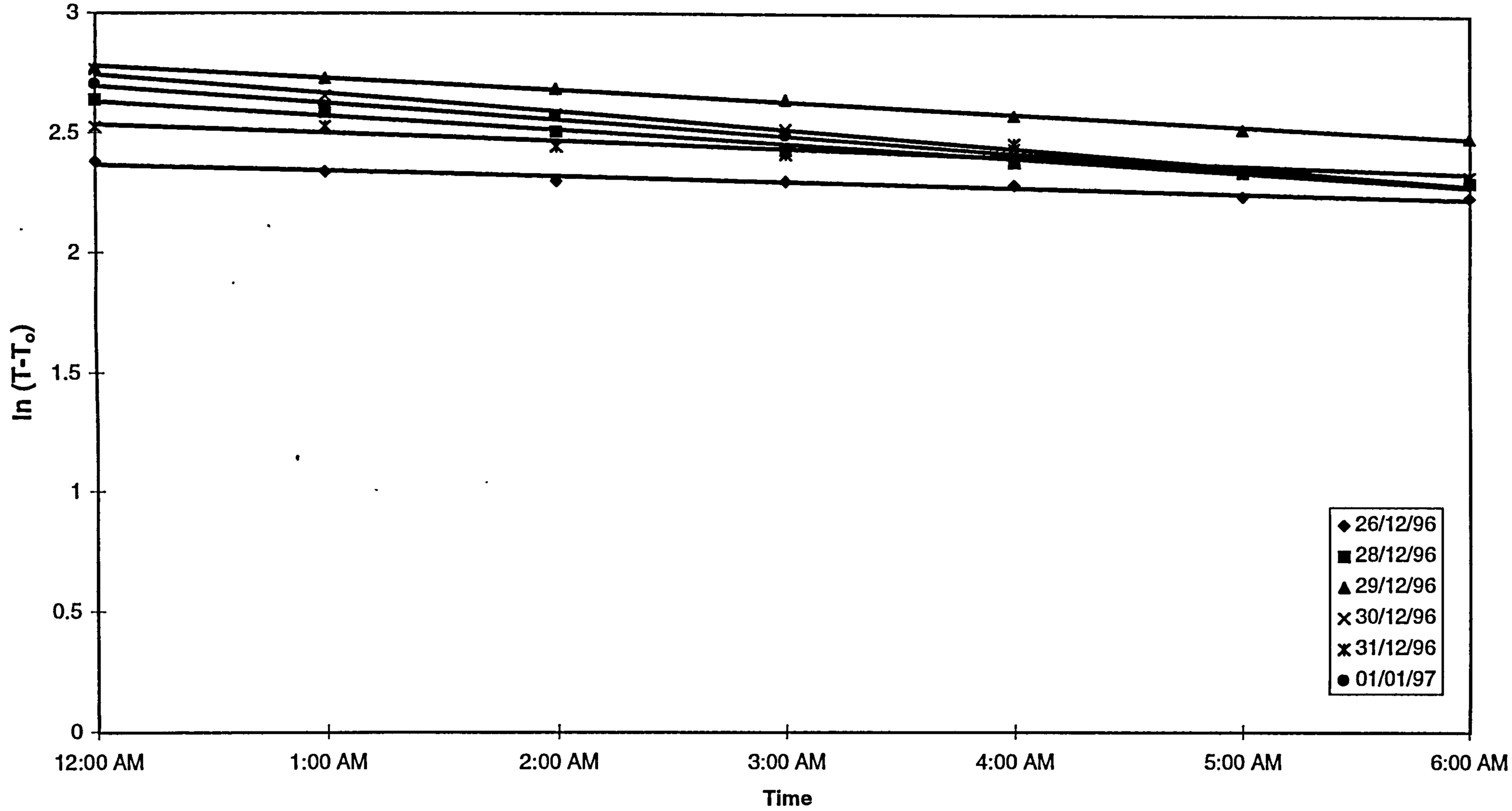

Figure 7.5 Building's cooling rate for certain days

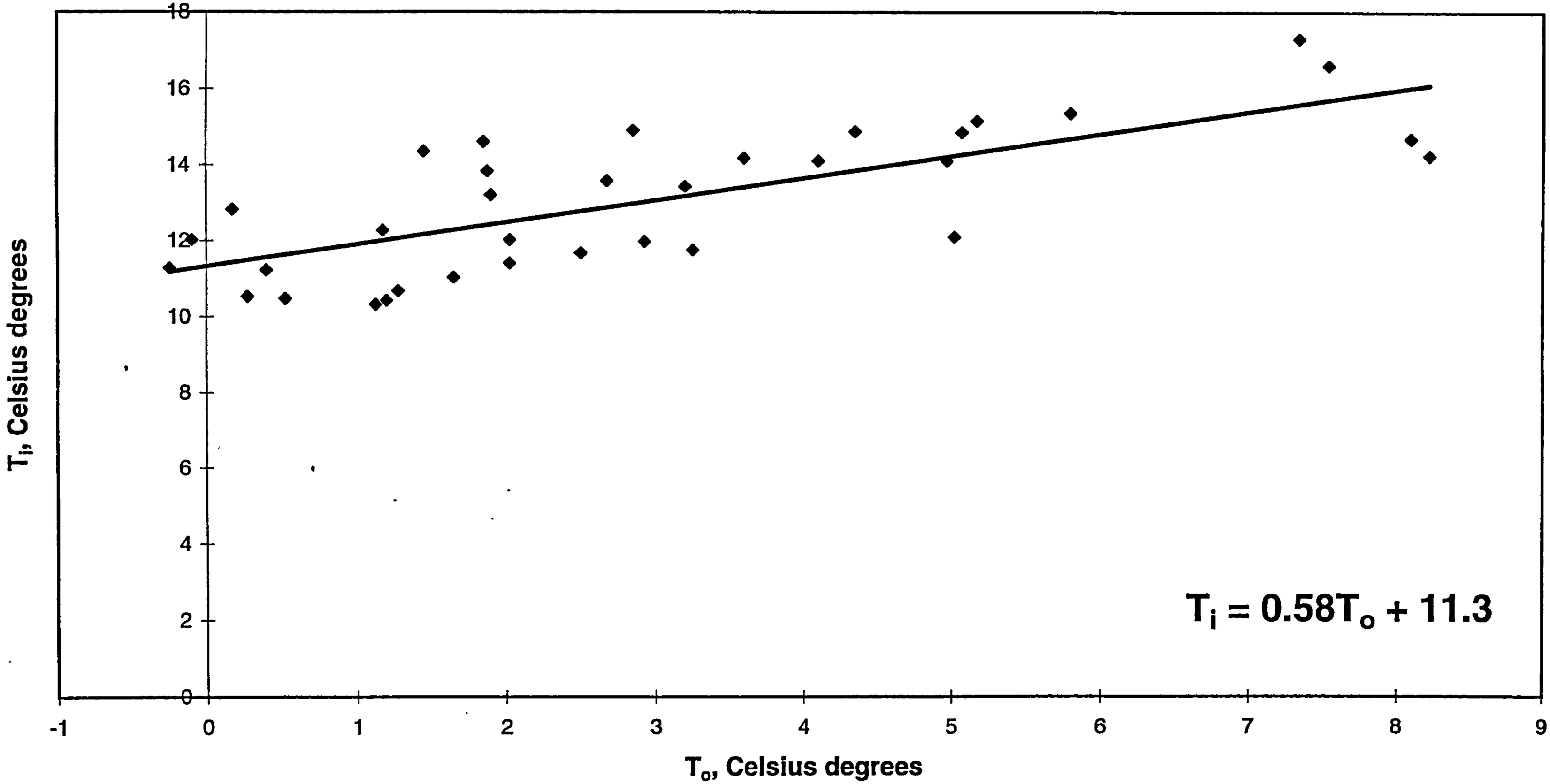

Figure 7.6 Nocturnal cooling performance of an occupied bedroom

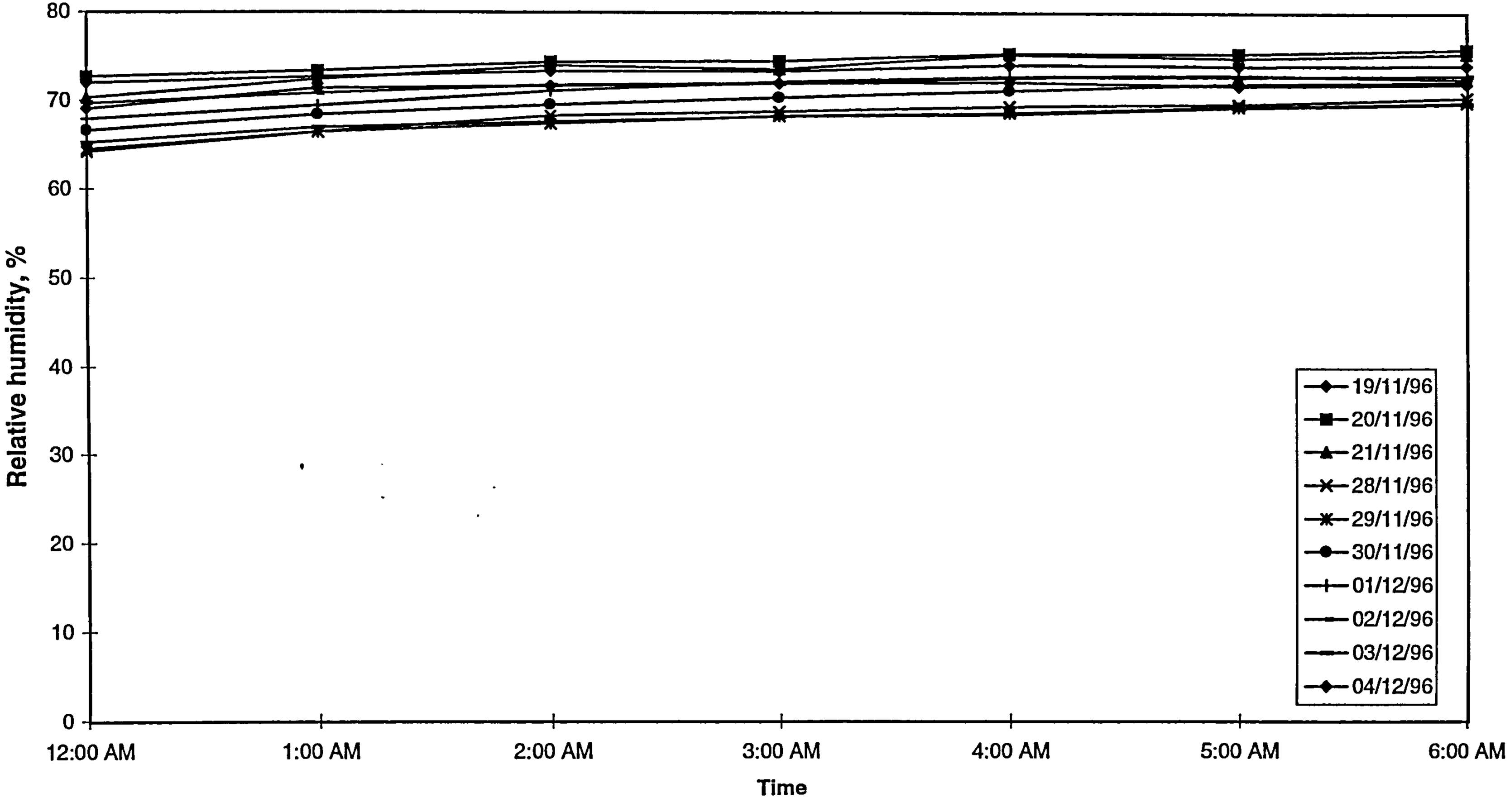

Figure 7.7 Nocturnal relative humidity for a single occupant bedroom

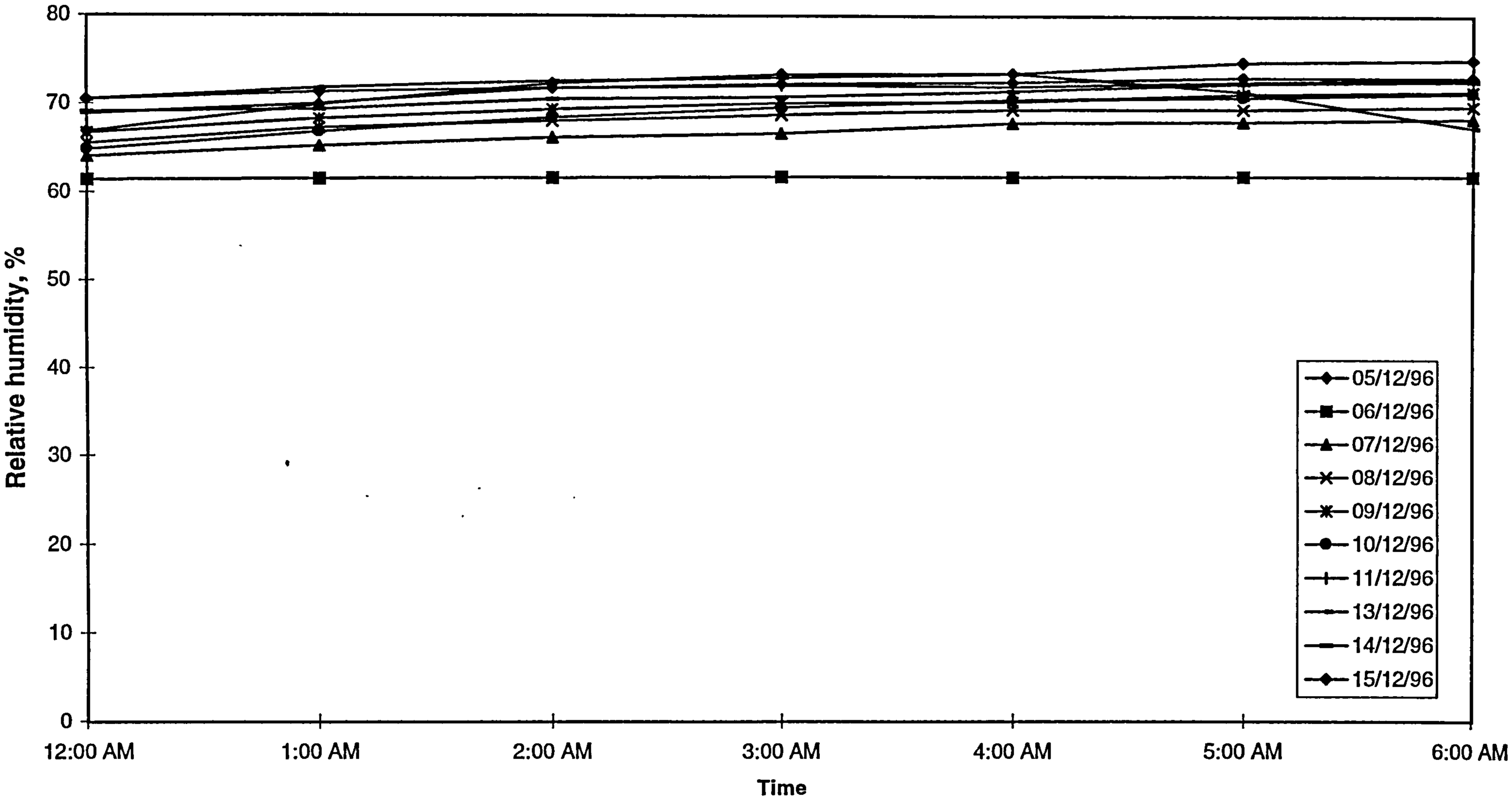

Figure 7.8 Nocturnal relative humidity for a single occupant bedroom

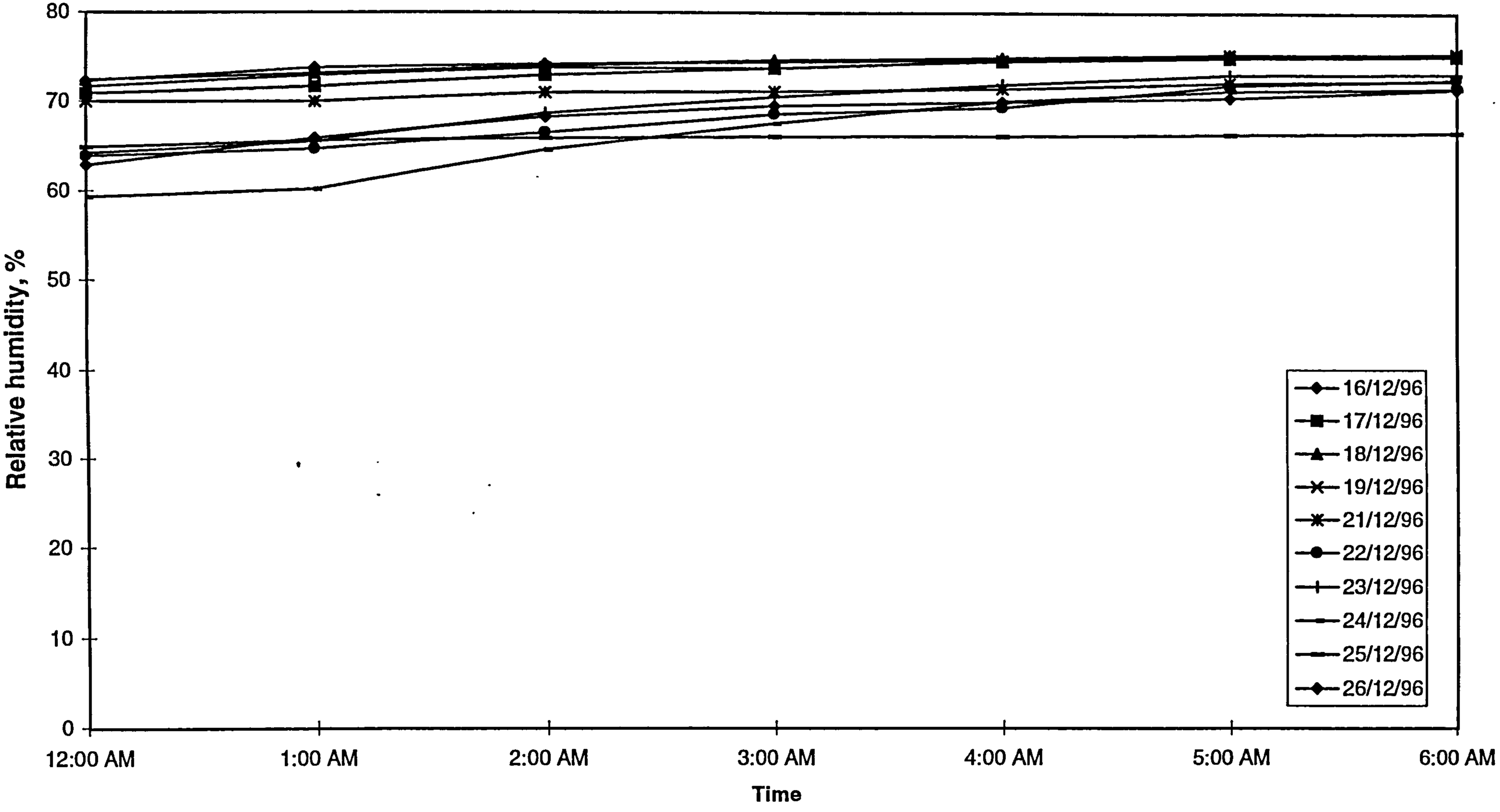

Figure 7.9 Nocturnal relative humidity for a single occupant bedroomTitle

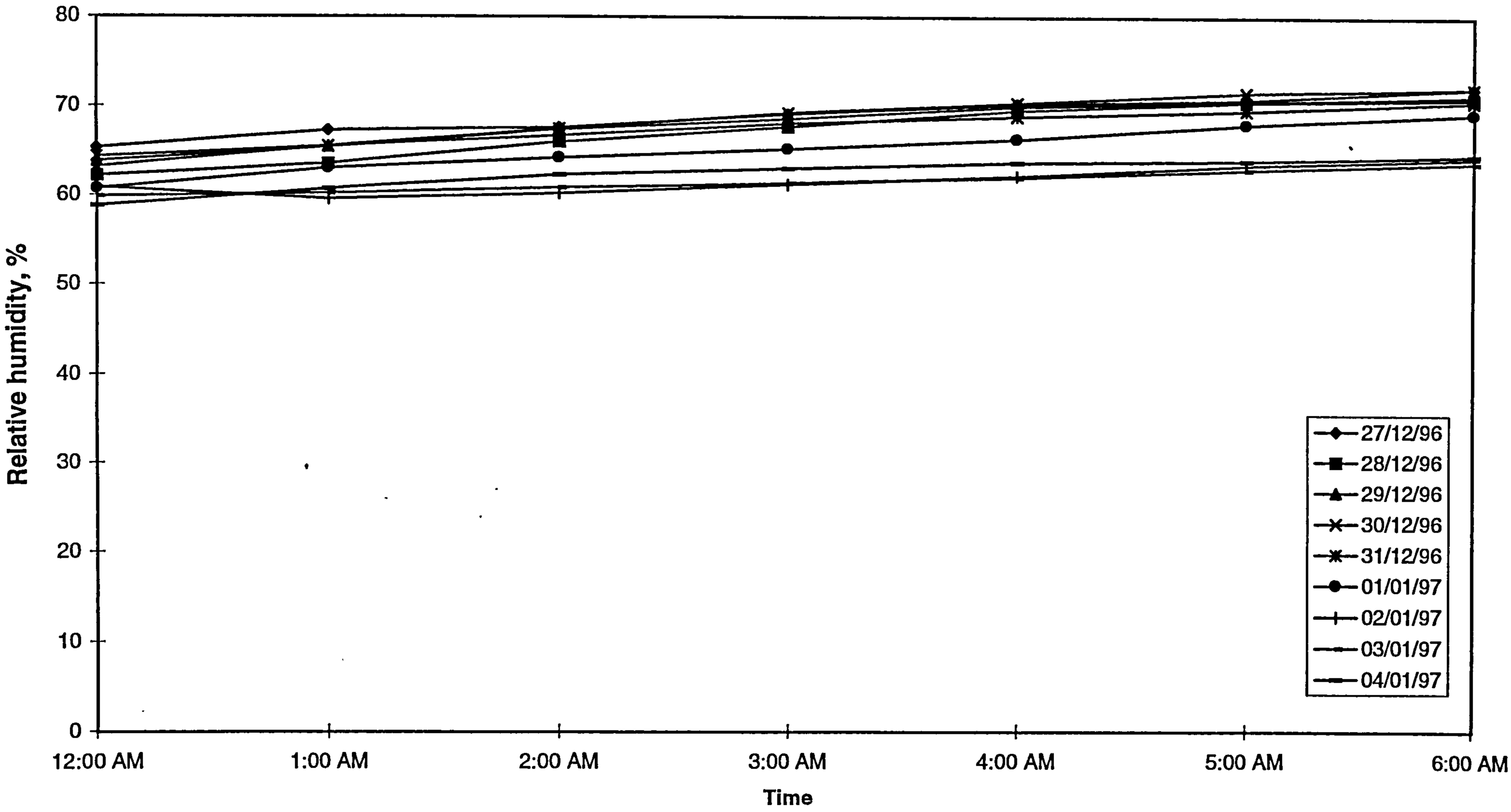

Figure 7.10 Nocturnal relative humidity for a single occupant bedroomTitle

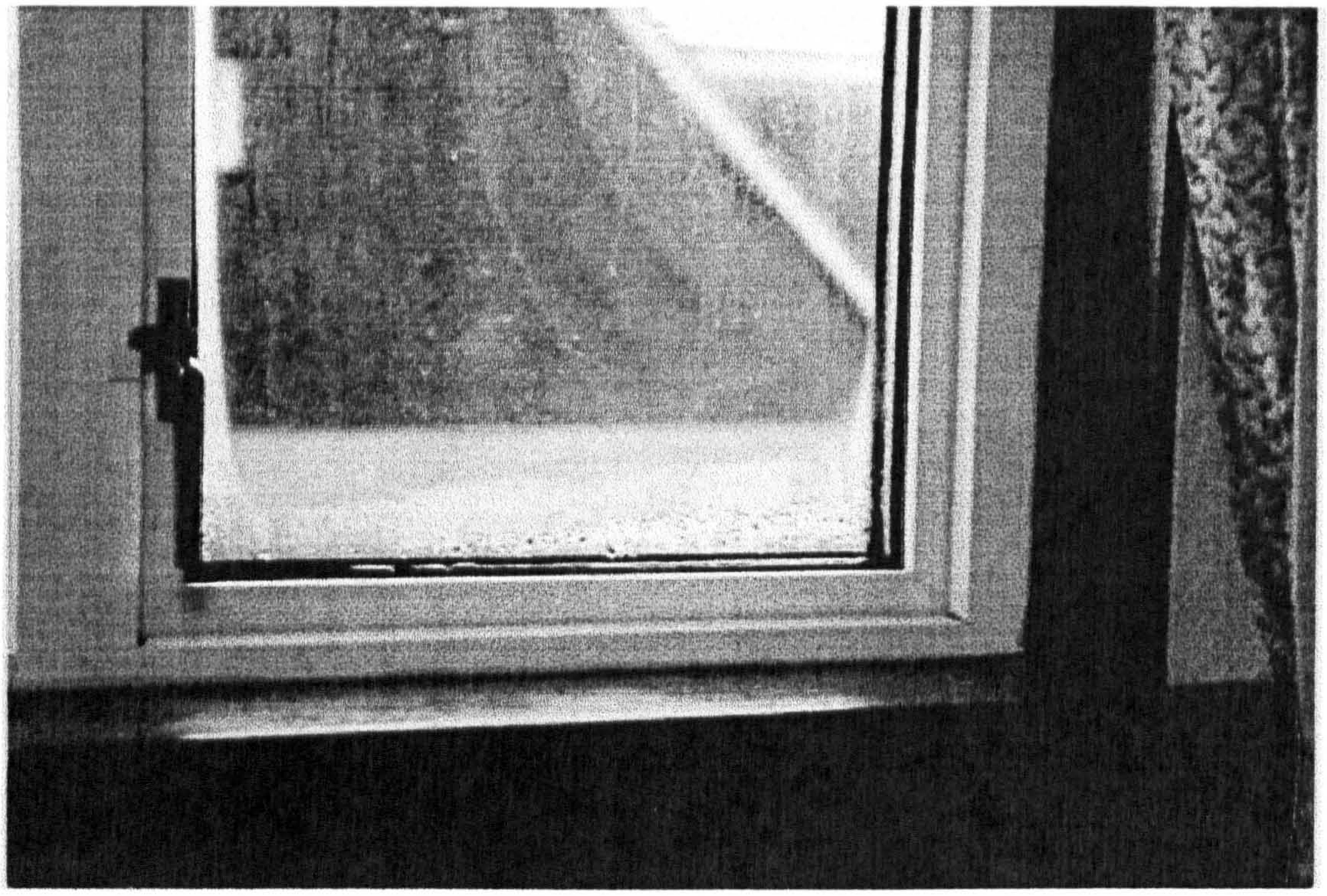

Figure 7.11a Condensation on double glazed window-experimental house (Zoom view)

Figure 7.11b Condensation on double glazed window-experimental house (Normal view)

Figure 7.12a Condensation on a double glazed window in a university flat

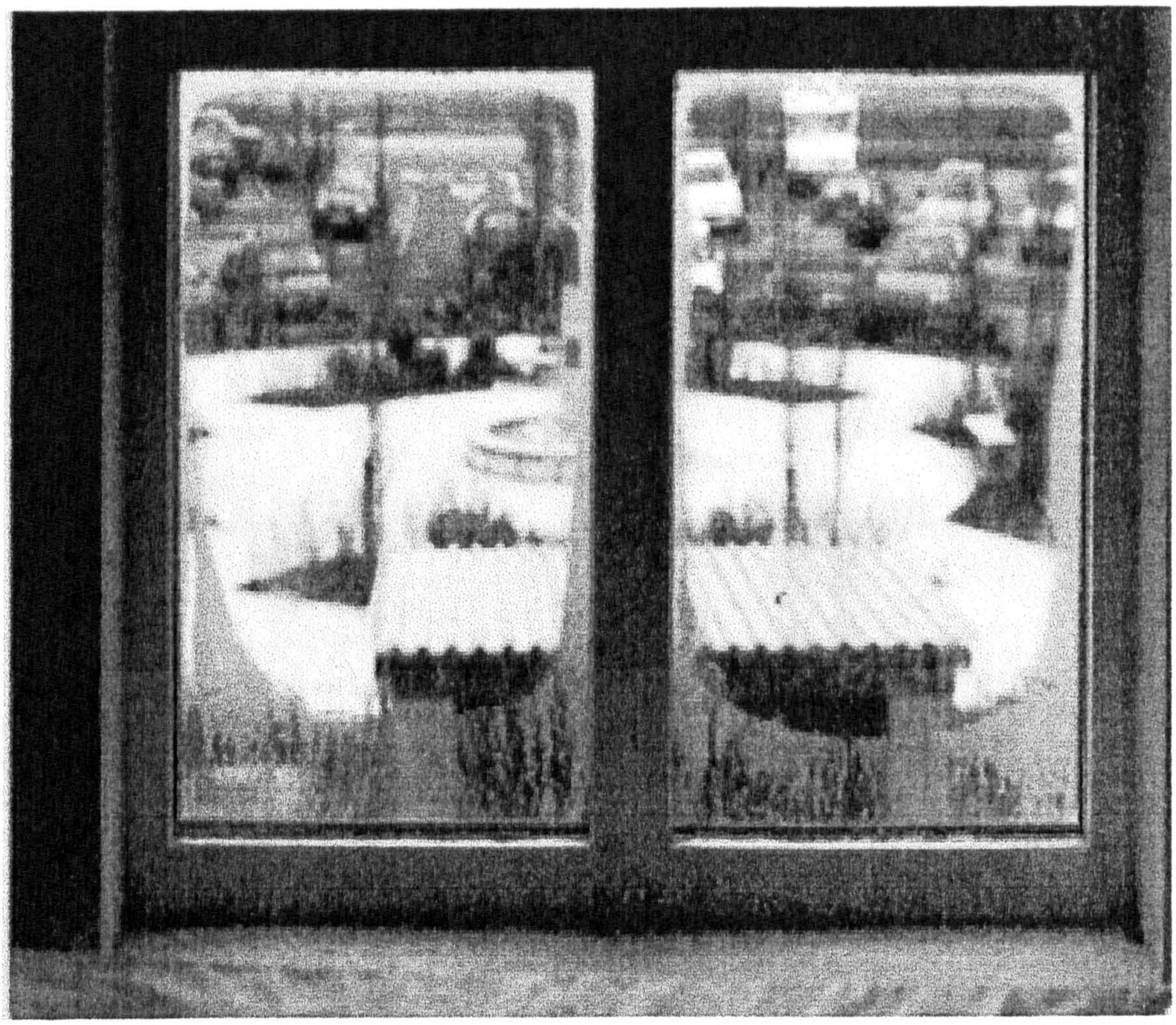

Figure 7.12b Condensation on double glazed window in a university flat – Zoom view

Table 7.3 Frequency of occurrence of condensation on window number 1

Year	Edinburgh	Manchester	London
1980	116	99	59
1981	127	112	62
1982	120	96	47
1983	98	92	52
1984	114	91	59
1985	129	104	78
1986	143	116	77
1987	122	95	70
1988	98	76	37
1989	104	85	39
Average	117	97	58

Table 7.4 Frequency of occurrence of condensation on window number 2

Year	Edinburgh	Manchester	London
1980	107	89	47
1981	121	101	58
1982	101	82	40
1983	91	84	42
1984	101	85	55
1985	119	98	70
1986	126	106	66
1987	109	86	59
1988	90	71	30
1989	92	77	33
Average	106	88	50

Table 7.5 Frequency of occurrence of condensation on window number 3

Year	Edinburgh	Manchester	London
1980	102	84	37
1981	117	90	52
1982	96	77	35
1983	88	77	38
1984	99	77	48
1985	112	91	63
1986	114	102	58
1987	101	83	57
1988	87	65	27
1989	88	74	26
Average	100	82	44

Table 7.6 Frequency of occurrence of condensation on window number 4

Year	Edinburgh	Manchester	London
1980	91	72	32
1981	104	77	46
1982	81	67	27
1983	82	68	33
1984	90	66	36
1985	103	76	60
1986	100	86	56
1987	94	74	51
1988	77	52	19
1989	79	61	19
Average	90	70	38

Table 7.7 Frequency of occurrence of condensation on window number 5

Year	Edinburgh	Manchester	London
1980	78	62	26
1981	94	70	40
1982	66	53	23
1983	74	57	29
1984	82	52	23
1985	93	70	51
1986	85	77	44
1987	82	69	47
1988	65	42	14
1989	65	55	10
Average	78	61	31

Table 7.8 Frequency of occurrence of condensation on window number 6

Year	Edinburgh	Manchester	London
1980	66	54	24
1981	85	65	40
1982	56	49	20
1983	69	53	24
1984	77	48	17
1985	86	66	49
1986	77	66	40
1987	80	61	42
1988	57	38	12
1989	56	49	9
Average	71	55	28

Table 7.9 Frequency of occurrence of condensation on window number 7

Year	Edinburgh	Manchester	London
1980	40	26	7
1981	63	42	20
1982	41	26	12
1983	40	26	9
1984	45	30	3
1985	62	56	31
1986	50	41	28
1987	55	42	24
1988	27	20	2
1989	33	30	-
Average	46	34	14

8 Conclusions and future work

This work presents several contributions to the understanding of the temperature distribution phenomenon in double glazed windows and the mechanism behind such variations and their effect on condensation occurrence on the inward facing pane of the window. A number of conclusions can be drawn based on the outcome of this research.

A. It has been proven, via measurements and computations, that there is a longitudinal temperature variation along the height of the inward facing glass of a double glazed window. This temperature stratification is primarily due to the buoyancy driven flow of gas within the sealed enclosure. An analytical model which computes the temperature at any given location along the vertical centre-line of the inner pane of double glazed window has been developed. This model is represented by the following equation:

$$t_i = T_f + (Q\,H / k)\,Na$$

B. A new dimensionless group, named the 'Napier Number', has been introduced. It is defined as, Napier number (Na) = ($\Delta T\ k / q\ H$). In this work a new relationship for obtaining the temperature at any given height along the window pane has been developed in terms of Napier number, i.e. $Na = [c_o + c_1\ U_{ref}][Ra^*_H\ Pr]^m$

C. A two-dimensional numerical model for obtaining the longitudinal temperature distribution for the bottom part of double-glazed windows has been developed. In contrast to the previous studies which solely addressed the spacer conduction effects, this model additionally includes the effects of radiative exchange between the glass panes and natural convection due to the circulating infill gas. It has been shown that the cavity gas convection is an important factor in the reduction of the bottom edge temperature. Cold bridging is also a significant factor for the conductive loss of heat at the edge surface. The present analysis has shown that the relative weighting for the conductive loss is only 17% for air filled windows. However, for the high-tech

windows with low-emissivity and heavier gases the edge effects dominate the temperature distribution.

The temperatures computed by this model were found to be in good agreement with the corresponding measured temperatures. Statistically, the average values of the mean bias error (MBE) and the root mean square error (RMSE) were found to be 0.5 and 0.7 degree Celsius respectively.

This model is of good use for the precise quantification of the condensation problem so commonly encountered in dwellings in the European and North American climates. It can also be used as a design tool in terms of selecting proper materials and dimensions for the spacer and frame.

D. It has been found that the temperature difference between the centre glazing and the bottom edge of the inner pane increases with decreasing U-value.

E. It is common experience that within dwellings condensation occurs on glazing surfaces during the early hours of the morning. To quantify this problem, a simplified model for assessing the nocturnal temperature inside a building subjected to a daytime heating schedule has been developed. This model relates the internal and external ambient temperatures at dawn by a linear relationship. For the given test room the following equation was obtained:

$$T_i = 0.58T_o + 11.3$$

This model may be used as a tool by building services professionals who are currently engaged in the use of nocturnal ventilation for cooling buildings.

F. It was noted that for any given double glazed window, the potential frequency of condensation occurrence for Edinburgh is over twice that for London.

G. The potential frequency of condensation occurrence can be significantly reduced by using modern, super-insulated windows. Condensation occurrence will be reduced by about 40-50% if an air-filled, float-glass double glazed window is replaced by a xenon-filled double glazed window using low-emissivity coating on both panes.

H. The potential of using an innovative window, i.e. one which employs a short baffle to suppress convection within the sealed cavity, has also been demonstrated. It was found that of all windows tested in the present programme of work, this innovative window is least susceptible to condensation occurrence. For example, the annual average potential frequency of condensation occurrence on the innovative window in Edinburgh is 46 compared with 71 for a xenon window using low-emissivity coating on two panes. This design can be successively introduced in window manufacturing. In high-tech windows installing a baffle will further suppress the occurrence of condensation.

Recommendations for further work have been identified and these are given below:

A. The use of the Computational Fluid Dynamic (CFD) technique to simulate the window in a more holistic manner, e.g. including air circulation indoors and the wind movement outside the building.

B. The outer pane was not the subject of attention in this work. As a next step therefore, it would be logical to query the effect of wind convection on the outer pane. Presently, attention was focused only on the temperature stratification of the inner pane.

C. The model developed in the present work for assessing the dawn temperature inside a given unheated building has only addressed the influence of the external ambient temperature. Other effects such as cloud cover, wind speed and direction, infiltration, and radiation exchange with exterior surfaces may be taken into account in future studies.

APPENDICES

APPENDIX A

Experimental Data for Eight Window Samples (Centreline measurements)

Table A1 Experimental data for the 4-air12-4 window (see Table 4.2 for design notation)

Date and Time	T_1	T_2	T_3	T_4	T_5	T_6	T_7	T_8	T_9	T_{10}	T_{11}	T_{12}	T_o	T_i	T_t	T_b
19/12/95 18:24	11.2	11.7	11.8	11.7	12.1	12.3	12.3	12.6	13.5	13.6	13.7	12.1	1.9	20.1	5.3	4.6
19/12/95 18:40	11.1	11.6	11.7	11.7	12.1	12.1	12.2	12.6	13.2	13.4	13.5	11.9	1.7	19.3	5.2	4.6
19/12/95 18:56	11.1	11.6	11.2	11.3	11.9	12.4	12.3	12.3	13.2	13.3	13.5	12.0	1.9	20.1	5.5	4.7
19/12/95 19:11	11.2	11.7	11.3	11.3	12.0	12.3	12.3	12.5	13.3	13.5	13.6	12.0	1.7	20.0	5.6	4.8
19/12/95 19:27	10.9	11.4	11.2	11.3	11.9	12.3	12.3	12.4	13.3	13.3	13.6	11.7	1.7	20.3	5.3	4.4
19/12/95 19:43	10.8	11.4	11.6	11.4	11.8	12.0	12.1	12.4	13.1	13.2	13.4	11.9	1.8	19.6	4.9	4.2
19/12/95 19:58	10.4	11.0	11.1	11.1	11.4	11.5	11.7	12.1	12.6	12.8	12.8	11.4	1.4	19.1	4.4	3.9
19/12/95 20:14	10.2	10.7	10.9	10.8	11.2	11.2	11.2	11.7	12.4	12.5	12.7	11.1	1.4	19.2	4.1	3.6
19/12/95 20:30	10.0	10.5	10.5	10.8	11.3	11.4	11.4	11.6	12.5	12.5	12.7	11.1	0.9	19.0	4.3	3.5
19/12/95 20:45	10.1	10.5	10.6	10.7	11.3	11.5	11.3	11.6	12.4	12.5	12.7	11.1	1.1	19.5	4.5	3.8
19/12/95 21:01	10.5	11.0	10.6	10.6	11.3	12.0	11.8	11.7	12.9	12.9	13.1	11.5	1.1	19.9	5.0	4.1
19/12/95 21:17	10.5	11.0	10.7	10.7	11.4	11.9	11.8	11.8	12.7	12.9	13.0	11.3	1.0	19.6	4.6	3.7
19/12/95 21:32	10.5	10.9	10.8	10.7	11.4	11.8	11.8	11.9	12.7	12.8	13.0	11.3	1.2	19.4	4.5	3.9
19/12/95 21:48	10.2	10.7	10.5	10.5	11.0	11.4	11.4	11.6	12.4	12.5	12.6	10.9	1.2	19.2	4.0	3.3
19/12/95 22:04	9.9	10.4	10.5	10.4	10.8	11.1	11.2	11.5	12.1	12.2	12.4	10.7	0.9	19.3	3.8	3.1
19/12/95 22:19	9.8	10.5	10.6	10.5	11.1	11.3	11.2	11.5	12.3	12.4	12.5	10.9	1.9	19.3	3.9	3.2
19/12/95 22:35	10.0	10.6	10.1	10.3	10.9	11.4	11.2	11.2	12.3	12.4	12.5	10.7	1.0	19.2	4.2	3.4
19/12/95 22:50	9.8	10.2	10.4	10.6	11.0	11.1	11.0	11.3	12.1	12.2	12.4	10.8	0.6	19.0	3.8	3.1
19/12/95 23:06	9.7	10.2	10.1	10.1	10.7	11.0	10.9	11.1	12.0	12.1	12.2	10.5	0.7	18.8	3.7	3.1
19/12/95 23:22	9.6	10.1	10.1	10.3	10.9	10.9	10.9	11.0	12.0	12.0	12.2	10.5	0.3	19.3	3.7	3.0
19/12/95 23:37	9.6	10.2	10.5	10.3	10.8	10.9	10.9	11.3	12.0	12.1	12.3	10.6	0.3	18.8	3.4	2.7
19/12/95 23:53	9.4	9.9	9.9	9.7	10.3	10.7	10.7	10.9	11.8	11.8	12.0	10.3	-0.2	18.7	3.2	2.5
20/12/95 00:09	9.2	9.8	10.0	9.9	10.2	10.5	10.5	10.9	11.6	11.7	11.8	10.2	0.1	18.2	3.1	2.5
20/12/95 00:24	9.2	9.7	9.5	9.6	10.1	10.6	10.6	10.7	11.5	11.5	11.7	10.0	0.2	18.6	3.2	2.5
20/12/95 00:40	9.1	9.7	9.8	9.6	10.1	10.4	10.4	10.7	11.4	11.4	11.6	10.0	0.1	18.2	3.0	2.4
20/12/95 00:56	8.8	9.4	9.9	9.8	10.1	10.2	10.2	10.7	11.4	11.6	11.7	10.0	-0.1	17.3	2.8	2.2
20/12/95 01:11	8.7	9.4	9.4	9.4	10.0	10.1	10.2	10.4	11.1	11.2	11.4	9.7	0.3	17.9	2.6	1.8
20/12/95 01:27	8.6	9.2	9.4	9.5	9.9	9.9	10.0	10.4	11.1	11.1	11.3	9.6	-0.1	17.9	2.4	1.6
20/12/95 01:43	8.4	9.0	9.3	9.3	9.6	9.9	9.9	10.3	10.9	11.0	11.0	9.5	-0.4	18.1	2.3	1.5
20/12/95 01:58	8.3	8.8	9.1	9.1	9.6	9.6	9.7	10.0	10.9	11.0	11.2	9.6	-0.4	17.5	2.5	1.5
20/12/95 02:14	8.1	8.6	9.0	8.9	9.4	9.4	9.4	9.8	10.5	10.7	10.8	9.2	-0.6	17.5	1.6	0.8
20/12/95 02:30	7.7	8.4	8.9	8.7	9.0	9.2	9.3	9.6	10.3	10.3	10.6	9.0	-0.5	17.4	1.5	0.6
20/12/95 02:45	7.5	7.9	8.2	8.4	8.9	9.1	9.1	9.2	10.0	10.1	10.3	8.6	-1.6	17.5	1.3	0.3
20/12/95 03:01	7.4	7.9	8.2	8.2	8.7	9.0	9.0	9.2	9.9	10.1	10.2	8.6	-1.6	17.3	1.2	0.1
20/12/95 03:17	7.3	7.9	8.2	8.4	8.9	9.1	9.1	9.2	10.1	10.2	10.3	8.6	-0.9	17.4	1.3	0.1
20/12/95 03:32	7.4	8.1	8.1	8.3	8.9	9.2	9.2	9.5	10.3	10.3	10.5	8.8	-1.3	17.7	1.2	0.1
20/12/95 03:48	7.5	8.1	8.1	8.3	9.0	9.3	9.3	9.5	10.2	10.4	10.5	8.8	-1.8	17.8	1.4	0.1
20/12/95 04:04	7.6	8.2	7.9	8.0	8.9	9.5	9.4	9.4	10.4	10.4	10.6	8.8	-1.9	17.8	1.6	0.2
20/12/95 04:19	7.6	8.2	8.3	8.6	9.1	9.3	9.2	9.5	10.3	10.4	10.6	8.9	-1.8	17.6	1.3	0.2
20/12/95 04:35	7.4	8.0	8.1	8.2	8.9	9.2	9.1	9.4	10.2	10.2	10.5	8.7	-1.7	17.8	1.2	-0.1
20/12/95 04:51	7.4	8.0	8.0	8.4	9.0	9.4	9.2	9.3	10.3	10.3	10.5	8.8	-2.1	17.9	1.3	0.0
20/12/95 05:06	7.4	8.0	8.3	8.6	9.0	9.1	9.0	9.4	10.2	10.3	10.5	8.8	-2.3	17.7	0.9	-0.2
20/12/95 05:22	7.4	8.0	8.1	8.2	9.0	9.1	9.1	9.3	10.1	10.2	10.4	8.6	-2.4	17.6	1.1	-0.2
20/12/95 05:37	7.2	7.8	8.1	8.4	9.0	9.1	9.1	9.2	10.0	10.0	10.3	8.7	-2.3	17.3	0.9	-0.3
20/12/95 05:53	6.8	7.5	7.7	8.0	8.5	8.8	8.7	8.8	9.7	9.7	9.9	8.3	-2.0	17.4	0.6	-0.6

Table A2 Experimental data for the 4-arg12-4 window (see Table 4.2 for design notation)

Date and Time	T_1	T_2	T_3	T_4	T_5	T_6	T_7	T_8	T_9	T_{10}	T_{11}	T_{12}	T_o	T_i	T_t	T_b
16/12/95 17:49	14.1	14.5	13.7	13.3	13.8	14.6	14.4	14.3	15.5	15.5	15.6	13.6	5.4	22.0	7.8	8.0
16/12/95 18:04	14.1	14.4	13.6	13.3	13.9	14.4	14.4	14.1	15.4	15.5	15.6	13.7	5.6	21.9	8.1	8.3
16/12/95 18:20	14.1	14.4	13.5	13.2	13.8	14.4	14.3	14.2	15.4	15.4	15.5	13.5	5.8	21.7	7.7	7.9
16/12/95 18:35	13.8	14.3	13.5	13.2	13.8	14.4	14.2	14.1	15.4	15.4	15.6	13.5	6.0	22.4	7.7	7.9
16/12/95 18:51	13.8	14.4	13.4	13.2	13.8	14.4	14.3	14.1	15.3	15.4	15.5	13.5	6.0	22.1	7.6	7.6
16/12/95 19:07	13.9	14.3	13.5	13.2	13.7	14.4	14.3	14.2	15.4	15.4	15.6	13.5	6.2	21.8	7.8	7.8
16/12/95 19:22	13.8	14.3	13.4	13.2	13.7	14.3	14.3	14.1	15.3	15.3	15.4	13.4	6.2	21.7	7.8	7.8
16/12/95 19:38	13.8	14.2	13.2	13.0	13.6	14.3	14.1	14.1	15.2	15.2	15.3	13.3	5.7	21.5	7.7	7.7
16/12/95 19:54	13.6	14.0	13.2	12.9	13.5	14.2	14.0	13.9	15.2	15.2	15.2	13.3	5.9	21.9	7.7	7.7
16/12/95 20:09	13.8	14.2	13.4	13.1	13.7	14.2	14.1	14.0	15.2	15.4	15.4	13.3	5.5	21.9	7.6	7.7
16/12/95 20:25	13.7	14.2	13.3	13.0	13.6	14.4	14.2	14.1	15.2	15.2	15.3	13.3	5.5	21.8	7.4	7.6
16/12/95 20:41	13.8	14.1	13.3	13.1	13.6	14.2	14.1	14.0	15.2	15.2	15.4	13.3	5.5	21.8	7.7	7.8
16/12/95 20:56	13.6	14.2	13.3	12.9	13.6	14.2	14.1	13.9	15.1	15.1	15.2	13.3	5.5	21.6	7.6	7.4
16/12/95 21:12	13.5	13.9	13.0	12.7	13.3	14.0	13.9	13.7	14.9	15.0	15.2	13.2	5.2	21.3	7.4	7.2
16/12/95 21:28	13.5	13.9	13.0	12.7	13.3	14.0	13.9	13.8	15.0	15.1	15.2	13.1	5.6	21.9	7.3	7.3
16/12/95 21:43	13.5	14.0	13.2	12.7	13.3	14.1	14.0	13.9	15.0	15.1	15.2	13.1	5.3	21.7	7.2	7.0
16/12/95 21:59	13.4	13.9	13.0	12.7	13.3	14.0	13.9	13.8	15.0	15.0	15.2	13.1	5.2	21.7	7.3	7.2
16/12/95 22:15	13.2	13.7	12.8	12.6	13.2	13.9	13.8	13.6	14.8	14.8	15.0	13.0	4.9	21.4	7.0	6.7
16/12/95 22:30	13.0	13.6	12.7	12.4	13.1	13.8	13.6	13.4	14.7	14.7	14.8	12.9	5.3	21.3	7.0	6.9
16/12/95 22:46	13.1	13.6	12.7	12.5	13.2	13.8	13.6	13.4	14.7	14.7	14.9	12.8	5.2	21.7	6.9	6.9
16/12/95 23:02	13.2	13.8	12.8	12.7	13.3	13.9	13.8	13.6	14.9	14.9	15.0	13.0	5.1	21.7	7.3	7.2
16/12/95 23:17	13.3	13.7	12.9	12.7	13.3	13.9	13.8	13.6	14.9	15.0	15.1	13.0	5.0	21.6	7.3	7.3
16/12/95 23:33	13.3	13.7	12.9	12.6	13.3	13.9	13.8	13.6	14.8	14.9	14.9	12.9	5.1	21.4	7.1	7.2
16/12/95 23:49	13.3	13.6	12.7	12.5	13.2	13.9	13.7	13.6	14.7	14.9	14.9	12.8	5.1	21.3	7.1	7.1
17/12/95 00:04	13.1	13.5	12.6	12.4	13.0	13.7	13.6	13.4	14.6	14.6	14.7	12.7	4.6	21.2	6.8	6.6
17/12/95 00:20	13.0	13.4	12.6	12.3	13.0	13.7	13.5	13.4	14.6	14.7	14.9	12.8	5.0	21.7	6.8	6.8
17/12/95 00:36	13.1	13.6	12.7	12.5	13.2	13.8	13.6	13.5	14.7	14.8	14.9	12.8	4.6	21.6	7.1	7.1
17/12/95 00:51	13.2	13.7	12.8	12.6	13.2	13.9	13.8	13.5	14.7	14.8	14.9	12.9	4.8	21.6	7.4	7.3
17/12/95 01:07	13.3	13.8	12.8	12.6	13.3	13.9	13.8	13.6	14.8	14.9	14.9	13.0	5.1	21.5	7.6	7.5
17/12/95 01:22	13.3	13.8	12.8	12.6	13.2	13.9	13.7	13.5	14.9	14.8	15.0	13.1	5.2	21.3	7.5	7.6
17/12/95 01:38	13.3	13.8	13.0	12.7	13.3	14.0	13.8	13.6	14.8	14.9	15.0	13.2	4.7	21.8	7.5	7.5
17/12/95 01:54	13.4	13.8	13.0	12.7	13.3	13.9	13.8	13.6	14.9	15.0	15.2	13.2	5.0	21.7	7.4	7.5
17/12/95 02:09	13.5	13.9	12.9	12.7	13.3	13.9	13.8	13.6	14.8	14.9	15.1	13.1	5.3	21.5	7.5	7.5
17/12/95 02:25	13.4	13.9	13.0	12.7	13.3	13.9	13.8	13.6	14.9	15.0	15.1	13.2	5.1	21.4	7.5	7.5
17/12/95 02:41	13.3	13.8	12.8	12.7	13.2	13.9	13.6	13.5	14.8	14.8	15.0	13.1	4.7	21.3	7.6	7.5
17/12/95 02:56	13.2	13.7	12.7	12.5	13.1	13.7	13.6	13.4	14.7	14.7	14.9	13.0	4.8	21.3	7.1	7.2
17/12/95 03:12	13.3	13.7	12.8	12.5	13.2	13.9	13.7	13.5	14.8	14.8	15.0	12.9	4.7	21.6	7.2	7.3
17/12/95 03:28	13.4	13.8	12.8	12.6	13.3	13.9	13.8	13.5	14.9	14.9	15.0	13.0	4.5	21.5	7.3	7.3
17/12/95 03:43	13.3	13.8	12.7	12.5	13.2	13.7	13.6	13.4	14.7	14.9	15.0	13.0	4.7	21.5	7.2	7.3
17/12/95 03:59	13.3	13.8	12.8	12.6	13.1	13.8	13.6	13.5	14.7	14.9	15.0	12.9	4.3	21.3	7.4	7.3
17/12/95 04:15	13.3	13.7	12.8	12.5	13.1	13.8	13.7	13.4	14.7	14.8	14.9	13.0	4.2	21.3	7.5	7.4
17/12/95 04:30	13.5	13.9	12.9	12.6	13.2	13.9	13.8	13.6	14.8	14.9	15.1	13.1	4.4	21.7	7.5	7.4
17/12/95 04:46	13.3	13.9	12.9	12.6	13.1	13.8	13.6	13.5	14.8	14.9	15.0	13.1	4.6	21.5	7.3	7.4
17/12/95 05:02	13.4	13.8	12.9	12.6	13.2	13.8	13.6	13.5	14.7	14.8	15.0	13.1	4.3	21.4	7.3	7.2
17/12/95 05:17	13.2	13.7	12.7	12.5	13.0	13.7	13.6	13.4	14.7	14.8	14.9	13.1	4.3	21.3	7.4	7.2
17/12/95 05:33	13.3	13.6	12.7	12.4	13.1	13.7	13.5	13.3	14.6	14.6	14.8	13.0	4.1	21.0	7.3	7.2
17/12/95 05:49	13.2	13.5	12.6	12.3	13.0	13.6	13.5	13.3	14.6	14.7	14.9	12.9	4.1	21.7	7.0	7.0

Table A3 Experimental data for the 4-air12-E4 window (see Table 4.2 for design notation)

Date and Time	T1	T2	T3	T4	T5	T6	T7	T8	T9	T10	T11	T12	To	Ti	Tt	Tb
20/12/95 18:06	11.0	12.5	12.2	12.1	12.9	13.8	13.8	13.7	14.4	14.5	14.7	12.3	-3.2	21.1	3.2	0.3
20/12/95 18:21	10.9	12.2	12.1	11.9	12.8	13.7	13.7	13.6	14.3	14.3	14.5	12.1	-3.6	20.7	2.6	-0.2
20/12/95 18:37	10.5	12.0	11.7	11.7	12.6	13.4	13.4	13.3	14.1	14.1	14.1	11.7	-3.1	20.4	2.1	-0.7
20/12/95 18:52	10.3	11.7	11.5	11.6	12.5	13.2	13.2	13.2	14.0	14.0	14.1	11.7	-2.5	20.3	2.9	0.0
20/12/95 19:08	10.3	11.7	11.4	11.4	12.3	13.1	13.1	13.0	13.8	13.8	14.0	11.6	-3.1	20.1	2.8	-0.1
20/12/95 19:24	10.1	11.6	11.3	11.3	12.3	13.0	13.0	13.0	13.8	13.8	14.0	11.6	-3.1	20.5	2.6	-0.2
20/12/95 19:39	10.2	11.7	11.5	11.3	12.3	13.1	13.2	13.0	13.7	13.9	13.9	11.5	-3.4	20.3	2.5	-0.5
20/12/95 19:55	10.0	11.6	11.3	11.2	12.2	12.9	13.0	12.9	13.6	13.8	13.8	11.4	-4.1	20.1	2.3	-0.7
20/12/95 20:11	9.8	11.3	11.0	11.0	11.9	12.7	12.8	12.6	13.4	13.5	13.6	11.1	-4.4	19.8	2.1	-0.8
20/12/95 20:26	9.8	11.1	10.9	11.0	11.8	12.6	12.7	12.5	13.3	13.4	13.5	11.1	-3.3	19.7	2.4	-0.7
20/12/95 20:42	9.6	11.0	10.8	10.8	11.7	12.5	12.5	12.4	13.1	13.3	13.3	11.0	-3.9	19.9	1.8	-1.1
20/12/95 20:58	9.6	11.2	10.9	10.8	11.8	12.5	12.5	12.5	13.1	13.3	13.4	10.9	-4.0	19.9	1.2	-1.7
20/12/95 21:13	9.4	10.8	10.7	10.6	11.6	12.4	12.4	12.3	13.1	13.2	13.3	10.7	-3.9	19.8	1.7	-1.2
20/12/95 21:29	9.5	10.8	10.6	10.6	11.6	12.3	12.4	12.2	13.0	13.0	13.1	10.7	-3.3	19.4	1.7	-1.0
20/12/95 21:45	9.4	10.9	10.5	10.5	11.4	12.2	12.2	12.1	13.0	13.0	13.1	10.7	-3.0	19.4	1.9	-0.9
20/12/95 22:00	9.3	10.8	10.5	10.5	11.5	12.2	12.3	12.1	13.0	13.0	13.0	10.7	-2.2	19.7	2.1	-0.8
20/12/95 22:16	9.4	10.9	10.7	10.5	11.4	12.4	12.4	12.3	13.0	13.2	13.3	10.8	-3.2	19.6	2.0	-0.9
20/12/95 22:32	9.5	10.9	10.6	10.6	11.5	12.4	12.3	12.3	13.0	13.1	13.2	10.8	-2.8	19.3	2.2	-0.7
20/12/95 22:47	9.4	10.8	10.5	10.4	11.3	12.2	12.2	12.2	12.9	13.0	13.1	10.6	-3.2	19.2	1.7	-1.1
20/12/95 23:03	9.2	10.7	10.3	10.2	11.2	12.1	12.1	12.0	12.7	12.8	12.8	10.4	-3.6	19.0	1.5	-1.2
20/12/95 23:19	9.2	10.6	10.2	10.2	11.2	12.0	12.0	11.9	12.7	12.7	12.8	10.5	-3.4	19.3	1.8	-1.0
20/12/95 23:34	9.3	10.7	10.4	10.3	11.3	12.1	12.1	12.0	12.8	12.9	13.0	10.6	-3.5	19.2	1.9	-1.0
20/12/95 23:50	9.2	10.7	10.4	10.2	11.2	12.1	12.1	12.0	12.6	12.8	12.9	10.4	-4.4	19.1	1.0	-1.6
21/12/95 00:06	9.1	10.6	10.2	10.0	11.0	11.8	11.9	11.8	12.5	12.6	12.7	10.4	-4.1	18.8	1.9	-1.1
21/12/95 00:21	9.1	10.4	10.0	10.0	10.9	11.8	11.7	11.6	12.5	12.6	12.6	10.3	-3.6	18.6	1.9	-1.0
21/12/95 00:37	9.1	10.5	10.1	10.0	11.0	11.9	11.9	11.9	12.6	12.6	12.8	10.4	-2.8	19.1	1.9	-0.9
21/12/95 00:53	9.2	10.7	10.3	10.2	11.1	12.0	12.0	11.9	12.6	12.7	12.7	10.3	-3.4	18.9	1.7	-1.0
21/12/95 01:08	9.1	10.6	10.3	10.1	11.0	11.9	11.9	11.8	12.6	12.7	12.8	10.4	-4.3	18.9	1.6	-1.3
21/12/95 01:24	9.1	10.6	10.2	9.9	10.9	11.8	11.8	11.7	12.4	12.5	12.6	10.3	-4.8	18.6	1.8	-1.4
21/12/95 01:39	8.9	10.4	10.1	9.9	10.7	11.7	11.7	11.6	12.4	12.4	12.5	10.3	-4.5	18.4	1.8	-1.3
21/12/95 01:55	8.9	10.4	9.9	9.8	10.8	11.7	11.7	11.6	12.3	12.4	12.5	10.3	-4.3	18.9	1.8	-1.0
21/12/95 02:11	9.0	10.4	10.0	9.8	10.8	11.7	11.7	11.7	12.4	12.6	12.6	10.2	-2.8	18.7	1.6	-1.1
21/12/95 02:26	9.1	10.6	10.1	9.9	10.8	11.6	11.8	11.7	12.4	12.5	12.6	10.3	-3.0	18.5	2.0	-0.7
21/12/95 02:42	9.0	10.4	9.9	9.9	10.8	11.5	11.6	11.5	12.4	12.4	12.5	10.1	-2.7	18.5	1.6	-0.8
21/12/95 02:58	8.9	10.2	9.8	9.7	10.6	11.4	11.5	11.4	12.2	12.3	12.4	9.9	-3.6	18.2	1.0	-1.3
21/12/95 03:13	8.7	10.0	9.5	9.6	10.5	11.3	11.3	11.2	12.0	12.2	12.2	9.4	-3.1	18.5	0.6	-1.4
21/12/95 03:29	8.8	10.2	9.8	9.7	10.6	11.4	11.4	11.4	12.2	12.3	12.3	9.6	-3.5	18.7	0.9	-1.1
21/12/95 03:45	8.7	10.2	9.8	9.7	10.6	11.5	11.5	11.4	12.2	12.2	12.3	9.6	-3.2	18.3	0.7	-1.2
21/12/95 04:00	8.9	10.2	9.8	9.7	10.7	11.3	11.4	11.3	12.1	12.2	12.2	9.5	-3.6	18.2	1.0	-0.9
21/12/95 04:16	8.7	10.0	9.7	9.7	10.6	11.3	11.3	11.1	11.9	12.0	12.0	9.3	-3.3	18.1	0.3	-1.2
21/12/95 04:32	8.7	9.8	9.4	9.4	10.4	11.1	11.2	11.0	11.9	11.9	11.9	9.0	-3.9	18.2	-0.1	-1.3
21/12/95 04:47	8.7	10.0	9.6	9.6	10.5	11.3	11.3	11.2	12.0	12.0	12.0	8.9	-3.6	18.5	-0.3	-1.5
21/12/95 05:03	8.7	10.0	9.5	9.5	10.5	11.3	11.3	11.1	11.9	12.1	11.9	9.0	-3.9	18.4	-0.3	-1.5
21/12/95 05:19	8.6	9.9	9.5	9.4	10.4	11.2	11.2	11.0	11.9	11.9	11.8	8.9	-3.7	18.1	-0.1	-1.5

Table A4 Experimental data for the 4-arg12-E4 window (see Table 4.2 for design notation)

Date and Time	T1	T2	T3	T4	T5	T6	T7	T8	T9	T10	T11	T12	To	Ti	Tt	Tb
14/12/95 16:57	17.0	18.4	17.8	18.0	18.7	19.3	19.2	18.9	19.8	19.8	19.6	15.5	4.6	23.8	8.0	7.8
14/12/95 17:13	16.3	17.5	17.1	17.1	17.9	18.5	18.3	18.2	19.0	19.1	18.8	14.9	4.3	23.2	7.3	6.9
14/12/95 17:28	15.6	16.9	16.4	16.5	17.3	17.7	17.7	17.5	18.5	18.5	18.3	14.3	4.0	22.7	6.7	6.1
14/12/95 17:44	15.1	16.4	15.9	16.0	16.8	17.3	17.3	17.0	18.0	18.0	17.8	13.8	3.5	22.5	6.3	5.9
14/12/95 18:00	14.9	16.1	15.7	15.9	16.6	17.2	17.1	16.8	17.9	17.9	17.8	13.8	3.5	22.7	6.6	6.0
14/12/95 18:15	14.9	16.2	15.7	15.8	16.5	17.2	17.1	16.9	17.9	17.9	17.7	14.0	3.6	22.4	7.0	6.4
14/12/95 18:31	14.8	16.1	15.6	15.6	16.4	17.0	17.0	16.7	17.8	17.8	17.7	14.0	4.3	22.3	7.3	6.6
14/12/95 18:47	14.7	15.9	15.5	15.6	16.3	16.9	16.8	16.6	17.6	17.7	17.5	14.0	3.6	22.0	7.2	6.4
14/12/95 19:02	14.7	15.9	15.4	15.5	16.2	16.7	16.7	16.5	17.4	17.4	17.3	13.8	4.0	21.7	6.8	6.3
14/12/95 19:18	14.6	15.8	15.3	15.4	16.2	16.8	16.7	16.4	17.5	17.5	17.4	13.7	3.9	22.2	6.9	6.4
14/12/95 19:34	14.6	15.8	15.3	15.4	16.1	16.7	16.7	16.4	17.4	17.5	17.4	13.6	3.7	22.0	7.0	6.5
14/12/95 19:49	14.6	15.9	15.3	15.4	16.0	16.7	16.6	16.5	17.4	17.5	17.4	13.8	3.7	21.9	7.0	6.5
14/12/95 20:05	14.4	15.6	15.1	15.3	16.0	16.6	16.5	16.3	17.3	17.3	17.3	13.7	3.4	21.7	7.0	6.4
14/12/95 20:21	14.4	15.6	15.0	15.1	15.9	16.5	16.4	16.1	17.2	17.2	17.0	13.4	4.6	21.5	6.5	6.1
14/12/95 20:36	14.2	15.5	15.0	15.2	15.8	16.5	16.3	16.0	17.2	17.2	17.1	13.1	4.8	22.1	6.6	6.4
14/12/95 20:52	14.3	15.6	15.1	15.3	16.0	16.6	16.5	16.3	17.3	17.2	17.1	13.1	4.4	22.0	6.4	6.3
14/12/95 21:08	14.1	15.5	15.0	15.1	15.9	16.5	16.4	16.2	17.2	17.2	17.0	13.1	4.2	21.8	6.2	5.8
14/12/95 21:23	14.1	15.4	14.9	15.1	15.8	16.4	16.3	16.1	17.1	17.0	16.9	13.0	4.7	21.6	6.2	5.7
14/12/95 21:39	14.0	15.3	14.7	15.0	15.6	16.3	16.2	15.9	17.0	17.0	16.8	12.9	4.1	21.3	6.2	6.0
14/12/95 21:54	14.1	15.2	14.8	15.0	15.7	16.3	16.2	16.0	17.0	17.0	16.8	12.9	4.7	21.8	6.1	5.9
14/12/95 22:10	14.1	15.3	14.9	15.0	15.7	16.3	16.2	16.0	17.1	17.0	16.9	12.9	4.9	21.6	6.3	5.9
14/12/95 22:26	14.2	15.4	15.0	15.0	15.8	16.5	16.3	16.1	17.1	17.1	17.0	12.9	5.0	21.7	6.4	6.2
14/12/95 22:41	14.1	15.3	14.8	15.0	15.7	16.3	16.2	16.0	17.1	17.1	16.8	12.8	4.7	21.4	6.4	6.2
14/12/95 22:57	14.1	15.2	14.8	14.9	15.6	16.2	16.1	16.0	16.9	16.9	16.6	12.7	5.2	21.2	6.3	6.3
14/12/95 23:13	14.0	15.2	14.7	14.9	15.7	16.3	16.2	15.9	17.0	17.0	16.7	12.8	5.4	21.4	6.6	6.5
14/12/95 23:28	14.1	15.4	14.8	15.0	15.7	16.4	16.3	16.1	17.1	17.1	16.8	12.9	5.1	21.8	6.6	6.4
14/12/95 23:44	14.2	15.4	14.9	15.1	15.9	16.5	16.3	16.0	17.1	17.0	16.8	12.7	5.5	21.5	6.6	6.4
15/12/95 00:00	14.2	15.4	14.8	15.1	15.8	16.5	16.4	16.1	17.1	17.1	16.8	12.9	4.9	21.6	6.7	6.4
15/12/95 00:15	14.2	15.3	14.8	15.1	15.7	16.3	16.2	16.0	17.0	17.0	16.7	13.0	5.4	21.4	6.6	6.3
15/12/95 00:31	14.1	15.3	14.8	15.0	15.6	16.3	16.2	15.9	16.9	16.9	16.9	12.9	5.3	21.4	6.8	6.5
15/12/95 00:47	14.1	15.3	14.8	14.9	15.7	16.3	16.2	16.0	17.0	17.1	16.9	12.9	5.1	21.7	6.5	6.3
15/12/95 01:02	14.2	15.4	14.9	15.0	15.7	16.3	16.3	16.1	17.1	17.1	16.8	12.9	5.4	21.5	6.4	6.3
15/12/95 01:18	14.1	15.3	14.8	14.9	15.7	16.3	16.2	16.0	17.0	17.0	16.7	12.5	4.8	21.4	6.2	6.1
15/12/95 01:34	14.1	15.2	14.6	14.9	15.6	16.3	16.1	15.9	16.9	16.9	16.6	12.5	4.9	21.1	6.2	6.0
15/12/95 01:49	14.0	15.2	14.7	14.7	15.5	16.2	16.1	15.9	16.9	16.8	16.5	12.4	5.0	21.1	6.2	6.1
15/12/95 02:05	13.9	15.1	14.6	14.8	15.5	16.1	16.1	15.7	16.8	16.8	16.5	12.5	4.3	21.7	6.2	6.0
15/12/95 02:21	14.1	15.3	14.8	15.0	15.8	16.4	16.1	15.9	17.0	17.0	16.7	12.7	4.1	21.6	6.4	6.1
15/12/95 02:36	14.0	15.2	14.7	14.9	15.6	16.3	16.1	16.0	17.1	17.0	16.8	12.8	4.3	21.6	6.4	6.2
15/12/95 02:52	13.9	15.2	14.7	14.8	15.6	16.2	16.0	15.8	16.9	16.9	16.7	12.7	3.9	21.4	6.1	6.0
15/12/95 03:08	14.0	15.2	14.6	14.8	15.5	16.1	16.0	15.8	16.9	16.8	16.7	12.7	3.9	21.4	5.9	5.6
15/12/95 03:23	13.8	15.0	14.5	14.7	15.4	16.0	15.9	15.6	16.7	16.7	16.6	12.5	4.2	21.4	5.9	5.8
15/12/95 03:39	13.9	15.1	14.6	14.7	15.5	16.1	16.1	15.8	16.8	16.9	16.6	12.6	4.3	21.5	5.9	5.8
15/12/95 03:55	13.9	15.1	14.6	14.9	15.5	16.1	16.1	15.8	16.8	16.8	16.6	12.6	3.7	21.4	5.8	5.5
15/12/95 04:10	13.8	14.9	14.5	14.7	15.4	16.0	15.9	15.7	16.7	16.7	16.5	12.6	3.4	21.3	5.5	5.0

Table A5 Experimental data for the 4E-kr12-E4 window (see Table 4.2 for design notation)

Date and Time	T1	T2	T3	T4	T5	T6	T7	T8	T9	T10	T11	T12	To	Ti	Tt	Tb
13/12/95 17:22	15.5	17.5	18.2	18.4	19.0	19.5	19.7	19.9	20.5	20.6	20.6	17.1	4.1	22.1	7.2	6.1
13/12/95 17:32	15.2	17.1	17.5	18.0	18.6	19.1	19.2	19.4	20.1	20.1	19.9	16.6	4.1	22.0	7.0	5.9
13/12/95 17:43	15.0	16.7	17.4	17.6	18.1	18.5	18.7	19.0	19.7	19.8	19.6	16.5	4.4	21.4	7.1	6.4
13/12/95 17:53	14.6	16.3	16.9	17.0	17.5	18.0	18.2	18.5	19.1	19.2	18.9	15.9	4.6	21.9	6.8	5.9
13/12/95 18:04	14.3	16.1	16.9	17.0	17.3	17.5	17.7	18.2	18.8	19.0	18.7	15.8	4.9	21.4	6.9	6.2
13/12/95 18:14	14.1	15.9	16.5	16.7	17.0	17.4	17.5	17.8	18.4	18.5	18.4	15.4	4.5	22.1	6.6	5.8
13/12/95 18:25	13.8	15.6	16.2	16.4	16.8	17.1	17.3	17.7	18.4	18.5	18.2	15.2	4.5	21.6	6.4	5.5
13/12/95 18:35	13.4	15.3	16.2	16.4	16.6	16.8	17.1	17.5	18.1	18.3	18.1	15.1	4.0	20.7	6.5	5.7
13/12/95 18:45	13.3	15.1	15.8	16.2	16.5	16.8	17.0	17.4	18.0	18.0	17.7	14.7	3.9	21.1	6.3	5.2
13/12/95 18:56	13.2	15.0	15.7	16.2	16.5	16.7	16.8	17.2	17.9	18.0	17.7	14.8	4.3	20.6	6.3	5.4
13/12/95 19:06	13.1	15.0	15.6	15.8	16.3	16.8	16.8	17.1	17.7	17.8	17.6	14.5	3.7	19.7	6.3	5.4
13/12/95 19:17	13.2	14.9	15.5	15.8	16.3	16.7	16.7	17.0	17.7	17.7	17.5	14.6	4.3	18.6	6.3	5.5
13/12/95 19:27	13.0	14.9	15.3	15.6	16.2	16.6	16.7	16.9	17.6	17.7	17.4	14.5	4.4	21.4	6.2	5.3
13/12/95 19:38	13.1	15.0	15.6	15.6	16.1	16.6	16.8	17.2	17.8	17.8	17.6	14.5	4.2	21.6	6.2	5.3
13/12/95 19:48	12.9	14.9	15.5	15.6	16.2	16.7	16.8	17.2	17.8	17.8	17.5	14.4	4.1	21.2	6.1	5.0
13/12/95 19:58	13.0	15.0	15.4	15.6	16.2	16.6	16.9	17.0	17.8	17.8	17.6	14.5	4.1	20.5	6.0	5.1
13/12/95 20:09	13.1	15.0	15.3	15.4	16.1	16.8	16.9	17.0	17.7	17.8	17.6	14.5	4.0	21.6	6.2	5.2
13/12/95 20:19	13.1	15.1	15.6	15.8	16.4	16.7	16.8	17.2	17.8	17.8	17.7	14.6	3.7	20.1	6.4	5.3
13/12/95 20:30	13.2	15.1	15.2	15.5	16.3	16.9	17.0	17.1	17.9	17.9	17.6	14.5	3.9	21.5	6.4	5.3
13/12/95 20:40	13.1	14.9	15.5	15.7	16.2	16.6	16.7	17.0	17.8	17.9	17.6	14.5	3.6	20.8	6.3	5.4
13/12/95 20:51	13.0	14.9	15.6	15.8	16.2	16.5	16.6	17.0	17.6	17.7	17.4	14.5	4.0	20.1	6.2	5.3
13/12/95 21:01	12.8	14.7	15.5	15.6	15.9	16.5	16.6	16.9	17.6	17.7	17.4	14.4	4.3	21.2	6.1	5.3
13/12/95 21:11	12.9	14.7	15.4	15.7	16.2	16.3	16.5	16.9	17.5	17.5	17.3	14.2	4.2	20.2	6.1	5.3
13/12/95 21:22	12.8	14.8	15.3	15.3	15.9	16.4	16.5	16.7	17.5	17.6	17.4	14.3	4.0	21.3	6.1	5.2
13/12/95 21:32	12.8	14.7	15.5	15.6	15.9	16.3	16.4	16.7	17.5	17.5	17.3	14.3	3.9	20.7	6.1	5.3
13/12/95 21:43	12.7	14.6	15.1	15.4	15.8	16.3	16.3	16.7	17.3	17.3	17.1	14.0	3.7	21.0	5.7	4.7
13/12/95 21:53	12.8	14.6	15.0	15.2	15.8	16.4	16.4	16.6	17.4	17.4	17.0	14.0	3.9	20.3	5.8	4.8
13/12/95 22:04	12.7	14.7	15.1	15.1	15.6	16.2	16.2	16.5	17.3	17.3	17.0	14.1	3.8	19.4	6.1	5.2
13/12/95 22:14	12.8	14.6	14.9	15.2	15.8	16.4	16.5	16.5	17.3	17.3	17.0	14.1	3.8	21.0	6.2	5.3
13/12/95 22:25	12.8	14.6	15.3	15.5	15.9	16.3	16.5	16.7	17.4	17.6	17.3	14.2	3.7	21.0	6.1	5.1
13/12/95 22:35	12.9	14.9	15.1	15.2	15.9	16.5	16.6	16.7	17.5	17.6	17.3	14.2	4.2	21.3	6.1	5.2
13/12/95 22:45	12.9	14.8	15.3	15.5	16.0	16.6	16.7	16.8	17.6	17.6	17.4	14.3	3.9	21.2	6.1	5.1
13/12/95 22:56	12.9	14.7	15.2	15.4	16.0	16.6	16.7	16.9	17.5	17.7	17.4	14.3	4.1	19.4	6.1	5.1
13/12/95 23:06	12.8	14.7	15.3	15.5	15.9	16.3	16.4	16.8	17.4	17.5	17.3	14.2	4.2	20.5	6.1	5.4
13/12/95 23:17	12.8	14.6	15.2	15.4	15.8	16.2	16.4	16.6	17.3	17.3	17.1	14.2	4.2	19.6	6.1	5.4
13/12/95 23:27	12.5	14.4	15.0	15.3	15.6	15.9	15.9	16.4	17.1	17.2	17.0	14.1	4.3	19.4	6.0	5.2
13/12/95 23:38	12.6	14.3	14.9	15.0	15.4	15.8	15.9	16.3	17.0	17.0	16.8	13.8	3.8	20.3	5.9	5.2
13/12/95 23:48	12.5	14.4	15.0	15.2	15.6	16.0	16.1	16.4	17.0	17.1	16.8	13.9	3.7	20.6	5.7	4.9
13/12/95 23:58	12.5	14.3	15.1	15.2	15.6	15.9	16.0	16.5	17.1	17.2	16.9	14.0	3.9	20.4	5.8	4.9
14/12/95 00:09	12.5	14.2	14.8	15.1	15.6	16.0	16.0	16.3	17.1	17.1	17.0	13.9	4.0	20.5	5.8	4.9
14/12/95 00:19	12.5	14.3	14.8	15.0	15.7	16.2	16.2	16.4	17.1	17.1	16.9	13.8	4.1	20.8	5.8	5.0
14/12/95 00:30	12.6	14.4	15.2	15.3	15.6	16.0	16.1	16.5	17.1	17.3	17.1	14.1	4.3	18.6	6.0	5.2
14/12/95 00:40	12.5	14.3	14.9	15.0	15.5	15.8	15.9	16.3	17.0	17.0	16.8	13.8	4.0	20.2	5.9	5.2
14/12/95 00:51	12.5	14.3	14.8	14.8	15.4	16.0	16.1	16.3	16.9	16.9	16.7	13.8	3.4	19.3	5.8	5.1

Table A6 Experimental data for the 4E-xe10-E4 window (see Table 4.2 for design notation)

Date and Time	T1	T2	T3	T4	T5	T6	T7	T8	T9	T10	T11	T12	To	Ti	Tt	Tb
12/12/95 16:48	16.0	18.0	18.5	19.0	19.5	20.3	20.2	20.1	20.8	20.8	20.3	16.1	1.8	24.4	8.1	5.6
12/12/95 17:03	15.9	17.8	18.2	18.6	19.2	20.0	20.0	19.8	20.6	20.6	20.0	15.7	2.1	24.5	7.7	5.6
12/12/95 17:19	15.7	17.7	18.2	18.6	19.2	19.9	19.9	19.8	20.4	20.5	20.0	15.5	2.7	24.3	7.3	4.7
12/12/95 17:35	15.4	17.5	17.9	18.5	19.1	19.7	19.7	19.6	20.3	20.2	19.7	15.5	2.4	24.1	7.4	4.8
12/12/95 17:50	15.4	17.4	17.7	18.2	18.9	19.5	19.5	19.3	20.2	20.2	19.6	15.4	3.2	24.0	7.7	5.3
12/12/95 18:06	15.5	17.3	17.7	18.1	18.7	19.4	19.5	19.2	20.0	20.0	19.4	15.4	3.2	23.6	7.8	5.7
12/12/95 18:22	15.4	17.3	17.6	18.1	18.6	19.4	19.4	19.1	20.0	20.0	19.4	15.4	3.8	23.8	8.0	5.9
12/12/95 18:37	15.5	17.4	17.8	18.1	18.8	19.4	19.5	19.3	20.1	20.1	19.5	15.5	3.7	24.0	8.3	6.1
12/12/95 18:53	15.6	17.5	17.8	18.1	18.8	19.5	19.6	19.3	20.1	20.1	19.6	15.5	3.8	23.8	8.3	6.0
12/12/95 19:09	15.5	17.5	17.7	18.1	18.8	19.5	19.5	19.2	20.1	20.0	19.5	15.4	4.1	23.7	8.3	6.2
12/12/95 19:24	15.6	17.4	17.6	18.1	18.7	19.4	19.4	19.1	20.0	20.0	19.4	15.4	3.6	23.6	8.2	6.2
12/12/95 19:40	15.5	17.3	17.6	17.9	18.5	19.3	19.3	19.1	19.8	19.8	19.2	15.3	3.8	23.4	8.2	6.2
12/12/95 19:56	15.5	17.3	17.6	17.9	18.5	19.3	19.3	19.1	20.0	19.9	19.4	15.3	4.2	23.8	8.2	5.9
12/12/95 20:11	15.5	17.4	17.6	17.9	18.6	19.3	19.4	19.2	19.9	19.9	19.4	15.4	3.3	23.7	8.1	5.8
12/12/95 20:27	15.5	17.3	17.6	18.0	18.6	19.3	19.4	19.1	19.8	19.8	19.3	15.3	5.5	23.5	8.2	6.1
12/12/95 20:43	15.5	17.3	17.6	17.9	18.6	19.3	19.4	19.1	19.9	19.9	19.3	15.5	4.0	23.5	8.6	6.4
12/12/95 20:58	15.4	17.2	17.5	17.9	18.5	19.3	19.3	18.9	19.9	19.9	19.4	15.6	4.1	23.4	8.7	6.4
12/12/95 21:14	15.6	17.3	17.6	17.9	18.6	19.4	19.4	19.1	19.9	19.9	19.3	15.7	4.7	23.8	8.8	6.5
12/12/95 21:30	15.7	17.5	17.8	18.1	18.7	19.4	19.5	19.3	20.0	20.0	19.6	15.6	3.9	23.8	8.4	6.3
12/12/95 21:45	15.7	17.6	17.7	18.1	18.7	19.4	19.4	19.1	20.0	20.0	19.5	15.6	5.0	23.6	8.6	6.3
12/12/95 22:01	15.7	17.5	17.6	18.0	18.6	19.3	19.3	19.1	20.0	20.0	19.5	15.7	5.2	23.4	8.7	6.3
12/12/95 22:17	15.6	17.4	17.6	18.0	18.6	19.4	19.3	19.0	19.9	19.9	19.5	15.6	4.7	23.4	8.7	6.4
12/12/95 22:32	15.7	17.4	17.7	18.0	18.6	19.3	19.3	19.0	19.8	19.8	19.4	15.7	5.0	23.4	8.9	6.6
12/12/95 22:48	15.8	17.6	17.8	18.0	18.6	19.5	19.5	19.2	20.0	20.0	19.5	15.7	3.9	23.7	8.7	6.5
12/12/95 23:04	15.6	17.5	17.8	18.1	18.7	19.4	19.5	19.2	20.0	20.0	19.6	15.6	3.9	23.6	8.6	6.3
12/12/95 23:19	15.6	17.4	17.7	18.1	18.7	19.4	19.4	19.1	19.9	19.9	19.5	15.6	5.6	23.5	8.7	6.5
12/12/95 23:35	15.6	17.4	17.6	18.0	18.6	19.4	19.4	19.1	19.8	19.8	19.4	15.6	4.8	23.3	8.6	6.4
12/12/95 23:50	15.6	17.3	17.6	17.9	18.5	19.2	19.2	19.0	19.9	19.8	19.4	15.7	4.0	23.2	8.5	6.4
13/12/95 00:06	15.5	17.3	17.6	17.9	18.4	19.2	19.2	19.0	19.9	19.8	19.4	15.6	5.2	23.5	8.5	6.3
13/12/95 00:22	15.6	17.5	17.6	18.0	18.6	19.3	19.4	19.1	20.0	19.9	19.5	15.6	3.8	23.7	8.3	6.3
13/12/95 00:37	15.5	17.2	17.6	18.0	18.6	19.3	19.4	19.2	19.9	19.9	19.4	15.4	5.1	23.5	8.3	6.1
13/12/95 00:53	15.5	17.3	17.5	18.0	18.5	19.3	19.4	19.2	19.9	19.7	19.3	15.3	5.5	23.3	8.3	6.4
13/12/95 01:09	15.3	17.1	17.7	18.1	18.6	19.0	19.1	19.1	19.8	19.7	19.2	15.2	5.5	22.9	8.3	6.5
13/12/95 01:24	15.1	16.9	17.7	18.1	18.4	18.6	18.7	18.9	19.5	19.5	19.0	15.0	5.8	23.0	8.1	6.2
13/12/95 01:40	15.0	16.8	17.3	17.9	18.5	19.0	19.0	18.9	19.7	19.6	19.1	15.0	5.2	23.5	7.8	5.8
13/12/95 01:56	14.8	16.8	17.6	18.1	18.5	18.6	18.8	19.0	19.7	19.5	19.1	15.0	5.1	23.0	7.7	5.5
13/12/95 02:11	14.7	16.6	17.4	17.8	18.3	18.6	18.7	18.7	19.5	19.4	18.9	14.8	5.3	23.0	7.5	5.5
13/12/95 02:27	14.5	16.3	17.2	17.6	17.9	18.3	18.4	18.4	19.2	19.2	18.6	14.6	5.2	22.7	7.4	5.3
13/12/95 02:43	14.4	16.3	16.9	17.4	17.8	18.2	18.2	18.3	19.1	19.1	18.5	14.5	4.8	22.6	7.2	5.2
13/12/95 02:58	14.2	16.3	16.8	17.3	17.8	18.4	18.4	18.2	19.2	19.1	18.6	14.5	4.5	23.1	7.1	4.8
13/12/95 03:14	14.4	16.3	17.1	17.5	18.0	18.3	18.5	18.5	19.2	19.2	18.6	14.6	4.9	22.2	7.3	5.2
13/12/95 03:30	14.2	16.4	17.2	17.6	17.9	18.1	18.2	18.5	19.1	19.1	18.5	14.5	5.0	22.4	7.2	5.3
13/12/95 03:45	14.1	16.1	17.0	17.4	17.7	18.0	18.1	18.2	19.0	18.9	18.4	14.5	4.9	22.0	7.1	5.0
13/12/95 04:01	14.0	15.7	16.6	17.1	17.6	17.8	17.9	18.0	18.9	18.8	18.3	14.3	4.8	22.3	7.0	5.0

Table A7 Experimental data for 4-air20-4 with baffle

Date and Time	T1	T2	T3	T4	T5	T6	T7	T8	T9	T10	T11	T12	To	Ti	Tb	Tt
29/12/95 18:30	7.2	8.4	7.6	6.7	6.7	7.6	8.1	9.1	10.2	10.7	11.5	8.8	-4.2	18.3	-2.7	0.9
29/12/95 19:01	7.4	8.6	7.7	6.7	6.8	7.7	8.1	9.0	10.2	10.7	11.3	8.8	-5.0	18.0	-2.7	0.8
29/12/95 19:32	8.0	8.4	7.4	6.7	7.1	7.7	8.0	8.9	10.1	10.6	11.2	8.5	-4.3	18.0	-3.0	-0.7
29/12/95 20:04	9.0	9.0	7.5	6.6	6.9	7.6	7.9	8.7	9.8	10.2	10.7	8.0	-4.5	17.9	-2.2	-0.7
29/12/95 20:35	9.0	8.8	7.6	6.8	7.1	7.8	8.1	8.8	9.9	10.3	10.8	8.0	-4.0	18.0	-2.0	-0.7
29/12/95 21:06	9.3	8.9	7.8	7.0	7.1	7.8	8.1	8.7	9.9	10.2	10.8	8.0	-3.9	17.7	-1.8	-0.7
29/12/95 21:38	9.3	9.1	7.6	6.7	6.8	7.5	7.9	8.7	9.9	10.2	10.8	8.0	-3.7	17.5	-1.6	-0.4
29/12/95 22:09	8.9	9.1	7.8	6.9	7.2	7.9	8.4	9.0	10.1	10.4	11.0	8.1	-3.5	18.0	-1.5	0.2
29/12/95 22:40	8.9	9.5	7.9	6.9	7.4	8.3	8.5	9.1	10.3	10.6	11.2	8.5	-2.6	17.8	-1.1	0.9
29/12/95 23:12	8.7	9.3	8.1	7.3	7.7	8.4	8.7	9.3	10.6	10.9	11.5	8.8	-2.8	18.1	-0.9	1.7
29/12/95 23:43	9.2	9.7	8.1	7.2	7.7	8.4	8.7	9.4	10.5	10.9	11.3	8.8	-3.0	17.7	-0.8	1.3
30/12/95 00:14	9.2	9.5	8.0	7.1	7.6	8.3	8.7	9.2	10.4	10.8	11.3	8.7	-2.5	17.5	-0.5	1.3
30/12/95 00:46	9.4	9.9	8.2	7.3	7.8	8.6	8.9	9.5	10.7	11.0	11.7	9.0	-2.8	17.8	-0.4	1.8
30/12/95 01:17	9.4	9.7	8.1	7.3	7.7	8.4	8.7	9.4	10.6	10.9	11.5	8.9	-2.8	17.6	-0.5	1.2
30/12/95 01:48	9.3	9.4	7.9	7.2	7.7	8.4	8.7	9.2	10.4	10.8	11.3	8.7	-3.3	18.0	-0.5	1.8
30/12/95 02:19	9.3	9.7	8.1	7.1	7.6	8.4	8.8	9.4	10.5	10.8	11.4	8.9	-3.1	17.7	-0.6	1.4
30/12/95 02:51	9.2	9.5	7.9	7.0	7.5	8.3	8.6	9.2	10.3	10.7	11.2	8.7	-2.9	17.4	-0.3	1.5
30/12/95 03:22	9.5	9.8	8.2	7.1	7.6	8.4	8.7	9.3	10.5	10.9	11.3	8.7	-2.9	17.7	-0.2	1.3
30/12/95 03:53	9.8	9.9	8.2	7.2	7.6	8.4	8.7	9.3	10.5	10.7	11.2	8.6	-2.7	17.3	0.0	1.2
30/12/95 04:25	9.8	9.7	8.1	7.2	7.7	8.4	8.8	9.3	10.5	10.7	11.2	8.7	-2.5	17.7	0.1	1.4
30/12/95 04:56	9.8	9.9	8.3	7.4	7.8	8.6	8.8	9.3	10.6	10.9	11.4	8.7	-1.7	17.4	0.3	1.6
30/12/95 05:27	9.6	9.8	8.3	7.4	7.8	8.5	8.8	9.3	10.4	10.8	11.2	8.8	-1.7	17.2	0.5	1.8
30/12/95 05:59	9.8	9.6	8.4	7.7	8.0	8.6	8.9	9.5	10.7	11.0	11.4	8.8	-1.1	17.5	0.5	1.7
30/12/95 18:30	10.5	10.4	9.5	9.1	9.3	9.7	10.0	10.5	11.8	11.8	12.1	9.6	1.5	17.7	2.7	3.4
30/12/95 19:01	10.2	10.1	9.4	9.1	9.3	9.8	10.1	10.4	11.7	11.9	12.2	9.7	1.5	18.1	2.7	3.4
30/12/95 19:33	10.3	10.2	9.5	9.2	9.6	9.9	10.2	10.6	11.8	11.9	12.1	9.7	1.7	17.8	2.8	3.4
30/12/95 20:04	10.4	10.4	9.6	9.0	9.3	9.8	10.1	10.4	11.7	11.9	12.2	9.7	1.6	17.7	2.9	3.6
30/12/95 20:35	10.7	10.4	9.5	9.2	9.5	9.9	10.2	10.6	11.7	11.8	12.2	9.7	1.5	18.1	3.0	3.7
30/12/95 21:07	11.2	10.6	9.6	9.2	9.3	10.0	10.1	10.6	11.7	11.8	12.1	9.8	1.7	17.6	2.9	3.5
30/12/95 21:38	11.0	10.5	9.6	9.1	9.4	9.9	10.0	10.5	11.6	11.8	12.1	9.7	1.7	18.0	3.0	3.5
30/12/95 22:09	10.9	10.5	9.5	9.1	9.3	9.9	10.1	10.5	11.8	11.8	12.1	9.8	1.9	17.7	3.0	3.5
30/12/95 22:40	10.7	10.2	9.4	8.9	9.2	9.7	9.9	10.4	11.7	11.7	12.0	9.6	1.7	17.4	2.8	3.4
30/12/95 23:12	10.5	10.3	9.5	9.1	9.4	9.9	10.1	10.4	11.6	11.8	12.1	9.6	1.9	17.4	2.9	3.5
30/12/95 23:43	10.5	10.1	9.4	9.2	9.5	9.9	10.1	10.5	11.7	11.7	12.0	9.6	2.2	17.3	3.1	3.6
31/12/95 00:14	10.6	10.4	9.5	9.0	9.3	9.8	10.0	10.4	11.6	11.7	12.0	9.6	2.1	17.3	3.0	3.6
31/12/95 00:46	10.6	10.3	9.5	9.3	9.6	10.0	10.2	10.6	11.8	11.9	12.2	9.7	1.9	17.8	3.1	3.7
31/12/95 01:17	10.5	10.4	9.5	9.1	9.2	9.9	10.0	10.5	11.7	11.8	12.0	9.7	2.1	17.5	3.2	3.9
31/12/95 01:48	10.6	10.4	9.5	9.1	9.4	9.9	10.2	10.5	11.8	11.8	12.2	9.7	2.0	17.9	3.1	3.7
31/12/95 02:20	10.8	10.5	9.6	9.0	9.3	9.8	10.0	10.6	11.7	11.8	12.1	9.7	1.9	17.6	3.2	3.8
31/12/95 02:51	10.8	10.5	9.6	9.1	9.3	9.8	10.1	10.5	11.7	11.7	12.0	9.7	2.0	17.5	3.5	3.9
31/12/95 03:22	10.8	10.5	9.7	9.3	9.6	10.0	10.2	10.7	11.9	11.9	12.3	9.8	2.3	17.8	3.3	3.9
31/12/95 03:54	11.1	10.6	9.6	9.3	9.5	10.0	10.2	10.7	11.8	11.9	12.1	9.8	2.1	17.7	3.6	4.0
31/12/95 04:25	10.7	10.3	9.6	9.4	9.6	10.0	10.1	10.5	11.8	11.9	12.2	9.9	2.2	17.9	3.4	3.9
31/12/95 04:56	11.0	10.6	9.6	9.3	9.6	10.0	10.2	10.5	11.8	11.9	12.2	9.8	2.2	17.6	3.6	3.9

Table A8 Experimental data for 4-air20-4 without baffle

Date and Time	T1	T2	T3	T4	T5	T6	T7	T8	T9	T10	T11	T12	To	Tl	Tb	Tt
21/12/95 18:01	9.3	9.2	8.8	9.1	9.4	10.1	10.2	10.5	11.8	12.1	12.4	10.0	-0.2	18.7	1.7	2.6
21/12/95 18:33	9.0	9.0	8.7	8.9	9.2	9.7	9.9	10.3	11.7	11.8	12.2	9.9	-0.3	18.2	1.4	2.4
21/12/95 19:04	9.0	8.7	8.4	8.8	9.1	9.6	9.8	10.1	11.5	11.7	12.1	9.8	-0.2	18.4	1.5	2.5
21/12/95 19:35	9.0	8.9	8.6	8.8	9.1	9.8	10.0	10.2	11.5	11.6	12.0	9.6	-0.4	18.3	1.4	2.5
21/12/95 20:07	8.9	8.8	8.3	8.4	8.8	9.5	9.6	9.9	11.2	11.5	11.8	9.6	-0.5	18.2	1.2	2.1
21/12/95 20:38	9.1	9.1	8.4	8.5	8.9	9.6	9.8	10.0	11.5	11.5	12.0	9.6	-0.2	18.5	1.6	2.8
21/12/95 21:09	9.3	9.3	8.7	8.6	9.1	9.8	9.9	10.2	11.5	11.7	12.0	9.7	-0.1	18.2	1.7	3.2
21/12/95 21:40	9.2	9.1	8.4	8.7	9.1	9.7	9.8	10.1	11.6	11.7	12.1	9.8	0.1	18.3	1.7	2.9
21/12/95 22:12	9.3	9.3	8.7	8.8	9.1	9.9	10.0	10.2	11.6	11.8	12.1	9.9	-0.2	18.4	1.8	3.1
21/12/95 22:43	9.5	9.5	8.8	8.8	9.2	9.8	10.1	10.2	11.7	11.8	12.0	9.8	0.3	18.1	2.0	3.4
21/12/95 23:14	9.5	9.4	8.9	9.0	9.3	10.0	10.2	10.4	11.7	11.8	12.1	9.9	0.2	18.5	2.1	3.3
21/12/95 23:46	9.6	9.4	8.9	9.0	9.3	10.0	10.2	10.5	11.9	11.9	12.2	10.0	0.5	18.2	2.2	3.6
22/12/95 00:17	9.6	9.5	8.9	9.0	9.4	10.1	10.2	10.4	11.7	11.7	12.0	9.9	0.6	18.3	2.3	3.5
22/12/95 00:48	10.0	9.9	9.0	8.9	9.5	10.2	10.3	10.6	11.8	12.1	12.3	10.1	0.6	18.3	2.6	3.9
22/12/95 01:20	10.0	10.1	9.2	9.0	9.5	10.2	10.4	10.6	11.9	12.0	12.3	10.2	0.5	18.2	2.8	4.0
22/12/95 01:51	10.1	10.2	9.3	9.1	9.6	10.3	10.5	10.6	12.1	12.2	12.5	10.4	0.3	18.6	2.9	4.2
22/12/95 02:22	10.2	10.1	9.2	9.2	9.7	10.4	10.4	10.7	12.1	12.2	12.4	10.5	0.2	18.2	2.9	4.1
22/12/95 02:54	10.0	9.9	9.2	9.2	9.5	10.2	10.4	10.6	11.9	12.0	12.4	10.3	0.5	18.5	2.8	3.9
22/12/95 03:25	10.1	10.0	9.3	9.3	9.6	10.4	10.5	10.8	12.2	12.2	12.5	10.4	0.9	18.5	3.1	4.3
22/12/95 03:56	10.0	10.0	9.2	9.1	9.5	10.2	10.4	10.6	12.1	12.2	12.4	10.4	1.0	18.2	3.0	4.1
22/12/95 04:27	10.3	10.2	9.4	9.4	9.9	10.6	10.7	10.9	12.4	12.5	12.7	10.6	1.3	18.9	3.6	4.9
22/12/95 04:59	10.5	10.5	9.7	9.5	10.0	10.7	10.8	11.1	12.4	12.6	12.7	10.7	1.4	18.6	3.7	4.7
22/12/95 05:30	10.5	10.5	9.8	9.6	10.0	10.6	10.8	11.0	12.3	12.4	12.6	10.7	1.2	18.4	3.5	4.6
22/12/95 18:01	10.1	10.0	9.8	10.1	10.3	10.7	10.9	11.1	12.5	12.6	13.0	10.8	2.8	18.5	3.4	4.3
22/12/95 18:33	10.1	9.9	9.5	9.9	10.2	10.7	10.8	11.1	12.4	12.4	12.8	10.6	2.3	18.3	3.3	4.1
22/12/95 19:04	9.8	9.7	9.5	9.9	10.2	10.8	10.8	11.0	12.3	12.4	12.7	10.5	1.8	18.6	3.0	3.8
22/12/95 19:35	10.1	9.9	9.5	9.8	10.1	10.8	10.9	11.2	12.4	12.5	12.8	10.7	2.2	18.4	3.2	3.9
22/12/95 20:07	9.6	9.6	9.3	9.6	9.9	10.5	10.6	10.8	12.2	12.3	12.6	10.5	2.2	18.8	2.7	3.6
22/12/95 20:38	9.5	9.6	9.3	9.6	9.9	10.3	10.5	10.8	12.2	12.3	12.6	10.4	2.1	18.4	2.8	3.7
22/12/95 21:09	9.4	9.5	9.2	9.6	9.9	10.4	10.5	10.7	12.2	12.2	12.5	10.4	2.0	18.1	2.9	3.7
22/12/95 21:41	9.8	9.7	9.3	9.6	9.9	10.5	10.7	10.9	12.3	12.4	12.6	10.5	1.8	18.6	2.9	3.9
22/12/95 22:12	9.6	9.4	9.3	9.6	10.0	10.5	10.6	10.8	12.1	12.2	12.5	10.5	1.9	18.2	2.8	3.7
22/12/95 22:43	9.2	9.3	9.1	9.7	10.0	10.2	10.3	10.5	12.0	12.1	12.5	10.3	1.7	18.3	2.4	3.1
22/12/95 23:15	8.9	9.2	9.2	9.5	9.8	10.0	10.2	10.4	11.9	12.0	12.4	10.2	1.8	18.1	2.3	3.1
22/12/95 23:46	9.0	9.2	9.0	9.3	9.5	10.0	10.1	10.3	11.7	11.9	12.2	10.0	1.2	17.8	2.3	3.1
23/12/95 00:17	9.2	9.1	8.9	9.3	9.6	10.0	10.2	10.5	11.9	12.0	12.3	10.1	1.6	18.2	2.3	3.3
23/12/95 00:48	8.9	8.9	8.8	9.1	9.5	9.9	10.1	10.4	11.6	11.8	12.1	10.0	1.5	17.9	2.2	2.9
23/12/95 01:20	8.8	8.7	8.5	9.0	9.3	9.8	10.1	10.2	11.4	11.6	12.0	9.7	1.1	18.4	2.0	2.6
23/12/95 01:51	8.4	8.6	8.6	9.1	9.3	9.6	9.8	10.1	11.6	11.7	12.0	9.8	1.1	17.7	1.9	2.5
23/12/95 02:22	8.7	8.8	8.7	9.0	9.3	9.8	9.9	10.0	11.6	11.6	12.0	9.8	1.3	17.7	1.8	2.4
23/12/95 02:54	8.9	9.0	8.7	9.0	9.4	9.8	10.0	10.3	11.6	11.7	12.0	9.7	1.0	17.9	2.0	2.9
23/12/95 03:25	9.0	9.0	8.7	9.0	9.4	9.8	10.0	10.3	11.5	11.8	12.0	9.8	1.5	18.1	2.3	2.9
23/12/95 03:56	8.7	8.8	8.6	9.0	9.4	10.0	10.1	10.3	11.5	11.7	11.9	9.8	0.7	17.8	1.5	2.3
23/12/95 04:28	8.6	8.4	8.3	8.9	9.3	9.6	9.7	10.0	11.4	11.6	11.8	9.6	1.4	18.0	1.8	2.6
23/12/95 04:59	8.8	8.8	8.6	8.9	9.2	9.7	9.8	10.0	11.5	11.5	11.8	9.6	0.9	17.5	2.0	2.8

APPENDIX B

Experimental Data for an Edinburgh Residence (In-situ Measurements)

Appendix B An abstract from the experimental data for an Edinburgh residence

Date	Time	T_{i1}	T_{i2}	T_{i3}	T_{i4}	T_{o1}	T_{o2}	T_{o3}	T_{o4}	V_w, m/s	ϕ, %
27/11/96	18:23:12	17.2	16.0	17.0	17.1	0.8	-0.9	-0.9	-1.1	1.0	58.8
27/11/96	19:23:12	17.8	16.4	17.3	17.3	1.1	-0.7	-0.5	-0.9	1.1	61.2
27/11/96	20:23:12	19.0	17.3	18.6	18.6	0.9	-1.2	-1.1	-1.4	1.2	60.6
27/11/96	21:23:12	19.3	17.9	19.0	19.0	0.8	-1.3	-1.3	-1.5	1.0	60.3
27/11/96	22:23:12	19.7	18.5	19.6	19.6	0.7	-1.2	-1.2	-1.4	0.8	60.6
27/11/96	23:23:12	18.4	18.0	18.4	18.4	1.4	-0.6	-0.6	-0.7	0.7	61.7
28/11/96	00:23:12	17.1	17.2	17.2	17.2	2.0	-0.3	-0.3	-0.6	0.4	64.2
28/11/96	01:23:12	15.9	16.2	16.0	15.9	2.1	-0.2	-0.1	-0.4	0.7	66.4
28/11/96	02:23:12	14.9	15.3	15.0	15.0	1.6	-0.6	-0.6	-0.9	0.6	68.3
28/11/96	03:23:12	14.1	14.6	14.3	14.2	1.3	-0.5	-0.4	-0.7	0.7	68.8
28/11/96	04:23:12	13.3	13.8	13.4	13.4	1.8	0.0	0.1	-0.2	0.8	69.4
28/11/96	05:23:12	12.7	13.1	12.8	12.8	2.2	0.6	0.7	0.4	0.3	69.7
28/11/96	06:23:12	12.1	12.5	12.2	12.3	2.3	0.8	1.0	0.6	0.1	70.5
28/11/96	18:23:12	16.9	14.6	16.6	16.8	4.7	4.2	4.1	4.2	3.0	60.3
28/11/96	19:23:12	18.0	15.8	17.7	17.9	5.2	4.9	4.9	4.9	3.3	58.6
28/11/96	20:23:12	19.3	17.1	19.2	19.3	5.4	4.5	4.5	4.5	4.0	57.7
28/11/96	21:23:12	18.7	17.5	18.4	18.3	4.9	3.8	3.8	3.7	4.4	58.8
28/11/96	22:23:12	17.6	17.0	17.3	17.3	4.4	3.5	3.6	3.6	5.0	60.8
28/11/96	23:23:12	16.1	16.2	16.1	16.1	4.8	4.0	4.1	3.9	4.4	62.0
29/11/96	00:23:12	14.9	15.2	15.0	15.0	5.1	4.5	4.6	4.2	2.2	64.5
29/11/96	01:23:12	14.2	14.5	14.3	14.2	4.4	4.0	3.9	3.9	2.0	66.4
29/11/96	02:23:12	13.7	14.0	13.8	13.8	4.0	3.5	3.5	3.3	1.7	67.4
29/11/96	03:23:12	13.1	13.4	13.2	13.2	3.5	2.8	2.9	2.6	1.9	68.3
29/11/96	04:23:12	12.7	13.0	12.8	12.8	3.2	2.8	2.8	2.8	2.0	68.7
29/11/96	05:23:12	12.3	12.5	12.4	12.4	3.3	2.7	2.7	2.8	2.3	69.4
29/11/96	06:23:12	11.8	12.1	12.0	12.0	3.2	2.8	2.8	2.9	2.3	69.9
29/11/96	18:23:12	16.1	13.8	16.0	16.0	3.4	3.0	3.0	3.4	2.7	63.4
29/11/96	19:23:12	16.9	15.2	16.9	17.0	3.8	3.4	3.3	3.6	2.5	61.2
29/11/96	20:23:12	18.7	16.6	18.6	18.6	3.6	3.2	3.2	3.4	2.5	61.1
29/11/96	21:23:12	17.7	16.7	17.4	17.5	3.9	3.4	3.4	3.6	2.8	62.0
29/11/96	22:23:12	16.7	16.2	16.5	16.5	4.0	3.4	3.5	3.6	2.7	63.8
29/11/96	23:23:12	16.2	15.9	16.1	16.1	4.3	3.8	3.7	4.1	2.8	65.5
30/11/96	00:23:12	15.4	15.4	15.4	15.3	4.6	4.2	4.1	4.5	2.7	66.6
30/11/96	01:23:12	14.3	14.7	14.5	14.5	5.0	4.6	4.6	4.9	2.3	68.4
30/11/96	02:23:12	13.7	14.0	13.7	13.7	5.0	4.8	4.6	5.2	2.5	69.5
30/11/96	03:23:12	13.2	13.5	13.2	13.3	4.9	4.6	4.5	5.0	2.5	70.4
30/11/96	04:23:12	12.7	13.0	12.8	12.8	4.5	4.4	4.3	4.7	2.1	71.2
30/11/96	05:23:12	12.3	12.6	12.4	12.5	4.6	4.5	4.4	4.7	1.4	72.0
30/11/96	06:23:12	11.9	12.3	12.1	12.1	5.0	5.0	4.8	5.3	1.2	72.3
30/11/96	18:23:12	20.0	19.1	19.8	19.8	4.6	3.3	3.8	2.7	1.0	66.3
30/11/96	19:23:12	19.1	18.8	19.1	19.1	4.6	3.1	3.6	2.6	1.1	64.9
30/11/96	20:23:12	19.1	18.5	18.7	18.6	4.7	3.7	4.1	3.4	0.9	66.1
30/11/96	21:23:12	18.8	18.5	18.7	18.6	5.1	4.0	4.3	3.7	1.1	66.6
30/11/96	22:23:12	18.3	18.1	18.2	18.2	5.7	4.9	5.0	4.9	1.6	67.1
30/11/96	23:23:12	18.0	17.9	18.0	18.0	6.0	5.2	5.4	5.0	2.0	66.3
01/12/96	00:23:12	17.6	17.7	17.7	17.6	6.4	5.7	5.8	5.5	1.6	67.9
01/12/96	01:23:12	17.0	17.3	17.1	17.1	6.9	6.2	6.4	6.2	2.0	69.4
01/12/96	02:23:12	15.9	16.4	16.0	16.0	7.0	6.4	6.6	6.3	2.4	71.1
01/12/96	03:23:12	15.2	15.7	15.4	15.4	7.4	6.9	7.0	6.9	3.4	72.2
01/12/96	04:23:12	14.8	15.2	14.9	14.9	7.8	7.4	7.5	7.4	3.3	72.8
01/12/96	05:23:12	14.4	14.7	14.5	14.4	8.2	8.0	8.1	7.8	3.7	73.0
01/12/96	06:23:12	14.1	14.4	14.2	14.2	8.3	8.0	8.4	8.2	2.8	72.6
01/12/96	18:23:12	20.0	18.3	19.8	19.9	5.5	5.2	5.4	3.9	2.3	65.3
01/12/96	19:23:12	20.4	19.0	20.3	20.3	5.3	4.9	5.2	4.0	2.8	63.2
01/12/96	20:23:12	20.4	19.3	20.1	20.1	4.8	4.1	4.6	3.4	2.9	63.2
01/12/96	21:23:12	19.9	19.2	19.6	19.6	4.6	4.1	4.5	3.5	3.1	64.9
01/12/96	22:23:12	19.1	18.8	19.0	18.9	4.3	3.6	3.9	2.9	3.1	66.8
01/12/96	23:23:12	17.8	18.1	18.1	18.0	4.3	3.7	3.9	3.4	3.5	67.7
02/12/96	00:23:12	17.0	17.4	17.4	17.4	4.6	4.0	4.3	3.8	2.5	69.7
02/12/96	01:23:12	16.3	16.7	16.4	16.3	5.0	4.6	4.7	4.2	2.9	70.8
02/12/96	02:23:12	15.8	16.1	15.9	15.9	4.8	4.3	4.5	4.1	3.0	71.8
02/12/96	03:23:12	15.2	15.5	15.3	15.3	4.7	4.4	4.4	4.2	3.2	72.0
02/12/96	04:23:12	14.8	15.1	14.9	14.9	5.1	4.8	4.8	4.7	2.9	72.7
02/12/96	05:23:12	14.4	14.7	14.5	14.6	5.2	4.9	5.0	4.9	2.7	72.8
02/12/96	06:23:12	14.0	14.2	14.1	14.1	5.2	4.9	5.0	4.8	3.0	73.0
03/12/96	00:30:01	16.3	16.6	16.6	16.5	2.8	2.0	2.8	2.9	0.0	65.2
03/12/96	01:30:01	16.0	16.4	15.8	15.8	2.7	1.8	2.6	2.7	0.0	66.9
03/12/96	02:30:01	15.4	15.5	15.1	15.1	2.9	2.3	2.9	3.0	0.0	67.6
03/12/96	03:30:01	15.0	14.9	14.5	14.3	3.2	2.8	3.1	3.2	0.0	68.2
03/12/96	04:30:01	14.2	14.3	14.0	13.9	3.3	2.8	3.1	3.1	0.0	68.5

Appendix B (cont'd) An abstract from the experimental data for an Edinburgh residence

Date	Time	T_{i1}	T_{i2}	T_{i3}	T_{i4}	T_{o1}	T_{o2}	T_{o3}	T_{o4}	V_w, m/s	ϕ, %
03/12/96	05:30:01	13.9	13.9	13.5	13.5	3.3	2.9	3.2	3.2	0.0	69.3
03/12/96	06:30:01	13.7	13.6	13.2	13.2	3.4	3.0	3.2	3.2	0.0	69.8
03/12/96	18:30:01	15.5	15.9	17.6	17.6	1.1	0.9	0.8	0.8	0.0	72.8
03/12/96	19:30:01	15.9	16.4	18.8	19.0	0.9	0.9	0.7	0.6	0.0	71.0
03/12/96	20:30:01	16.3	16.9	19.3	19.5	0.7	0.5	0.4	0.3	0.0	68.4
03/12/96	21:30:01	15.8	16.2	17.7	17.4	0.8	0.6	0.5	0.5	0.0	68.0
03/12/96	22:30:01	15.7	15.9	16.5	16.5	1.1	0.8	0.8	0.8	0.0	68.2
03/12/96	23:30:01	14.6	14.9	15.1	14.9	1.2	0.3	0.9	0.8	0.0	70.4
04/12/96	00:30:01	14.0	14.2	14.1	14.0	1.4	0.1	1.1	0.9	0.0	72.0
04/12/96	01:30:01	13.5	13.8	13.5	13.3	1.1	0.2	1.3	1.2	0.0	72.7
04/12/96	02:30:01	12.9	13.2	12.8	12.8	0.9	0.1	1.6	1.7	0.0	73.4
04/12/96	03:30:01	12.4	12.7	12.4	12.4	1.3	0.1	2.2	2.2	0.0	73.4
04/12/96	04:30:01	12.3	12.2	11.9	11.9	1.5	0.2	2.2	2.2	0.0	74.1
04/12/96	05:30:01	11.9	11.9	11.6	11.5	1.7	0.2	2.4	2.4	0.0	74.0
04/12/96	06:30:01	11.6	11.6	11.2	11.2	2.0	0.1	3.0	3.0	0.0	74.1
04/12/96	18:30:01	14.8	15.1	16.9	17.2	3.9	4.3	4.5	4.4	0.0	64.5
04/12/96	19:30:01	16.2	16.4	18.4	18.7	3.8	4.2	4.3	4.3	0.0	64.1
04/12/96	20:30:01	17.5	18.0	20.0	20.3	3.9	4.3	4.5	4.4	0.0	62.2
04/12/96	21:30:01	17.0	17.4	18.2	18.1	3.9	4.2	4.3	4.2	0.0	64.3
04/12/96	22:30:01	16.2	16.4	16.9	16.9	3.9	4.1	4.1	4.0	0.0	66.5
04/12/96	23:30:01	15.1	15.4	15.4	15.4	3.4	3.2	3.2	3.3	0.0	69.1
05/12/96	00:30:01	14.1	14.4	14.3	14.2	2.6	2.4	2.3	2.3	0.0	70.5
05/12/96	01:30:01	13.6	13.9	13.6	13.6	2.2	2.1	2.1	2.2	0.0	71.3
05/12/96	02:30:01	13.4	13.5	13.1	13.2	1.4	1.0	0.9	0.9	0.0	71.8
05/12/96	03:30:01	12.9	12.9	12.6	12.6	0.9	0.6	0.5	0.6	0.0	72.3
05/12/96	04:30:01	12.4	12.3	12.0	12.1	0.5	0.4	0.4	0.4	0.0	72.5
05/12/96	05:30:01	11.9	11.9	11.6	11.7	0.1	0.0	-0.1	-0.1	0.0	73.1
05/12/96	06:30:01	11.4	11.4	11.1	11.2	-0.1	-0.3	-0.3	-0.3	0.0	73.1
05/12/96	18:30:01	18.8	19.2	20.7	21.0	1.4	0.7	0.6	0.7	0.0	60.1
05/12/96	19:30:01	17.9	18.1	18.6	18.6	0.8	0.2	0.1	0.1	0.0	62.7
05/12/96	20:30:01	17.1	17.2	17.7	17.7	0.5	-0.4	-0.6	-0.5	0.0	64.3
05/12/96	21:30:01	16.7	16.9	17.5	17.5	0.0	-0.7	-0.8	-0.7	0.0	64.5
05/12/96	22:30:01	18.1	18.6	20.6	21.0	-0.3	-1.2	-1.4	-1.4	0.0	61.8
05/12/96	23:30:01	18.5	19.1	21.3	22.1	-0.4	-1.6	-1.7	-1.6	0.0	61.6
06/12/96	00:30:01	18.9	19.4	21.8	22.4	-0.7	-1.8	-2.1	-2.0	0.0	61.4
06/12/96	01:30:01	19.3	19.5	21.9	22.6	-1.4	-2.5	-2.8	-2.6	0.0	61.5
06/12/96	02:30:01	19.1	19.6	21.7	22.3	-1.7	-2.5	-2.7	-2.6	0.0	61.6
06/12/96	03:30:01	18.9	19.6	21.6	22.0	-1.9	-2.8	-3.1	-2.9	0.0	61.8
06/12/96	04:30:01	18.9	19.3	21.3	21.9	-2.1	-3.0	-3.3	-3.1	0.0	61.8
06/12/96	05:30:01	19.0	19.4	21.4	21.8	-2.1	-2.8	-3.0	-3.0	0.0	61.9
06/12/96	06:30:01	18.6	19.2	21.2	21.8	-2.3	-3.2	-3.6	-3.5	0.0	61.9
06/12/96	18:30:01	17.2	17.7	19.7	19.9	0.3	0.4	0.4	0.4	0.0	59.2
06/12/96	19:30:01	18.6	19.1	21.3	21.3	0.2	0.4	0.5	0.5	0.5	58.5
06/12/96	20:30:01	19.8	20.3	22.4	22.2	0.2	0.4	0.5	0.5	0.2	57.6
06/12/96	21:30:01	18.4	18.6	19.4	19.4	-0.1	-0.3	-0.3	-0.3	0.1	59.1
06/12/96	22:30:01	16.5	16.7	17.0	16.9	-0.2	-0.5	-0.3	-0.3	0.3	61.7
06/12/96	23:30:01	16.0	16.3	16.4	16.3	-0.1	0.1	0.1	0.1	0.1	62.5
07/12/96	00:30:01	15.5	15.9	16.1	16.1	-0.1	0.0	0.2	0.2	0.5	64.0
07/12/96	01:30:01	14.8	15.0	14.5	14.7	0.3	1.1	1.3	1.2	0.8	65.2
07/12/96	02:30:01	13.9	14.0	13.6	13.7	0.4	0.9	1.1	1.0	0.9	66.2
07/12/96	03:30:01	13.2	13.3	12.9	12.9	0.4	0.6	0.8	0.8	0.4	66.7
07/12/96	04:30:01	12.7	12.8	12.3	12.2	0.7	1.4	1.5	1.5	1.2	67.9
07/12/96	05:30:01	12.0	12.2	11.9	11.9	1.2	2.1	2.3	2.2	2.3	68.1
07/12/96	06:30:01	11.7	11.9	11.5	11.6	1.9	2.6	2.8	2.7	2.2	68.4
07/12/96	18:30:01	17.7	17.8	18.3	18.2	5.6	5.2	5.1	5.2	3.2	62.5
07/12/96	19:30:01	17.8	18.1	19.6	19.6	5.6	5.4	5.3	5.3	2.9	62.5
07/12/96	20:30:01	19.3	19.7	21.8	21.4	5.8	5.8	5.7	5.7	2.9	65.3
07/12/96	21:30:01	20.3	20.6	22.4	22.6	6.1	6.0	6.1	6.1	3.5	62.8
07/12/96	22:30:01	19.6	19.7	20.6	20.4	6.6	6.5	6.6	6.5	3.6	62.9
07/12/96	23:30:01	18.8	18.9	19.5	19.4	6.9	6.6	6.6	6.6	2.8	64.5
08/12/96	00:30:01	17.7	18.1	18.2	18.2	7.2	6.8	6.8	6.9	2.7	65.5
08/12/96	01:30:01	16.7	17.2	17.0	16.9	7.4	6.9	6.9	7.0	2.8	67.3
08/12/96	02:30:01	16.4	16.5	16.2	16.2	7.5	7.1	7.0	7.1	2.8	68.1
08/12/96	03:30:01	15.8	16.0	15.7	15.7	7.7	7.2	7.2	7.3	2.7	68.8
08/12/96	04:30:01	15.5	15.5	15.3	15.2	7.7	7.2	7.2	7.2	2.5	69.4
08/12/96	05:30:01	15.1	15.1	15.0	15.0	8.0	7.8	7.9	7.9	2.7	69.5
08/12/96	06:30:01	14.7	14.8	14.6	14.6	8.2	8.0	8.1	8.1	2.4	69.8
08/12/96	18:30:01	21.2	20.8	23.3	23.3	9.0	8.1	8.0	8.0	2.3	63.0
08/12/96	19:30:01	20.9	20.6	22.3	22.4	8.8	8.0	7.8	7.8	1.9	62.5
08/12/96	20:30:01	20.1	20.0	20.8	20.8	8.8	7.8	7.6	7.6	1.8	64.8

Appendix B (cont'd) An abstract from the experimental data for an Edinburgh residence

Date	Time	T_{I1}	T_{I2}	T_{I3}	T_{I4}	T_{o1}	T_{o2}	T_{o3}	T_{o4}	V_w m/s	ϕ, %
08/12/96	21:30:01	20.4	20.3	21.9	21.9	8.6	7.7	7.7	7.7	2.2	64.6
08/12/96	22:30:01	20.7	20.3	21.8	21.9	8.3	7.4	7.4	7.4	2.5	62.9
08/12/96	23:30:01	20.4	20.2	21.4	21.5	8.1	7.1	7.3	7.3	1.7	64.3
09/12/96	00:30:01	19.4	19.6	19.9	19.9	7.9	7.3	7.2	7.3	2.0	66.7
09/12/96	01:30:01	18.9	19.0	19.0	19.0	7.9	7.2	7.2	7.2	2.2	68.3
09/12/96	02:30:01	18.6	18.5	18.3	18.4	7.7	7.1	7.0	7.1	2.2	69.4
09/12/96	03:30:01	18.1	17.9	17.8	17.7	7.9	7.5	7.5	7.5	2.0	70.1
09/12/96	04:30:01	17.8	17.5	17.2	17.2	8.0	7.5	7.3	7.4	1.3	70.3
09/12/96	05:30:01	17.1	17.1	16.9	16.9	8.1	7.5	7.3	7.4	1.8	71.2
09/12/96	06:30:01	16.7	16.7	16.5	16.5	8.1	7.5	7.3	7.3	2.0	71.5
09/12/96	18:30:01	18.5	17.8	20.6	21.1	9.2	8.4	8.0	8.0	0.0	61.9
09/12/96	19:30:01	19.5	18.6	21.8	22.1	9.1	8.4	7.9	7.9	0.0	62.7
09/12/96	20:30:01	20.9	19.8	23.1	23.5	9.2	8.5	8.0	8.0	0.0	62.2
09/12/96	21:30:01	21.3	20.4	23.4	24.1	9.2	8.7	8.1	8.2	0.1	63.3
09/12/96	22:30:01	22.5	21.5	25.3	26.1	8.9	7.8	7.7	7.7	0.5	61.4
09/12/96	23:30:01	22.2	21.7	23.9	24.6	8.8	7.8	7.3	7.5	0.2	60.2
10/12/96	00:30:01	20.8	21.0	21.4	21.5	9.0	7.7	7.3	7.4	0.2	64.8
10/12/96	01:30:01	19.8	20.1	20.2	20.3	9.1	8.2	7.4	7.5	0.0	66.8
10/12/96	02:30:01	19.2	19.5	19.4	19.4	9.2	8.1	7.1	7.2	0.0	68.5
10/12/96	03:30:01	18.7	18.9	18.7	18.6	9.1	8.0	6.9	7.1	0.0	69.6
10/12/96	04:30:01	18.2	18.4	18.1	18.1	8.7	7.1	6.6	6.7	0.2	70.5
10/12/96	05:30:01	17.7	17.8	17.7	17.5	8.6	7.4	6.7	6.8	0.1	70.8
10/12/96	06:30:01	17.3	17.4	17.3	17.2	8.6	7.3	6.7	6.8	0.1	71.3
10/12/96	18:30:01	19.8	18.7	22.0	22.7	6.1	5.2	4.8	4.8	1.0	60.6
10/12/96	19:30:01	20.3	19.3	22.1	22.5	6.0	5.1	4.7	4.7	0.6	61.6
10/12/96	20:30:01	20.5	19.9	22.5	22.7	6.1	5.3	4.9	5.0	0.9	62.2
10/12/96	21:30:01	20.2	19.9	21.1	21.1	6.0	5.1	4.6	4.7	1.0	63.6
10/12/96	22:30:01	19.7	19.6	20.2	20.2	5.7	4.8	4.4	4.4	1.1	65.2
10/12/96	23:30:01	18.6	18.8	18.7	18.6	5.7	4.8	4.4	4.4	0.4	67.6
11/12/96	00:30:01	18.0	18.0	17.7	17.7	5.8	5.0	4.5	4.6	0.2	68.9
11/12/96	01:30:01	17.6	17.4	17.2	17.1	6.0	5.1	4.6	4.7	0.2	70.0
11/12/96	02:30:01	16.5	16.8	16.5	16.4	6.2	5.3	4.6	4.7	0.0	71.8
11/12/96	03:30:01	16.5	16.3	16.0	15.9	6.2	5.2	4.7	4.8	0.0	72.1
11/12/96	04:30:01	15.9	15.8	15.6	15.5	6.2	5.3	4.7	4.8	0.0	72.0
11/12/96	05:30:01	15.3	15.4	15.1	15.0	6.2	5.2	4.7	4.8	0.2	72.6
11/12/96	06:30:01	15.1	14.9	14.7	14.7	5.9	5.0	4.7	4.7	0.1	73.0
13/12/96	00:00:01	15.0	15.2	15.1	15.0	2.3	1.4	1.2	1.2	0.8	70.5
13/12/96	01:00:01	14.4	14.7	14.3	14.3	1.7	1.2	0.9	0.9	0.5	71.8
13/12/96	02:00:01	14.0	14.0	13.7	13.5	1.3	0.9	0.7	0.7	0.2	72.6
13/12/96	03:00:01	13.4	13.5	13.1	13.1	0.9	0.4	0.1	0.1	0.2	73.0
13/12/96	04:00:01	13.0	13.1	12.6	12.6	0.5	0.2	0.0	0.0	0.6	73.5
13/12/96	05:00:01	13.2	13.5	14.4	14.5	0.1	-0.2	-0.4	-0.4	0.2	71.5
13/12/96	06:00:01	15.1	15.6	17.8	18.0	-0.4	-0.9	-1.5	-1.5	0.1	67.4
13/12/96	18:00:01	16.6	17.3	19.1	19.4	-0.3	-0.5	-0.7	-0.7	1.8	60.5
13/12/96	19:00:01	17.2	18.1	19.6	19.9	-0.5	-0.7	-0.7	-0.7	1.9	61.1
13/12/96	20:00:01	17.6	18.4	20.1	20.2	-0.5	-0.7	-0.7	-0.6	2.0	61.1
13/12/96	21:00:01	17.2	17.6	18.6	18.7	-0.1	-0.1	0.0	0.0	2.4	64.9
13/12/96	22:00:01	15.6	16.0	16.2	16.3	0.5	0.7	0.7	0.7	2.6	68.6
13/12/96	23:00:01	15.6	15.9	16.2	16.1	1.1	1.0	1.0	1.1	2.7	68.3
14/12/96	00:00:01	15.2	15.5	15.8	15.8	1.6	1.3	1.3	1.3	3.1	69.1
14/12/96	01:00:01	14.2	14.6	14.5	14.5	1.9	1.3	1.3	1.4	3.1	69.4
14/12/96	02:00:01	13.5	13.7	13.4	13.4	2.1	1.5	1.6	1.6	3.1	70.5
14/12/96	03:00:01	12.6	12.8	12.6	12.6	2.3	1.9	1.8	1.9	3.1	70.8
14/12/96	04:00:01	12.0	12.4	12.1	12.1	2.6	2.6	2.6	2.6	3.1	71.5
14/12/96	05:00:01	11.8	11.9	11.7	11.6	3.1	3.3	3.3	3.3	3.0	72.4
14/12/96	06:00:01	12.0	12.3	12.9	12.8	3.4	3.7	3.7	3.7	2.4	72.7
14/12/96	18:00:01	18.6	19.1	19.8	19.4	7.3	6.9	6.9	7.0	0.0	66.6
14/12/96	19:00:01	18.8	19.1	20.0	19.6	7.4	7.2	7.2	7.2	0.0	64.5
14/12/96	20:00:01	18.7	19.0	19.9	19.5	7.6	7.3	7.4	7.4	0.0	63.8
14/12/96	21:00:01	19.2	19.5	20.4	20.0	7.7	7.4	7.4	7.4	0.0	65.1
14/12/96	22:00:01	19.3	19.6	20.3	20.0	7.7	7.3	7.3	7.4	0.0	65.3
14/12/96	23:00:01	19.2	19.6	20.1	19.9	7.6	7.0	7.1	7.1	0.0	65.2
15/12/96	00:00:01	18.7	19.0	19.5	19.3	7.6	7.0	7.0	7.0	0.0	66.9
15/12/96	01:00:01	18.1	18.3	18.2	18.2	7.3	6.8	6.8	6.8	0.0	69.9
15/12/96	02:00:01	16.9	17.2	17.0	16.9	6.8	6.3	6.2	6.3	0.0	72.3
15/12/96	03:00:01	16.7	16.7	16.3	16.3	6.3	5.9	5.9	5.9	0.0	73.4
15/12/96	04:00:01	16.3	16.2	15.8	15.7	5.9	5.4	5.4	5.4	0.0	73.5
15/12/96	05:00:01	15.7	15.6	15.4	15.3	6.1	5.7	5.7	5.7	0.0	74.8
15/12/96	06:00:01	15.3	15.3	15.0	15.0	5.6	5.1	5.0	5.0	0.0	75.1
15/12/96	18:00:01	20.6	21.0	22.7	23.0	6.3	5.3	5.3	5.4	0.0	67.1

Appendix B (cont'd) An abstract from the experimental data for an Edinburgh residence

Date	Time	T_{I1}	T_{I2}	T_{I3}	T_{I4}	T_{o1}	T_{o2}	T_{o3}	T_{o4}	V_w m/s	ϕ, %
15/12/96	19:00:01	20.9	21.5	22.9	23.3	6.5	6.0	6.0	6.0	0.0	66.1
15/12/96	20:00:01	20.7	21.2	22.3	22.5	6.5	5.9	5.8	5.9	0.0	65.3
15/12/96	21:00:01	20.1	20.6	21.5	21.5	6.4	5.8	5.8	5.9	0.0	66.0
15/12/96	22:00:01	19.9	20.2	20.4	20.5	6.8	6.2	6.2	6.2	0.0	67.4
15/12/96	23:00:01	19.7	19.6	19.1	19.1	7.1	6.4	6.4	6.4	0.0	70.3
16/12/96	00:00:01	18.9	18.7	18.2	18.2	7.2	6.6	6.6	6.6	0.0	72.3
16/12/96	01:00:01	17.7	17.8	17.4	17.4	7.2	6.3	6.3	6.3	0.0	73.8
16/12/96	02:00:01	17.2	17.2	17.0	16.9	6.8	6.1	6.1	6.1	0.0	74.2
16/12/96	03:00:01	16.9	16.8	16.5	16.5	6.6	5.9	5.8	5.9	0.0	74.5
16/12/96	04:00:01	16.2	16.2	15.9	15.9	6.2	5.6	5.6	5.6	0.0	74.8
16/12/96	05:00:01	16.1	15.8	15.5	15.5	5.9	5.3	5.2	5.3	0.0	75.2
16/12/96	06:00:01	15.6	15.5	15.2	15.1	6.1	5.7	5.7	5.7	0.0	75.2
16/12/96	18:00:01	17.5	18.4	20.3	20.6	7.2	6.2	6.3	6.3	0.6	64.3
16/12/96	19:00:01	18.6	19.5	21.0	21.5	6.9	6.1	6.2	6.2	1.2	64.4
16/12/96	20:00:01	19.8	20.3	21.8	22.5	7.0	6.3	6.3	6.3	1.1	65.5
16/12/96	21:00:01	20.2	20.5	21.6	21.8	7.1	6.2	6.3	6.3	1.1	65.7
16/12/96	22:00:01	19.4	19.7	20.0	20.0	6.8	6.0	6.0	6.1	0.8	66.7
16/12/96	23:00:01	18.6	19.1	19.4	19.2	7.0	5.7	5.7	5.8	0.3	68.0
17/12/96	00:00:01	18.4	18.4	18.2	18.2	6.9	5.5	5.3	5.3	0.1	70.9
17/12/96	01:00:01	17.4	17.4	17.0	17.0	6.8	5.5	5.4	5.4	0.2	71.7
17/12/96	02:00:01	16.8	16.8	16.5	16.5	6.8	5.2	5.1	5.1	0.0	73.0
17/12/96	03:00:01	16.1	16.2	16.0	16.0	6.6	5.1	5.0	5.0	0.1	73.8
17/12/96	04:00:01	15.8	15.7	15.5	15.5	6.2	4.7	4.5	4.5	0.1	74.6
17/12/96	05:00:01	15.5	15.5	15.1	15.0	5.7	4.3	4.2	4.2	0.3	75.0
17/12/96	06:00:01	15.1	15.0	14.7	14.7	5.5	4.1	3.9	3.9	0.3	75.2
17/12/96	18:00:01	17.1	17.8	19.5	20.3	3.3	2.2	2.1	2.2	0.5	64.3
17/12/96	19:00:01	18.0	18.7	20.3	20.8	3.0	1.7	1.6	1.7	0.1	64.1
17/12/96	20:00:01	19.3	20.1	21.9	22.2	2.5	1.9	1.8	1.8	0.2	62.6
17/12/96	21:00:01	19.9	20.1	21.3	21.6	2.9	2.8	2.9	2.9	0.2	64.6
17/12/96	22:00:01	18.8	19.1	19.4	19.4	3.5	3.0	3.0	3.0	0.0	66.6
17/12/96	23:00:01	18.1	18.2	18.5	18.4	4.0	3.1	3.0	3.1	0.1	70.1
18/12/96	00:00:01	17.1	17.4	17.0	16.9	4.4	3.2	3.1	3.2	0.1	72.4
18/12/96	01:00:01	16.5	16.5	16.2	16.2	4.6	2.9	2.8	2.9	0.1	73.2
18/12/96	02:00:01	16.1	16.0	15.6	15.6	4.6	2.8	2.6	2.7	0.0	74.0
18/12/96	03:00:01	15.3	15.4	15.1	15.1	4.5	2.7	2.6	2.6	0.0	74.7
18/12/96	04:00:01	15.2	15.3	14.8	14.7	4.3	2.9	2.7	2.8	0.1	75.0
18/12/96	05:00:01	15.0	14.7	14.4	14.3	4.3	3.0	2.9	2.9	0.1	75.4
18/12/96	06:00:01	14.5	14.4	13.9	13.9	4.4	3.4	3.3	3.3	0.1	75.4
18/12/96	18:00:01	16.8	17.7	20.1	20.3	6.6	6.2	6.2	6.2	1.2	66.3
18/12/96	19:00:01	18.1	18.8	20.6	20.8	6.2	5.7	5.6	5.6	1.3	64.2
18/12/96	20:00:01	19.0	19.6	21.6	21.5	5.7	4.8	4.8	4.8	1.5	64.4
18/12/96	21:00:01	19.8	20.1	21.5	21.4	5.5	4.6	4.6	4.6	1.7	64.9
18/12/96	22:00:01	18.7	19.0	19.5	19.4	5.4	4.6	4.6	4.6	1.1	66.0
18/12/96	23:00:01	17.8	18.0	18.3	18.2	5.3	4.4	4.4	4.4	1.0	68.8
19/12/96	00:00:01	16.7	17.0	16.8	16.7	5.1	4.0	3.9	3.9	1.0	71.7
19/12/96	01:00:01	16.0	16.3	16.0	15.9	4.9	3.7	3.7	3.9	0.9	73.0
19/12/96	02:00:01	15.8	15.8	15.4	15.4	4.7	3.9	3.6	4.2	0.7	73.8
19/12/96	03:00:01	15.3	15.2	14.8	14.8	4.4	3.5	3.1	3.5	1.1	73.8
19/12/96	04:00:01	14.7	14.7	14.4	14.4	4.0	2.9	2.9	2.9	1.2	74.7
19/12/96	05:00:01	14.2	14.2	13.9	13.9	3.7	2.5	2.6	2.5	1.4	75.3
19/12/96	06:00:01	13.6	13.7	13.5	13.5	3.4	2.4	2.3	2.6	1.2	75.5

APPENDIX C

Experimental Data for Two Window Samples (Two-dimensional Matrix)

Table C1 An abstract from the experimental data for the 4-air12-4 window (see Table 4.2 for design notation)
Temperatures for nodes 1-17 (see Fig. 4.4)

Date	Time	T_1	T_2	T_3	T_4	T_5	T_6	T_7	T_8	T_9	T_{10}	T_{11}	T_{12}	T_{13}	T_{14}	T_{15}	T_{16}	T_{17}
20/01/97	18:05:01	8.8	10.1	9.7	9.7	10.3	10.6	10.7	10.7	11.9	11.6	10.4	9.7	10.7	10.9	10.6	10.7	9.6
20/01/97	18:10:01	9.0	10.1	9.5	9.7	10.3	10.5	10.7	10.7	12.0	11.6	10.4	9.8	10.6	11.0	10.6	10.7	9.6
20/01/97	18:15:01	8.9	9.9	9.6	9.7	10.3	10.6	10.6	10.6	11.9	11.4	10.2	9.7	10.6	10.8	10.6	10.6	9.6
20/01/97	18:20:01	8.9	9.9	9.5	9.7	10.3	10.6	10.6	10.6	11.9	11.5	10.4	9.7	10.7	10.9	10.5	10.7	9.5
20/01/97	18:25:01	8.8	9.8	9.5	9.6	10.3	10.5	10.6	10.7	11.8	11.4	10.3	9.7	10.5	10.9	10.5	10.7	9.5
20/01/97	18:30:01	8.8	9.9	9.5	9.6	10.2	10.5	10.5	10.7	11.8	11.4	10.4	9.7	10.6	10.8	10.5	10.6	9.5
20/01/97	18:35:01	8.8	9.9	9.4	9.6	10.2	10.5	10.5	10.5	11.8	11.4	10.2	9.7	10.5	10.8	10.6	10.6	9.4
20/01/97	18:40:01	8.8	9.9	9.5	9.6	10.2	10.5	10.6	10.6	11.8	11.4	10.3	9.6	10.5	10.7	10.4	10.6	9.4
20/01/97	18:45:01	8.7	9.8	9.4	9.6	10.1	10.4	10.4	10.5	11.7	11.3	10.1	9.5	10.5	10.7	10.4	10.6	9.4
20/01/97	18:50:01	8.7	9.8	9.3	9.4	10.1	10.3	10.4	10.5	11.8	11.3	10.2	9.6	10.5	10.8	10.3	10.5	9.3
20/01/97	18:55:01	8.7	9.8	9.4	9.6	10.3	10.5	10.5	10.5	11.7	11.4	10.2	9.5	10.5	10.7	10.5	10.7	9.3
20/01/97	19:00:01	8.7	9.8	9.5	9.7	10.4	10.4	10.6	10.6	11.8	11.4	10.1	9.5	10.6	10.9	10.6	10.7	9.3
20/01/97	19:05:01	8.6	9.8	9.4	9.6	10.3	10.5	10.6	10.6	11.8	11.5	10.3	9.6	10.6	10.9	10.7	10.8	9.3
20/01/97	19:10:01	8.8	9.9	9.5	9.7	10.4	10.6	10.7	10.7	11.9	11.5	10.3	9.6	10.6	10.9	10.6	10.8	9.3
20/01/97	19:15:01	8.7	9.9	9.6	9.8	10.3	10.6	10.6	10.7	11.9	11.5	10.3	9.5	10.6	11.0	10.6	10.8	9.3
20/01/97	19:20:01	8.7	9.8	9.6	9.7	10.3	10.6	10.6	10.7	11.9	11.5	10.3	9.6	10.7	11.0	10.7	10.7	9.4
20/01/97	19:25:01	8.8	9.9	9.5	9.8	10.4	10.6	10.7	10.7	11.9	11.5	10.3	9.6	10.6	10.9	10.6	10.7	9.4
20/01/97	19:30:01	8.8	9.9	9.6	9.8	10.4	10.6	10.7	10.7	11.8	11.5	10.3	9.6	10.6	11.0	10.6	10.7	9.4
20/01/97	19:35:01	8.7	9.8	9.5	9.7	10.3	10.6	10.6	10.7	11.8	11.4	10.3	9.6	10.6	10.8	10.5	10.7	9.3
20/01/97	19:40:01	8.7	9.8	9.5	9.6	10.3	10.6	10.6	10.6	11.9	11.5	10.3	9.5	10.6	10.9	10.6	10.6	9.3
20/01/97	19:45:01	8.6	9.9	9.5	9.6	10.2	10.5	10.5	10.5	11.8	11.3	10.2	9.5	10.5	10.8	10.5	10.6	9.3
20/01/97	19:50:01	8.7	9.7	9.5	9.6	10.2	10.5	10.5	10.5	11.8	11.3	10.2	9.5	10.4	10.7	10.5	10.6	9.3
20/01/97	19:55:01	8.6	9.8	9.5	9.5	10.1	10.4	10.4	10.4	11.6	11.3	10.1	9.4	10.3	10.6	10.3	10.5	9.2
20/01/97	20:00:01	8.6	9.8	9.4	9.5	10.1	10.4	10.4	10.4	11.6	11.2	10.0	9.3	10.3	10.7	10.4	10.5	9.2
20/01/97	20:05:01	8.5	9.7	9.5	9.6	10.3	10.3	10.4	10.5	11.8	11.4	10.1	9.4	10.3	10.8	10.3	10.6	9.2
20/01/97	20:10:01	8.6	9.8	9.4	9.7	10.2	10.4	10.6	10.5	11.8	11.4	10.1	9.3	10.3	10.7	10.3	10.7	9.2
20/01/97	20:15:01	8.7	9.9	9.5	9.7	10.2	10.5	10.6	10.6	11.8	11.4	10.1	9.4	10.4	10.8	10.5	10.6	9.2
20/01/97	20:20:01	8.7	9.8	9.5	9.7	10.2	10.5	10.5	10.6	12.0	11.4	10.2	9.3	10.5	10.7	10.5	10.7	9.2
20/01/97	20:25:01	8.6	9.8	9.5	9.7	10.2	10.5	10.5	10.6	11.9	11.3	10.0	9.4	10.4	10.9	10.5	10.7	9.2
20/01/97	20:30:01	8.6	9.8	9.5	9.7	10.3	10.5	10.5	10.5	11.8	11.4	10.1	9.4	10.4	10.7	10.5	10.7	9.1
20/01/97	20:35:01	8.6	9.7	9.5	9.6	10.1	10.4	10.5	10.5	11.7	11.3	10.0	9.3	10.4	10.7	10.4	10.6	9.1
20/01/97	20:40:01	8.5	9.8	9.4	9.6	10.1	10.5	10.6	10.5	11.7	11.3	10.1	9.4	10.4	10.8	10.4	10.6	9.1
20/01/97	20:45:01	8.4	9.7	9.4	9.5	10.2	10.5	10.5	10.4	11.6	11.2	10.0	9.3	10.4	10.7	10.4	10.5	9.1
20/01/97	20:50:01	8.4	9.6	9.3	9.5	10.2	10.3	10.4	10.3	11.6	11.2	10.0	9.3	10.4	10.7	10.3	10.5	9.1
20/01/97	20:55:01	8.5	9.6	9.3	9.6	10.1	10.3	10.5	10.3	11.6	11.2	10.0	9.3	10.4	10.7	10.3	10.4	9.1
20/01/97	21:00:01	8.6	9.7	9.3	9.6	10.1	10.4	10.5	10.3	11.7	11.2	10.0	9.3	10.3	10.7	10.3	10.5	9.0
20/01/97	21:05:01	8.5	9.5	9.2	9.5	10.1	10.4	10.4	10.4	11.7	11.2	10.0	9.3	10.3	10.7	10.3	10.5	9.1
20/01/97	21:10:01	8.5	9.5	9.1	9.5	10.0	10.2	10.3	10.3	11.7	11.3	10.0	9.3	10.4	10.6	10.3	10.5	9.0

Table C1 Experimental data for the 4-air12-4 window (see Table 4.2 for design notation)
Temperatures for nodes 18-34 (see Fig. 4.4)

Date	Time	T_{18}	T_{19}	T_{20}	T_{21}	T_{22}	T_{23}	T_{24}	T_{25}	T_{26}	T_{27}	T_{28}	T_{29}	T_{30}	T_{31}	T_{32}	T_{33}	T_{34}
20/01/97	21:15:01	8.5	9.6	9.2	9.6	10.1	10.3	10.4	10.4	11.7	11.3	10.0	9.2	10.3	10.6	10.4	10.5	9.0
20/01/97	21:20:01	8.4	9.6	9.4	9.6	10.2	10.5	10.5	10.5	11.8	11.4	10.1	9.2	10.3	10.7	10.5	10.6	8.9
20/01/97	21:25:01	8.5	9.7	9.5	9.7	10.3	10.6	10.6	10.7	11.8	11.4	10.1	9.2	10.4	10.8	10.5		
20/01/97	18:05:01	9.9	9.8	9.5	9.4	10.2	11.1	11.0	10.7	10.4	10.0	10.7	10.1	11.1	10.0	11.0	10.6	11.6
20/01/97	18:10:01	9.9	9.8	9.4	9.4	10.2	11.0	11.0	10.7	10.5	10.0	10.7	10.1	11.1	10.0	11.0	10.6	11.6
20/01/97	18:15:01	9.9	9.8	9.4	9.4	10.2	11.0	11.0	10.7	10.4	9.9	10.6	10.0	11.1	10.0	11.1	10.5	11.5
20/01/97	18:20:01	9.8	9.8	9.4	9.4	10.2	10.9	11.0	10.7	10.4	9.9	10.6	10.0	11.0	10.0	11.0	10.6	11.5
20/01/97	18:25:01	9.8	9.7	9.4	9.3	10.1	10.9	11.0	10.7	10.4	9.9	10.6	10.0	11.0	9.9	11.0	10.5	11.5
20/01/97	18:30:01	9.8	9.7	9.4	9.3	10.1	10.9	11.0	10.6	10.3	9.8	10.6	9.9	11.0	9.9	11.0	10.5	11.5
20/01/97	18:35:01	9.8	9.7	9.3	9.3	10.1	10.8	10.9	10.6	10.3	9.8	10.5	9.9	11.0	9.9	10.9	10.5	11.5
20/01/97	18:40:01	9.7	9.7	9.3	9.3	10.0	10.9	10.9	10.6	10.3	9.8	10.5	9.9	11.0	9.9	11.0	10.5	11.5
20/01/97	18:45:01	9.7	9.6	9.3	9.2	10.0	10.8	10.8	10.5	10.3	9.8	10.5	9.9	10.9	9.8	10.9	10.4	11.3
20/01/97	18:50:01	9.7	9.6	9.3	9.2	10.0	10.8	10.8	10.5	10.2	9.8	10.5	9.8	10.9	9.8	10.9	10.4	11.3
20/01/97	18:55:01	9.7	9.6	9.2	9.2	10.0	10.8	10.8	10.5	10.2	9.8	10.5	9.8	10.9	9.8	10.8	10.3	11.5
20/01/97	19:00:01	9.7	9.6	9.3	9.2	10.0	10.9	10.9	10.6	10.3	9.8	10.6	9.8	11.0	9.8	11.0	10.3	11.5
20/01/97	19:05:01	9.7	9.6	9.3	9.2	10.1	10.9	11.0	10.6	10.3	9.8	10.6	9.9	11.0	9.8	11.0	10.3	11.4
20/01/97	19:10:01	9.7	9.7	9.3	9.3	10.0	10.9	11.0	10.7	10.3	9.8	10.6	9.9	11.0	9.8	11.0	10.3	11.5
20/01/97	19:15:01	9.7	9.7	9.3	9.2	10.0	10.9	11.0	10.7	10.4	9.8	10.6	9.9	11.1	9.8	11.0	10.3	11.5
20/01/97	19:20:01	9.7	9.7	9.3	9.2	10.1	10.9	11.0	10.7	10.4	9.8	10.6	9.9	11.1	9.8	11.0	10.5	11.6
20/01/97	19:25:01	9.7	9.7	9.3	9.2	10.0	10.9	11.0	10.7	10.4	9.8	10.6	9.9	11.1	9.8	11.0	10.5	11.6
20/01/97	19:30:01	9.7	9.7	9.3	9.2	10.0	10.9	11.0	10.7	10.4	9.8	10.6	9.9	11.0	9.8	11.0	10.5	11.5
20/01/97	19:35:01	9.7	9.6	9.3	9.2	10.0	10.9	10.9	10.6	10.3	9.8	10.6	9.9	11.1	9.8	11.1	10.5	11.5
20/01/97	19:40:01	9.7	9.6	9.3	9.2	10.0	10.9	10.9	10.6	10.3	9.8	10.6	9.8	11.0	9.8	11.0	10.4	11.5
20/01/97	19:45:01	9.7	9.6	9.2	9.2	10.0	10.8	10.9	10.6	10.3	9.7	10.5	9.8	10.9	9.8	10.9	10.3	11.4
20/01/97	19:50:01	9.6	9.5	9.2	9.1	10.0	10.8	10.8	10.5	10.2	9.7	10.5	9.8	10.9	9.7	10.8	10.3	11.3
20/01/97	19:55:01	9.5	9.5	9.1	9.1	9.9	10.7	10.8	10.5	10.2	9.6	10.4	9.7	10.8	9.7	10.7	10.2	11.2
20/01/97	20:00:01	9.5	9.4	9.1	9.0	9.9	10.7	10.8	10.4	10.1	9.6	10.4	9.7	10.8	9.6	10.7	10.2	11.2
20/01/97	20:05:01	9.6	9.5	9.1	9.0	9.9	10.8	10.8	10.4	10.1	9.6	10.4	9.7	10.8	9.6	10.8	10.2	11.2
20/01/97	20:10:01	9.6	9.5	9.1	9.1	9.9	10.8	10.8	10.5	10.2	9.6	10.4	9.7	10.8	9.6	10.8	10.2	11.3
20/01/97	20:15:01	9.6	9.5	9.1	9.1	9.9	10.8	10.8	10.5	10.2	9.7	10.5	9.7	10.9	9.6	10.8	10.2	11.3
20/01/97	20:20:01	9.6	9.5	9.2	9.1	9.9	10.9	10.9	10.5	10.2	9.6	10.5	9.7	10.9	9.6	10.9	10.1	11.3
20/01/97	20:25:01	9.6	9.5	9.2	9.1	9.9	10.8	10.9	10.5	10.2	9.6	10.5	9.7	10.9	9.6	10.8	10.2	11.3
20/01/97	20:30:01	9.6	9.5	9.1	9.1	9.8	10.7	10.9	10.5	10.2	9.6	10.5	9.6	10.9	9.6	10.8	10.1	11.2
20/01/97	20:35:01	9.5	9.4	9.1	9.0	9.8	10.7	10.8	10.5	10.2	9.6	10.4	9.6	10.8	9.6	10.8	10.1	11.2
20/01/97	20:40:01	9.5	9.4	9.0	9.0	9.8	10.7	10.7	10.4	10.1	9.6	10.4	9.6	10.8	9.6	10.8	10.1	11.2
20/01/97	20:45:01	9.5	9.4	9.0	9.0	9.8	10.6	10.8	10.4	10.1	9.5	10.4	9.6	10.8	9.5	10.8	10.2	11.3
20/01/97	20:50:01	9.5	9.4	9.0	9.0	9.8	10.7	10.7	10.4	10.1	9.5	10.4	9.6	10.8	9.5	10.8	10.2	11.3
20/01/97	20:55:01	9.5	9.4	9.0	8.9	9.8	10.7	10.7	10.4	10.1	9.5	10.4	9.6	10.8	9.5	10.8	10.2	11.3

Table C1 Experimental data for the 4-air12-4 window (see Table 4.2 for design notation)
Temperatures for nodes 35-48, i and o (see Fig. 4.4)

Date	Time	T_{35}	T_{36}	T_{37}	T_{38}	T_{39}	T_{40}	T_{41}	T_{42}	T_{43}	T_{44}	T_{45}	T_{46}	T_{47}	T_{48}	T_o	T_i
20/01/97	21:00:01	9.5	9.4	9.0	8.9	9.8	10.7	10.7	10.4	10.1	9.5	10.4	9.6	10.8	9.5	10.7	10.2
20/01/97	21:05:01	9.5	9.4	9.0	8.9	9.8	10.7	10.7	10.4	10.1	9.5	10.4	9.5	10.8	9.5	10.8	10.1
20/01/97	21:10:01	9.4	9.4	9.0	9.0	9.7	10.6	10.7	10.4	10.0	9.5	10.3	9.5	10.8	9.4	10.7	10.0
20/01/97	21:15:01	9.4	9.4	9.0	8.9	9.7	10.6	10.7	10.4	10.1	9.4	10.3	9.5	10.8	9.4	10.7	10.0
20/01/97	21:20:01	9.4	9.4	9.0	9.0	9.7	10.7	10.8	10.5	10.1	9.5	10.4	9.5	10.8	9.4	10.8	10.0
20/01/97	18:05:01	11.1	12.0	11.3	12.1	11.5	12.2	12.4	12.4	12.0	10.9	11.3	11.6	11.4	10.6	1.0	16.0
20/01/97	18:10:01	11.0	11.8	11.3	12.1	11.4	12.2	12.3	12.3	11.9	10.9	11.3	11.5	11.3	10.6	1.0	15.5
20/01/97	18:15:01	11.0	11.7	11.2	12.0	11.2	12.1	12.3	12.3	11.9	10.9	11.1	11.4	11.2	10.5	1.0	16.0
20/01/97	18:20:01	11.0	11.8	11.2	12.0	11.3	12.1	12.3	12.3	11.9	10.9	11.1	11.4	11.3	10.5	1.0	15.5
20/01/97	18:25:01	11.0	11.8	11.2	12.0	11.3	12.2	12.3	12.3	11.8	10.8	11.2	11.5	11.3	10.5	1.0	16.0
20/01/97	18:30:01	10.9	11.7	11.1	12.0	11.2	12.1	12.2	12.2	11.8	10.8	11.2	11.5	11.3	10.5	1.0	16.0
20/01/97	18:35:01	11.0	11.7	11.1	12.0	11.2	12.1	12.2	12.2	11.7	10.7	11.1	11.5	11.2	10.5	1.0	15.5
20/01/97	18:40:01	11.0	11.7	11.1	12.0	11.2	12.1	12.2	12.2	11.7	10.7	11.0	11.4	11.2	10.4	1.0	15.5
20/01/97	18:45:01	10.8	11.7	11.1	12.0	11.2	12.1	12.2	12.2	11.7	10.8	11.0	11.3	11.1	10.4	1.0	15.5
20/01/97	18:50:01	10.8	11.6	11.1	11.8	11.2	12.0	12.0	12.1	11.6	10.7	11.0	11.3	11.1	10.3	1.0	16.0
20/01/97	18:55:01	10.8	11.7	11.1	12.0	11.2	12.1	12.1	12.2	11.7	10.7	11.1	11.4	11.2	10.4	1.5	16.0
20/01/97	19:00:01	10.9	11.7	11.1	12.0	11.3	12.1	12.2	12.3	11.7	10.7	11.2	11.5	11.2	10.4	1.0	16.5
20/01/97	19:05:01	10.8	11.7	11.1	11.9	11.2	12.1	12.2	12.3	11.8	10.7	11.1	11.4	11.3	10.4	1.5	16.0
20/01/97	19:10:01	10.8	11.7	11.1	12.1	11.2	12.2	12.2	12.3	11.8	10.6	11.1	11.4	11.3	10.4	1.0	16.0
20/01/97	19:15:01	10.9	11.8	11.1	12.1	11.3	12.2	12.2	12.3	11.8	10.7	11.1	11.4	11.3	10.4	1.0	16.0
20/01/97	19:20:01	11.0	11.9	11.2	12.1	11.3	12.2	12.2	12.3	11.8	10.6	11.1	11.5	11.3	10.4	1.0	16.0
20/01/97	19:25:01	11.0	11.8	11.2	12.1	11.3	12.2	12.3	12.3	11.8	10.8	11.1	11.5	11.2	10.4	1.0	16.0
20/01/97	19:30:01	11.0	11.8	11.2	12.1	11.3	12.2	12.2	12.3	11.7	10.8	11.1	11.4	11.2	10.4	1.5	16.0
20/01/97	19:35:01	11.0	11.8	11.2	12.1	11.3	12.2	12.2	12.3	11.9	10.7	11.1	11.4	11.2	10.4	1.5	16.0
20/01/97	19:40:01	10.8	11.7	11.1	12.0	11.2	12.1	12.2	12.2	11.8	10.6	11.0	11.4	11.2	10.3	1.0	16.0
20/01/97	19:45:01	10.8	11.7	11.1	12.0	11.2	12.1	12.1	12.2	11.7	10.6	10.9	11.2	11.0	10.2	1.5	16.0
20/01/97	19:50:01	10.8	11.6	11.0	11.8	11.1	12.0	12.1	12.1	11.6	10.5	10.8	11.2	11.0	10.1	1.0	16.0
20/01/97	19:55:01	10.7	11.6	11.0	11.8	11.1	12.0	12.0	12.0	11.5	10.5	10.8	11.1	10.9	10.0	1.0	15.5
20/01/97	20:00:01	10.7	11.6	11.0	11.7	11.1	12.0	12.0	12.1	11.5	10.5	10.8	11.2	10.9	10.0	1.0	16.0
20/01/97	20:05:01	10.7	11.6	11.0	11.8	11.1	12.0	12.1	12.2	11.6	10.5	10.8	11.1	10.9	10.0	1.0	16.5
20/01/97	20:10:01	10.7	11.6	11.0	11.9	11.1	12.1	12.2	12.2	11.6	10.5	10.8	11.2	11.0	10.0	0.0	16.5
20/01/97	20:15:01	10.7	11.6	11.0	12.0	11.1	12.1	12.2	12.2	11.7	10.6	10.9	11.2	11.0	10.1	0.5	16.5
20/01/97	20:20:01	10.7	11.6	11.0	11.9	11.1	12.0	12.2	12.2	11.6	10.5	10.9	11.2	11.0	10.0	0.0	16.5
20/01/97	20:25:01	10.7	11.7	11.0	12.0	11.1	12.1	12.2	12.2	11.6	10.5	10.9	11.3	11.1	10.2	-0.5	16.0
20/01/97	20:30:01	10.6	11.6	10.9	11.9	11.1	12.0	12.2	12.2	11.7	10.5	10.9	11.3	11.1	10.2	-0.5	16.0
20/01/97	20:35:01	10.7	11.6	11.0	11.8	11.1	12.0	12.1	12.2	11.6	10.5	10.9	11.3	11.1	10.2	-0.5	16.0
20/01/97	20:40:01	10.6	11.6	11.0	11.8	11.1	12.0	12.1	12.2	11.6	10.5	10.9	11.3	11.0	10.1	0.5	16.0
20/01/97	20:45:01	10.7	11.6	11.0	11.8	11.1	12.1	12.0	12.1	11.5	10.5	10.8	11.2	11.0	10.1	0.0	16.0

Table C2 An abstract from the experimental data for the 4E-xe10-E4 window (see Table 4.2 for design notation)
Temperatures for nodes 1-17 (see Fig. 4.4)

Date	Time	T_1	T_2	T_3	T_4	T_5	T_6	T_7	T_8	T_9	T_{10}	T_{11}	T_{12}	T_{13}	T_{14}	T_{15}	T_{16}	T_{17}
16/01/97	18:05:01	14.4	16.6	17.0	17.4	18.2	18.5	18.2	18.0	18.7	17.8	14.3	14.3	17.2	18.0	18.2	18.3	14.0
16/01/97	18:10:01	14.6	16.8	16.9	17.4	18.1	18.5	18.4	18.0	18.8	17.8	14.4	14.4	17.2	18.1	18.2	18.2	14.1
16/01/97	18:15:01	14.5	16.7	17.0	17.4	18.2	18.5	18.4	17.9	18.7	17.9	14.6	14.5	17.2	18.2	18.2	18.3	14.2
16/01/97	18:20:01	14.7	16.8	17.1	17.6	18.2	18.6	18.4	18.0	18.8	17.9	14.7	14.6	17.3	18.2	18.3	18.4	14.2
16/01/97	18:25:01	14.7	16.7	17.0	17.4	18.2	18.5	18.4	18.0	18.8	17.8	14.7	14.6	17.3	18.2	18.3	18.3	14.3
16/01/97	18:30:01	14.8	16.9	17.1	17.5	18.2	18.6	18.4	18.0	18.9	18.0	14.8	14.6	17.3	18.2	18.4	18.4	14.3
16/01/97	18:35:01	14.7	16.9	17.1	17.5	18.2	18.6	18.5	18.0	18.9	18.0	14.6	14.5	17.3	18.1	18.3	18.3	14.3
16/01/97	18:40:01	14.8	16.8	17.0	17.5	18.3	18.7	18.5	18.0	18.9	18.0	14.7	14.5	17.3	18.2	18.3	18.4	14.3
16/01/97	18:45:01	14.8	16.9	17.1	17.6	18.3	18.6	18.4	18.1	18.8	17.9	14.7	14.5	17.3	18.2	18.3	18.4	14.3
16/01/97	18:50:01	14.7	16.9	17.1	17.6	18.5	18.7	18.4	18.2	18.9	18.0	14.7	14.6	17.3	18.3	18.4	18.5	14.3
16/01/97	18:55:01	14.8	17.0	17.2	17.7	18.4	18.8	18.6	18.2	19.0	18.1	14.7	14.6	17.4	18.4	18.5	18.5	14.4
16/01/97	19:00:01	14.8	17.1	17.4	17.8	18.6	18.9	18.7	18.3	19.1	18.2	14.8	14.6	17.5	18.4	18.6	18.7	14.3
16/01/97	19:05:01	14.8	17.1	17.4	17.9	18.6	18.9	18.7	18.4	19.2	18.2	14.7	14.6	17.5	18.5	18.6	18.7	14.4
16/01/97	19:10:01	14.8	17.1	17.4	17.8	18.6	19.0	18.8	18.4	19.1	18.2	14.8	14.7	17.6	18.5	18.6	18.7	14.4
16/01/97	19:15:01	14.8	17.1	17.4	17.8	18.7	19.0	18.8	18.3	19.2	18.3	14.8	14.7	17.6	18.5	18.6	18.7	14.4
16/01/97	19:20:01	15.0	17.2	17.4	17.8	18.6	19.0	18.8	18.3	19.2	18.2	14.8	14.7	17.6	18.5	18.7	18.7	14.4
16/01/97	19:25:01	14.8	17.1	17.4	17.8	18.6	19.0	18.7	18.4	19.1	18.2	14.9	14.7	17.5	18.5	18.6	18.6	14.5
16/01/97	19:30:01	14.7	17.1	17.4	17.8	18.6	18.9	18.8	18.4	19.2	18.3	14.9	14.8	17.6	18.5	18.6	18.7	14.4
16/01/97	19:35:01	14.7	17.0	17.3	17.8	18.5	18.8	18.6	18.4	19.2	18.3	14.9	14.8	17.6	18.5	18.6	18.7	14.4
16/01/97	19:40:01	14.8	17.0	17.3	17.8	18.6	19.0	18.7	18.3	19.1	18.2	14.9	14.7	17.6	18.4	18.5	18.6	14.4
16/01/97	19:45:01	14.6	17.0	17.3	17.7	18.5	18.9	18.7	18.4	19.1	18.2	14.9	14.8	17.6	18.5	18.6	18.6	14.4
16/01/97	19:50:01	14.8	17.1	17.4	17.8	18.5	18.9	18.7	18.2	19.1	18.1	14.9	14.8	17.5	18.5	18.6	18.7	14.4
16/01/97	19:55:01	14.6	16.9	17.2	17.7	18.5	18.8	18.6	18.3	19.1	18.1	14.8	14.6	17.5	18.4	18.5	18.6	14.3
16/01/97	20:00:01	14.5	17.0	17.3	17.7	18.5	18.8	18.6	18.2	19.0	18.2	14.7	14.5	17.5	18.4	18.5	18.5	14.3
16/01/97	20:05:01	14.4	16.8	17.2	17.6	18.4	18.7	18.5	18.3	19.0	18.0	14.5	14.4	17.5	18.3	18.5	18.6	14.2
16/01/97	20:10:01	14.4	16.8	17.2	17.8	18.6	18.8	18.6	18.4	19.0	18.1	14.4	14.3	17.4	18.4	18.5	18.6	14.1
16/01/97	20:15:01	14.4	17.0	17.2	17.8	18.6	18.9	18.7	18.4	19.2	18.3	14.5	14.3	17.4	18.5	18.5	18.6	14.0
16/01/97	20:20:01	14.4	17.0	17.4	17.8	18.6	18.9	18.8	18.3	19.2	18.1	14.5	14.3	17.4	18.4	18.7	18.6	14.1
16/01/97	20:25:01	14.3	17.0	17.3	17.8	18.6	18.9	18.7	18.4	19.1	18.1	14.5	14.3	17.4	18.5	18.6	18.6	14.0
16/01/97	20:30:01	14.3	16.8	17.3	17.8	18.7	18.9	18.7	18.5	19.1	18.2	14.4	14.3	17.4	18.4	18.5	18.6	14.0
16/01/97	20:35:01	14.3	16.8	17.2	17.7	18.6	18.9	18.7	18.3	19.1	18.0	14.3	14.2	17.4	18.4	18.6	18.6	13.9
16/01/97	20:40:01	14.2	16.8	17.2	17.7	18.5	18.9	18.7	18.2	19.1	18.1	14.2	14.0	17.3	18.4	18.5	18.6	13.8
16/01/97	20:45:01	14.1	16.7	17.2	17.7	18.5	18.8	18.5	18.1	18.9	17.9	13.9	13.8	17.2	18.2	18.4	18.5	13.7
16/01/97	20:50:01	14.1	16.8	17.1	17.7	18.4	18.8	18.6	18.2	18.9	17.9	13.9	13.8	17.1	18.2	18.4	18.5	13.7
16/01/97	20:55:01	14.1	16.6	17.0	17.5	18.3	18.7	18.5	18.1	19.0	17.9	13.9	13.8	17.1	18.2	18.3	18.5	13.6
16/01/97	21:00:01	14.0	16.5	17.1	17.6	18.3	18.7	18.5	18.0	18.8	17.8	13.9	13.8	17.0	18.2	18.3	18.5	13.6
16/01/97	21:05:01	14.0	16.5	17.0	17.6	18.2	18.7	18.5	18.0	18.8	17.8	13.9	13.7	17.0	18.1	18.3	18.4	13.5

Table C2 (cont'd) Experimental data for the 4E-xe10-E4 window (see Table 4.2 for design notation)
Temperatures for nodes 18-34 (see Fig. 4.4)

Date	Time	T_{18}	T_{19}	T_{20}	T_{21}	T_{22}	T_{23}	T_{24}	T_{25}	T_{26}	T_{27}	T_{28}	T_{29}	T_{30}	T_{31}	T_{32}	T_{33}	T_{34}
16/01/97	21:10:01	13.8	16.5	16.9	17.5	18.3	18.6	18.4	17.9	18.8	17.8	13.8	13.7	17.0	18.1	18.2	18.4	13.5
16/01/97	21:15:01	13.8	16.4	16.8	17.5	18.2	18.5	18.4	17.8	18.7	17.6	13.9	13.7	17.0	18.0	18.3	18.3	13.4
16/01/97	21:20:01	13.8	16.4	16.9	17.4	18.2	18.6	18.4	17.8	18.7	17.6	13.8	13.6	16.9	18.1	18.2	18.2	13.4
16/01/97	18:05:01	14.6	14.8	14.6	14.4	15.2	16.9	17.3	17.1	16.9	14.7	17.2	15.1	17.8	14.7	17.5	15.2	18.0
16/01/97	18:10:01	14.6	14.9	14.6	14.5	15.2	16.9	17.3	17.2	16.9	14.7	17.2	15.2	17.8	14.7	17.5	15.3	18.1
16/01/97	18:15:01	14.7	14.9	14.7	14.6	15.3	16.9	17.4	17.2	16.9	14.8	17.2	15.3	17.8	14.8	17.6	15.3	18.1
16/01/97	18:20:01	14.8	15.0	14.7	14.7	15.3	17.0	17.4	17.3	17.0	14.9	17.3	15.3	17.9	14.9	17.6	15.3	18.1
16/01/97	18:25:01	14.9	15.0	14.8	14.7	15.4	17.1	17.5	17.3	17.0	15.0	17.3	15.4	18.0	15.0	17.7	15.4	18.1
16/01/97	18:30:01	14.8	15.0	14.8	14.7	15.4	17.1	17.5	17.3	17.0	14.9	17.3	15.4	18.0	14.9	17.7	15.5	18.2
16/01/97	18:35:01	14.8	15.0	14.8	14.7	15.4	17.0	17.5	17.3	17.0	14.9	17.3	15.3	17.9	14.9	17.7	15.4	18.2
16/01/97	18:40:01	14.8	15.0	14.8	14.7	15.3	17.0	17.4	17.3	17.0	14.9	17.3	15.3	17.9	14.8	17.6	15.3	18.1
16/01/97	18:45:01	14.8	15.1	14.8	14.7	15.4	17.1	17.4	17.3	17.1	14.9	17.3	15.4	17.9	14.9	17.7	15.3	18.1
16/01/97	18:50:01	14.9	15.1	14.9	14.7	15.4	17.2	17.5	17.4	17.1	15.0	17.5	15.4	18.0	15.0	17.8	15.6	18.3
16/01/97	18:55:01	14.9	15.1	14.9	14.8	15.5	17.2	17.6	17.5	17.2	15.0	17.5	15.4	18.1	14.9	17.8	15.6	18.3
16/01/97	19:00:01	14.9	15.1	14.9	14.8	15.5	17.3	17.7	17.5	17.2	15.0	17.5	15.4	18.1	15.0	17.9	15.6	18.3
16/01/97	19:05:01	15.0	15.2	14.9	14.8	15.5	17.3	17.7	17.5	17.3	15.0	17.6	15.5	18.2	15.0	17.9	15.4	18.3
16/01/97	19:10:01	15.0	15.2	14.9	14.8	15.5	17.3	17.7	17.5	17.3	15.0	17.6	15.5	18.2	15.0	17.9	15.6	18.4
16/01/97	19:15:01	15.0	15.2	15.0	14.8	15.5	17.3	17.7	17.5	17.3	15.0	17.6	15.5	18.2	15.0	17.9	15.6	18.5
16/01/97	19:20:01	15.0	15.2	14.9	14.8	15.5	17.3	17.7	17.6	17.3	15.1	17.6	15.5	18.2	15.1	17.9	15.6	18.4
16/01/97	19:25:01	15.0	15.2	14.9	14.8	15.5	17.3	17.7	17.6	17.3	15.1	17.6	15.5	18.2	15.1	17.9	15.6	18.5
16/01/97	19:30:01	15.0	15.2	14.9	14.8	15.5	17.3	17.7	17.5	17.3	15.1	17.6	15.6	18.2	15.1	17.9	15.6	18.3
16/01/97	19:35:01	15.0	15.2	14.9	14.8	15.5	17.3	17.7	17.5	17.2	15.1	17.6	15.6	18.2	15.2	18.0	15.6	18.4
16/01/97	19:40:01	15.0	15.2	14.9	14.7	15.5	17.3	17.7	17.5	17.2	15.1	17.6	15.6	18.2	15.1	18.0	15.6	18.3
16/01/97	19:45:01	15.0	15.1	14.9	14.7	15.5	17.2	17.6	17.5	17.2	15.1	17.6	15.6	18.2	15.1	17.9	15.7	18.4
16/01/97	19:50:01	14.9	15.1	14.8	14.7	15.5	17.3	17.6	17.5	17.2	15.1	17.6	15.5	18.2	15.1	17.9	15.7	18.4
16/01/97	19:55:01	14.9	15.0	14.8	14.6	15.5	17.2	17.6	17.4	17.1	15.0	17.5	15.5	18.2	15.0	17.9	15.6	18.3
16/01/97	20:00:01	14.8	15.0	14.7	14.5	15.4	17.1	17.5	17.4	17.1	14.9	17.5	15.3	18.1	14.8	17.8	15.4	18.2
16/01/97	20:05:01	14.7	14.9	14.6	14.4	15.3	17.1	17.5	17.3	17.0	14.8	17.4	15.2	18.1	14.7	17.8	15.3	18.2
16/01/97	20:10:01	14.7	14.9	14.6	14.4	15.3	17.1	17.5	17.3	17.1	14.8	17.5	15.2	18.1	14.7	17.8	15.2	18.2
16/01/97	20:15:01	14.6	14.8	14.6	14.4	15.2	17.1	17.5	17.3	17.0	14.8	17.4	15.2	18.1	14.6	17.8	15.2	18.2
16/01/97	20:20:01	14.7	14.8	14.6	14.4	15.2	17.1	17.5	17.3	17.1	14.8	17.5	15.2	18.1	14.7	17.8	15.2	18.3
16/01/97	20:25:01	14.6	14.8	14.5	14.4	15.2	17.1	17.5	17.3	17.1	14.7	17.5	15.2	18.1	14.7	17.8	15.2	18.3
16/01/97	20:30:01	14.6	14.8	14.5	14.4	15.2	17.1	17.5	17.4	17.0	14.7	17.4	15.1	18.1	14.6	17.8	15.2	18.3
16/01/97	20:35:01	14.5	14.7	14.4	14.3	15.1	17.0	17.5	17.3	17.0	14.6	17.4	15.0	18.0	14.5	17.7	15.1	18.2
16/01/97	20:40:01	14.4	14.6	14.3	14.2	15.0	17.0	17.4	17.2	17.0	14.5	17.3	14.9	18.0	14.4	17.7	15.0	18.1
16/01/97	20:45:01	14.3	14.5	14.2	14.1	14.9	16.9	17.3	17.1	16.9	14.4	17.3	14.8	17.9	14.2	17.6	14.8	18.0
16/01/97	20:50:01	14.3	14.4	14.2	14.0	14.8	16.8	17.2	17.1	16.8	14.3	17.2	14.7	17.8	14.2	17.5	14.7	17.9

Table C2 (cont'd) Experimental data for the 4E-xe10-E4 window (see Table 4.2 for design notation)
Temperatures for nodes 35-48 and I, o nodes (see Fig. 4.4)

Date	Time	T_{35}	T_{36}	T_{37}	T_{38}	T_{39}	T_{40}	T_{41}	T_{42}	T_{43}	T_{44}	T_{45}	T_{46}	T_{47}	T_{48}	T_o	T_I
16/01/97	20:55:01	14.2	14.4	14.2	14.0	14.8	16.8	17.2	17.1	16.8	14.3	17.2	14.7	17.8	14.1	17.5	14.7
16/01/97	21:00:01	14.2	14.3	14.1	13.9	14.7	16.7	17.2	17.0	16.8	14.2	17.1	14.6	17.7	14.1	17.4	14.6
16/01/97	21:05:01	14.1	14.3	14.0	13.9	14.7	16.7	17.1	17.0	16.7	14.2	17.1	14.6	17.7	14.1	17.4	14.6
16/01/97	21:10:01	14.0	14.3	14.0	13.8	14.6	16.6	17.1	16.9	16.7	14.1	17.0	14.5	17.7	14.0	17.3	14.6
16/01/97	21:15:01	14.0	14.2	13.9	13.7	14.6	16.6	17.0	16.9	16.6	14.1	17.0	14.5	17.6	14.0	17.3	14.6
16/01/97	21:20:01	14.0	14.2	13.9	13.8	14.5	16.5	17.0	16.9	16.6	14.1	17.0	14.5	17.6	13.9	17.3	14.6
16/01/97	18:05:01	15.6	18.3	15.8	18.5	15.8	18.3	18.7	18.8	18.2	15.3	16.2	16.5	16.3	15.5	7.0	22.0
16/01/97	18:10:01	15.7	18.5	16.0	18.5	16.0	18.3	18.6	18.8	18.1	15.5	16.3	16.5	16.4	15.6	7.5	23.0
16/01/97	18:15:01	15.7	18.4	16.0	18.4	16.0	18.3	18.7	18.9	18.3	15.7	16.5	16.8	16.6	15.9	7.5	22.0
16/01/97	18:20:01	15.8	18.5	16.1	18.5	16.1	18.3	18.7	18.9	18.3	15.8	16.5	16.8	16.6	15.9	7.0	22.5
16/01/97	18:25:01	15.8	18.5	16.1	18.5	16.1	18.3	18.7	18.8	18.3	15.6	16.4	16.7	16.4	15.8	5.5	22.0
16/01/97	18:30:01	15.9	18.6	16.1	18.6	16.1	18.5	18.7	18.8	18.2	15.6	16.5	16.7	16.5	15.8	5.0	22.5
16/01/97	18:35:01	15.8	18.6	16.1	18.6	16.1	18.4	18.8	18.9	18.4	15.6	16.4	16.7	16.5	15.8	5.0	23.0
16/01/97	18:40:01	15.8	18.5	16.1	18.5	16.0	18.3	18.7	18.9	18.3	15.5	16.3	16.7	16.5	15.8	4.5	23.0
16/01/97	18:45:01	15.8	18.4	16.1	18.6	16.1	18.3	18.8	19.0	18.4	15.8	16.5	16.7	16.6	15.9	5.5	23.5
16/01/97	18:50:01	15.9	18.7	16.2	18.8	16.2	18.6	18.9	19.1	18.4	15.6	16.8	17.1	16.8	16.0	4.5	23.5
16/01/97	18:55:01	16.0	18.7	16.2	18.8	16.3	18.7	19.1	19.2	18.6	15.8	16.6	16.9	16.8	16.0	5.0	23.5
16/01/97	19:00:01	16.0	18.8	16.3	18.8	16.2	18.7	19.1	19.2	18.6	15.8	16.7	17.0	16.7	15.9	4.5	23.5
16/01/97	19:05:01	15.9	18.8	16.2	18.8	16.2	18.7	19.1	19.2	18.6	15.8	16.7	17.0	16.8	16.0	5.0	23.5
16/01/97	19:10:01	16.0	18.8	16.3	18.9	16.3	18.7	19.1	19.3	18.6	15.9	16.7	17.1	16.8	16.0	4.5	23.5
16/01/97	19:15:01	16.1	18.8	16.3	19.0	16.3	18.8	19.1	19.2	18.7	15.9	16.8	17.1	16.8	16.1	4.5	23.5
16/01/97	19:20:01	16.1	18.8	16.3	18.9	16.2	18.7	19.1	19.2	18.6	15.9	16.7	17.0	16.8	16.0	4.5	23.5
16/01/97	19:25:01	16.0	18.8	16.3	18.9	16.3	18.7	19.1	19.2	18.6	15.8	16.7	17.0	16.8	16.0	5.0	23.5
16/01/97	19:30:01	15.9	18.8	16.3	18.8	16.3	18.7	19.0	19.2	18.6	15.9	16.8	17.1	16.9	16.1	5.0	23.5
16/01/97	19:35:01	16.0	18.8	16.3	18.8	16.3	18.7	19.1	19.3	18.6	15.9	16.7	17.0	16.9	16.1	4.5	23.5
16/01/97	19:40:01	15.9	18.7	16.3	18.8	16.3	18.7	19.1	19.3	18.6	16.0	16.8	17.1	16.8	16.1	4.0	23.5
16/01/97	19:45:01	16.1	18.8	16.4	18.9	16.4	18.8	19.1	19.2	18.6	15.9	16.7	17.1	16.8	16.1	4.5	23.0
16/01/97	19:50:01	16.1	18.8	16.3	18.8	16.4	18.7	19.1	19.3	18.6	15.9	16.8	17.1	16.8	16.1	4.5	23.5
16/01/97	19:55:01	16.0	18.8	16.3	18.8	16.3	18.7	19.0	19.1	18.5	15.6	16.5	16.8	16.5	15.9	4.0	23.0
16/01/97	20:00:01	15.8	18.7	16.1	18.7	16.0	18.6	18.9	19.0	18.4	15.4	16.4	16.8	16.5	15.8	4.0	23.0
16/01/97	20:05:01	15.7	18.7	16.1	18.7	16.0	18.6	19.0	19.1	18.5	15.5	16.3	16.6	16.4	15.7	4.0	23.5
16/01/97	20:10:01	15.7	18.6	15.9	18.7	15.9	18.5	19.0	19.2	18.5	15.5	16.4	16.7	16.5	15.7	4.0	23.5
16/01/97	20:15:01	15.7	18.6	16.0	18.7	16.0	18.6	19.0	19.2	18.5	15.5	16.4	16.8	16.5	15.7	4.0	23.5
16/01/97	20:20:01	15.7	18.7	16.1	18.8	16.0	18.7	19.0	19.2	18.5	15.5	16.5	16.8	16.6	15.8	4.0	23.5
16/01/97	20:25:01	15.7	18.7	16.1	18.8	16.0	18.7	19.0	19.1	18.5	15.5	16.6	16.8	16.5	15.7	3.5	23.5
16/01/97	20:30:01	15.7	18.7	16.0	18.8	16.0	18.7	19.0	19.2	18.5	15.3	16.2	16.6	16.3	15.6	4.0	23.5
16/01/97	20:35:01	15.6	18.7	15.8	18.7	15.8	18.6	18.9	19.1	18.4	15.2	16.0	16.4	16.1	15.4	3.5	23.5